UNT™

Practical Applications of FTIR to Characterize Paving Materials

Technical Report 0-5608-1

Cooperative Research Program

**UNIVERSITY OF NORTH TEXAS
DENTON, TEXAS**

TEXAS DEPARTMENT OF TRANSPORTATION

in cooperation with the
Federal Highway Administration and the
Texas Department of Transportation

1. Report No. FHWA/TX-11/0-5608-1	2. Government Accession No.	3. Recipient's Catalog No.
4. Title and Subtitle PRACTICAL APPLICATIONS OF FTIR TO CHARACTERIZE PAVING MATERIALS		5. Report Date November 2009; Published: December 2010
		6. Performing Organization Code
7. Author(s) Seifollah Nasrazadani, David Mielke, Tyler Springfield, and Naresh Ramasamy		8. Performing Organization Report No. Report 0-5608-1
9. Performing Organization Name and Address University of North Texas 3940 N. Elm Denton, Texas 76207		10. Work Unit No. (TRAIS)
		11. Contract or Grant No. Project 0-5608
12. Sponsoring Agency Name and Address Texas Department of Transportation Research and Technology Implementation Office P.O. Box 5080 Austin, Texas 78763-5080		13. Type of Report and Period Covered Technical Report: September 2007–August 2009
		14. Sponsoring Agency Code
15. Supplementary Notes Project performed in cooperation with the Texas Department of Transportation and the Federal Highway Administration. Project Title: Practical Applications of FTIR to Characterize Paving Materials		

16. Abstract

Practical applications of Fourier Transform Infrared Spectroscopy in determination of quality and uniformity of antistripping additives, curing membrane compounds, concrete spall repair epoxy materials, evaporation retardants, and concrete cement were investigated. Polymer content in a number of polymer modified asphalt samples were measured based on calibration curves developed for two sets of samples (received from asphalt suppliers to TxDOT) with known polymer contents. Quantification of polymer in asphalt was based on the relationship between the intensity ratio of 966 cm^{-1}/1375 cm^{-1} absorption bands to the polymer concentration (wt%). Correlation factor for this relationship for the two sets of data was above 0.96. FTIR technique appears to be capable of quantifying alkali content in concrete cement. A linear relationship was observed relating absorption bands ratio of 750 cm^{-1}/923 cm^{-1} to Na_2O equivalent (as measured with X-ray Fluorescence) with $R^2 = 0.97$. FTIR fingerprints of spall repair patching epoxy, concrete curing membrane, and evaporation retardants were obtained. A separate practical protocol for each kind of analysis was developed for identification and quantification (where applicable) for paving materials constituents. Despite successful applications of FTIR in the analysis of polymer content in asphalt binders, alkali content assessment in concrete cement, and fingerprinting of spall repair epoxy, curing membranes, and evaporation retardants, FTIR was not found to be a suitable technique to detect and quantify antistripping agents in asphalt materials due to low concentration of the antistripping agents and possibly band overlap in the spectra of organic compounds.

17. Key Words Polymer modified asphalt, emulsion asphalt, concrete curing compound, alkali equivalent, concrete spall repair epoxy, evaporation retardant, fly ash	18. Distribution Statement No restrictions. This document is available to the public through NTIS: National Technical Information Service Springfield, Virginia 22161 http://www.ntis.gov		
19. Security Classif.(of this report) Unclassified	20. Security Classif.(of this page) Unclassified	21. No. of Pages 160	22. Price

Form DOT F 1700.7 (8-72)   Reproduction of completed page authorized

PRACTICAL APPLICATIONS OF FTIR TO CHARACTERIZE PAVING MATERIALS

by

Seifollah Nasrazadani
Associate Professor
University of North Texas

David Mielke
Graduate Student
University of North Texas

Tyler Springfield
Graduate Student
University of North Texas

and

Naresh Ramasamy
Graduate Student
University of North Texas

Disclaimers

Author's Disclaimer: The contents of this report reflect the views of the authors, who are responsible for the facts and the accuracy of the data presented herein. The contents do not necessarily reflect the official view or policies of the Federal Highway Administration or the Texas Department of Transportation (TxDOT). This report does not constitute a standard, specification, or regulation.

Engineering Disclaimer
NOT INTENDED FOR CONSTRUCTION, BIDDING, OR PERMIT PURPOSES.
Project Engineer: Seifollah Nasrazadani

Acknowledgments

Products

This final report is the Product 1 listed in the deliverables table. Detailed documentation of the research performed is included in this report.

Table of Contents

LIST OF FIGURES

Page

LIST OF TABLES

1. INTRODUCTION

Texas Department of Transportation annually spends a sizable portion of its budget in purchasing paving materials including asphalt binders, emulsions, cutbacks, and neat binders, curing membranes, epoxy materials for concrete spall repair, cements, and paint. A common characteristic of these paving materials is a certain degree of variability in the quality and uniformity of starting materials used in processing and production of these products. For example, the base materials used in production of asphalt binders, emulsions, cutbacks, and neat binders is heavily dependent on crude oil sources. The chemical makeup of crude oil from different parts of the world is different, and such a difference leads to minor variation in product quality made from petroleum. The main purpose of this investigation was to study applicability of Fourier Transform Infrared spectroscopy (FTIR) in characterization of these materials.

FTIR is a rapid non-destructive technique that requires minimal sample preparation and minimal training of operators. It can also be field portable and inexpensive compared to other characterization methods. Availability of a large library (in both printed and electronic formats) of organic and inorganic compounds used in paving materials makes analysis and interpretation of FTIR spectra relatively easy.

In this investigation, attempts were made to successfully apply FTIR in both quantitative and qualitative analysis of paving materials. Specifically, polymer concentration in polymer-modified asphalt binders were quantitatively measured using AASHTO T302 standard procedure. A new exploratory analysis method was developed to quantitatively assess alkali concentration in concrete cements using FTIR. In addition to these two quantitative methods, fingerprints of concrete spall repair epoxy, curing membrane compound, and evaporation retardants were obtained for qualitative analysis of these products.

1.1 Research Objectives

The main objective of this research was to address practical applicability of the FTIR technique in characterization of commonly used paving materials. In order to accomplish our main objective, the following sub-objectives are considered:

1. Determination of antistripping agents quality in emulsions, cut-backs, and neat binders
2. Determination of polymer content in asphalt binders
3. Determination of quality and uniformity of curing membranes

4. Determination of quality and uniformity of epoxy materials used for concrete spall repair
5. Determination of quality and uniformity of cements

FTIR testing procedures has been developed as related to some of the above items and presented in appendices B, C, and F. Transfer of knowledge and experience gained from this project to TxDOT practice methods will facilitate ease of quality assurance processes in materials procurement.

1.2 Scope of Research

A comprehensive literature review on state-of-the-art practical applications of FTIR in characterization of paving materials is required to enable development of test procedures for routine analysis by TxDOT engineers. FTIR fingerprint spectra of concrete spall repair epoxy, curing membrane compound, and evaporation retardants were developed. Comparison of these spectra will be used to assess quality and uniformity of the products. Samples from different batches of each material were collected and analyzed for quality and uniformity. Given the research objectives above, the research team collected multiple sample batches from different suppliers of the mentioned products and performed FTIR analysis/characterization. In addition, quantification of polymer content in polymer-modified asphalt binders as well as development of a new analytical method for quantification of equivalent alkali content in concrete cement was completed.

This report contains nine sections including: literature review (section 2), description of fundamentals of FTIR (section 3), quantification of polymer content in polymer-modified asphalt binders (section 4), study of the quality and uniformity of antistripping agents (section 5), quality and uniformity of epoxy materials (section 6), quality and uniformity of curing membrane (section 7), and cement quality and uniformity (section 8) followed by conclusions (section 9).

2. REVIEW OF LITERATURE

An extensive literature search on "practical" applications of FTIR on pavement materials resulted in a compilation of journal papers, technical reports, and standards that are summarized in the following sections. Each section describes salient features of the research work of other investigators on practical applications of FTIR in the given material.

2.1 Asphalt Binders

According to Y. Yildirim (2007), pavements with polymer modification exhibit greater resistance to rutting and thermal cracking, decreased fatigue damage, stripping, and temperature susceptibility. Generally desirable characteristics of polymer-modified binders include greater elastic recovery, a higher softening point, greater viscosity, greater cohesive strength and greater ductility. Typical polymers used in asphalt include the following: styrene-butadiene-styrene (SBS), styrene-butadine-rubber (SBR), natural rubber (NR), tyre rubber (TR), and Elvaloy^{TM}. J-F Masson et al. (2001) documented FTIR spectra for polystyrene (PS), polybutadiene (PB), and SBS.

Table 2.1 contains assigned FTIR absorption bands for these polymers. The absorption band for polybutadiene at wavenumber 966 cm^{-1} is completely independent of that of polystyrene at a wavenumber 699 cm^{-1}. The distinct FTIR spectra features of these two copolymers allows for the identification and quantification of these copolymers in asphalt. J-F Masson et al. (2001) further assigned absorption bands due to C-H out of plane (oop) bending in monoalkylated aromatics and C-H out of plane bending of *trans*-alkene for 699 cm^{-1} and 966 cm^{-1}, respectively. Table 2.1 shows absorptions between 650 cm^{-1} and 966 cm^{-1} in FTIR spectra of bitumen, PS, and PB. This research group further measured molar absorptivity of PB (at 966 cm^{-1}) and PS (at 699 cm^{-1}) based on Beer's law, a = A/bc (a=absorptivity, A= absorbance, b = cell path length, and c is the copolymer concentration), as 266 mol^{-1}cm^{-1}and 73 L mol^{-1}cm^{-1}, respectively. They have shown that PS and PB molar absorptivities were affected by copolymer structure and composition. For this reason, their calculated polymer content came within +/- 0.5 wt% of the expected value that translated into an average error of 10% of the actual polymer contents [J-F Masson et al. (2001)].

Table 2.1: Absorption between 650 and 966 cm^{-1} in FTIR Spectra of PS and PB.

Compound	Assigned band (cm-1)	Origin
PS	699 and 750	C – H oop* bending in monoalkylated aromatic
PB	993	C – H oop bending of cis-alkene
	966	C – H oop bending of *trans*-alkene
	911	C – H oop bending of terminal-alkene
	730-650	C – H wagging of *cis*-alkene

* oop = out of plane

American Association of State Highway and Transportation Officials (AASHTO) published a standard method test for "Polymer Content of Polymer-Modified Emulsified Asphalt Residue and Asphalt Binders," as AASHTO T-302-05, to formalize a method of quantifying polymer content in asphalt. The method consists of first preparing a sample. Asphalt binder is heated to less than 163°C and placed in a vacuum of 20 mm Hg. The sample is then diluted with 10 ml of solvent and applied in an infrared window. This method, presented by AASHTO T-302, was utilized by the Virginia Department of Transportation.

S. Diefenderfer (2006) presented a report for the evaluation of polymer detection methods for binder quality assurance. This report considered the practicality of FTIR for regular use for the detection and quantification of SBS and SB content in polymer-modified asphalt. The report concluded that FTIR is a suitable test for determining the polymer content of asphalt. It gave accurate results with no false positive identification and has shown acceptable repeatability of the results. However, one thing the report showed was that FTIR failed to determine different performance grades of the asphalt binders. FTIR analysis of the above-prepared sample shows peaks at 965cm^{-1}, attributed to SB and SBS, and 1375 cm^{-1}, attributed to asphalt, in agreement with the above literature. The ratio of the SB and SBS peak versus the asphalt peak is then used to determine the polymer content of the asphalt. By varying the initial concentration of polymer in asphalt, a calibration curve can be constructed from the peak ratios, as shown below in Figure 2.1. Such calibration curves can be used for a fast and accurate means of testing asphalts.
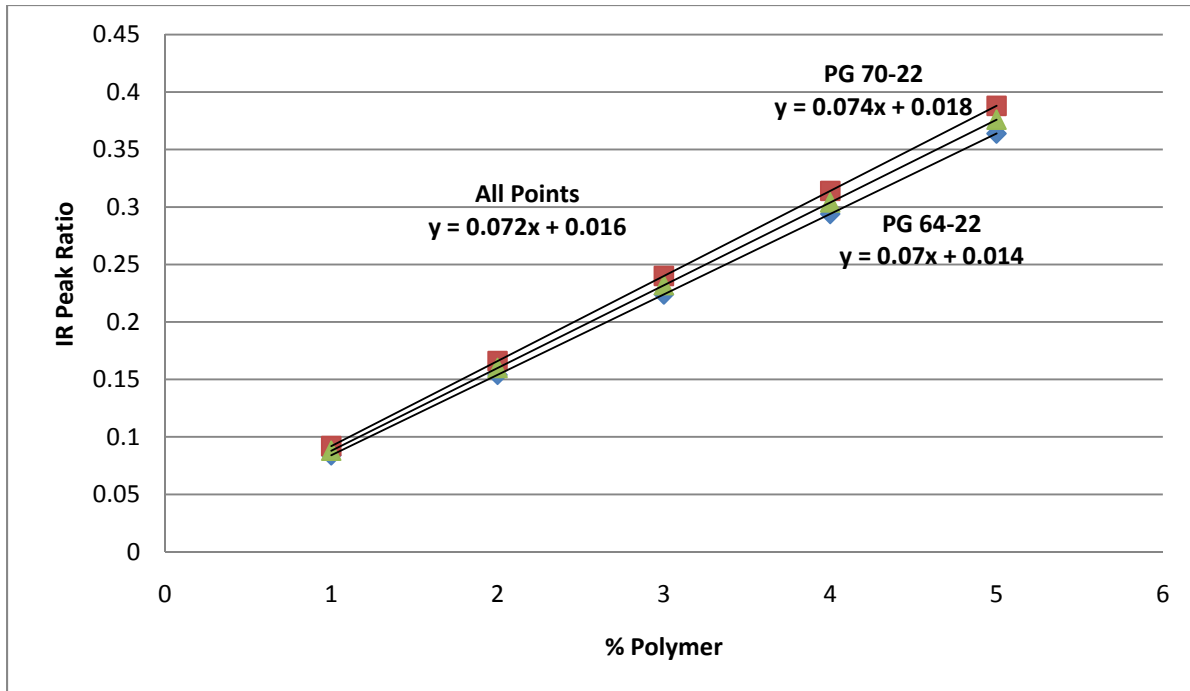
Figure 2.1: Calibration Curve for Polymer Content of Asphalt Based on Data Given by Diefenderfer (2006).

Natural rubber (NR) and styrene-butadiene-rubber (SBR), a polymer used in polymer-modified asphalt, were analyzed by M. Fernandez-Berridi et al. (2006). In their analysis, they incorporated the use of FTIR with the use of TGA in an effort to characterize and quantify amounts of natural rubber and SBR in mixtures of unknown composition. In this study, peaks of 750 cm^{-1} and 700 cm^{-1} were attributed to out-of-plane bending vibrations of aromatic = C-H and C = C, respectively, peaks of 990 cm^{-1} and 910 cm^{-1}, attributed to out-of-plane bending vibrations of = C-H of vinyl groups, 960 cm^{-1} was attributed to butadiene, and finally the peak at 815 cm^{-1} was attributed to vibrations of natural rubber. Special note is taken to the peaks located at 966 cm^{-1} (butadiene) and 700 cm^{-1} (styrene), since these are prominent peaks not located in the range of absorption of asphalt. FTIR has therefore shown a great ability to serve as a qualitative test to SBR and natural rubber. FTIR was further used to quantify amounts of natural rubber and SBR in the samples. Absorption band of 2960-2820 cm^{-1} attributed to CH$_2$ and CH$_3$ stretching vibrations were used as a means to normalize the sample. Peak ratios of the styrene and butadiene peaks verses the normalized peaks were taken and used as a means to quantify amounts of styrene and butadiene in samples.

G.N. Ghebremeskel et al. (2003) utilized FTIR absorption bands of 1602 cm^{-1}, 1639 cm^{-1} and 2237 cm^{-1} for quantification of styrene, butadiene, and acrylonitrile, respectively. In their investigation, they used the absorption intensity ratio of 1602/1639 to quantify SBR content in the SBR/NBR (acrylonitrile-butadiene rubber) blends and showed a correlation of R^2= 0.9986 for a plot of absorbance ratio vs. the % SBR. The NBR quantification was done using the absorption intensity ratio of peaks at 2237 cm^{-1} and 1639 cm^{-1}, and similarly the absorption ratio of 2237 cm^{-1} to 1639 cm^{-1} that correspond to acrylonitrile and butadiene. The correlation coefficient for a plot of 2237/1639 vs. %SBR was shown as R^2= 0.9997.

C.W. Curtis et al. (1995) applied FTIR to quantify polymer content in asphalt cement. Curtis's group evaluated two SBR latexes, ethylene vinyl acetate (EVA) and SBS polymers, in three different asphalts. They used TEX 533-C (1999) test procedure as the starting point in their analysis. They indicated, "Although the behavior of SBR latex in each asphalt yielded somewhat different calibration curves, each latex-modified asphalt cement was successfully quantified." Their calibration curves for SBR latex, EVA, and SBS materials in asphalt yielded R^2 values that ranged from 0.92 to 0.99.

J.C. Petersen et al. (1977, 1986) have successfully applied IR spectroscopy to analyze asphalt. E.A. Mercado et al. (2005) found FTIR technique very useful for studying factors affecting binder properties between production and construction in an effort to understand the mechanism of asphalt degradation and unacceptable performance. Their FTIR results based on spectral region of 1695 cm^{-1} to 1714 cm^{-1} showed a clear relationship to their Rolling Thin Film Oven (RTFO) results. They suggested that asphalt degradation could be due to an oxidation process that was consistent with FTIR absorption band observations related to carbonyl area (1650 cm^{-1} – 1820 cm^{-1}).

2.2 Application of FTIR in Aging Resistance Analysis of Asphalt Cements

Mechanical properties and chemical structures of asphalts change with time due to the aging phenomenon. Specifically oxidative aging (aging due to oxidation) of asphalt causes hardening of asphalts and leads to deterioration of asphalt pavements. Traditionally, physical and rheological properties of an asphalt sample are measured to assess aging resistance of the asphalt. Recently, FTIR technique has been successfully applied to investigate the aging resistance characteristics of polymer-modified asphalt (PMA) cements (C. Ouyang 2006, C.

Ouyang 2006). C. Ouyang et al. (2006) showed addition of about 1% of antioxidants (zinc dialkyldithiophospaht (ZDDP) zinc dibutyl dithiocarbamate (ZDBC)) modified asphalt to improve resistance of PMA to the formation of carbonyl. Both ZDDP and ZDBC containing PMA showed resistance to the formation of carbonyl to some extent, so ZDDP and ZDBC can be considered antioxidants that retard oxidation of PMA through the inhibition of peroxides and radical scavenging (C. Ouyang 2006). Studies of this type indicate the possibility of utilizing FTIR technique in developing new antioxidants that would enhance PMA performance. J. Lamontagne et al. (2001) artificially accelerated aging of bitumen samples and showed that one hour of cell oxidation (accelerated laboratory testing) is equivalent to two years of road service. Rolling Thin Film Oven Test (RTFOT) and Pressure Ageing Vessel (PAV) were two laboratory techniques used to artificially age asphalts, and their effects on asphalt were determined by FTIR. It was concluded that oxidation from the above tests can partly simulate actual asphalt aging. This was verified by using FTIR to track chemical changes due to aging. A thin layer of asphalt was placed on a potassium bromide pellet and placed in an oxygen-rich heating cell to simulate the aging process. A continuous FTIR spectrum was produced as the heating cell gradually increased the temperature of the asphalt sample.

2.3 Application of FTIR in Analysis of Antistripping Agents

Antistripping agents are chemicals used to facilitate strong bonding between aggregates and asphalt. Strength and durability of the mentioned bond determines performance of the asphalt cement. Presence or penetration of moisture to the aggregate-asphalt interface is believed to be the major cause of bond failures and the purpose of adding antistripping agents is to eliminate moisture or prevent its accumulation at the interface to allow formation of a cohesive bond. Addition of lime or Portland cement to the mix, lime slurry treatment of aggregates, bitumen pre-coating of the aggregates, inhibition of hydrophilic aggregates, washing or blending of aggregates, and addition of antistripping chemical agents are among methods employed to strengthen asphalt to aggregate adhesion and reduce stripping from intrusion of moisture (Curtis 1990) . C. Curtis (1990), in his review article, lists liquid antistripping agents, discusses lime and other mineral agents, and reviews test methods for measurement of stripping agents. As suggested by C. Curtis (1990), most of the commonly used liquid antistripping agents contain nitrogen in the form of amines, fatty amines, substituted amines, and polyamines. U.

Bagampadde and U. Isacsson (2006) did not find infrared spectroscopy suitable for the analysis of amines in the blends. T. Nguyen et al. (1996) developed an application method for measuring water-stripping resistance of asphalt/siliceous aggregate mixtures based on FTIR. They have quantified the thickness of the water layer at the interface, developed a technique to measure the adhesion loss of an asphalt/aggregate system exposed to water environment, and related the quantity of interfacial water thickness with adhesion loss data. Water absorption bands, one at 3000-3650 cm^{-1} and the other at 1625-1645 cm^{-1}, are clear indications of the presence of water. T. Nguyen et al. (1996) used these absorption bands to quantify water level at the interface by subtracting spectra collected before and after siliceous exposure to water for different exposure times. When Nguyen measured and plotted FTIR absorption band intensity at 3650 cm^{-1} of four antistripping agents as a function of time, they observed that lime and a low-grade aliphatic polyamine performed most effectively and least effectively respectively, as far as antistripping quality is concerned (T. Nguyen 1996). Recently, a procedure based on spectroscopy has been developed for the qualitative and quantitative analysis of amine-based antistripping additives in asphalt binders and mixes (C. Chen 2006).

Emulsion asphalts are currently being used for surface treatment, chip seal, and tack coat. Through project 0-1710 sponsored by TxDOT, a group of Texas Transportation Institute (TTI) researchers studied physical properties of surface treatment binders. They evaluated binders at multiple temperatures simulating corresponding performance in specific environmental conditions to develop a guide for emulsion selection for environmental conditions of the state of Texas. They indicated that application of cutback has been discontinued due to environmental concerns.

G.L. Anderson and L.H. Lewandowski (1994) compiled a database for commercially available additives to bitumen using FTIR analysis. They have shown that FTIR is the most suitable technique for the analysis of chemical additives in bitumen. The concentration range of additives they studied was from 0 to 10%. U. Bagampadde and U. Isacsson (2006) reported that the most commonly used liquid antistripping additives are amine-based and were not able to detect amines at a dosage of 0.5%, as the observed FTIR band did not show discernible differences from those of plain bitumens. M.A. Rodriguez –Valverde et al. (2008) studied N-alkyl propylendiamines, and alkylamidoamines that were derived from tallow in rapid and medium setting cationic bitumen emulsions for surface dressing at the concentration of 0.5%

w/w% and manufacturing of bituminous mixture at 0.1% w/w%. They did not use FTIR to characterize emulsion samples, but they have developed an imaging technique for this purpose.

M. Siddiqui et al. (2003) have taken advantage of hydrogen bonds in asphaltenes in an effort to characterize asphalt. The OH peak intensity of phenol, the enthalpies of hydrogen bond formation, and the content of heteroatoms in asphaltenes were analyzed to explain the hydrogen bonding and structure of asphalt. They mixed asphalt samples with a one to one ratio of asphaltenes to phenol solution and analyzed with FTIR within the region of 4000-3000 cm^{-1}. The suggested absorption band of 3610 cm^{-1} was attributed to free OH stretching vibrations and 3294 cm^{-1} was attributed to as NH group.

F. Lima et al. (2004) have used Near Infrared Spectroscopy (NIR) for determination of properties used in characterizing and classifying asphalt cement grade. Some of the properties analyzed were penetration value, absolute viscosity at 60°C, kinematics viscosity at 135°C, and flash point of asphalt cement.

2.4 Application of FTIR in the Analysis of Hot-Mix Asphalt (HMA)

T. Arnold et al. (2006) used FTIR for quantitative determination of lime in hot-mix asphalt. Their results show that hydrated lime exhibited a sharp peak at a wavenumber of 3640 cm^{-1} due to the presence of the hydroxyl group in $Ca(OH)_2$. They suggested that this sharp peak could be used to demonstrate the presence and quantification of the amount of lime. They assigned a peak at about 1390 cm^{-1} to C-O stretching that they related to a calcium carbonate impurity. The presence of calcium carbonate could be explained by reaction 1.

$$Ca(OH)_2 + CO_2 \rightarrow CaCO_3 + H_2O \quad (1)$$
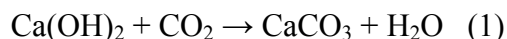
They clearly showed that the FTIR spectrum of calcium carbonate does not show one peak at 3640 cm^{-1}, but rather shows two peaks: one at 1390cm^{-1} and the other at 866 cm^{-1}. Their analysis, based on the linearity of the relationship between the 3640 cm^{-1} peak area and the lime concentration, showed a correlation factor of $R^2 = 0.968$ and, based on peak height yielded an R^2 of 0.977. They did a similar analysis for calcium carbonate based on 1390 cm^{-1} and 866 cm^{-1} peaks, and obtained an R^2 of roughly 0.97, irrespective of the peak used, peak area, or height.

The T. Arnold et al. (2006) group further suggested that visual examination of the FTIR spectrum provides an instant indication of lime quality. To demonstrate this, they used the existence of the peak at 1390 cm^{-1} to indicate the presence of calcium carbonate impurity.

2.5 Application of FTIR in the Analysis of Epoxy

W. Brittan (1991) studied prehardened epoxies with varying ratios of hardener and resins by Attenuated Total Reflectance Fourier Transform Infrared Spectroscopy (ATR- FTIR). A method of partial least squares was used with the results of FTIR to determine unknown mixing ratios. Seven samples of epoxies were used with an average of 0.1 part of hardener out of 11 parts. The results of these tests concluded that FTIR is simpler than more traditional methods and that it has provided superior results also. Thus, FTIR has been shown to have the ability to quantify resin and hardener ratios in cured epoxies. While tests like the above have been done in characterizing properties of cured epoxies, N. Poisson et al. (1996) has used FTIR to study epoxy curing and epoxy reactive systems. A diglycidyl ether of bisphenol A was used as a prepolymer with dicyandiamide as a hardener. A conventional FTIR range of 400-4000 cm^{-1}, was used in the analysis using KBr pellets and also used was near infrared in the 4000-7000 cm^{-1} range using a glass window for the samples. The resulting scans of the epoxy samples produced complicated spectra. About 20 peaks were analyzed and its functional group was determined. Epoxy conversion rate was determined by analyzing the epoxy group band at 915 cm^{-1} and the phenyl group band at 830 cm^{-1}.

Uncured analysis of epoxy resin using FTIR was studied by Y. Li et al. (2006). The epoxy resin studied was a common thiirane/epoxy resin of bisphenol A. The original experiment consisted of creating a novel separation method of pure epoxy resin from thiirane/epoxy resin. To validate this separation method, it was important to develop a complementary method to quantify the amount of bisphenol A epoxy in a given sample.

Besides using FTIR in qualitative and quantitative analysis of epoxy resins, cures, and curing processes, FTIR has been further utilized in studying the physical and mechanical properties of epoxies. T. Scherzer (2003) presented a paper on the 'First Application of Rheooptical FTIR Spectroscopy to Monitor Complex Orientation Phenomena in Highly Cross-Linked Epoxy Networks During Uniaxial Deformation and Relaxation.' There are many types of polymers (linear, branched, cross-linked, and network), and each type of polymer contributes a unique spectral signature to that polymer. The amount of cross-linking has been directly attributed to the interconnection of polymers and thus the overall strength of the sample. This theory was put to test by T. Scherzer (2003). By using Rheooptical FTIR, he attributed the highly

cross-linked epoxy network to higher stress strength of Bisphenol A/ Epichlorohydrin epoxies. He also concluded in his studies that the orientation of epoxy networks is completely reversible in their rubbery state and that no fatigue was evident from gradual chain ruptures of polymers in epoxy samples.

S. Lin et al. (1978) studied thermal and oxidative degradation of cured epoxy systems as a means of characterizing aging. FTIR was used in the analysis of degradation of epoxy systems. Three different kinds of epoxy systems were studied: diglyadyl ethers of bisphenol A (DGEBA), phnophtalalein (DGEPP), and 9, 9-bis (40hydroxyphenyl) fluorine (DGEBF). The three samples from above were cured and exposed to various thermal, oxidative, and photo degradation. The epoxy resin mixed with 9.5 g of trimethoxyboroxine was dissolved in acetone, which had been dehydrated by K_2CO_3 and distilled at 56°C. Photodegradation was accomplished by exposing samples with mercury-xenon arc 1000-W power ultraviolet light. Thermal degradation was simulated with elevated temperatures up to 300°C. The FTIR results of oxidative, thermal, and photo degradation was found to be related to the autocatalytic oxidation of aliphatic hydrocarbon segments. Comparing results with natural degradation of samples allowed suggestions to be made of actual degradation mechanism of epoxy systems.

FTIR has been successfully applied as a research tool to study different aspects of epoxy behavior, including epoxy curing (Y. Zhang et al. 2007, J. Canavate et al. 2000, T. Scherzer 1995, I.E. dell'Erba 2007, M. Sanchez-Soto et al. 2007), epoxy thermal oxidative degradation (P. Musto 2003), nano-particles in epoxy (J. Vega-Baudrit et al. 2007, Jia et al. 2007), hydrogen bond formation in epoxy adhesives on hydrated cement (F. Djouani et al. DOI 10.1002/sia.2783 www.interscience.com), and epoxy coating for corrosion protection of steel in concrete environment (K. Saravanan et al. 2007).

2.6 Application of FTIR in the Analysis of Concrete, Fly Ash, and Slag

FTIR Spectroscopy was used by T. Hughes et al. (1995) in determining cement composition. This study is part of a large endeavor of FTIR methods in cement chemistry, direct analysis of performance properties of cement, and in-situ monitoring of hydration reactions. Hughes applied diffuse reflectance mid-infrared Fourier transform spectroscopy (DRIFTS) in his study. This study was conducted due to the inconsistent composition and hydration properties of cements and the need for quality control. Cement samples from different sources with different

compositions were analyzed. KBr pellets containing various amounts of cement were made and the DRIFT technique was found to produce a clear and distinct spectrum for each cement sample with a high degree of reproducibility. Calibration curves produced by the 156 cements of known content lead to very reliable quantitative information on the chemical content of unknown samples. Table 2.2 show FTIR characteristic absorbance bands for cement minerals.

In the continuation of the above study, P. Fletcheret et al. (1995) applied FTIR in predicting the quality and performance of oil-field cements. They defined inherent batch-to-batch variability, aging, contamination, and variable slurry as factors affecting performance of cements.

Diffuse reflectance FTIR can be used to determine the particle size, composition, and crystallinity, as well as impurities in cement. Physiochemical properties are determined by constructing a large database of various kinds of cement along with information such as weight percent of cement minerals, weight percent of cement oxide composition, binned particle size composition, weight loss on ignition, free lime content, insoluble residue, and thickening time for neat cement slurry. Complex models are then used to determine quality and performance.

Table 2.2: Characteristic Absorbance Bands for Cement Minerals (T. Hughes et al. 1995).

Material	Fundamentals			Overtones	O-H Stretch	O-H Bend
Sulfates	v_1	v_3	v_4			
Gypsum	1005	1117	669, 604	2500-1900	3553, 3399	1686, 1618
Bassanite	1009 1117 1098	1152 600	660,629	2500-1900	3611, 3557	1618
Syngenite	1001	1192 1130 1113	658,644 604	2500-1900	3309	1678
Anhydrite	1015	1163	677, 615 600	2500-1900		
Carbonate Hydroxides	v_2	v_3	v_4			
Calcium Carbonate	876,849	1458	714	2980-2500, 1794		
Calcium Hydroxide					3646	
Magnesium Hydroxide					3696	

Clinker phases		Unassigned Fundamentals		
C_3S	Si-O	935, 521	2 000-1600	
C_2S	Si-O	991,879	2060-1600	
C_3A	Al-O	889, 860, 812, 785 762, 621, 586, 578, 506		
C_4AF	Fe-O	700-500		

M.J. Varas et al. (2005) applied FTIR to differentiate between natural and artificial (Portland) cements. In their research, they showed four wide regions where the main transmission bands of Si-Al, S, Ca, and OH were concentrated. They assigned different FTIR spectra regions to the bonds present in the cement constituents. Detailed descriptions of each FTIR region and corresponding bonds are given in their paper. A noticeable difference in their FTIR spectra compared to previous ones is the fact that they plotted FTIR transmittance bands rather than absorption bands.

Recently A.A.P. Mansur et al. (2007) evaluated the degree of polymerization of silicate units in cement-based materials using FTIR. Their results indicate the spectrum of anhydrous cement with an Si-O band at 927 cm^{-1} and an Si-O band at 525cm^{-1}. They showed bands associated with gypsum and anhydrite in the range of 1165 cm^{-1} to 1096 cm^{-1}. They further showed carbonate bands at 2516 cm^{-1}, 1793 cm^{-1}, 1497 cm^{-1}, 1420 cm^{-1}, 875 cm^{-1}, and 713 cm^{-1}. Substitution of byproducts of smelting of ore (slag), coal combustion power plant (fly ash), and silicon smelting (silica fume) into Portland cement has gained popularity due to the pozzolanic properties of these byproducts. Fly ash, silica fume, and slag offer an inexpensive bulk material that is used to substitute for cement materials. A few typical pieces of research on application of FTIR in the analysis of byproduct-substituted cement are referenced in B. Yilmaz et al. 2008, F. Puertas et al. 2000, R.K. Vempati et al. 1994, N.J. Saikia et al. 2002, A. Fernandez et al. 2003, F. Puertas et al. 2003, and T. Bakharev 2005.

B. Yilmaz and A. Olgun (2008) used FTIR in studying the effects of fly ash on the properties of cement and mortar. Ordinary Portland cement and composite cement were used as samples and hydrated up to 28 days. FTIR results showed a strong Si-O stretching band at 961cm^{-1} and a weak band at 457 cm^{-1}. C-O bending at 872 cm^{-1} and stretching at 1417 cm^{-1} are also shown. A peak at 3637-3641 cm^{-1} is attributed to the OH band from calcium hydroxide; the intensity of this peak is found to correspond to the fly ash concentration.

F. Puertas et al. (2000) further studied fly ash and slag using FTIR. Fly ash/slag ratios of 100/0, 70/30, 50/50, 30/70, and 0/100 with curing temperatures of 25 ºC and 65 ºC were used with an activator of NaOH with concentrations of 2M and 10M. FTIR analysis showed a stretching vibration of SiO$_4$ tetrahedra for slag at 956 cm^{-1} and from fly ash at 1075 cm^{-1}. It was concluded that different reaction products had formed from comparing infrared spectra of the pastes with a 2M and 10M NaOH solution.

2.7 Summary

In this literature search, attention was focused on papers that discuss "practical" applications of FTIR Spectroscopy and specifically applications related to the interest of Texas Department of Transportation. Papers related to major issues of paving materials, including polymer modified asphalt, aging resistance of asphalt cements, stripping agents characteristics,

hot mix asphalt analysis, analysis of epoxy systems, and slag/fly ash substituted for concrete were also researched.

3. PRINCIPLES OF FOURIER TRANSFORM INFRARED SPECTROSCOPY

3.1 Introduction

Fourier Transform Infrared Spectroscopy (FTIR) is one of the two vibrational spectroscopy (Infrared and Raman) techniques that are widely used in industry. FTIR provides qualitative (through fingerprinting), semi-quantitative, and quantitative information on chemical structures and physical characteristics. Solid, liquid, or gas samples can be analyzed in bulk or thin film forms. Accessories are available to investigate materials properties at different temperatures. Typical examples of paving materials characterization include identification and quantification of polymers in polymer-modified asphalt, aging and oxidation of asphalt binders, characterization of concrete curing membranes, identification of concrete constituent phases, analysis of alkali content in concrete, analysis of pozzollons in concrete, to name a few. Texas Department of Transportation spends a sizable budget on purchasing large quantities of paving materials and systematic quality control/quality assurance is an absolute necessity in ensuring construction of durable pavements. FTIR is a rapid, non-destructive, inexpensive, and reliable technique that is applicable both in the laboratory and the field.

3.2 Working Principle

FTIR involves the twisting, rotating, bending, and vibration of the chemical bonding (Figure 3.1). Let incident infrared radiation intensity be I_o and I be the intensity of the beam after it interacts with the sample. The ratio of intensities I/I_o as a function of frequency of light gives a spectrum, which can be in three formats: as transmittance, reflectance, and absorbance. The multiplicity of vibrations occurring simultaneously produces a highly complex absorption spectrum, which is a unique characteristic of the functional groups comprising the molecule and also the configuration of the atoms. A detector is used to read out the intensity of light after it interacts with the sample. The typical setup of an FTIR is shown in the Figure 3.2. The author has successfully applied this technique for the identification and characterization of iron oxides (S. Nasrazadani and H. Namduri, 2006, S. Nasrazadani 1997, S. Nasrazadani and A. Raman 1993, J. Stevens et al. 2006). Specifically, magnetite and maghemite that are not differentiable with popular x-ray diffraction technique were successfully identified by FTIR (S. Nasrazadani

and A. Raman 1993). Advantages of applying this technique for quantification of organic and inorganic materials include:

- Minimal sample preparation
- Fast, reliable, and robust analysis
- No need for messy chemicals
- No spectra interferences
- Fully computerized analysis
- Ease of operation and minimal operator training and expertise
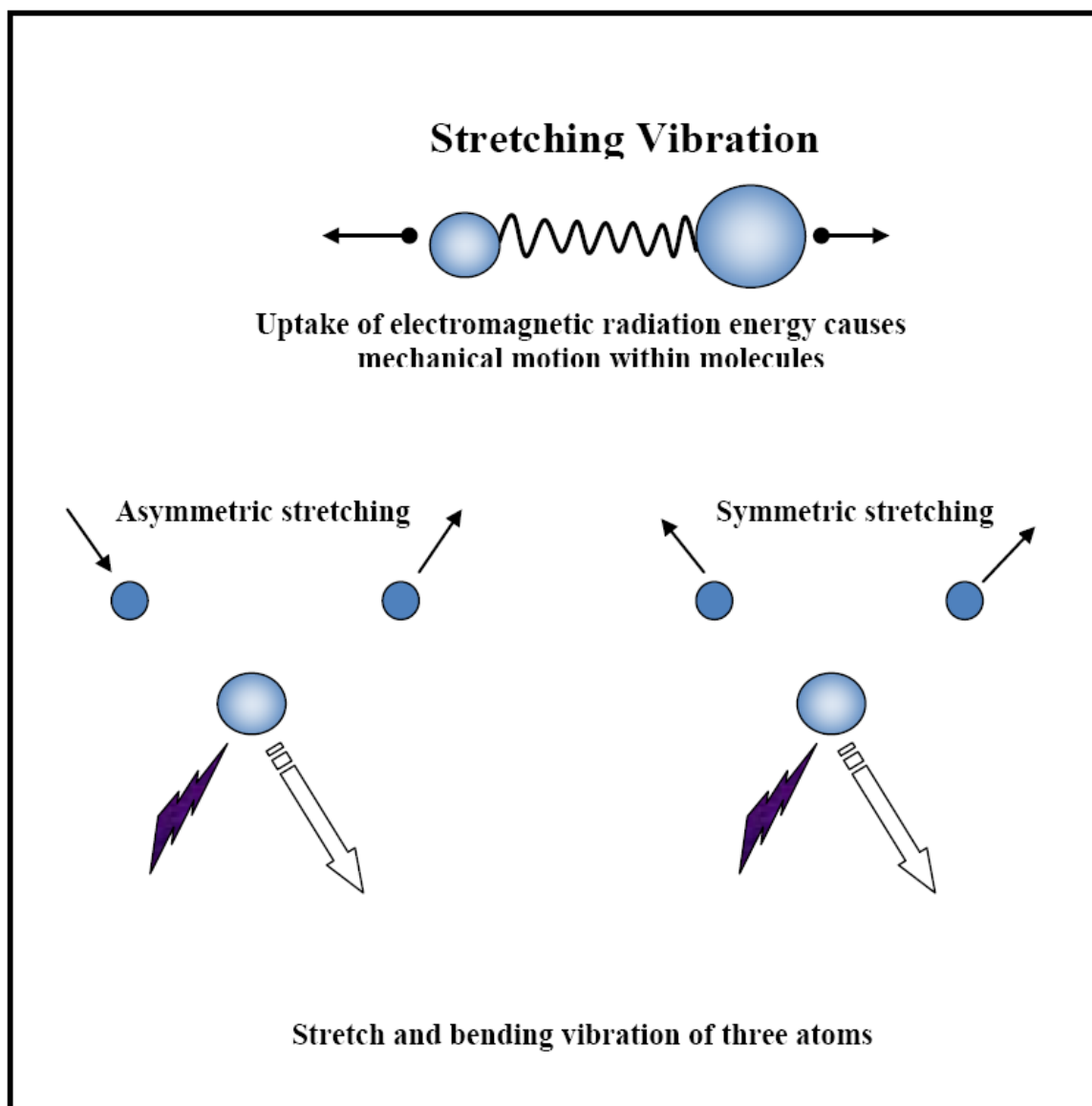
Figure 3.1: Stretching and Bending Vibrations of Atoms due to Absorption of IR Radiation.
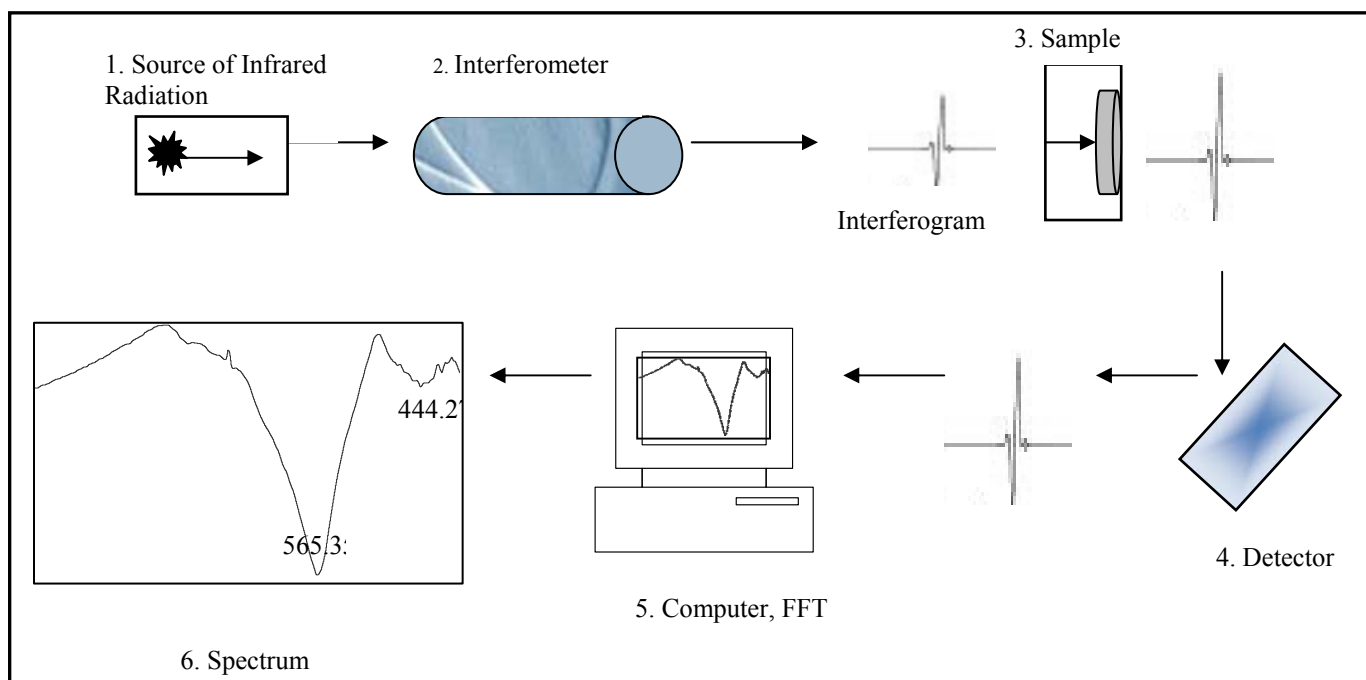
Figure 3.2: Experimental Set-up for Fourier Transform Infrared Spectroscopy.

Probing beam in FTIR spectroscopy is a radiation in the Infrared range. Figure 3.3 shows electromagnetic spectrum and position of mid-IR spectral range in relation to the rest of electromagnetic radiation. Mid-IR range includes wavelength of 2.5 to 25 μm that corresponds to a wavenumber (inverse of wavelength) range of 4000-400 cm^{-1} range, respectively. Because time and frequency are inversely proportional, a mathematical Fourier transform allows conversion of intensity versus time spectrum into intensity versus frequency spectrum that is typically used in FTIR analysis.
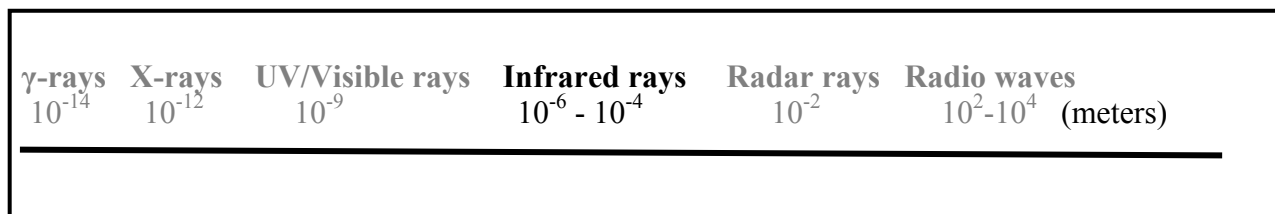
Figure 3.3: Electromagnetic Spectrum.

3.3 Origin of FTIR Spectrum

Atomic bonding in a given molecule can be modeled as a set of masses and a spring with masses representing atoms and the spring that models the bond. Absorption of unique pockets of energy (**E**) from the incident IR radiation source by the molecules produces a spectrum showing an interferogram that contains the spectrum of the source minus the spectrum of the sample. According to Einstein's equation (given below), the absorbed energy is related to the frequency of the vibration and each range of frequencies is related to a molecular mechanical motion generated by such an increase in molecular energy.

$$E = h\,\upsilon = h\,c/\lambda = h\,c\,\tilde{\upsilon}$$

In the above equation, **c** is the speed of light in vacuum, **h** is Planck's constant, and $\tilde{\upsilon}$ is the wavenumber (cm^{-1}) that is inversely proportional to the wavelength.

When energy is absorbed by a given molecule, a range of mechanical motions is possible that includes symmetrical and anti-symmetrical stretching, scissoring, rocking, wagging, and twisting. Photons with discrete energy levels are required for each mode of mechanical motion, and this fact enables identification and assignment of absorption bands in the FTIR spectrum.

3.4 Practical Interpretation of FTIR Spectra

The beauty of FTIR technique from a practical point of view is the fast and easy interpretation of its spectra for known materials. Practitioners oftentimes are interested in identifying a commonly used material and quick analysis of its quality. There are rigorous mathematical methods for interpretation of FTIR spectra, but general assignment of FTIR absorption bands are given by John M. Chalomers and Geoffery Dent (1997). Organic materials, such as paint systems, epoxies, and polymers exhibit bands in the higher wavenumber range, while inorganic materials such as concrete, cement, and generally oxide containing materials, exhibit major bands in the wavenumber ranges below 1000 cm^{-1}.

4. APPLICATION OF FTIR IN QUANTIFICATION OF POLYMER CONTENT IN POLYMER-MODIFIED ASPHALT

Polymer Modified Asphalt (PMA) has been successfully applied in high-stress locations such as busy intersections and airports (G. King 1999). Asphalt binders are modified with polymers to enhance binders rutting resistance, fatigue resistance, and stripping resistance (C.W. Curtis 1995). In unmodified condition, asphalt binders crack at low temperatures and soften at high temperatures. Polymers are added to asphalt binders to provide elasticity and durability with greater temperature stability. Commonly used polymer asphalt modifiers include styrene-butadiene-styrene (SBS), styrene-butadiene-rubber (SBR), and ethyl-vinyl-acetate (EVA). SBS is an elastomeric tri-block copolymer that improves elasticity of asphalt to prevent permanent deformation and cohesive failures. Elastomers stretch under load and regain their original shape upon removal of load. SBR is a random copolymer used as dispersion in water (latex) improving low temperature ductility, increase in viscosity, increase in elastic recovery, and enhancement in adhesive and cohesive properties of asphalt (Y. Yildirim, 2007). EVA is a plastomeric copolymer with chemical formula $[C_2H_4]_n[C_4H_6O_2]_m$.
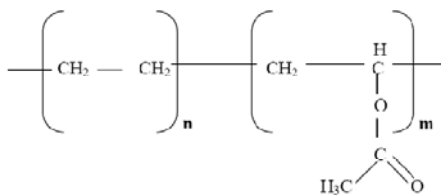
Plastomeric copolymers are added to asphalt to improve thermal cracking resistance at low temperatures.

FTIR analysis can differentiate between SBS/SBR and ethylene vinyl acetate (EVA) containing asphalts. FTIR spectra of SBS and SBR containing asphalts are similar since both contain the same monomer (see molecular structure of SBS below) and their spectra show a band at 966 cm^{-1} attributed to =C-H bend in trans-1,4-butadiene (C.W. Curtis 1995). However, FTIR spectrum of EVA shows two bands at 1242 cm^{-1} (attributed to C-O-C) and 1736 cm^{-1} (attributed to C=O in acetate) (C.W. Curtis 1995). Structure composition of PB in SBS is shown below as 1,4 *cis*, 1,4 *trans*, and 1,2 *vinil* from left to right respectively (L. B. Canto et al.).

$$CH_2 \quad CH_2 \qquad CH_2 \quad H \qquad H \quad H$$
$$\diagdown \diagup \qquad \diagdown \diagup \qquad | \quad |$$
$$C = C \qquad C = C \qquad C - C$$
$$\diagup \diagdown \qquad \diagup \diagdown \qquad | \quad \|$$
$$H \qquad H \qquad H \qquad CH_2 \qquad H \quad CH_2$$
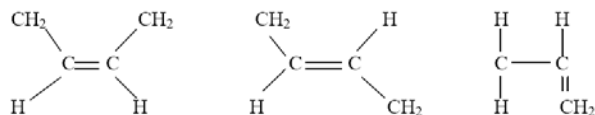
Two groups of samples with known polymer concentrations from two asphalt manufacturers were acquired and their corresponding FTIR calibration curves were generated based on AASHTO T-302-05 Attenuated Total Reflectance (ATR) method as well as standard transmission FTIR method. The calibration curves were then used to quantify the polymer contents of a number of samples with unknown amounts of polymers. Unknown samples were received from TxDOT's asphalt laboratory at Cedar Park. Following sections provide details of calibration procedures, results obtained, and conclusions drawn from the measured FTIR spectra.

4.1 Calibration Curve Generation for Polymer-Modified Asphalt by FTIR

4.1.1 ATR Method

AASHTO T-302-05 standard method was used for the ATR method. Polymer-modified asphalt sample was heated in an oven at a maximum temperature of 100°C until the asphalt assumed a workable viscosity. Approximately 10 g of the asphalt was placed on wax paper that was cut to a size slightly larger than the face of an ATR crystal. Enough material was used to result in a layer that covered the face of the crystal. Asphalt thickness on the paper was about 1 mm. ATR accessories was installed according to the manufacturer guidelines. Material was allowed to cool for several minutes prior to affixing the asphalt surface in direct contact with the top face of the prepared ATR crystal. Air bubbles were removed to ensure that material is in direct contact with ATR crystal.

4.1.2 Transmission FTIR Method

Polymer-modified asphalt sample was heated in an oven at a maximum temperature of 100°C until the asphalt assumed a workable viscosity. For standard FTIR analysis, approximately 10 g of the asphalt was placed on wax paper. About 100 mg of potassium bromide (KBr) was pressed in a 13 mm die of about 10,000 psi for two minutes to achieve a solid KBr pellet. This pellet was then placed on top of the asphalt that was previously prepared on wax paper to achieve a thin transparent coat of asphalt on the pellet.

Six samples of pre-made polymer-modified asphalts with varying percentages of polymer from 0 to 5% were provided by supplier A. Each FTIR analysis was done on a Thermo Nicolet Avatar 370 DTGS from 4000 cm^{-1} to 400 cm^{-1} using 32 scans with a resolution of 2 cm^{-1}. Eight separate samples and tests were done for the asphalt to determine quality and repeatability of measurements.

4.2 Results

Figure 4.1 shows the overlay of Transmittance spectra of 0, 1, 2, 3, 4, and 5% polymer modified asphalt in the range of 1400 cm^{-1} to 675 cm^{-1}. Quantification of polymer content is done in accordance with AASHTO T-302. An infrared spectrum is generated and considered in the range of 1500 cm^{-1} to 675 cm^{-1}, as shown in Figure 4.1. A baseline adjustment is then made between 1400 cm^{-1} and 925 cm^{-1} and the heights of the peaks of 1375 cm^{-1} and 966 cm^{-1} are measured from the baseline. Each spectrum in Figure 4.2 shows two distinct absorbance bands: one at 966 cm^{-1} that represents the polymer modifiers (SBR, SB, or SBS), and the other at 1375 cm^{-1} that is attributed to the base asphalt binder. Relative intensities of these two absorbance bands are utilized in quantification of the polymer contents. Accurate and precise measurement of relative intensities requires correctly drawn baseline. Measurement of ratios of these two absorbance bands for different samples containing various polymer content were based on the heights of the two measured peaks and are averaged for each polymer sample, and are shown in Table 4.1.
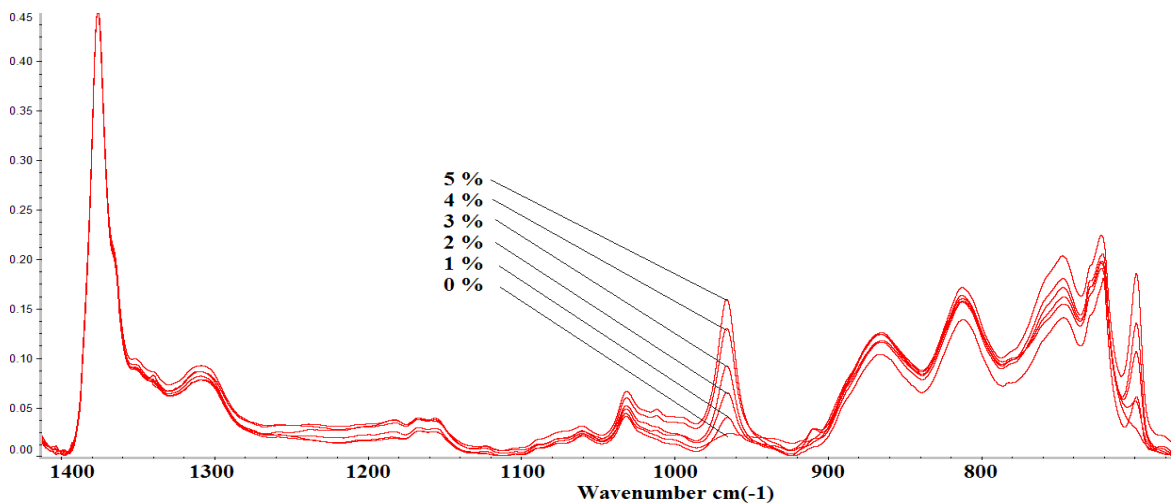
Figure 4.1: FTIR Spectra of Asphalt Samples Containing Various Amounts of Polymer Received from Asphalt Supplier A.
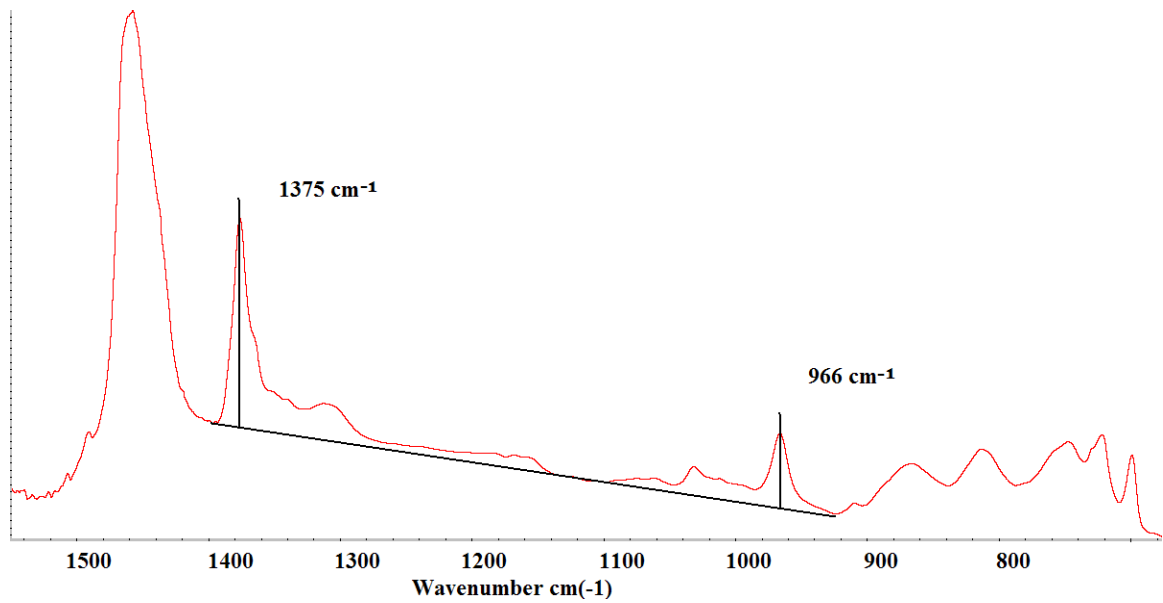
Figure 4.2: FTIR Spectrum of a Typical Polymer-Modified Asphalt Sample with Baseline Drawn for Absorbance Measurement.

Table 4.1: Relative Absorbance Ratios of the Polymer-Modified Asphalt Samples with Known Amounts of Polymer in Asphalt Samples Received from Supplier A.

Percent Polymer Content	966 cm^{-1}	1375 cm^{-1}	Absorbance band Ratio	Standard Deviation
0 %	0.013225	0.425625	0.031368	0.00203
1 %	0.033775	0.3955	0.085734	0.005949
2 %	0.040725	0.288875	0.14066	0.004879
3 %	0.078725	0.388	0.202761	0.006916
4 %	0.0922	0.369875	0.27819	0.017633
5 %	0.1265	0.3615	0.349976	0.009291

All resulting absorbance ratios are plotted in Figure 4.3 along with an extrapolated linear trendline showing an R^2 value of 0.99 and an equation of y=0.0638*X+0.022.
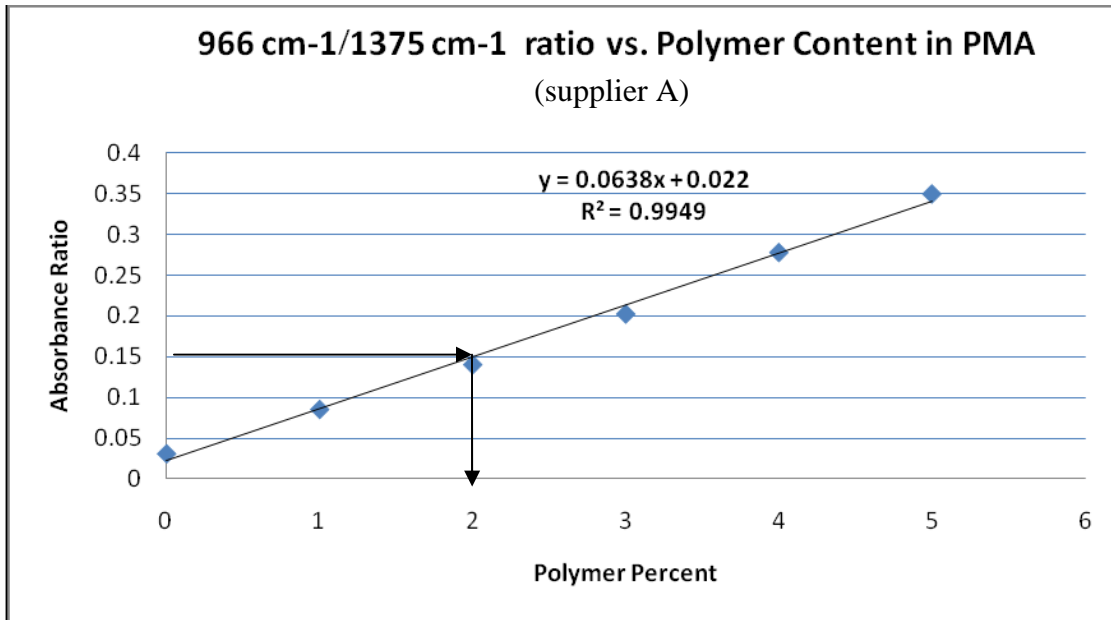
Figure 4.3: Calibration Curve for Samples with Known Concentrations of Polymers from Supplier A.

The calibration curve presented in Figure 4.3 can be used to calculate polymer content of an unknown asphalt binder. For example, if the absorbance bands ratio (for 966 cm^{-1} to 1375 cm^{-1} bands) for an unknown sample is measured to be 0.15, then one can calculate the polymer content of the sample by substituting y=0.15 in the equation y=0.06838x+0.022 and getting x=(0.15-0.022)/0.06838 that would represent polymer content of 2%. Obviously a graphical method shown in Figure 4.3 would produce similar results.

4.2.1 Calibration Curve Generation for Polymer-Modified Asphalt by FTIR (Supplier B)

Three samples of asphalt with polymer contents of 2.4%, 3.0%, and 3.9% were received from supplier B and similar procedures as the one for supplier A was followed. Figure 4.4 shows FTIR spectra of the three samples. As indicated by the concentration, as the polymer concentration in the asphalt increased, the intensity of the 966 cm^{-1} absorption band increased. Figure 4.5 show an example of the baseline measurement of relative intensities of 966 cm^{-1} to 1375 cm^{-1} absorption bands. Calibration curve based on these three known samples were generated (Figure 4.6) in order to quantitatively analyze samples received from supplier B. Table 4.2 shows measured relative intensities for absorption bands of the three samples. It must be noted that ATR method produced a poor absorbance ratio relationship to polymer

concentration for supplier B samples, but when the same samples were tested using the transmittance method discussed in the next section a much stronger relationship was obtained as indicated in Figure 4.6.
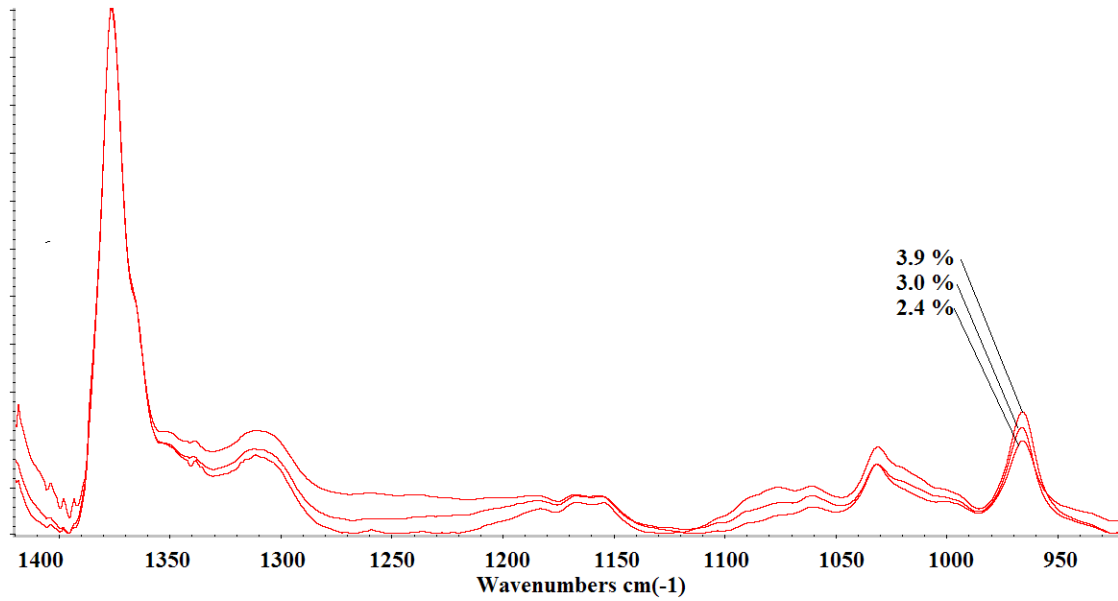
Figure 4.4: FTIR Spectra of Three Asphalt Samples Provided by Supplier B.
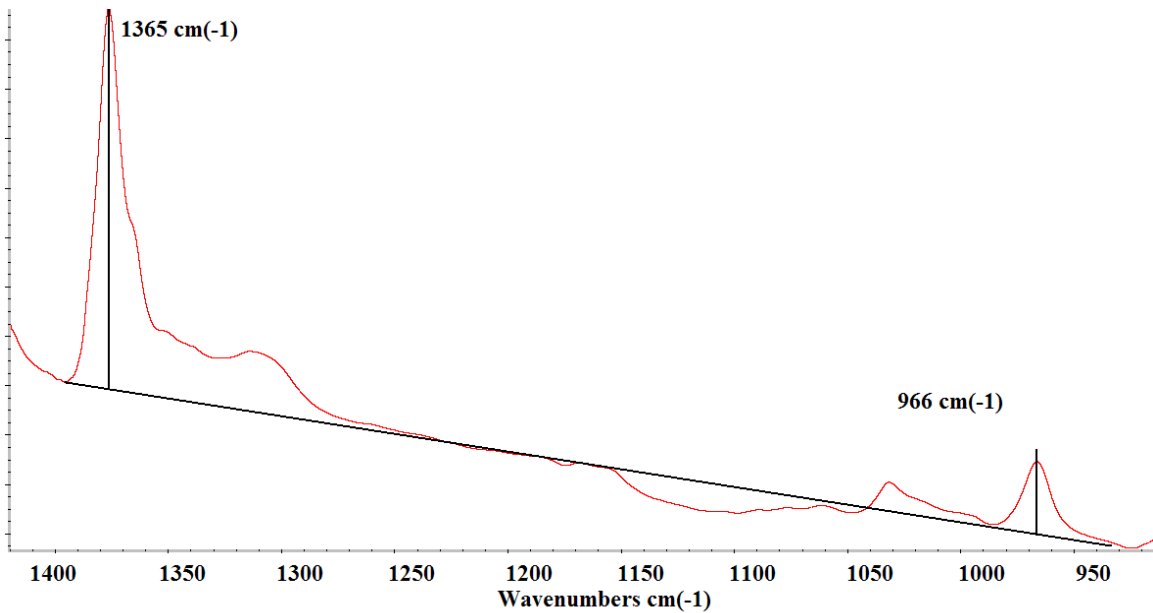
Figure 4.5: Background Line Selected for the Measurement of the Relative Intensities.

Table 4.2: Relative Intensities Measured for 966 cm^{-1} and 1375 cm^{-1} Absorption Bands of Three Samples Provided by Supplier B.

Percent Polymer	966 cm^{-1}	1375 cm^{-1}	Peak Ratio	Standard Deviation
2.4 %	0.046133	0.2595	0.177478	0.0058
3.0 %	0.090167	0.432667	0.208281	0.006593
3.9 %	0.068422	0.283833	0.240786	0.007182
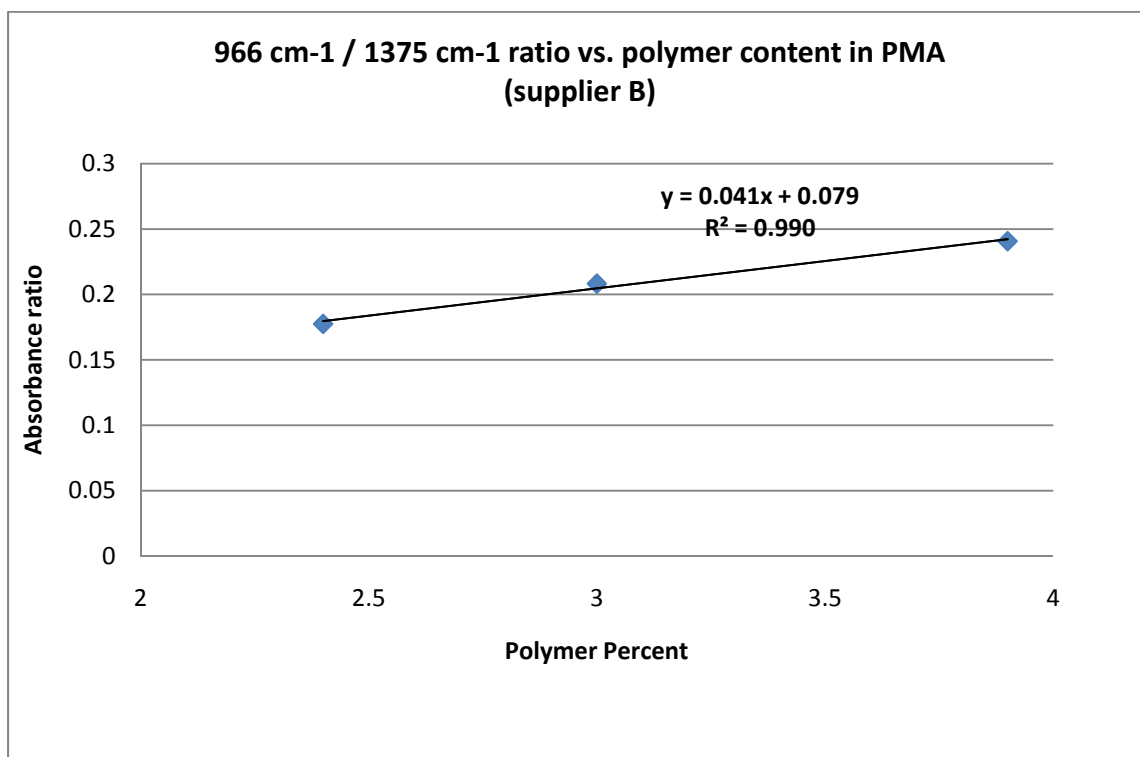
Figure 4.6: Calibration Curve for Samples with Known Concentrations of Polymers from Supplier B.

Figure 4.7 presents a comparison of the data generated for both supplier A and supplier B materials. Comparison of both products show about the same polymer content in their respective asphalt samples with corresponding polymer concentrations. Obvious differences could be due to the fact that only three samples with nearly close polymer concentrations (2.4%, 3.0%, and 3.9%) were received and the linear line is drawn based on the linear fit curve using only these three samples. Another possible source of deviation could be testing techniques (ATR for supplier A samples vs Transmittance method for supplier B samples). Other than this deviation, a convincing linear relationship between polymer concentration and relative absorbance intensity ratio was observed in all cases for both ATR and Transmittance FTIR methods.
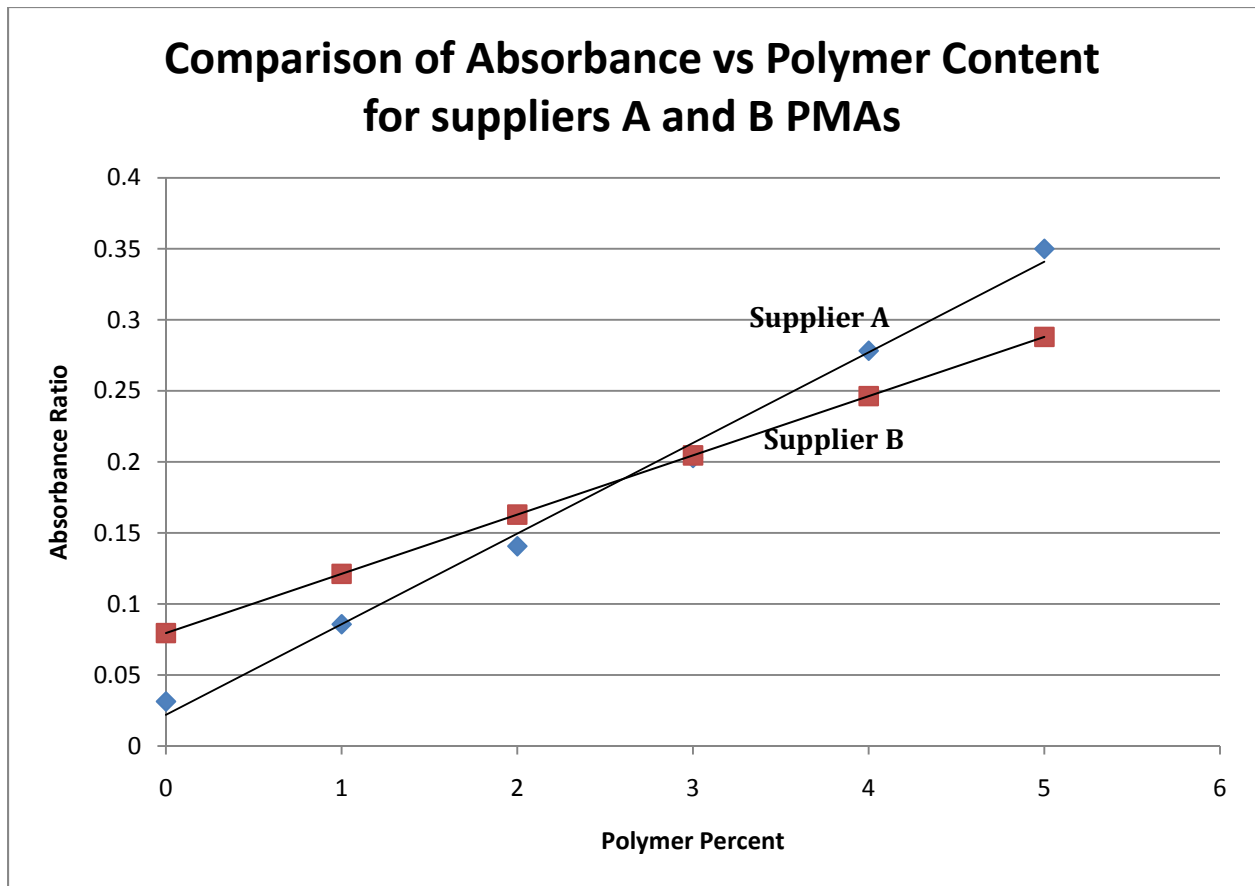
Figure 4.7: Comparison of Calibration Curves for Both Suppliers A and B Samples.

A number of asphalt samples received fron Cedar Park laboratory of TxDOT were tested for their polymer contents, and Table 4.3 shows measured polymer content based on the generated calibration curves shown in Figure 4.7. Actual polymer content of these samples were not known, so no comparison of the results could be made. FTIR spectra of polymer-modified samples tested are shown in Appendix A. A complete protocol for application of FTIR in polymer qualtification in asphalt samples is given in Appendix B.

Table 4.3: Measured Polymer Contents Using FTIR Based on Calibration Curves Generated for Supplier A and Supplier B Samples.

TxDOT sample ID	Supplier A	Supplier B
3	0 %	0 %
4	0 %	0 %
5	0 %	0 %
0142	1.8 %	1.4 %
0143	2.9 %	3.0 %
0144	3.1 %	3.4 %
0145	3.2 %	3.5 %
0156	3.0 %	3.2 %
0157	1.9 %	1.6 %
0158	3.3 %	3.8 %
0159	3.4 %	3.8 %
07B	2.0 %	1.6 %
164	0 %	0 %

4.2.2 Comparison of ATR and Transmission FTIR in Quantifying Polymer Content in Asphalt

Six independent tests of a given sample were conducted on asphalt samples using ATR and transmission methods of FTIR. The results from transmission and ATR methods in quantifying polymer content in asphalt were compared. Tables 4.4 and 4.5 present results from ATR and Transmission methods, respectively. The peak height of 966 cm^{-1} and 1375 cm^{-1} were measured from a baseline adjustment and the ratio of these two values were used to calculate the polymer content by means of the method presented in AASHTO T-302. Average polymer content of the sample using both ATR and Transmission methods along with standard deviations are given in Table 4.6. Figure 4.8 shows scatter of intensity ratios for both ATR and transmission methods where it clearly demonstrates that the transmission method is by far more reproducible with less intensity ratio deviation from one run to the next. Generally, FTIR spectra of the sample as shown in Figure 4.9 indicated that ATR FTIR spectrum is noisier which influences background adjustment, resulting in larger errors associated with polymer content measurements of asphalt samples.

Table 4.4: Results of Six Independent Polymer-Modified Asphalt Samples Using ATR Method.

File Name	966 cm^{-1} intensity	1375 cm^{-1} intensity	966 cm^{-1}/1375 cm^{-1} RATIO	% POLYMER
ATR0301	.00108	.00497	.217304	4.4
ATR0302	.00156	.00559	.27907	5.7
ATR0308	.001015	.005235	.193887	3.9
ATR0323	.00126	.00482	.261411	5.4
ATR0336	.00039	.00169	.230769	4.7
ATR0339	.00154	.00541	.279492	5.8

Table 4.5: Results of Six Independent Polymer-Modified Asphalt Samples Using Transmission Method.

File Name	966 cm^{-1} intensity	1375 cm^{-1} intensity	966 cm^{-1}/1375 cm^{-1} RATIO	% POLYMER
TRAN0928	.0429	.195	.220000	4.4
TRAN0929	.026	.115	.226087	4.6
TRAN0930	.0437	.2	.2185	4.4
TRAN0931	.0393	.184	.213587	4.3
TRAN0932	.0417	.188	.221809	4.5
TRAN0933	.0389	.174	.223563	4.5

Table 4.6: Polymer Content of the Samples Used for Comparison of ATR and Transmission Methods along with Standard Deviation and Percent Differences.

FTIR METHOD	Absorbance RATIO	Standard Deviation	% POLYMER	% Difference
ATR	.243656	.035188	4.9	+/- 0.781959
TRAN	.220591	.004343	4.4	+/- 0.0965
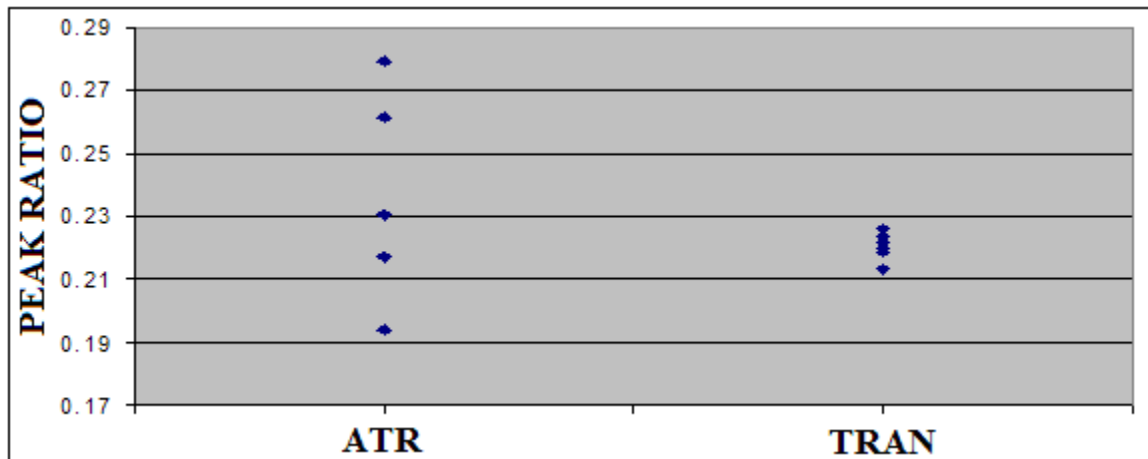
Figure 4.8: Comparison of the Absorbance Ratios in Both ATR and Transmission Methods.
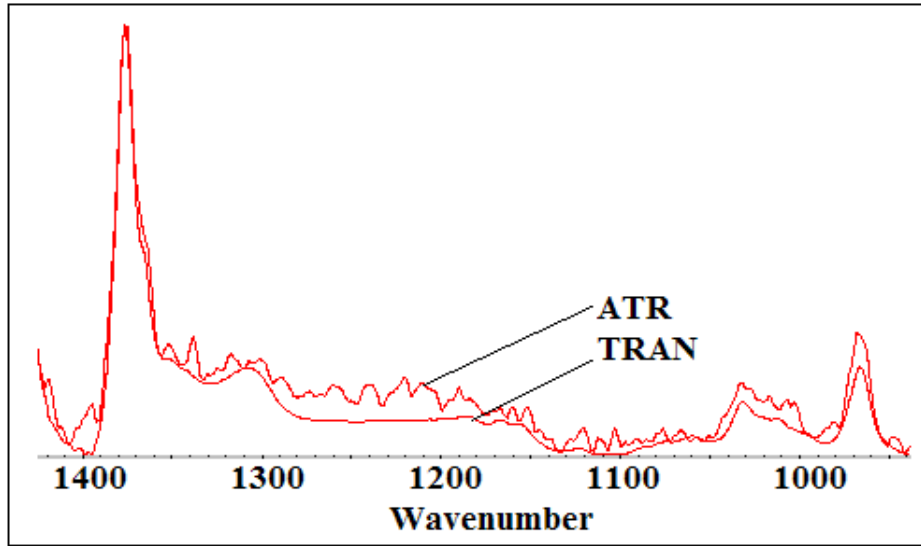
Figure 4.9: FTIR Spectra of a Polymer-Modified Asphalt Sample Showing Noise Level in ATR and Transmission Methods.

4.3 Additional Polymer Quantification in PMA

In order to gain confidence in the ability of FTIR to quantify polymer contents of asphalt binder reproducibly, two additional sets of data were gathered using asphalt binder samples with known polymer contents which were produced by dilution of the original samples received from suppliers A and B. Enough additional base asphalt was added to polymer-modified asphalt to produce a fresh set of samples with known polymer content. Figures 4.10 and 4.11 show their corresponding data.
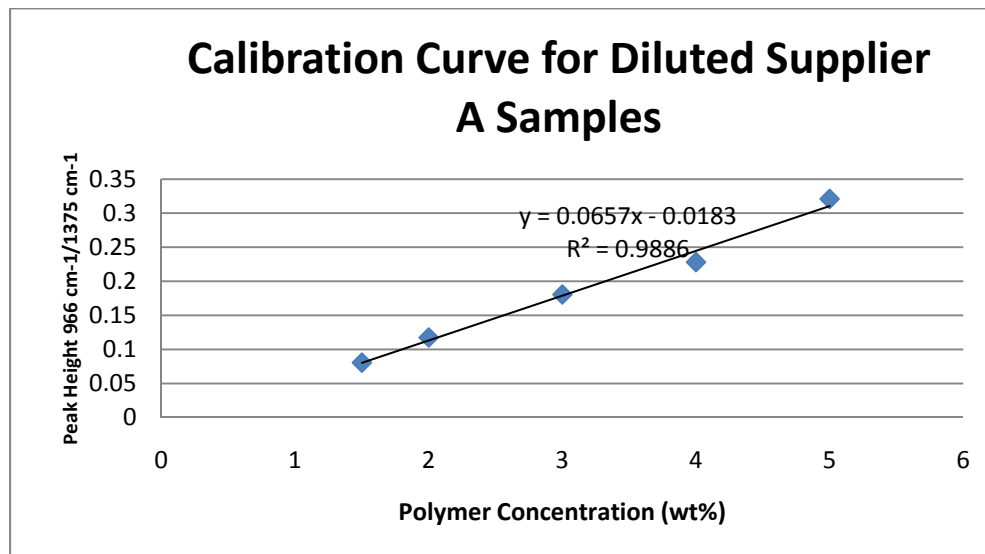
Figure 4.10: Additional Calibration Curve for Samples with Known Concentrations of Polymers from Supplier A.
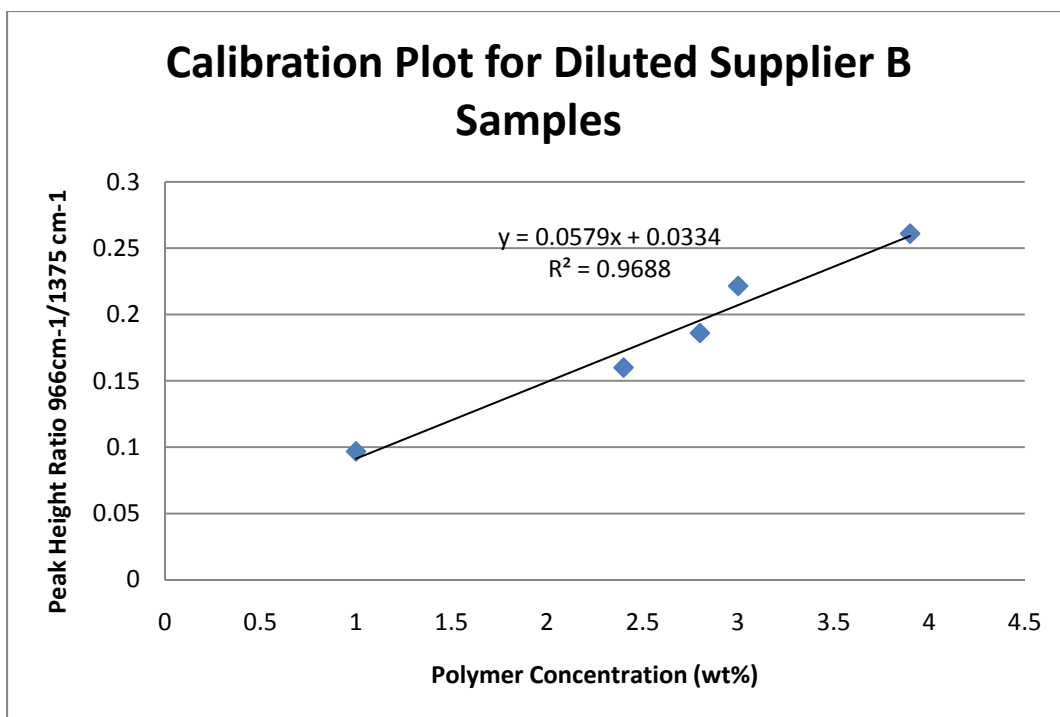
Figure 4.11: Additional Calibration Curve for Samples with Known Concentrations of Polymers from Supplier B.

Standard diviation for measurements of peak ratios for suppliers A and B samples were calculated based on at least five measurements for each set. Supplier A samples showed standard deviations of 0.0069, 0.0075, 0.016, 0.043, and 0.024 for asphalt samples containing 1.5%, 2%, 3%, 4%, and 5% respectively. Standard deviation for samples from supplier B were 0.012, 0.02, 0.032, 0.047, and 0.041 for samples containing 1%, 2.4%, 2.8%, 3%, and 3.9% polymer.

4.4 Comparison of Results Obtained with Literature Data

Table 4.7 presents a comparison of the mathematical relationship between the FTIR peak ratio of 966 cm^{-1}/1375 cm^{-1} bands and polymer concentration (wt%) for two sets of data obtained from supplier A and B with similar data from literature. As can be seen in Table 4.7, a high degree of linearity in the relationship between FTIR peak height and polymer concentration exists in all cases. Slight variation is due to experimental errors and differences in base asphalt materials. Specifically, base asphalt used in this research was PG 64-22 whereas base asphalt used in Curtis's group was AC/20 binder.

Table 4.7: Mathematical Relationships for FTIR Peak Height Ratio to Polymer Concentration of Data Obtained in This Research and Literature Data.

Samples Used	Linear Equation	Comments
Supplier A original set	Y= 0.0638 X + 0.022	$R^2 = 0.99$
Supplier B original set	Y= 0.041 X + 0.079	$R^2 = 0.99$
Supplier B diluted set	Y = 0.057 X + 0.033	$R^2 = 0.96$
Supplier A diluted set	Y = 0.065 X + 0.018	$R^2 = 0.98$
AC/20 Coastal/Exxon SBS*	Y = 0.036925 X + 0.052617	$R^2 = 0.98$
AC/20 Ergon/Exxon SBS*	Y = 0.034325 X + 0.081267	$R^2 = 0.98$
AC/20 Hunt/Exxon SBS*	Y = 0.043969 X + 0.045046	$R^2 = 0.92$

* data from Christine W. Curtis et al. (1995)

According to Table 4.7, the mathematical relationship between peak ratio and polymer concentration for both original and diluted samples (received from both suppliers A and B) are nearly similar. For example, when using data for supplier A samples if one measures a peak ratio of 0.25 corresponding polymer concentrations are calculated as 3.57% irrespective of which equation (equation for original or dilute set) is used. Same analysis (calculation of polymer concentration for a peak ratio of 0.25) using the original and dilute equations for supplier B show polymer concentration of 4.17% and 3.81% indicating 9% difference.

4.5 Summary

A method of quantifying polymer content in asphalt was developed by FTIR in accordance with technical report AASHTO T 302-05. The resulting calibration curve and quantification equation is in general agreement with the one generated by AASHTO. Results of this investigation indicated a linear relationship between polymer content in polymer-modified asphalt samples and the absorbance ratio of 966 cm^{-1}/1375 cm^{-1} bands. Calibration curves generated for both sample sets received from suppliers A and B showed close agreement in the range of data samples for the supplier B source (2.4-3.9%) and differ slightly above 3.9% and below 2.4%. The observed slope difference seen in Figure 4.7 may be a result of lack samples with known polymer concentrations below 2.4% and above 3.9% from supplier B. It is highly recommended to generate a calibration curve for a given asphalt source for the full polymer content range of 0%-5%. In addition, transmission FTIR results are more reproducible than their ATR counterparts.

5. STUDY OF THE QUALITY AND UNIFORMITY OF ANTISTRIPPING AGENTS IN EMULSIONS, CUTBACKS, AND NEAT BINDERS

Antistripping agents are used to reduce or eliminate stripping of asphalt cement from aggregate in Hot Mix Asphalt (HMA) mixtures (F.L. Roberts 1996).   Stripping is defined as loss of bonding between the aggregates and the asphalt cement. Symptoms of stripping include raveling, rutting, shoving, corrugation, and cracking (F.L. Roberts 1996). Moisture penetration is believed to be one of the factors contributing to stripping and FTIR techniques have been used to study this phenomenon (U. Bagampadde and U. Isacsson 2006). Liquid antistripping additives are added to emulsion systems to enhance performance of asphalt emulsions. The following sections provide classification and chemistry of asphalt emulsions.

5.1 Asphalt Emulsion Classification

Asphalt emulsion system consists of three constituents including asphalt, water, and emulsifying agents. Other additives are added as stabilizers, coating improvers, antistrips, or break control agents. Asphalt emulsions are classified as anionic, cationic, and non-ionic. According to ASTM D 2397 and D977, cationic asphalt emulsions are identified with a letter C (on its label) followed by a setting speed of slow (SS), medium (MS), or rapid (RS). Absence of the letter "C" indicates that the asphalt emulsion is anionic. All asphalt emulsions are also classified by the viscosity of the starting asphalt; low viscosity is indicated as class 1 and high viscosity as class 2. In addition, harder starting asphalt is designated with "H" and softer starting asphalt is designated with "S" after viscosity designation. Polymer-modified asphalt emulsions (with 3-5% polymer) are designated with "P" after viscosity classification. A group of gel quality anionic asphalt emulsion with a high float characteristic as qualified by the float test has "HF" designation before their setting.

5.2 Chemistry of Asphalt Emulsion

The main source of asphalt binders is the refined crude petroleum that is composed of hydrocarbons with large molecules. Figure 5.1 shows a schematic diagram of a complete emulsified asphalt production process.

Water is the second main/predominant constituent of an asphalt emulsion. Water quality in terms of type and amounts of mineral content affects asphalt emulsion quality in anionic and

cationic groups differently. For example, while presence of calcium and magnesium ions stabilizes cationic asphalt emulsion, these ions adversely affect anionic asphalt emulsion by forming soap scum. Likewise, carbonates and bicarbonates stabilize anionic asphalt emulsion, but destabilize cationic asphalt emulsion by reacting with water soluble amine hydrochloride emulsifiers (AEMA 2004).

The third constituent of an asphalt emulsion is an emulsifying agent. Emulsifiers control quality of the final product significantly. Emulsifiers are basically surfactants. Their function is to control stability of asphalt droplets and breaking time. Typical anionic emulsifiers are acids produced from wood derivatives, such as tall oils, rosins, and lignins that react with sodium or potassium hydroxide to turn the emulsifier into soap (AEMA 2004). Cationic emulsifiers are fatty amines (diamines, imidazolines, and amidoamines). Reaction with hydrochloric acid turns these amines into soap (AEMA 2004). The following provides dissociation characteristics of three types of surfactants in water as given in AEMA 2004 document:

1─Anionic Surfactants- Where the electrovalent and polar hydrocarbon group is part of the negatively charged ion, when the compound ionizes: $CH_3(CH_2)_n\ COO^-Na^+$

2─Nonionic Surfactant- Where the hydrophilic group is covalent and polar, and which dissolves without ionization: $CH_3(CH_2)_nCOO\ (CH_2CH_2O)_x\ H$

3─Cationic Surfactants- Where the electrovalent and polar hydrocarbon group is part of the positively charged ion when the compound ionizes: $CH_3(CH_2)_n\ NH_3^+Cl^-$
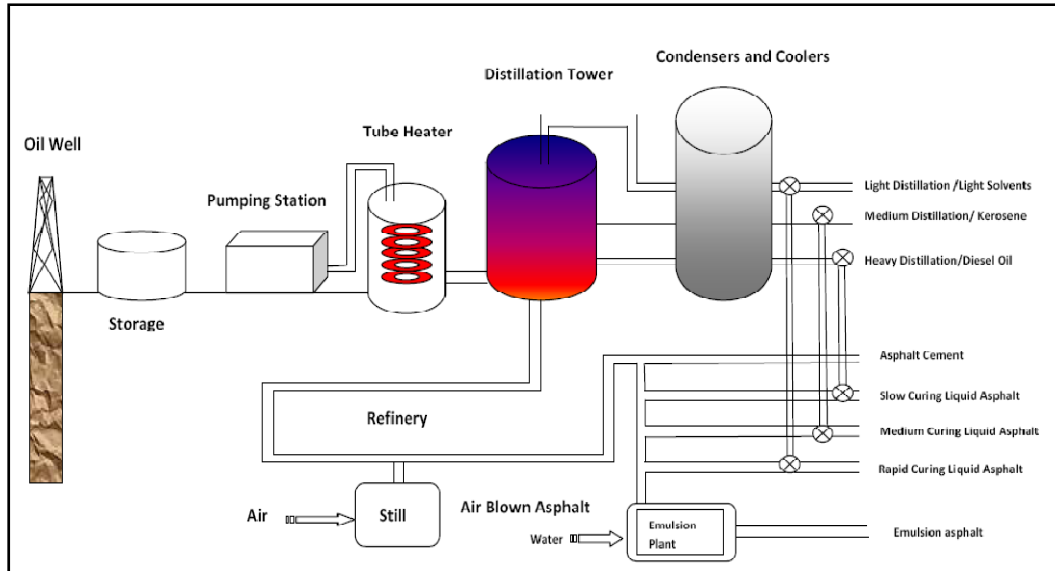
Figure 5.1: Schematic of a Complete Cycle in Emulsion Asphalt Production.

Figure 5.2 shows the nonpolar oil-loving section and polar water-loving portion of surfactants. Surfactants usually concentrate at the interface of liquid-gas or liquid-solid interfaces as shown in Figure 5.3. The oil-loving hydrocarbon tail of a typical emulsifier is 12-18 carbon atoms long (James 2006). If one represents this hydrocarbon tail as R, the following formulations of emulsion agents are produced by neutralizing with an acid or base to form a neutralized cationic or anionic emulsion agent. Tables 5.1 and 5.2 show typical emulsion recopies.

RNH_2 (insoluble form) $+ HCl = RNH_3 + Cl^-$ (water-soluble cationic form)
$RCOOH$ (insoluble form) $+ NaOH = RCOO^- + Na^+ + H_2O$ (water-soluble anionic form)
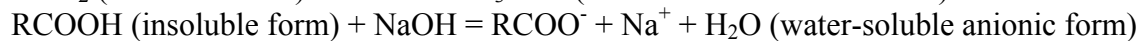
Table 5.1: Chemistry of Asphalt Emulsifiers.

Lipophilic Portion	Head Group
Tallowalkyl-	$[-NH_2CH_2CH_2CH_2NH_3]^{2-}$
Tallowalkyl-	$[-N (CH_3)_3]^-$
Nonylphenyl-	$[-O(CH_2CH_2O)_{100}H$
Tall Oil-	$[-COO]-$
Alkylbenzene	$[-SO3]^-$
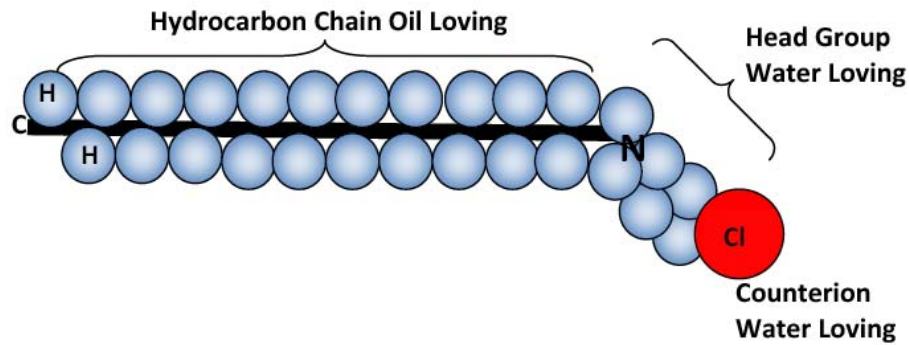
Figure 5.2: Water-Loving and Oil-Loving Sections of a Surfactant.
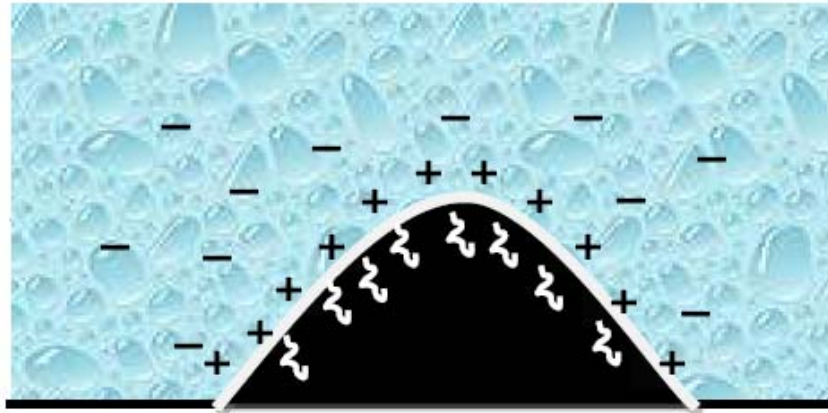
Figure 5.3: Solid-liquid Interface where Surfactant Molecules Accumulate.

Table 5.2 Typical Recipes for Emulsion Asphalt (James 2006).

CRS	65% Asphalt	0.2%Tallowdiamine	0.15% HCl (35%)	Water to 100%	Soap pH=1.5-2.5
CSS	60% Asphalt	0.6% Tallow diquaternary ammonium chloride	NA	Water to 100%	Soap pH=3-7
Anionic RS	65% Asphalt	0.3% Tall Oil	0.2% Sodium hydroxide	Water to 100%	Soap pH=11-12
Anionic SS	60% Asphalt	0.5% Ethoxylated nonyl phenol	0.5% Lignins	Water to 100%	Soap pH=10-12

5.3 FTIR Spectrum of an Antistripping Agent from TxDOT Cedar Park Laboratory

A sample of a liquid antistripping agent was provided by TxDOT to obtain FTIR spectrum and Figure 5.4 shows the resulting spectra. The presence of a number of absorption bands in the spectrum (Figure 5.4 red trace) proves that there are bonds between constituents of this organic liquid and FTIR is capable of detecting them if there is sufficient quantity of it

available in an unknown sample. However, if the concentration of the antistripping agent is below the detection limit of the FTIR technique, there will not be any discernible absorption bands to enable their detection and identification. This issue was experimented by comparing spectra of PG 64-22 base asphalt with (Figure 5.4 blue trace) and without (Figure 5.4 purple trace) 2% antistripping additive and Figure 5.4 shows no difference between the two spectra.
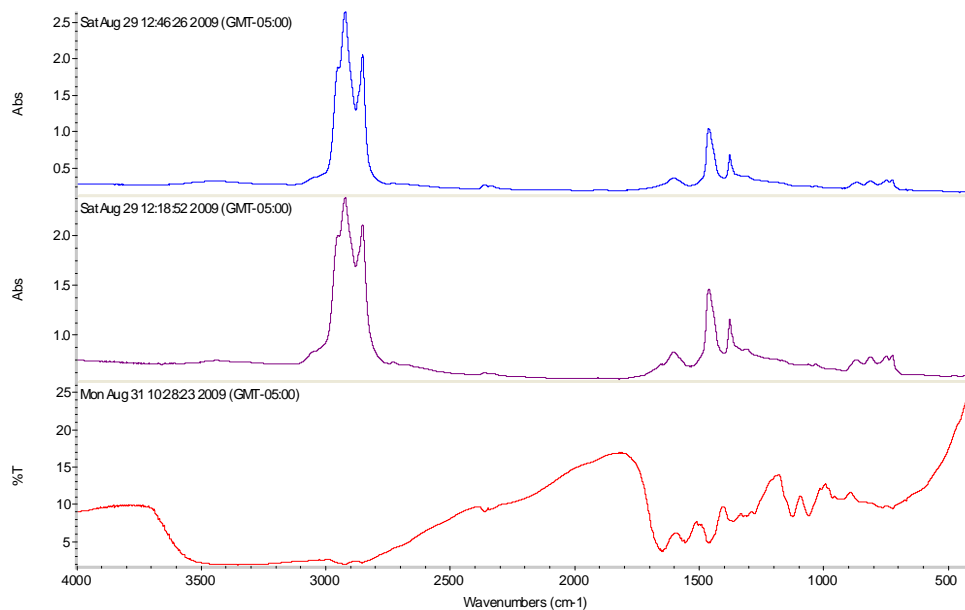
Figure 5.4 FTIR Spectrum of an Antistripping Agent Obtained from Cedar Park Laboratory of TxDOT and Its Comparison with PG 64-22+2% Antistripping Agent (Blue Trace), without 2% Antistripping (Purple Trace).

5.4 Identification of Antistripping and Emulsion Agents in Asphalt Binders

Samples of anionic asphalt emulsion binders including SS-1, SS-1H, HFRS -2, and cationic asphalt emulsion binders such as CHFRS-2P, CSS-1, CSS-1H, CRS-2, and CRS-2P are studied in this research.   Figure 5.5 (a-c) shows three possible emulsifying and antistripping agents present in SS-1. Trimethyl tallow ammonium chloride, dimethyl di(coco) ammonium chloride, and N-tallow propylenediamine with 79.99%, 79.19%, and 79.03% percent match, respectively, were possible emulsifying agents present in SS-1. In each case, red trace represents unknown sample and all other traces with different colors represent possible agents matching the given trace.

	Index	Match	Compound Name	Library Name
1	169	79.99	Trimethyl tallow ammonium chloride	FDM FTIR Spectra of Surfactants
2	429	79.19	N-tallow-propylenediamine	FDM FTIR Spectra of Surfactants
3	321	79.09	Ammonium lauryl sulfate	FDM FTIR Spectra of Surfactants
4	167	79.03	Dimethyl di(coco) ammonium chloride	FDM FTIR Spectra of Surfactants
5	338	78.40	POE oleyl amine (2 mol EtO)	FDM FTIR Spectra of Surfactants
6	427	77.78	N-coco-propylenediamine	FDM FTIR Spectra of Surfactants
7	265	77.67	POE soya amine (2 mol EtO)	FDM FTIR Spectra of Surfactants
8	170	76.66	Trimethyl cocoammonium chloride	FDM FTIR Spectra of Surfactants

(a)

Figure 5.5 Shows FTIR Spectra of a Typical SS-1 Sample.

	Index	Match	Compound Name	Library Name
1	169	79.99	Trimethyl tallow ammonium chloride	FDM FTIR Spectra of Surfactants
2	429	79.19	N-tallow-propylenediamine	FDM FTIR Spectra of Surfactants
3	321	79.09	Ammonium lauryl sulfate	FDM FTIR Spectra of Surfactants
4	167	79.03	Dimethyl di(coco) ammonium chloride	FDM FTIR Spectra of Surfactants
5	338	78.40	POE oleyl amine (2 mol EtO)	FDM FTIR Spectra of Surfactants
6	427	77.78	N-coco-propylenediamine	FDM FTIR Spectra of Surfactants
7	265	77.67	POE soya amine (2 mol EtO)	FDM FTIR Spectra of Surfactants
8	170	76.66	Trimethyl cocoammonium chloride	FDM FTIR Spectra of Surfactants

(b)

	Index	Match	Compound Name	Library Name
1	169	79.99	Trimethyl tallow ammonium chloride	FDM FTIR Spectra of Surfactants
2	429	79.19	N-tallow-propylenediamine	FDM FTIR Spectra of Surfactants
3	321	79.09	Ammonium lauryl sulfate	FDM FTIR Spectra of Surfactants
4	167	79.03	Dimethyl di(coco) ammonium chloride	FDM FTIR Spectra of Surfactants
5	338	78.40	POE oleyl amine (2 mol EtO)	FDM FTIR Spectra of Surfactants
6	427	77.78	N-coco-propylenediamine	FDM FTIR Spectra of Surfactants
7	265	77.67	POE soya amine (2 mol EtO)	FDM FTIR Spectra of Surfactants
8	170	76.66	Trimethyl cocoammonium chloride	FDM FTIR Spectra of Surfactants

(c)

Figure 5.5 Shows FTIR Spectra of a Typical SS-1 Sample (cont.).

Figure 5.6 (a-c) shows FTIR spectra of HFRS-2 emulsion showing similar FTIR spectrum with SS-1 sample indicating lack of FTIR ability to detect minute changes in the chemistry of these materials. Similar identification as SS-1 is shown in the tables below the spectra.

41

	Index	Match	Compound Name	Library Name
1	321	88.33	Ammonium lauryl sulfate	FDM FTIR Spectra of Surfactants
2	169	87.26	Trimethyl tallow ammonium chloride	FDM FTIR Spectra of Surfactants
3	167	86.36	Dimethyl di(coco) ammonium chloride	FDM FTIR Spectra of Surfactants
4	429	85.86	N-tallow-propylenediamine	FDM FTIR Spectra of Surfactants
5	338	85.83	POE oleyl amine (2 mol EtO)	FDM FTIR Spectra of Surfactants
6	265	84.61	POE soya amine (2 mol EtO)	FDM FTIR Spectra of Surfactants
7	427	83.29	N-coco-propylenediamine	FDM FTIR Spectra of Surfactants
8	170	82.90	Trimethyl cocoammonium chloride	FDM FTIR Spectra of Surfactants

(a)

	Index	Match	Compound Name	Library Name
1	321	88.33	Ammonium lauryl sulfate	FDM FTIR Spectra of Surfactants
2	169	87.26	Trimethyl tallow ammonium chloride	FDM FTIR Spectra of Surfactants
3	167	86.36	Dimethyl di(coco) ammonium chloride	FDM FTIR Spectra of Surfactants
4	429	85.86	N-tallow-propylenediamine	FDM FTIR Spectra of Surfactants
5	338	85.83	POE oleyl amine (2 mol EtO)	FDM FTIR Spectra of Surfactants
6	265	84.61	POE soya amine (2 mol EtO)	FDM FTIR Spectra of Surfactants
7	427	83.29	N-coco-propylenediamine	FDM FTIR Spectra of Surfactants
8	170	82.90	Trimethyl cocoammonium chloride	FDM FTIR Spectra of Surfactants

(b)

Figure 5.6 (a-c) Shows HFRS-2 Spectra.

	Index	Match	Compound Name	Library Name
1	321	88.33	Ammonium lauryl sulfate	FDM FTIR Spectra of Surfactants
2	169	87.26	Trimethyl tallow ammonium chloride	FDM FTIR Spectra of Surfactants
3	167	86.36	Dimethyl di(coco) ammonium chloride	FDM FTIR Spectra of Surfactants
4	429	85.86	N-tallow-propylenediamine	FDM FTIR Spectra of Surfactants
5	338	85.83	POE oleyl amine (2 mol EtO)	FDM FTIR Spectra of Surfactants
6	265	84.61	POE soya amine (2 mol EtO)	FDM FTIR Spectra of Surfactants
7	427	83.29	N-coco-propylenediamine	FDM FTIR Spectra of Surfactants
8	170	82.90	Trimethyl cocoammonium chloride	FDM FTIR Spectra of Surfactants

(c)
Figure 5.6 (a-c) Shows HFRS-2 Spectra (conti.)

Figure 5.7 (a-c) shows FTIR spectra and corresponding analysis of cationic emulsion asphalts of CHFRS-2, showing similar results as HFRS-2 and SS-1 results, indicating insensitivity of FTIR to differentiation of antistripping agents. Figure 5.8 (a-c) shows FTIR spectra corresponding to a typical CRS-2 sample.

	Index	Match	Compound Name	Library Name
1	321	88.35	Ammonium lauryl sulfate	FDM FTIR Spectra of Surfactants
2	169	88.32	Trimethyl tallow ammonium chloride	FDM FTIR Spectra of Surfactants
3	167	87.69	Dimethyl di(coco) ammonium chloride	FDM FTIR Spectra of Surfactants
4	429	87.62	N-tallow-propylenediamine	FDM FTIR Spectra of Surfactants
5	338	86.45	POE oleyl amine (2 mol EtO)	FDM FTIR Spectra of Surfactants
6	265	85.62	POE soya amine (2 mol EtO)	FDM FTIR Spectra of Surfactants
7	427	85.42	N-coco-propylenediamine	FDM FTIR Spectra of Surfactants
8	170	84.85	Trimethyl cocoammonium chloride	FDM FTIR Spectra of Surfactants

(a)
Figure 5.7 FTIR Spectra of CHFRS-2 and Corresponding Analysis.

43

	Index	Match	Compound Name	Library Name
1	321	88.35	Ammonium lauryl sulfate	FDM FTIR Spectra of Surfactants
2	169	88.32	Trimethyl tallow ammonium chloride	FDM FTIR Spectra of Surfactants
3	167	87.69	Dimethyl di(coco) ammonium chloride	FDM FTIR Spectra of Surfactants
4	429	87.62	N-tallow-propylenediamine	FDM FTIR Spectra of Surfactants
5	338	86.45	POE oleyl amine (2 mol EtO)	FDM FTIR Spectra of Surfactants
6	265	85.62	POE soya amine (2 mol EtO)	FDM FTIR Spectra of Surfactants
7	427	85.42	N-coco-propylenediamine	FDM FTIR Spectra of Surfactants
8	170	84.85	Trimethyl cocoammonium chloride	FDM FTIR Spectra of Surfactants

(b)

	Index	Match	Compound Name	Library Name
1	321	88.35	Ammonium lauryl sulfate	FDM FTIR Spectra of Surfactants
2	169	88.32	Trimethyl tallow ammonium chloride	FDM FTIR Spectra of Surfactants
3	167	87.69	Dimethyl di(coco) ammonium chloride	FDM FTIR Spectra of Surfactants
4	429	87.62	N-tallow-propylenediamine	FDM FTIR Spectra of Surfactants
5	338	86.45	POE oleyl amine (2 mol EtO)	FDM FTIR Spectra of Surfactants
6	265	85.62	POE soya amine (2 mol EtO)	FDM FTIR Spectra of Surfactants
7	427	85.42	N-coco-propylenediamine	FDM FTIR Spectra of Surfactants
8	170	84.85	Trimethyl cocoammonium chloride	FDM FTIR Spectra of Surfactants

(c)

Figure 5.7 FTIR Spectra of CHFRS-2 and Corresponding Analysis (conti.).

	Index	Match	Compound Name	Library Name
1	169	89.63	Trimethyl tallow ammonium chloride	FDM FTIR Spectra of Surfactants
2	429	89.17	N-tallow-propylenediamine	FDM FTIR Spectra of Surfactants
3	321	89.04	Ammonium lauryl sulfate	FDM FTIR Spectra of Surfactants
4	167	88.95	Dimethyl di(coco) ammonium chloride	FDM FTIR Spectra of Surfactants
5	338	87.18	POE oleyl amine (2 mol EtO)	FDM FTIR Spectra of Surfactants
6	427	87.04	N-coco-propylenediamine	FDM FTIR Spectra of Surfactants
7	265	86.20	POE soya amine (2 mol EtO)	FDM FTIR Spectra of Surfactants
8	170	85.84	Trimethyl cocoammonium chloride	FDM FTIR Spectra of Surfactants

(a)

	Index	Match	Compound Name	Library Name
1	169	89.63	Trimethyl tallow ammonium chloride	FDM FTIR Spectra of Surfactants
2	429	89.17	N-tallow-propylenediamine	FDM FTIR Spectra of Surfactants
3	321	89.04	Ammonium lauryl sulfate	FDM FTIR Spectra of Surfactants
4	167	88.95	Dimethyl di(coco) ammonium chloride	FDM FTIR Spectra of Surfactants
5	338	87.18	POE oleyl amine (2 mol EtO)	FDM FTIR Spectra of Surfactants
6	427	87.04	N-coco-propylenediamine	FDM FTIR Spectra of Surfactants
7	265	86.20	POE soya amine (2 mol EtO)	FDM FTIR Spectra of Surfactants
8	170	85.84	Trimethyl cocoammonium chloride	FDM FTIR Spectra of Surfactants

(b)

Figure 5.8 FTIR Spectra of a Typical CRS-2 Sample.

	Index	Match	Compound Name	Library Name
1	169	89.63	Trimethyl tallow ammonium chloride	FDM FTIR Spectra of Surfactants
2	429	89.17	N-tallow-propylenediamine	FDM FTIR Spectra of Surfactants
3	321	89.04	Ammonium lauryl sulfate	FDM FTIR Spectra of Surfactants
4	167	88.95	Dimethyl di(coco) ammonium chloride	FDM FTIR Spectra of Surfactants
5	338	87.18	POE oleyl amine (2 mol EtO)	FDM FTIR Spectra of Surfactants
6	427	87.04	N-coco-propylenediamine	FDM FTIR Spectra of Surfactants
7	265	86.20	POE soya amine (2 mol EtO)	FDM FTIR Spectra of Surfactants
8	170	85.84	Trimethyl cocoammonium chloride	FDM FTIR Spectra of Surfactants

(c)

Figure 5.8 FTIR Spectra of a Typical CRS-2 Sample (conti.).

5.5 FTIR Fingerprints and Uniformity of Anionic, Cationic Emulsions and Cutback Asphalt Binders

5.5.1 Procedures

Eight emulsifiers, given in Table 5.3, were provided by their producers and used as samples for FTIR analysis.

Table 5.3: List of Products Analyzed (Fall 2008) (samples received from TxDOT).

Label	Producer	Grade/Product
A3042	A	HFRS-2P Tank 202
B3044	A	HFRS-2 Tank 204
C3044	B	SS-1
D3045	B	CRS-2
E3046	B	CRS-2P
F3047	B	PCE
3	C	MC-30
4	C	RC-250

Approximately 1 g of the emulsifier is placed on wax paper from the batch being sampled. Next 100 mg of potassium bromide (KBr) is pressed in a 13 mm die under pressure

46

(10,000 psi) for two minutes to achieve a solid KBr pellet. This pellet is then placed on the emulsifier still on the wax paper to achieve a thin transparent coat of emulsifying agent on the pellet. FTIR analysis was done on a Thermo Nicolet Avatar 370 DTGS from 4000 to 400 cm^{-1} using 32 scans with a resolution of 2 cm^{-1}. Tests were done from 0 to 90 minutes at intervals of 15 minutes. Each sample is analyzed five independent times to ensure repeatability of results. Further tests were conducted to analyze the change in time to the emulsifier spectrum due to evaporation on the KBr pellet. Also the spectrums of Transmitted and ATR Spectroscopy were compared.

5.5.2 Results

The general spectrum of each emulsifier is shown below in Figures 5.9-5.16 in the range of 4000 to 400 cm^{-1}.
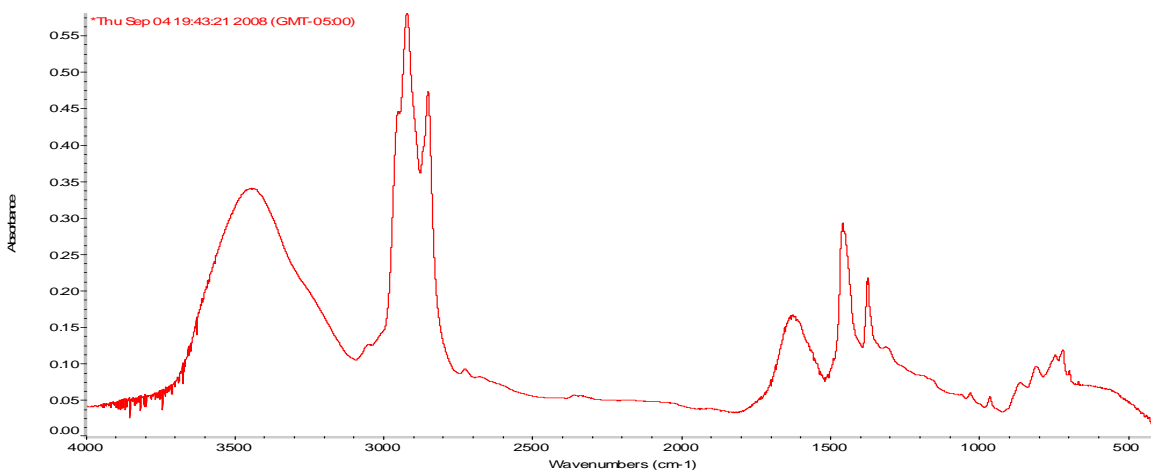
Figure 5.9: FTIR Spectrum of Sample A3042, HFRS-2 Tank 202 from Supplier A.
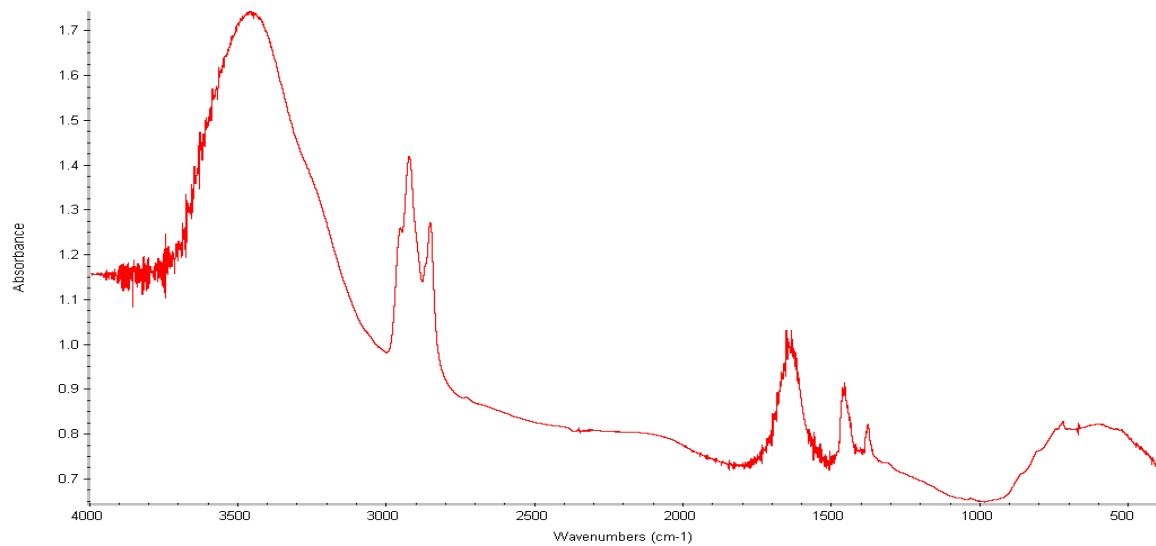
Figure 5.10: FTIR Spectrum of Sample B 3044, HFRS-2P Tank 204 from Supplier A.

*Mon Nov 03 17:38:18 2008 (GMT-06:00)
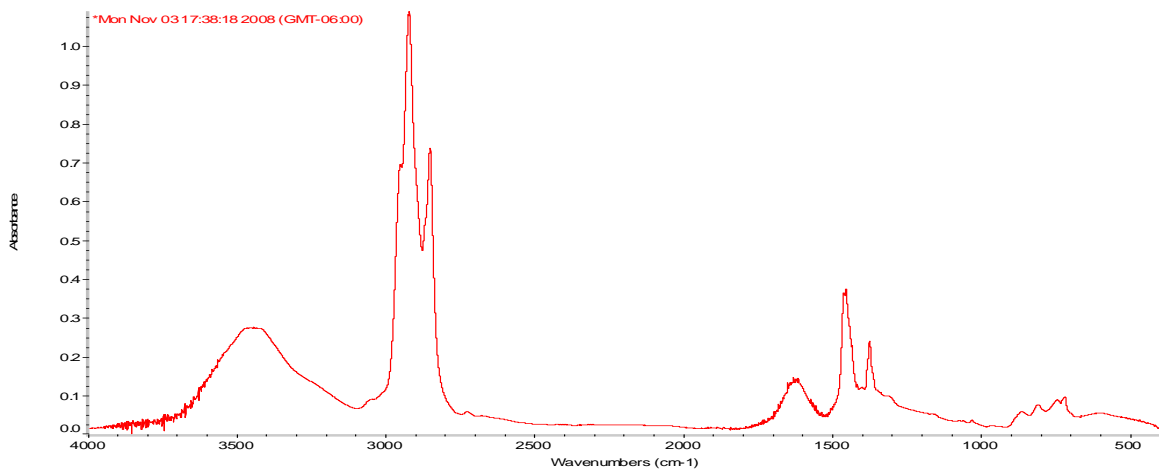
Figure 5.11: FTIR Spectrum of Sample C3044, SS-1 from Supplier B.

*Sat Nov 08 11:11:09 2008 (GMT-06:00)
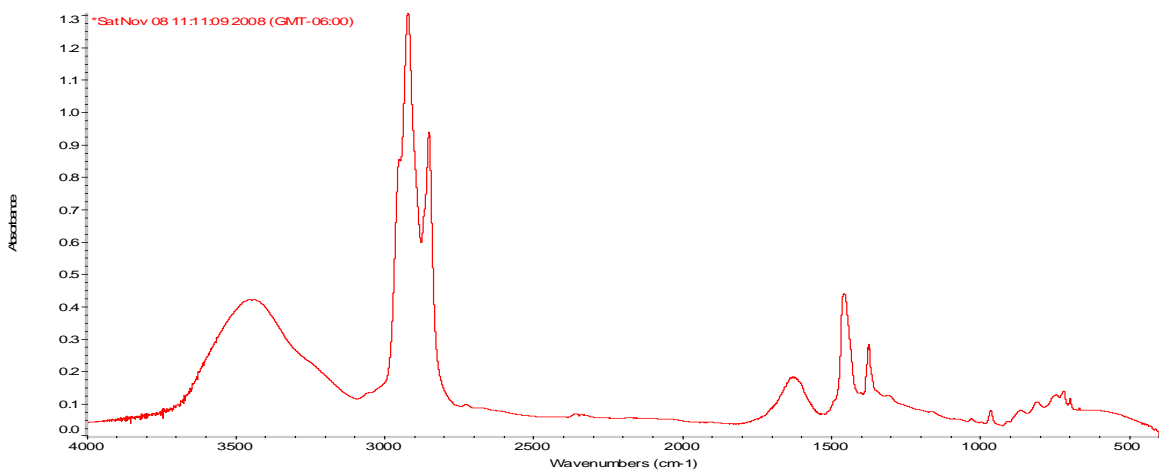
Figure 5.12: FTIR Spectrum of Sample D3045, CRS-2 from Supplier B.
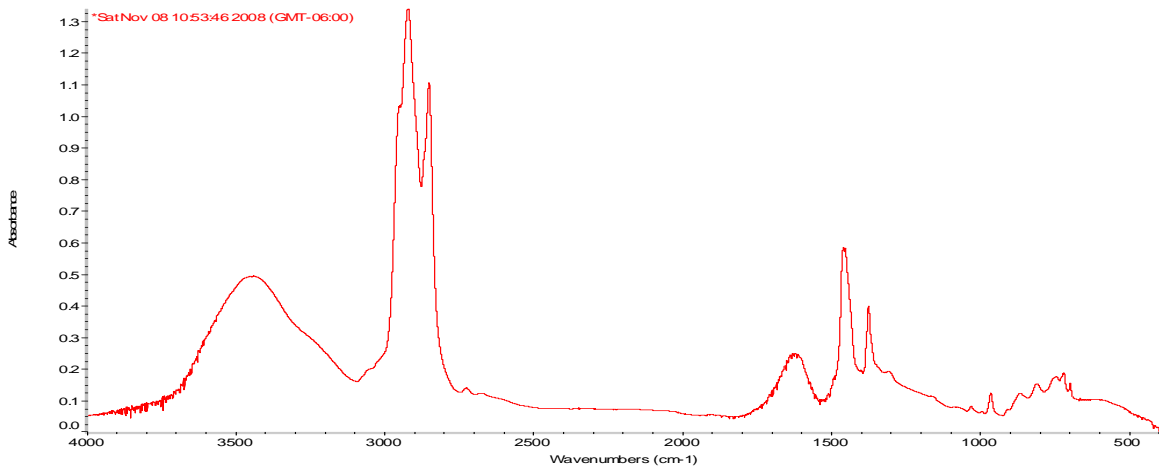
Figure 5.13: FTIR Spectrum of Sample E3046, CRS-2P from Supplier B.
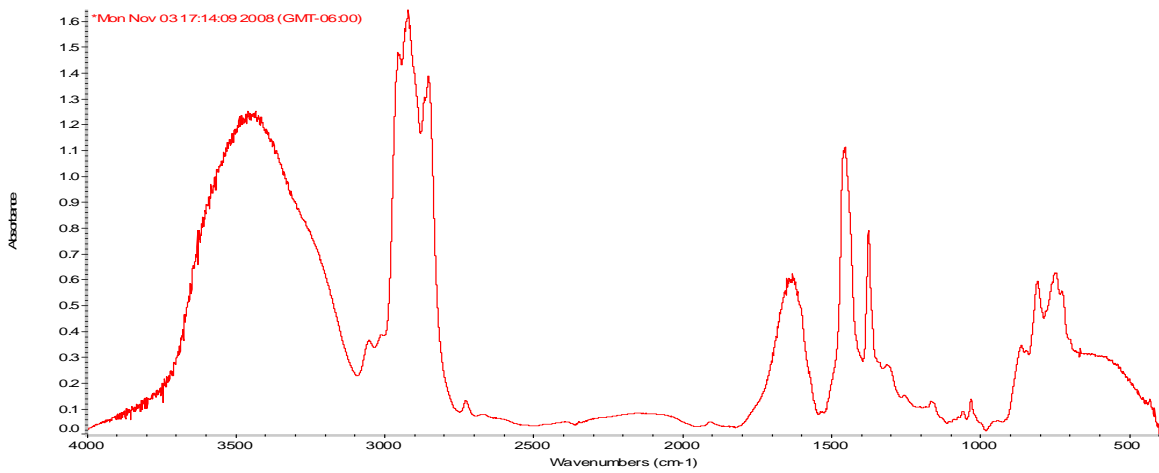
Figure 5.14: FTIR Spectrum of Sample F3047, PCE from Supplier B.
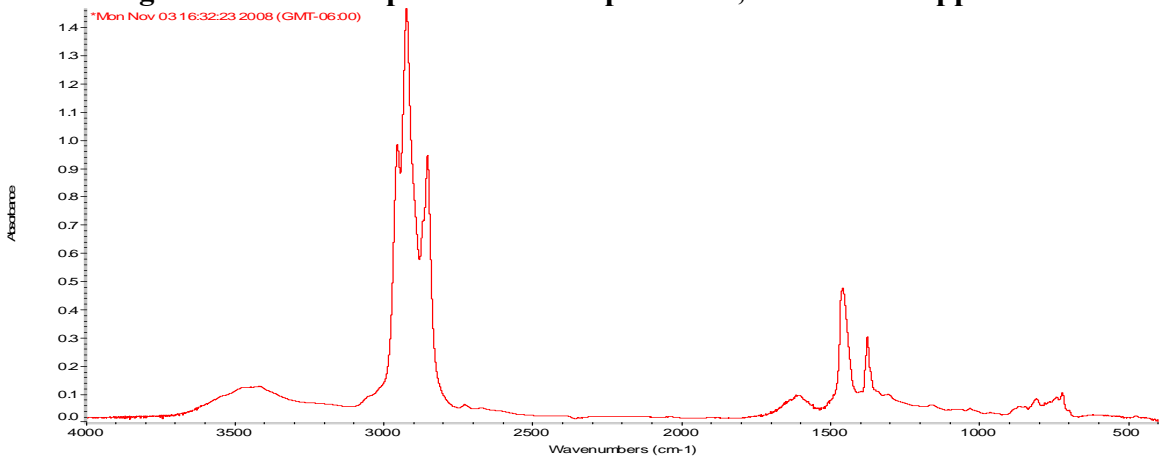
Figure 5.15: FTIR Spectrum of Sample 3, CCAT MC-30 from Supplier C.
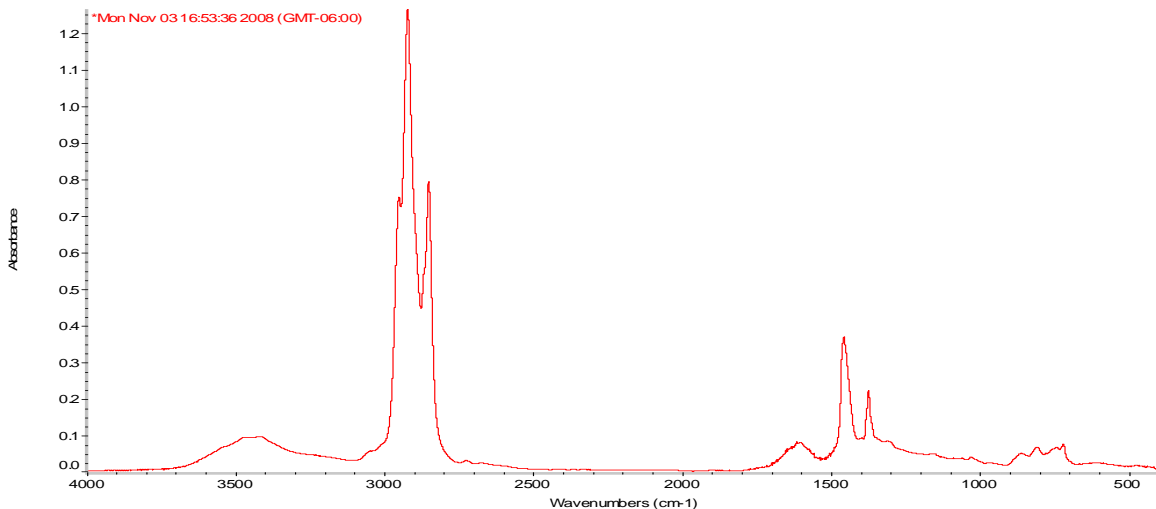
Figure 5.16: FTIR Spectrum of Sample 4, CCAT RC-250 from Supplier C.

Functional analysis of the spectra was conducted by Thermo Nicolet Avatar analyzing software. This allows an immediate analysis of functional groups within a spectrum for quick qualitative and fingerprinting purposes. Figure 5.17 shows a functional group analysis conducted on C3044 sample. Note the presence and range of Inorganic Carbonates shown in purple, Aliphatic Primary Amide shown in green, and Secondary Aliphatic Alcohols shown in blue.
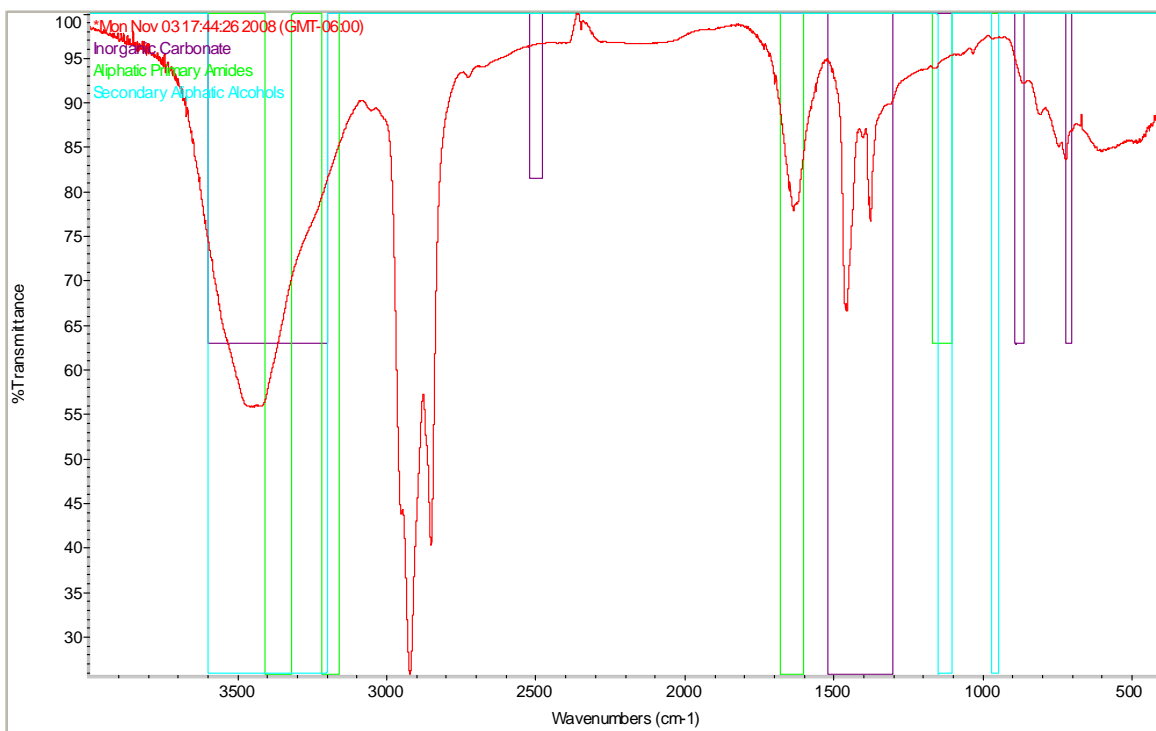
Figure 5.17: Functional Group Analysis of SS-1 (C3044).

Comparative analysis of all spectra was conducted and the samples were divided into two groups. The first group compares samples from A3042 and F3048 and is shown in Figure 5.18. The range of interest is from 1500 to 400 cm⁻¹. Note the spectral variations around 700 cm⁻¹ and 966 cm⁻¹. The second group consists of samples 3 and 4 and is shown in Figure 5.19 with a spectral range of 900 cm⁻¹to 650 cm⁻¹. Note spectral variations at 845 cm⁻¹, 835 cm⁻¹, 790 cm⁻¹, and 687 cm⁻¹. These bands are associated with kerosene that is the base material used in production of cutbacks (S. Garrigues (1995)).
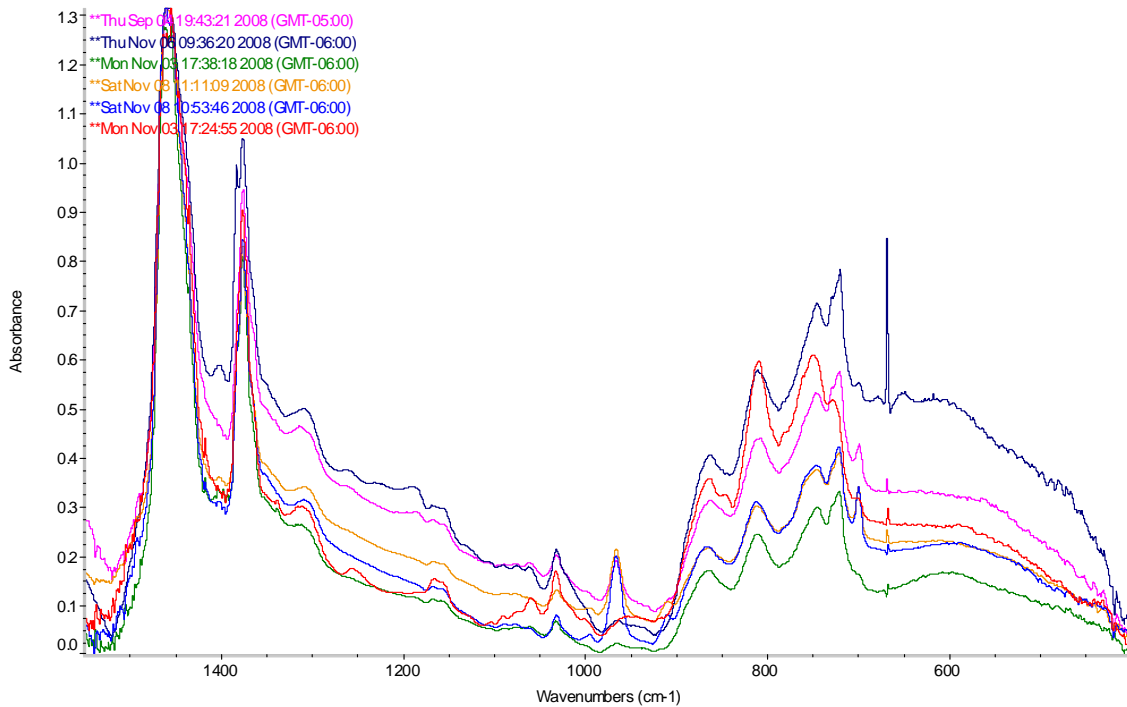
Figure 5.18: Comparison of FTIR Spectra for A3042 (Pink), B3044 (Purple), C3044 (Green), D3045 (Yellow), E3046 (Blue), and F3047 (Red) Samples.
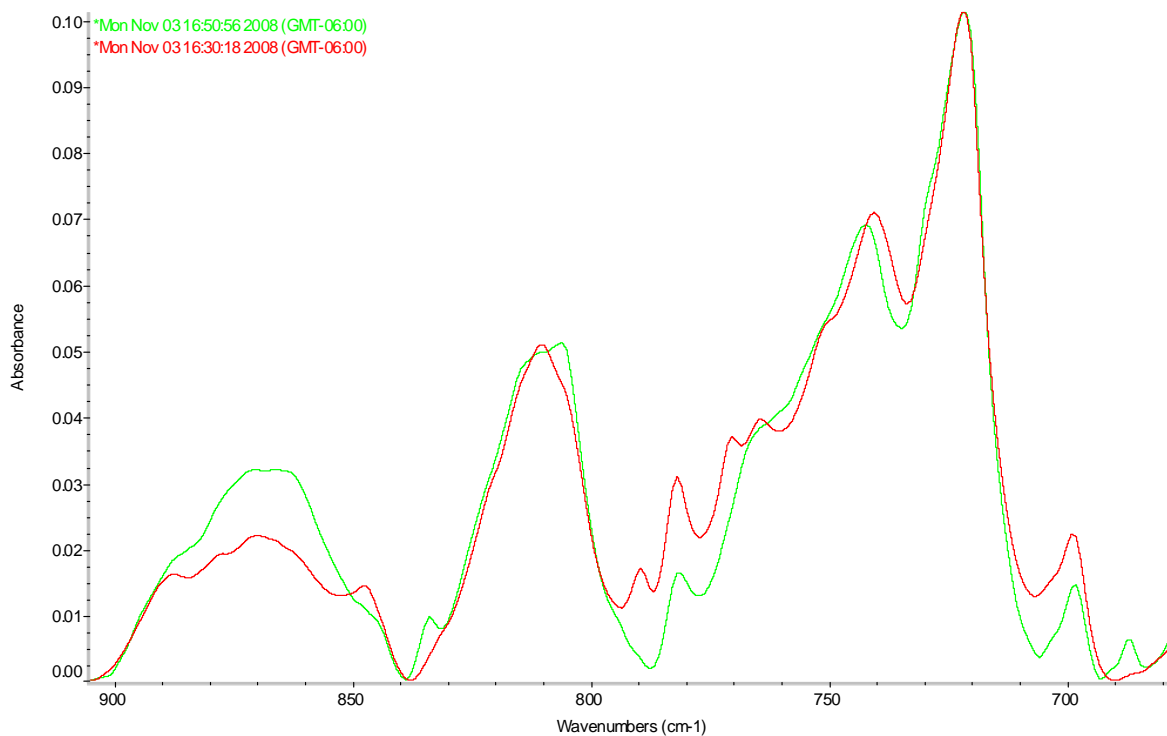
Figure 5.19: Comparison of FTIR Spectra for CCAT RC-250 (Green) and CCAT MC-50 (Red) Samples.

Conducting the Transmittance FTIR tests, it was noted that the very visible physical change of the emulsifier on the KBr pellet mostly attributed to the fast evaporative property of the emulsifier. Tests were done to analyze the spectrum of emulsifier that was subjected to ambient conditions over a period of time to ensure consistency in the spectra. Figure 5.20 shows sample D3045 that was analyzed at zero, five, and ten minutes at ambient conditions. It was determined that there were significant changes to the water bands, at 3500 cm^{-1} and 650cm^{-1}, and also to the carbonyl band at 1625 cm^{-1}.
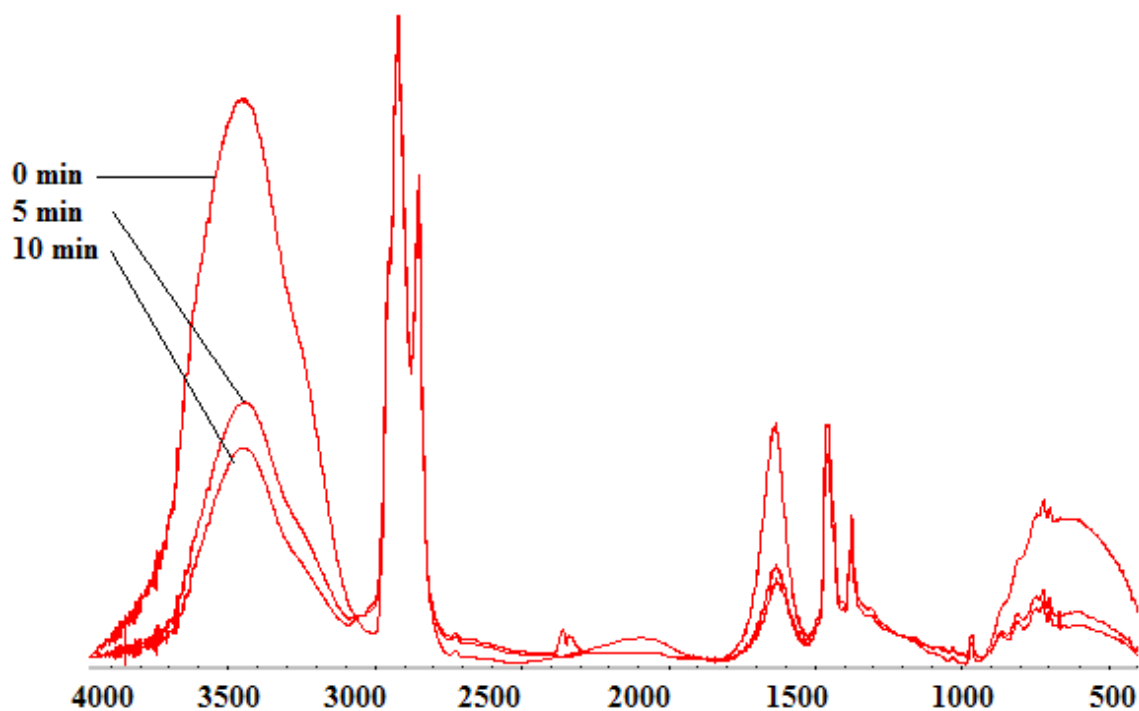
Figure 5.20: Comparison of FTIR Spectra of CRS-2 (D3045) Sample when Tested at 0, 5, and 10 Minutes.

Approximately 2 to 3 g of emulsifying agent is placed on a Germanium optical crystal within the ATR accessory. ATR-FTIR analysis is done on a Thermo Nicolet Avatar 370 DTGS with the ATR accessory from 4000 cm^{-1} to 700 cm^{-1} using 48 scans with a resolution of 4 cm^{-1}. The samples were analyzed five times to ensure the reproducibility of the results. FTIR fingerprint spectra of all products listed in Table 5.4 are given in Figures 5.21-5.31 (see Appendix G). Batch 1 samples are the same samples used previously (stored in ambient conditions) and re-analyzed. Batch 2 samples are from a new batch received from the same manufacturer.

Table 5.4: List of Products Analyzed (Spring 2009).

Product	Supplier #1	Supplier #2	Supplier #3	Supplier #4
CRS-2	B (batch 1)	B (batch 2)	N/A	D
CRS-2P	B (batch 1)	B (batch 2)	N/A	N/A
CHFRS-2P	B (batch 1)	B (batch 2)	N/A	N/A
HFRS-2	N/A*	N/A	A	D
HFRS-2P	N/A	N/A	A	D

*N/A = Not Available

5.6 Summary

FTIR spectra of both cationic and anionic asphalt emulsions were obtained for all products listed in Tables 5.3 and 5.4. Fingerprint spectra of these products showed a reproducible pattern for five repeated measurements. Specifically, samples received from TxDOT (listed in Table 5.3) in early September 2008 were analyzed and stored in ambient conditions at the UNT Materials laboratory. When these samples were used again in February and March of 2009 (batch 1 in Table 5.4), no detectable changes in their respective FTIR spectra were observed, indicating that these materials are very chemically stable if kept at room temperature.

The functional groups of the SS-1 product were identified as "Aliphatic primary Amide," "Secondary Aliphatic Alcohol," and "Inorganic carbonate." HFRS-2P, HFRS-2, SS-1, CRS-2, CRS-2P, and PCE products showed the same FTIR spectra as presented in Figure 5.18. However, RC-250 and MC-250 products showed FTIR spectra nearly identical yet distinctly different from the other products. The FTIR spectrum for the MC-50 product shows a slight shift to lower wave numbers, indicating a slight molecular structure change compared to that of RC-250 product. Chemically, both MC-50 and RC-250 products are the same. FTIR absorption bands shown in the spectra of both cutback samples were all associated with kerosene that is the base material used in the making of these products.

Samples given in Table 5.3 were analyzed using KBr pellets, while samples given in Table 5.4 were all analyzed using the ATR-reflectance method that eliminates KBr pellet preparation. However, as observed and discussed previously, FTIR spectra taken by KBr pellets showed smoother traces, whereas their ATR counterparts were somewhat noisy. The level of background noise in those traces taken using the ATR method was not strong enough to interfere with the analysis.

A second batch of CRS-2 and CRS-2P products received from supplier B showed exactly the same FTIR spectra as first batch products from this supplier, indicating uniformity in these products. Similarly, the same products received from suppliers D and B showed identical FTIR spectra that are indicative of the product uniformity between these suppliers. In addition, HFRS and HFRS-2P products of both suppliers D and A showed a very similar FTIR trace.

In order to be able to observe the FTIR band related to the polymer content of HFRS-2P, CRS-2P, and CHFRS-2P products, samples of these products need to be heated. Samples heated to 100°C showed a typical 966 cm^{-1} absorption band associated with SBS polymer in these products. AASHTO T302-05 recommends to heat emulsions to a temperature of 82 °C.

In summary, the FTIR technique is not suitable for characterization of antistripping agents in asphalt materials due to the fact that the concentration level of antistripping agents is low (about 0.1-2%), and band overlap between emulsion agents (surfactants) and antistripping agents is possible (U. Bagampadde and U. Isacsson 2006). Previous investigators concluded that amine-containing emulsion cannot be analyzed using FTIR (U. Bagampadde and U. Isacsson 2006).

6. QUALITY AND UNIFORMITY OF CONCRETE SPALL REPAIR EPOXY MATERIALS

6.1 Background

Punchout formation and deep spalling are two distress types that are consequences of transverse cracking in continually reinforced concrete pavements (CRCP). Delamination of concrete from reinforcing rebar possibly due to temperature or moisture variation is believed to be responsible for transverse cracking. Punchout and spalling are prevalent in Houston which is a large urban district. These types of distresses usually require costly Full Depth Repair (FDR). Successful application of spall repair epoxy materials saves money and time in eliminating the need of FDR. TxDOT has sponsored Project 0-5110 through which mechanical properties of a number of spall patching materials were evaluated and guidelines for repair procedures were developed. In this research, FTIR fingerprint spectra of all components of commonly used spall repair materials were obtained to ensure quality and uniformity of these materials.

6.2 Protocol for FTIR Analysis of Epoxy

6.2.1 ATR Method

Approximately 10 g of epoxy is placed on a Germanium optical crystal within the ATR accessory. ATR-FTIR analysis is done on a Thermoelectric Avatar 370 DTGS with ATR accessory from 4000 to 500 cm^{-1} using 48 scans with a resolution of 4 cm^{-1}. Five separate samples are prepared to determine quality and repeatability of measurements. The Germanium crystal is cleaned with acetone, then washed with water and dried between sample tests. The manufacturer instruction manual can be utilized for functional group analysis using the available library component of the FTIR software package.

6.2.2 Transmittance Method

Approximately 10 g of epoxy is placed on a wax sheet, and approximately 10 g of the catalyst additive is placed on another wax sheet and placed under a fume hood. Then 100 mg of potassium bromide (KBr) is pressed in a 13 mm die for two minutes to achieve a solid KBr pellet. This pellet is then placed on top of the epoxy that was previously prepared on wax paper, to achieve a thin transparent coat of asphalt on the pellet. FTIR analysis is done on a Thermoelectric Avatar 370 DTGS from 4000 to 400 cm^{-1} using 32 scans with a resolution of

2 cm^{-1}. Five separate samples are prepared and tested to determine quality and repeatability of measurements. The manufacturer instruction manual can be utilized for functional group analysis using the available library component of the FTIR software package.

6.3 ATR-FTIR Analysis of Concrete Spall Repair Product 1 (CSRP 1)

CSRP 1 is a urethane-based repair product that comes in a three-part kit. Part A and part B are the two liquid components, and part C is a pre-weighed aggregate, which contains a mix of fiberglass and sand. Part A and part B components are blended together at a two-to-one ratio for approximately ten seconds, immediately after which component C is added and mixed for an additional two minutes. This product also requires that a primer be added to the repair surface and allowed to cure before placement of the repair material. A catalyst can be added to speed up set time for cold weather applications in low temperature tests. CSRP 1 is an elastomeric concrete repair material that is used for highways and airports. A sample of CSRP 1 product was acquired, and the FTIR- ATR method is applied for qualitatively analysis. CSRP 1 contains part A and B as well as aggregate. Parts A and B are analyzed independently and unmixed, and their physical contents are shown in Tables 6.1 and 6.2.

Table 6.1: CSRP 1 A Chemical Contents.

CSRP 1 Part A		
Contents	**WT.%**	**CAS Registry #**
Proprietary	-	Proprietary
2,4-Toluene Diisocyanate (TDI)	<6%	584-84-9
2,6-Toluene Diisocyanate (TDI)	<2%	91-08-7

Table 6.2: CSRP 1 B Chemical Contents.

CSRP 1 Part B		
Contents	**WT.%**	**CAS Registry #**
Proprietary	-	Proprietary
4,4'-Methylene bis (2-chloroaniline)	39.0%	101-14-4

Figures 6.1 and 6.2 show FTIR-ATR Spectra of the CSRP 1 part A. Spectral results of the FTIR-ATR analysis of the CSRP 1 part B are given in Figures 6.3 and 6.4.
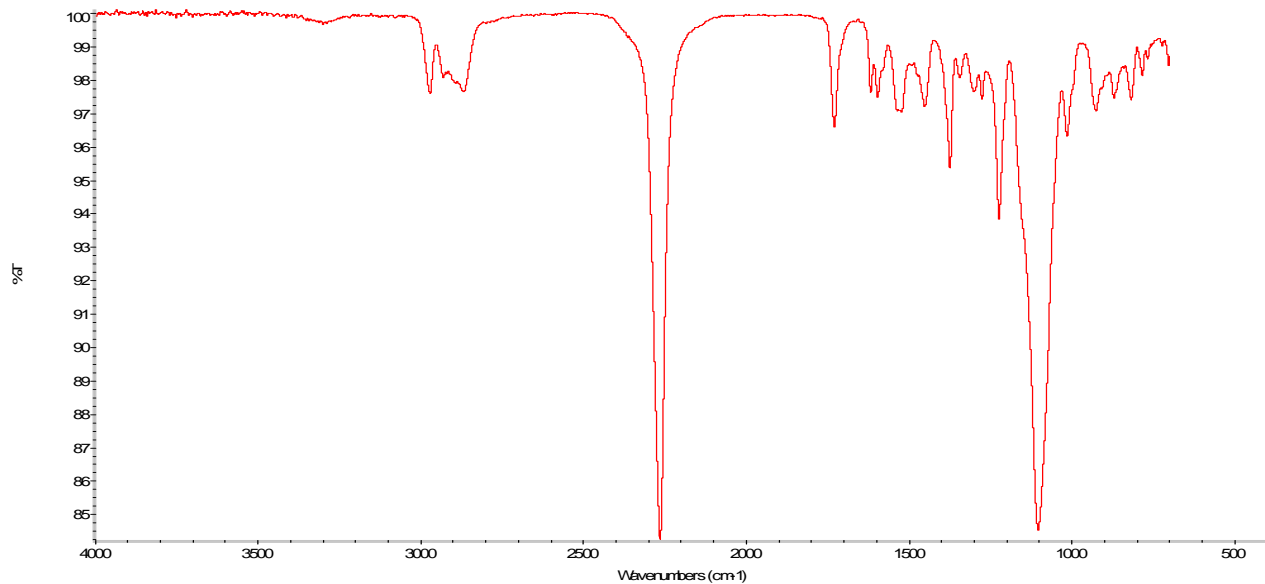
Figure 6.1: ATR-FTIR CSRP 1 Part A Spectrum.
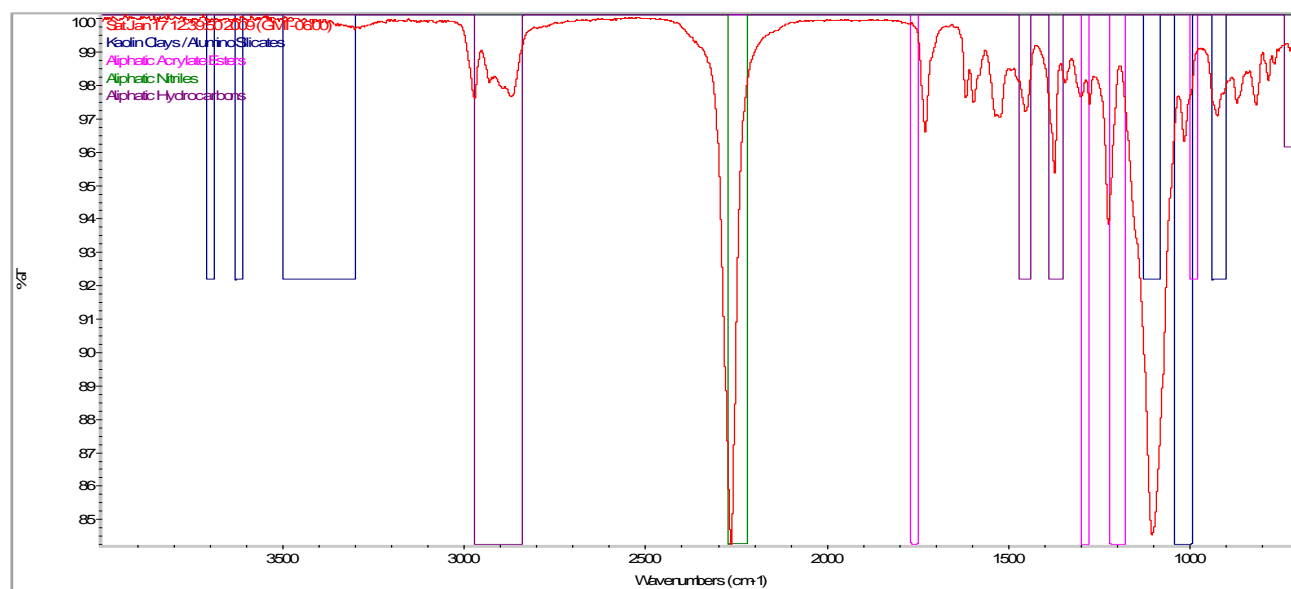
Figure 6.2: Superposition of FTIR Spectrum for CSRP 1 Part A and Absorption Bands for Kaolin Clays/ Alumino Silicates (Blue), Aliphatic Acrylate Esters (Pink), Aliphatic Nitriles (Green), Aliphatic Hydrocarbons (Purple).

59
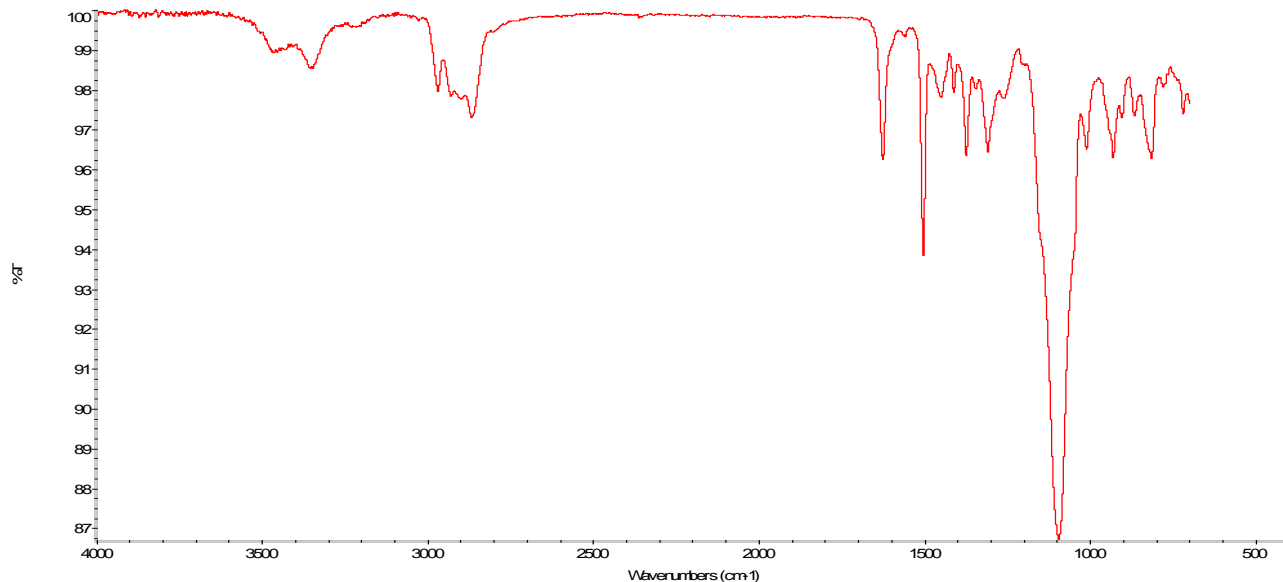
Figure 6.3: ATR-FTIR Spectrum for CSRP 1 Part B.
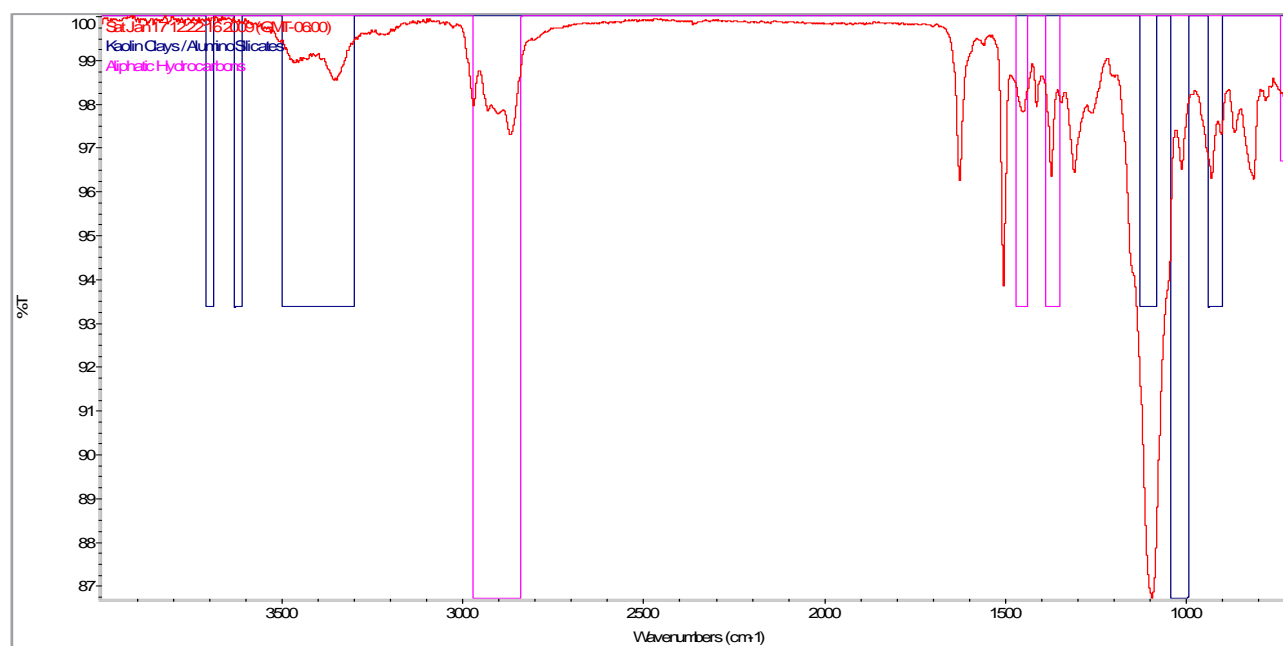
Figure 6.4: Superposition of FTIR Spectrum for CSRP 1 Part B and Absorption Bands for Kaolin Clays/Alumino Silicates (Blue), Aliphatic Hydrocarbons (Purple).

The repeatability and quality of spectrums produced was verified by testing each sample five times and comparing prominent peaks for reproducibility of the test. Figure 6.5 shows an overlay of the five tests done on CSRP 1 part A. The similarity of the spectrums was found to be high if not better for the other three samples, deeming the FTIR-ATR analysis dependable and repeatable.
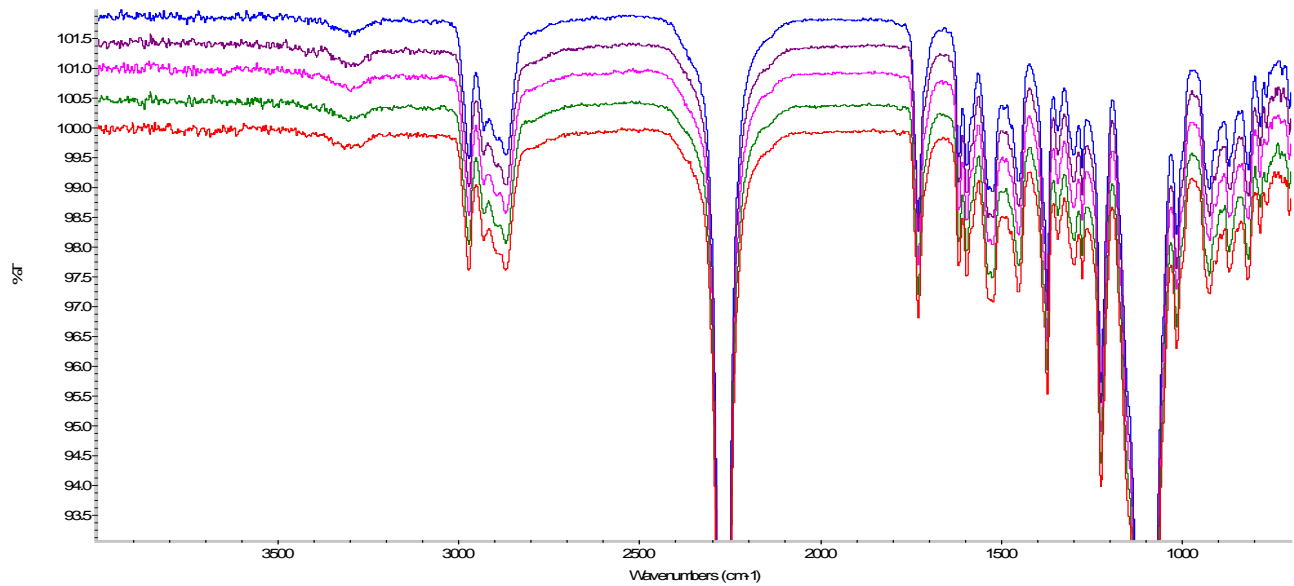
Figure 6.5: Spectra of CSRP 1 Part A test 1 (Blue), 2 (Purple), 3 (Pink), 4 (Green), and 5 (Red).

6.4 ATR and Transmittance FTIR Analysis of Concrete Spall Repair Product 2 (CSRP 2)

CSRP 2 is a thermosetting vinyl polymer that comes in a five-gallon bucket from which the amount required for the size of the repair is measured. Then 1.2 oz of a liquid catalyst is added to a gallon of CSRP 2 and mixed for 30 to 60 seconds. After being mixed, a small amount of this liquid is used to prime the repair surface. Next, blast sand is added to the catalyzed liquid, at a volume ratio of approximately 3 to 4 parts sand per liquid base.

Figure 6.6 shows the overlap of ATR and Transmittance spectra of CSRP 2 in the range of 4000 cm^{-1} to 2400 cm^{-1}, and Figure 6.7 shows the same spectra in the range of 2000 cm^{-1} to 500 cm^{-1}. Figure 6.8 shows the functional group analysis, as provided by EZ OMNIC software, of the transmittance spectrum in the range of 4000 cm^{-1} to 2400 cm^{-1} and 2000 cm^{-1} to 500 cm^{-1} in Figure 6.9. A catalyst is typically used with CSRP 2. FTIR spectra along with the functional group characterization of the catalyst are shown in Figures 6.10-6.13.
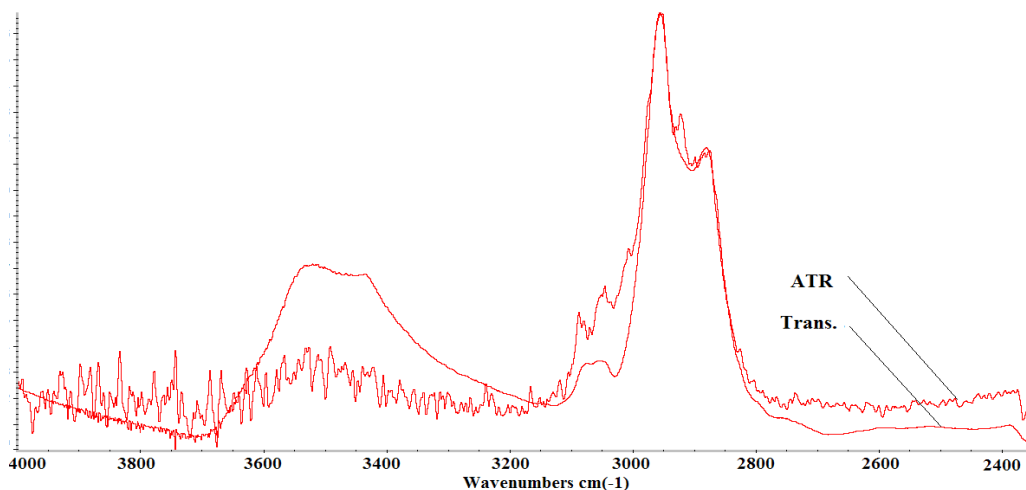
Figure 6.6 FTIR ATR and Transmittance Spectra for CSRP 2 in 4000 – 2400 cm⁻¹ Range.
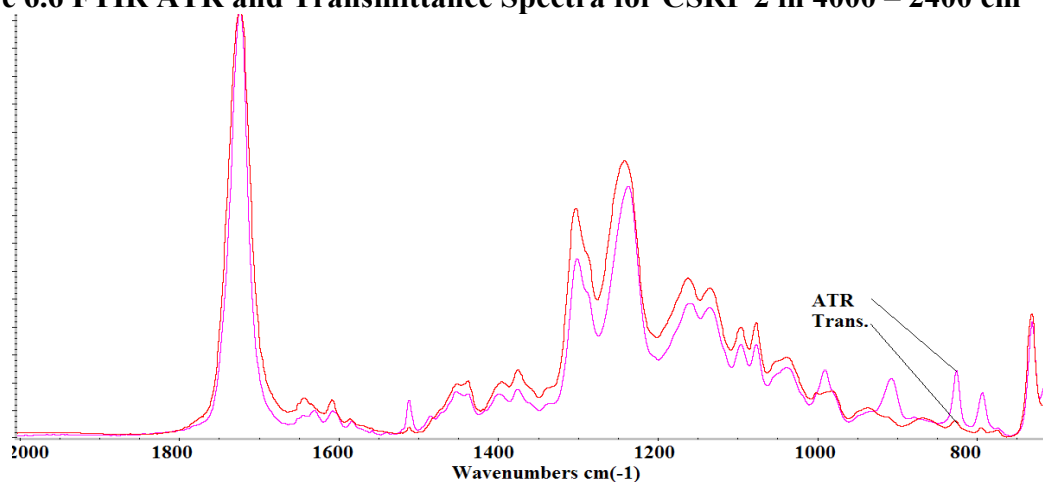
Figure 6.7: FTIR ATR and Transmittance Spectra for CSRP 2 in 2000 – 500 cm⁻¹ Range.
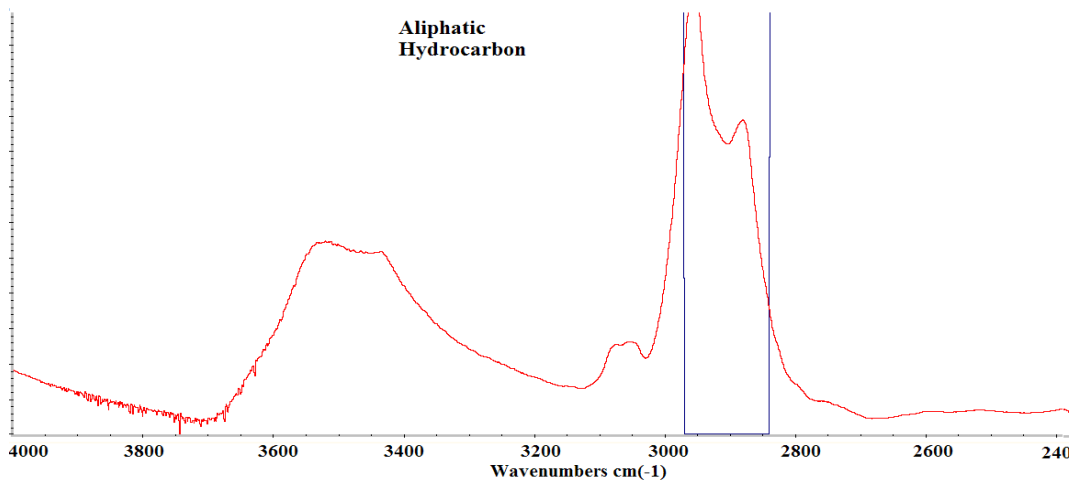
Figure 6.8: Superposition of FTIR Spectrum for CSRP 2 and Absorption Bands for Aliphatic Hydrocarbon.
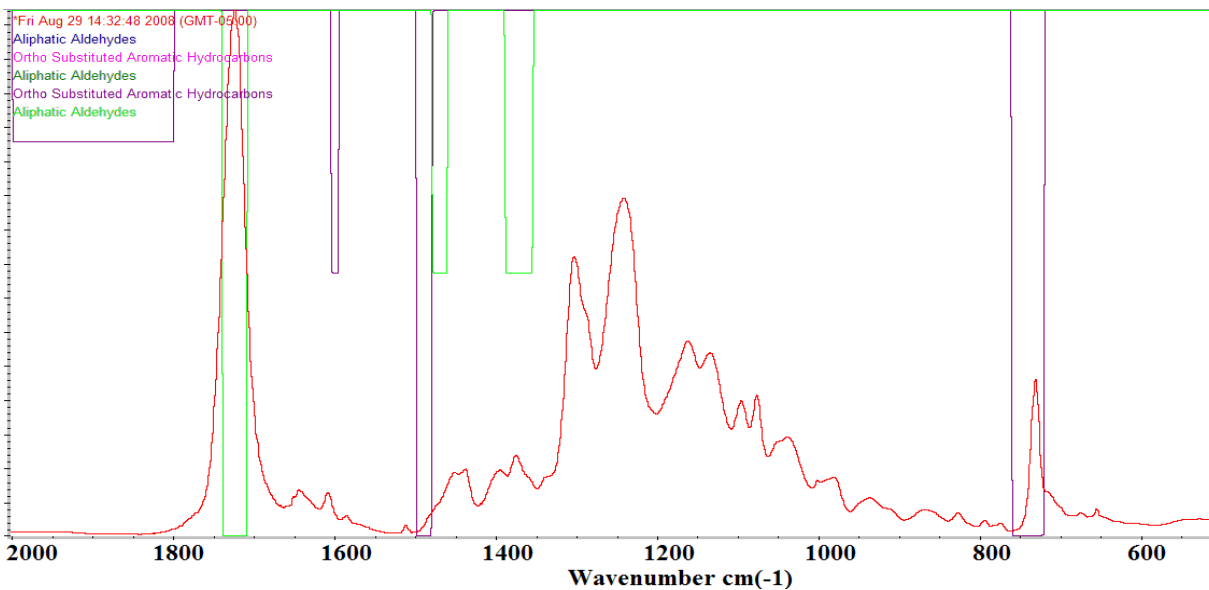
Figure 6.9: Superposition of FTIR Spectrum for CSRP 2 and Absorption Bands for Aliphatic Aldehydes (Green).
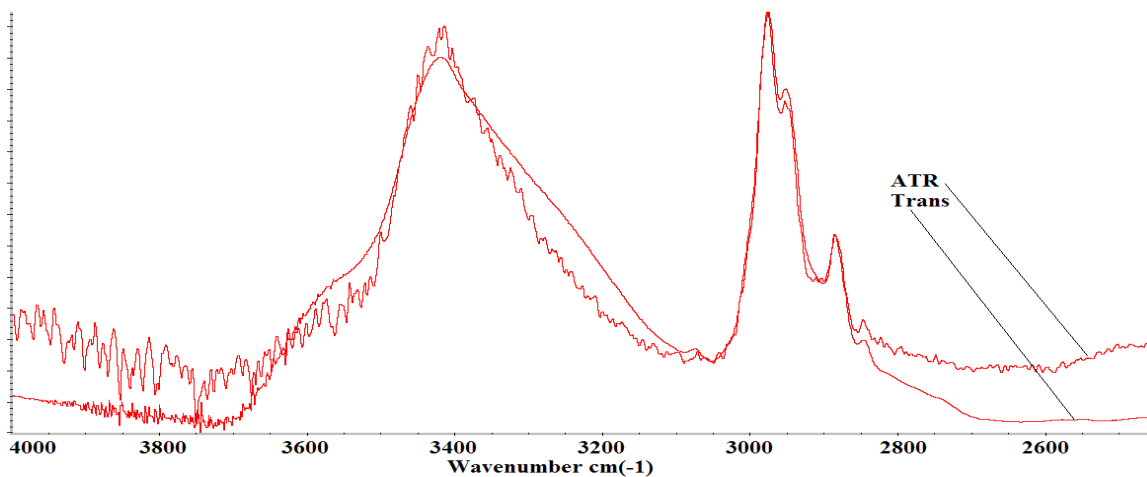
Figure 6.10: FTIR ATR and Transmittance Spectra of CSRP 2 Catalyst.
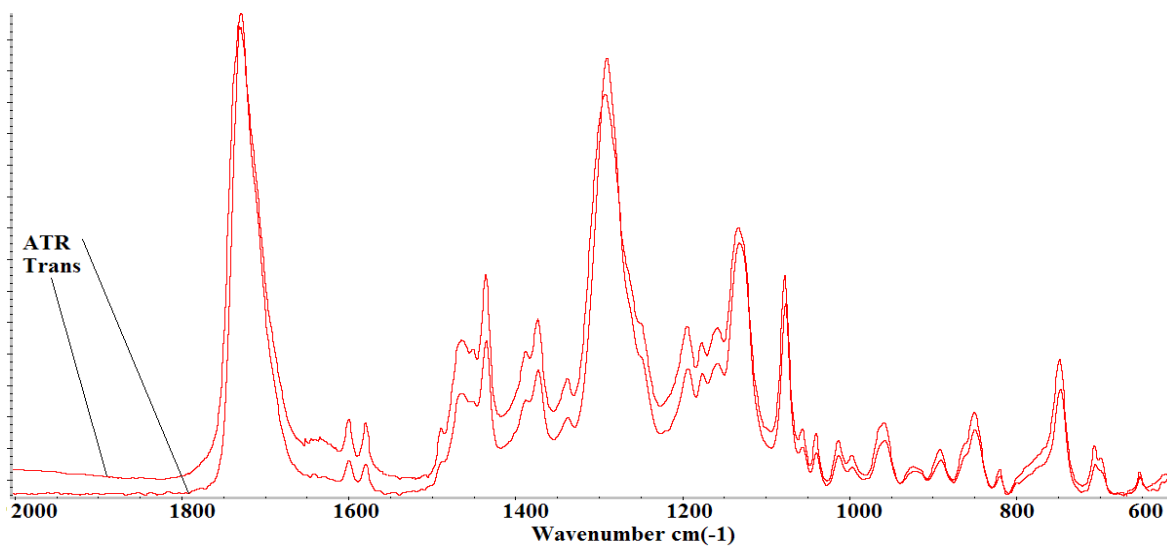
Figure 6.11: FTIR ATR and Transmittance Spectra of CSRP 2 Catalyst.
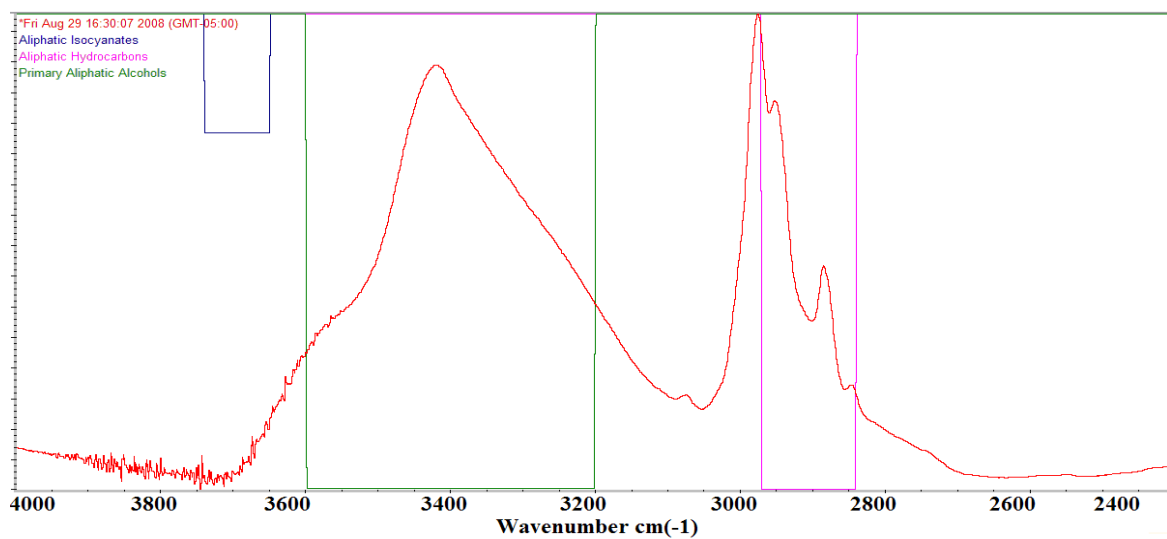
Figure 6.12: Superposition of FTIR Spectrum of CSRP 2 Catalyst and Aliphatic Hydrocarbon (Purple) and Primary Aliphatic Alcohols (Green).
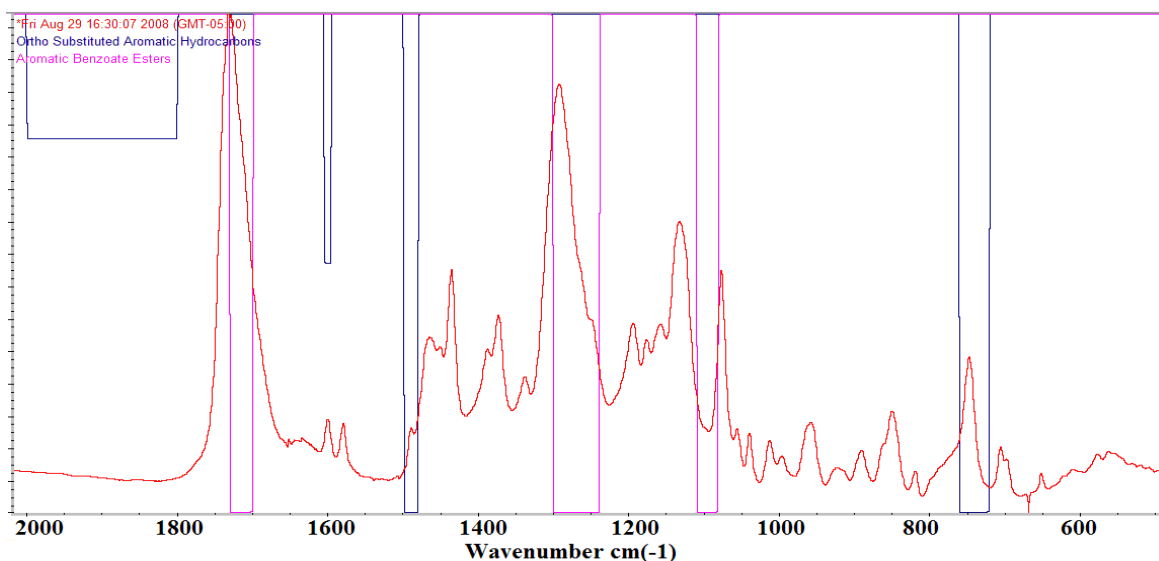
Figure 6.13: Superposition of FTIR Spectra of CSRP 2 Catalyst and Aromatic Benzenate Esters (Purple), Aromatic Hydrocarbon (Blue).

FTIR has been shown to successfully fingerprint CSRP 2 for qualitative purposes in the ATR and transmittance modes. The ATR method is shown to be relatively noisier than transmittance especially in the range of 4000 cm^{-1} to 3000 cm^{-1}, which contains important water content information, as shown in Figure 6.6. Figure 6.7 shows notable differences in peaks 1630 cm^{-1}, 1512 cm^{-1}, 1485 cm^{-1}, 990 cm^{-1}, 908 cm^{-1}, 826 cm^{-1}, 794 cm^{-1}, and 715 cm^{-1}. These results are consistent on all five tests results. Major aromatic and aliphatic hydrocarbons are shown in Figure 6.8 and 6.9 and may serve as a further qualitative, and possibly quantitative, means of analysis.

FTIR has been shown to successfully fingerprint the catalyst additive for CSRP 2 for qualitative purposes in the ATR and transmittance modes. The ATR method is shown to be relatively noisier than transmittance especially in the range of 4000 to 3000 cm^{-1}, which contains important water content information, as shown in Figure 6.10. No major differences can be seen between ATR and transmittance methods. Lack of differences may be verified in Figures 6.10 and 6.11, and are further verified in all five tests. The transmittance method is recommended for use in analyzing the catalyst additive due to its larger spectral range and its cleaner spectrum, especially in the mentioned water band area. Major aromatic and aliphatic hydrocarbons are shown in Figure 6.12 and 6.13, and may serve as a further qualitative, and possibly quantitative, means of analysis.

6.5 ATR and Transmittance FTIR Analysis of Concrete Spall Repair Product 3 (CSRP 3)

CSRP 3 is an epoxy resin that contains parts A and B as well as aggregate. Parts A and B are analyzed independently and unmixed, and their chemical contents (as specified by supplier) are shown in Tables 6.3 and 6.4, respectively.

Table 6.3: CSRP 3 A Chemical Contents.

CSRP 3 Part A		
Contents	**WT.%**	**CAS Registry #**
Proprietary	-	Proprietary
Alkyl Glycidyl Ether	10-30%	68609-97-2
Bisphenol A Diglycidyl Ether Resin	60-100%	25068-38-6

Table 6.4: CSRP 3 B Chemical Contents.

CSRP 3 Part B		
Contents	**WT.%**	**CAS Registry #**
Proprietary	-	Proprietary
Amine	-	-
1,6-Hexanediamine, trimethyl-Trimethylhexamethylenekiamine	-	25620-52-3
Amins, coco alkyl Tetradecylamine	-	61788-46-3
Phenol 2, 4, 6-tris[(dimethylamino)methyl]	-	90-72-2
Phenol	-	108-95-2

Spectral results of the FTIR-ATR analysis of the CSRP 3 part A are given in Figure 6.14, and Figure 6.15.
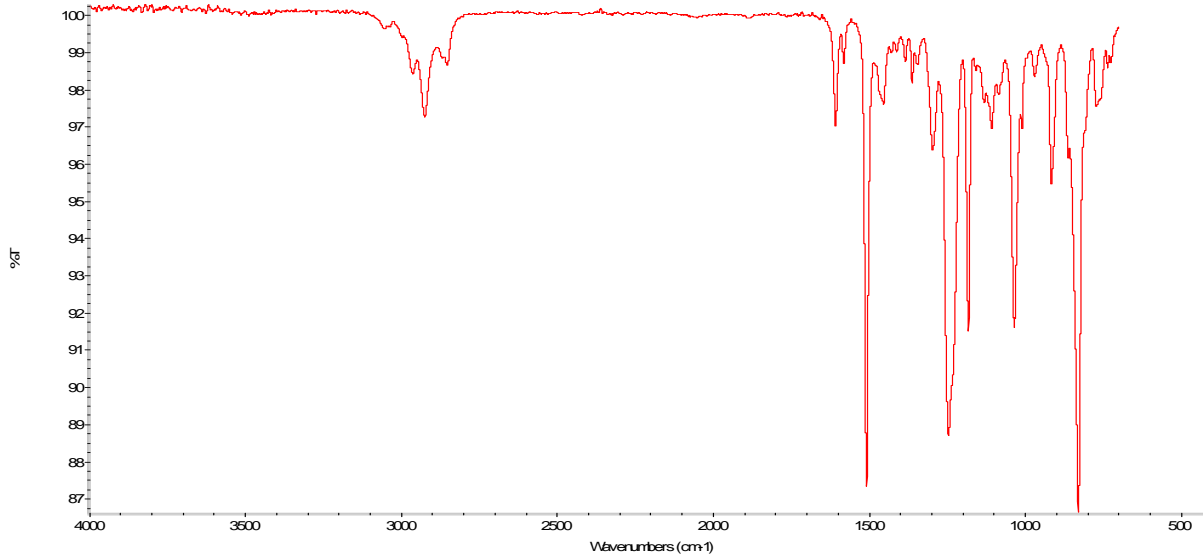
Figure 6.14: ATR-FTIR CSRP 3 Part A Spectrum.
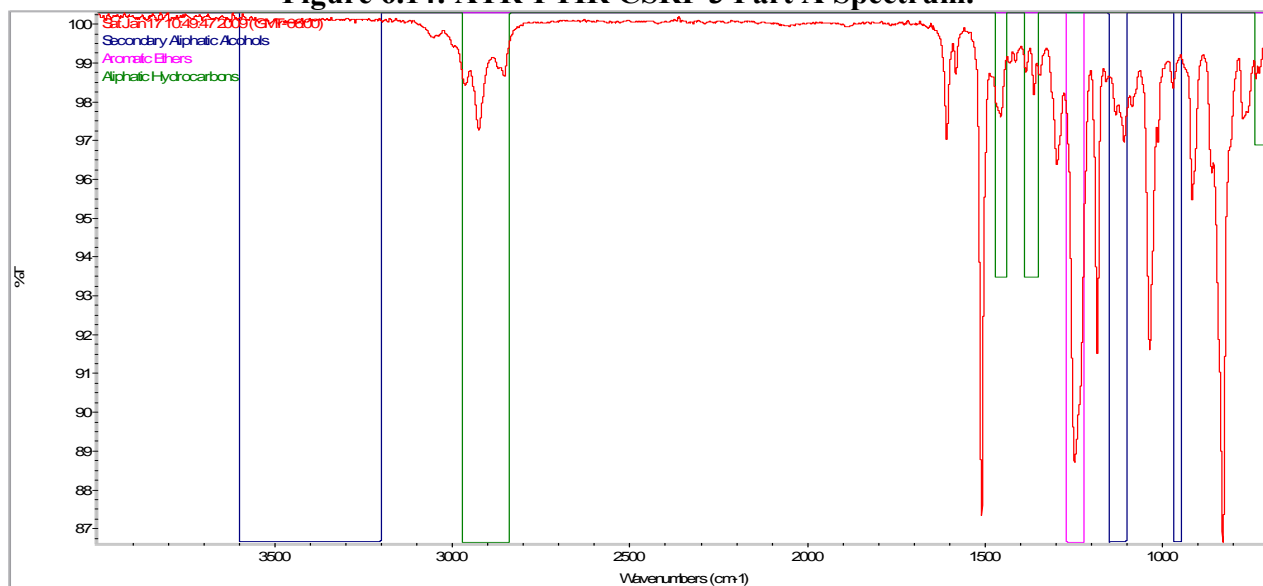
Figure 6.15: Superposition of FTIR Spectrum of CSRP 3 Part A and Absorption Bands of Secondary Aliphatic Alcohols (Blue), Aromatic Ethers (Pink), Aliphatic Hydrocarbons (Green).

Spectral results of the FTIR-ATR analysis of CSRP 3 part B are given in Figure 6.16, and Figure 6.17.
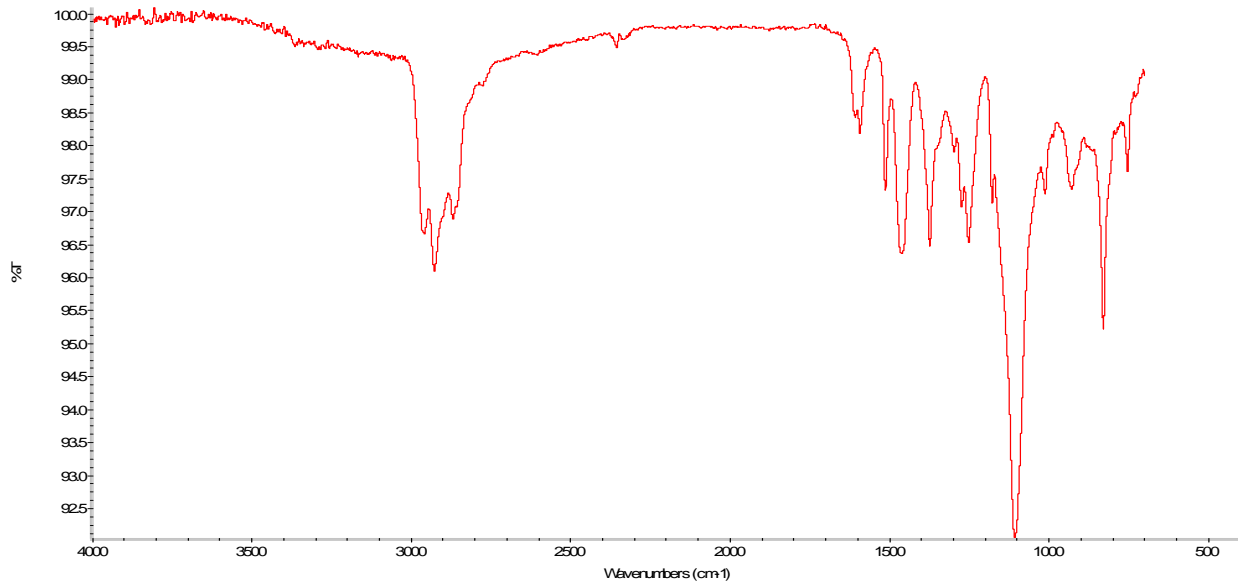
Figure 6.16: ATR-FTIR CSRP 3 Part B Spectrum.
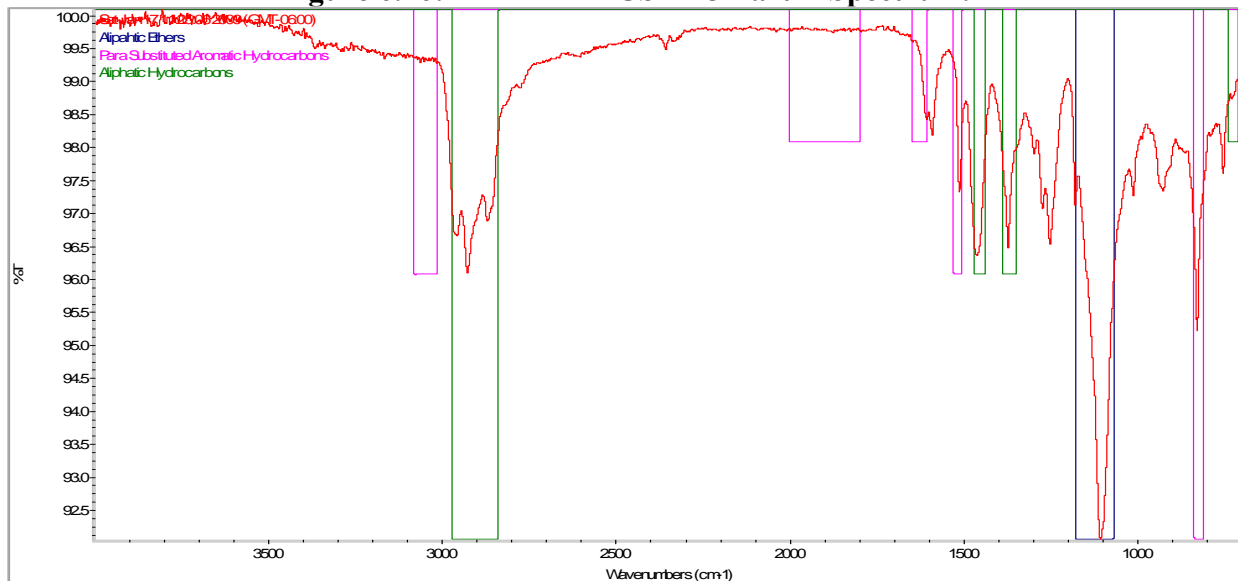
Figure 6.17: Superposition of FTIR Spectrum of CSRP 3 Part B and Absorption Bands of Aliphatic Ethers (Blue), Para Substituted Aromatic Hydrocarbons (Pink), Aliphatic Hydrocarbons (Green).

6.6 ATR and Transmittance FTIR Analysis of Concrete Spall Repair Product 4 (CSRP 4)

CSRP 4 is a two-component epoxy repair material. The product consists of two pre-measured liquid components, part A and part B, which are mixed together at a one-to-one ratio for three minutes. A third component, C, which consists of pre-weighed coarse sand, is then slowly added to the liquid and mixed thoroughly. The product is then placed in the repair area. No primer is needed. The company produces a different formulation for cold weather applications. FTIR transmittance and ATR methods are applied in qualitative analysis of CSRP 4

component A and B. Five independent samples of each resin and hardener are analyzed. FTIR will be employed to analyze and quantify these samples by Thermoelectron Avatar 370 infrared spectrometer.

The transmittance spectrum of the CSRP 4 Component A is shown in Figure 6.18 in the range of 4000 to 400 cm⁻¹. Figure 6.19 shows the overlap of ATR and Transmittance spectra of CSRP 4 Component A in the range of 4000 to 2400 cm⁻¹, and Figure 6.20 shows the same spectra in the range of 2000 to 800 cm⁻¹. Figure 6.21 shows the functional group analysis of the transmittance spectrum, as provided by EZ OMNIC software.
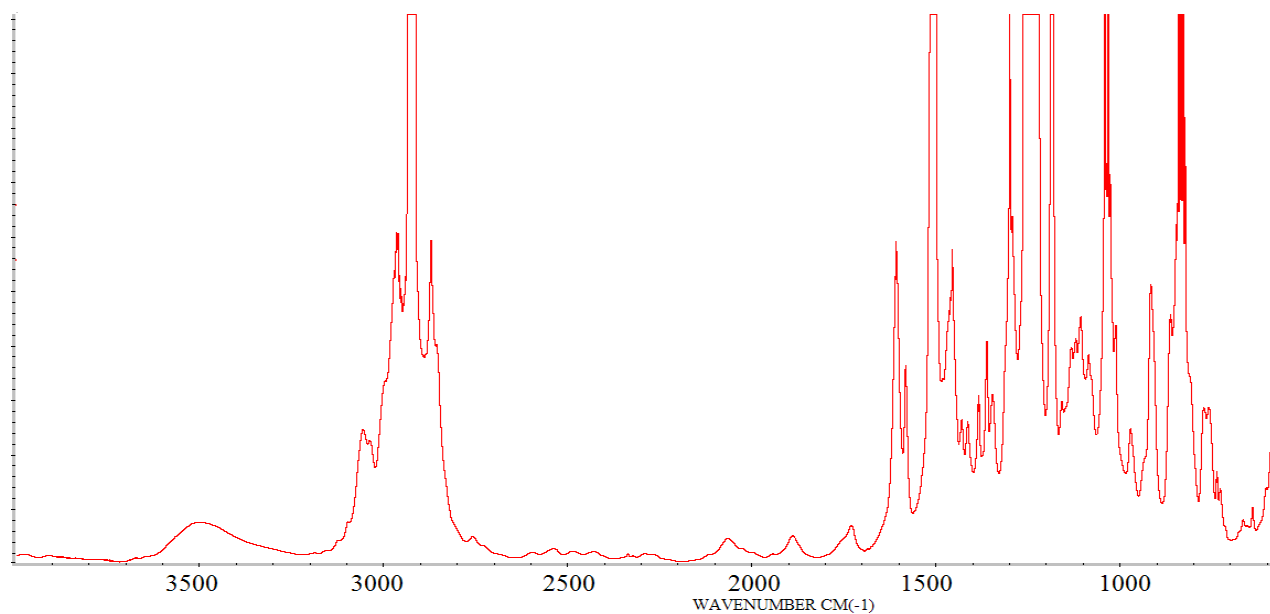
WAVENUMBER CM(-1)
Figure 6.18: FTIR Spectrum of CSRP 4 Component A.
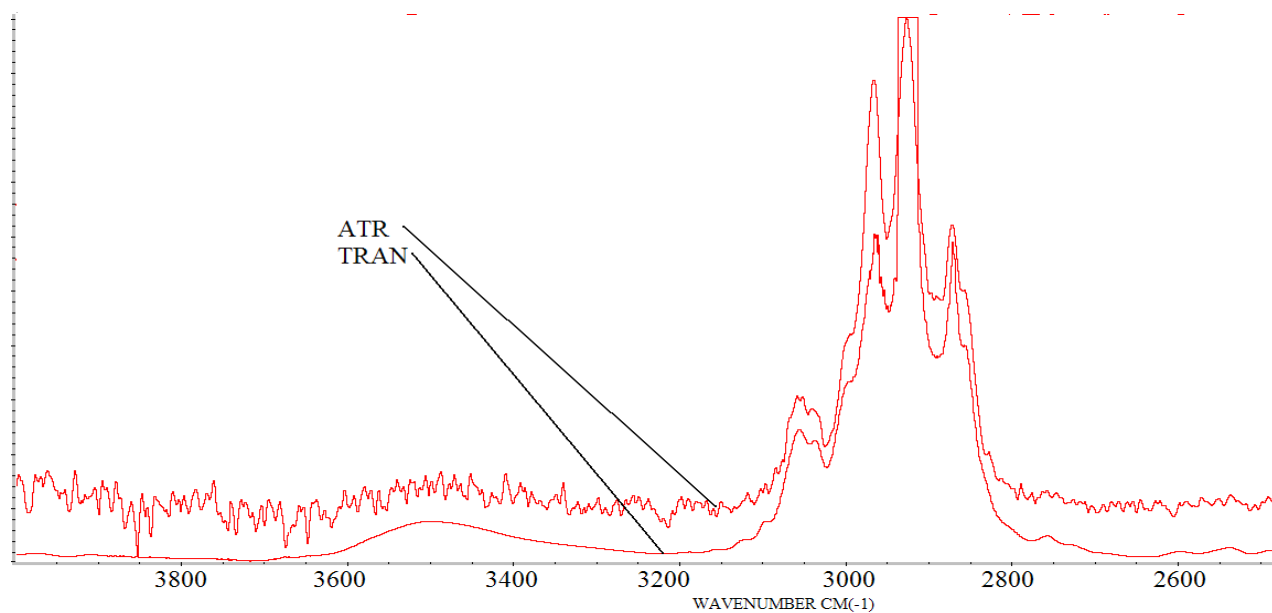
Figure 6.19: FTIR ATR and Transmittance Spectra of CSRP 4 Component A.
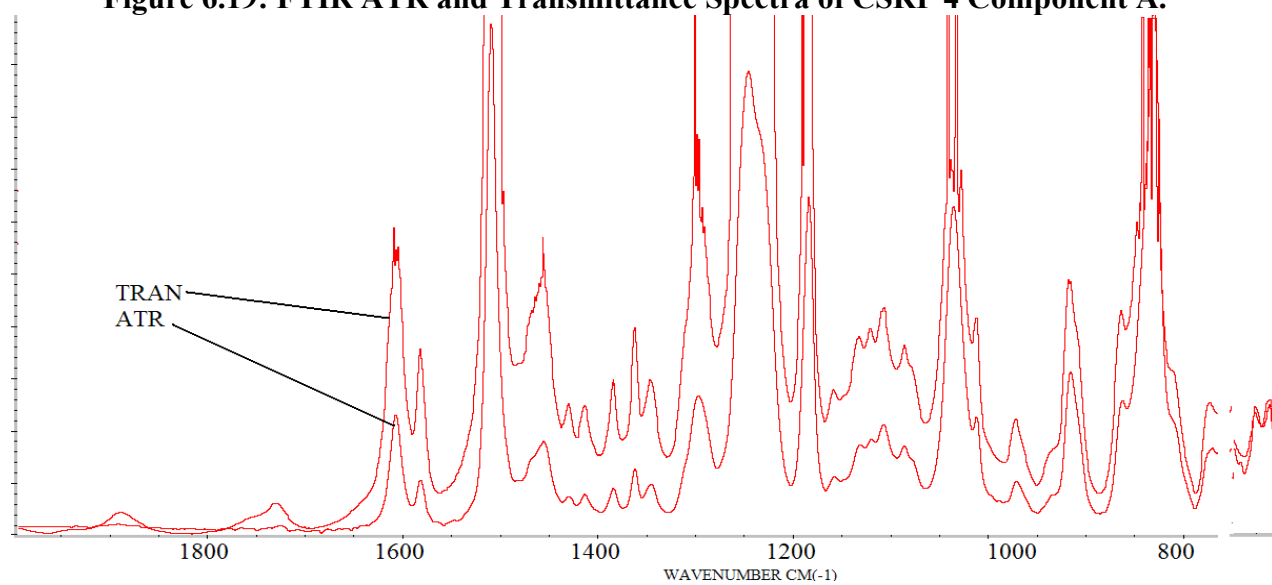
Figure 6.20: FTIR ATR and Transmittance Spectra of CSRP 4 Component A.

WAVENUMBER CM(-1)
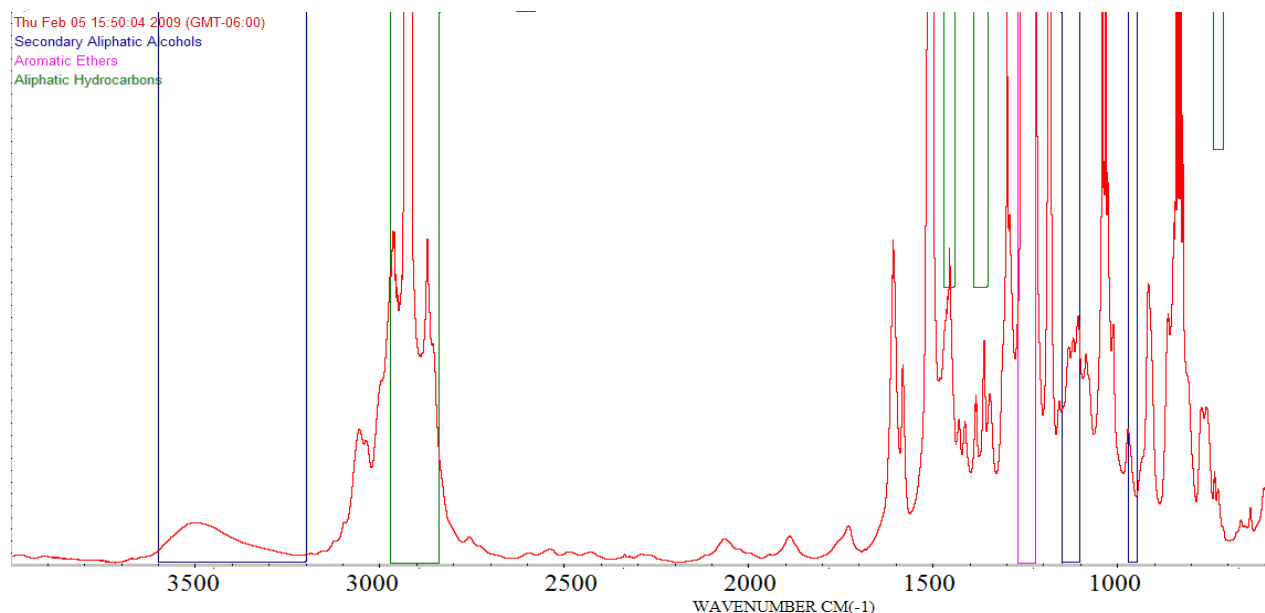
Figure 6.21: Superposition of FTIR Spectrum of CSRP 4 Component A and Absorption Bands of Aliphatic Hydrocarbon (Green), and Aliphatic Alcohols (Blue).

The transmittance spectrum of CSRP 4 Component B is shown in Figure 6.22 in the range of 4000 to 400 cm⁻¹. Figure 6.23 shows the overlap of ATR and Transmittance spectra of CSRP 4 Component B in the range of 4000 to 2400 cm⁻¹, and Figure 6.24 shows the same spectra in the range of 2400 to 800 cm⁻¹. Figure 6.25 shows the functional group analysis of the transmittance spectrum, as provided by EZ OMNIC software. Figure 6.26 shows an overlay of the spectrum of component A and B.

WAVENUMBER CM(-1)
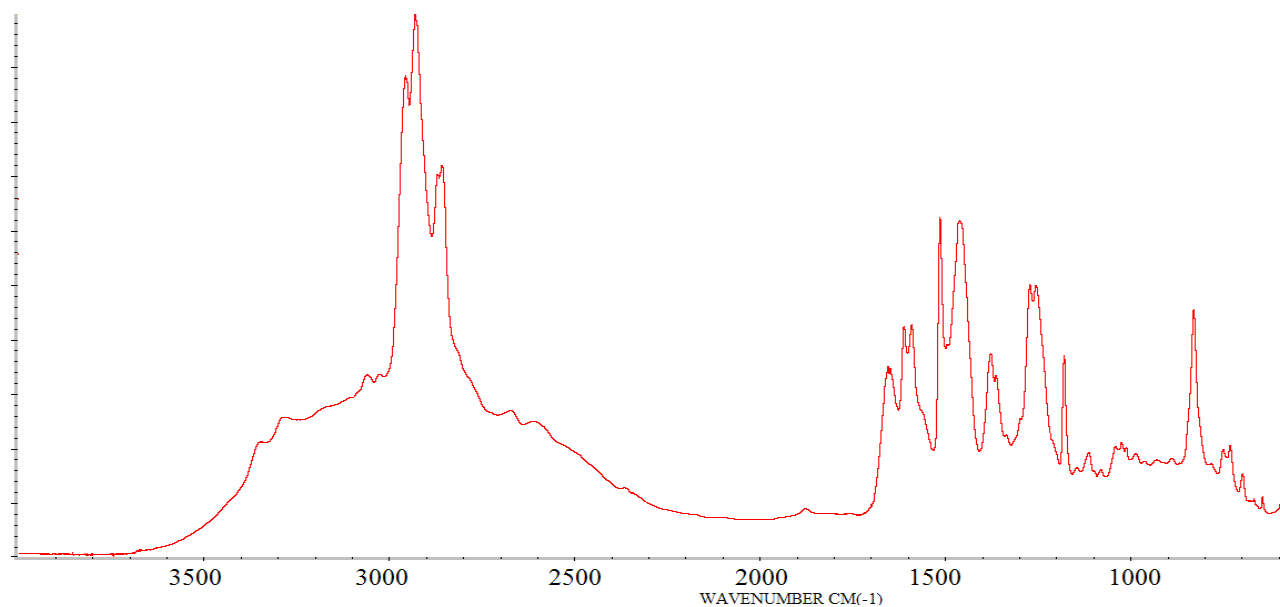
Figure 6.22: Transmittance FTIR Spectrum of CSRP 4 Component B.

71
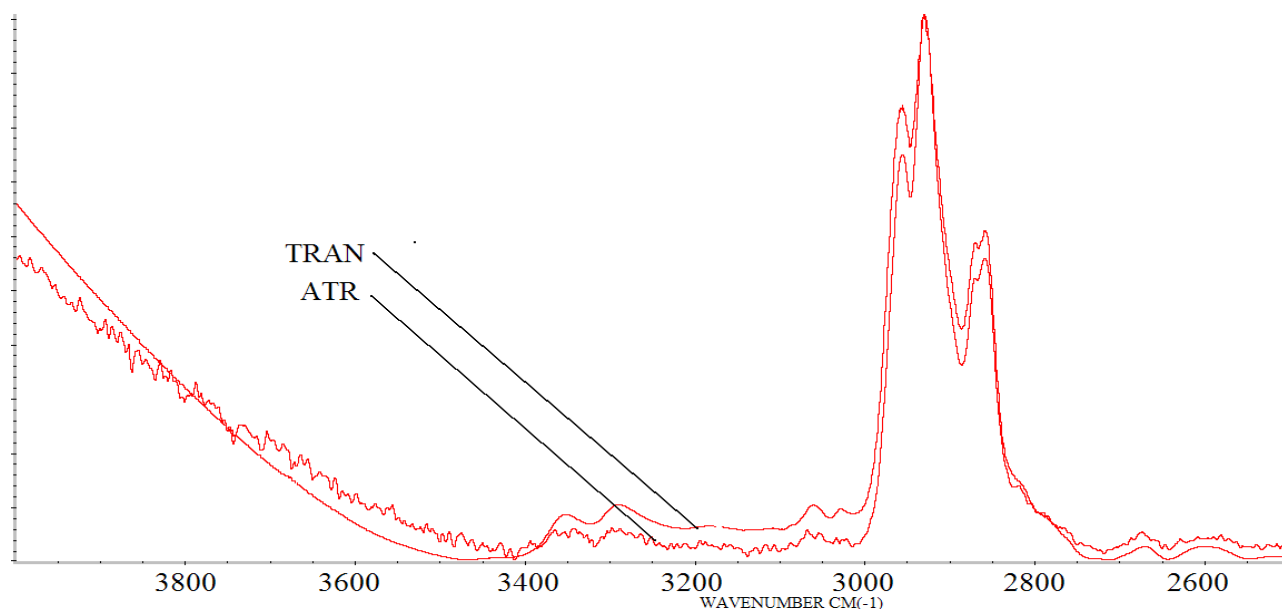
Figure 6.23: FTIR ATR and Transmittance Spectra CSRP 4 Component B 4000 – 2400 cm⁻¹ Range.
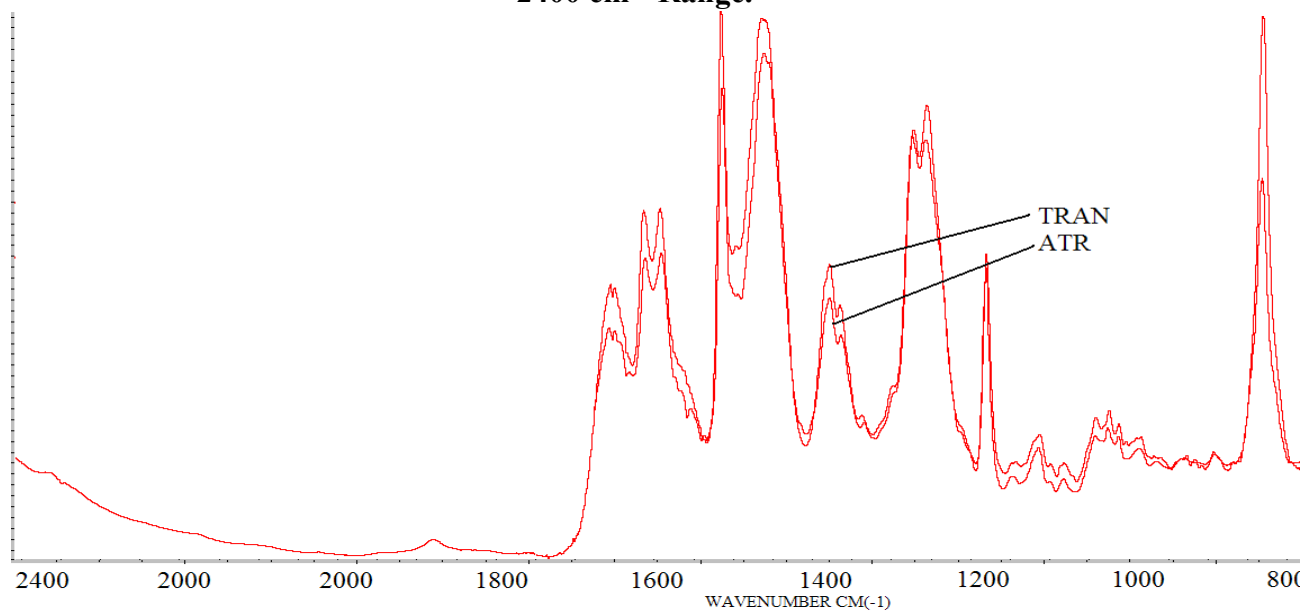
Figure 6.24: FTIR ATR and Transmittance Spectra CSRP 4 Component B 2400 – 800 cm⁻¹ Range.
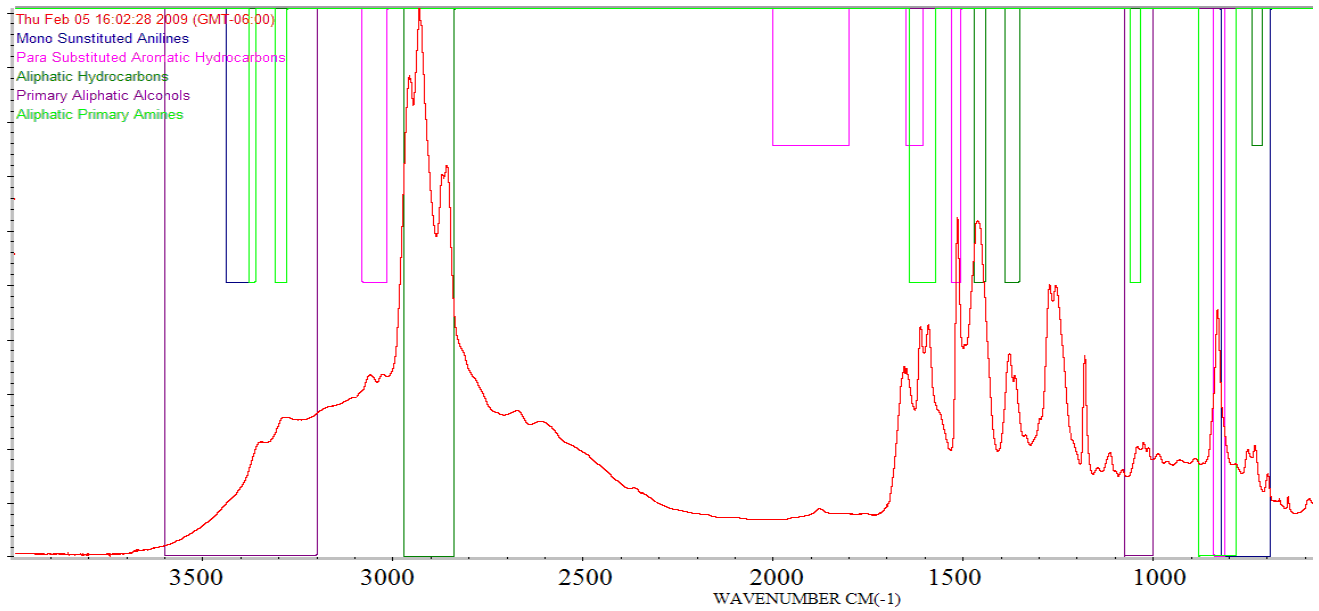
Figure 6.25: Superposition of FTIR Spectrum of CSRP 4 Component B and Absorption Bands for Aliphatic Amines (Green), Aromatic Hydrocarbons (Purple), and Aliphatic Hydrocarbons (Dark Green).
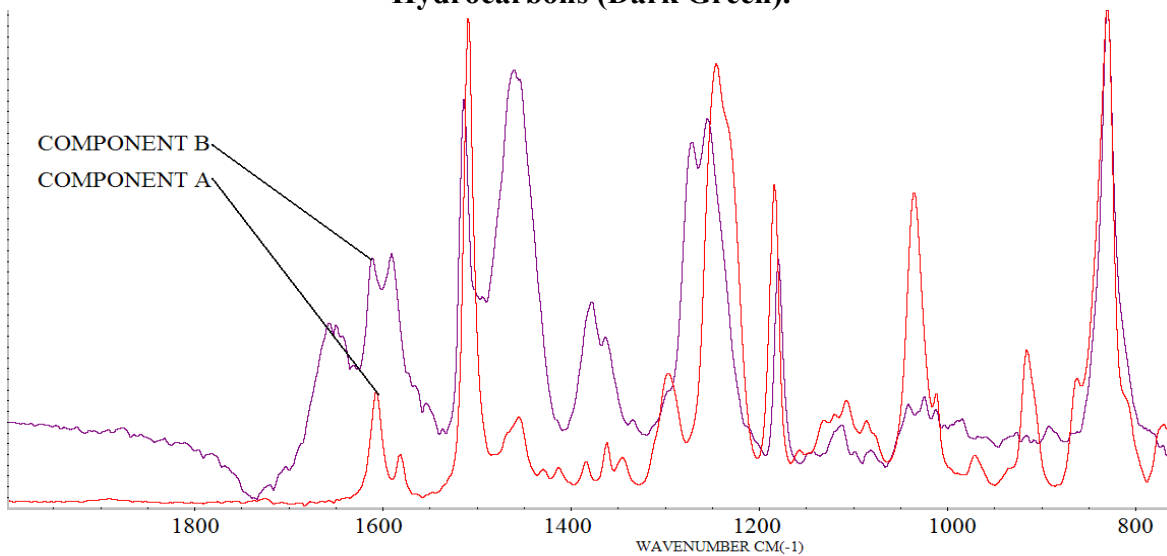
Figure 6.26: Overlay of FTIR Spectra of CSRP 4 Components A and B.

6.7 Uniformity Analysis of Concrete Spall Repair Epoxy Products

Epoxy products received from different suppliers were analyzed in January 2009 and same products were analyzed again in July 2009, as well as a new batch of the same products obtained from the same suppliers. Results are shown in Figures 6.27 through 6.32.
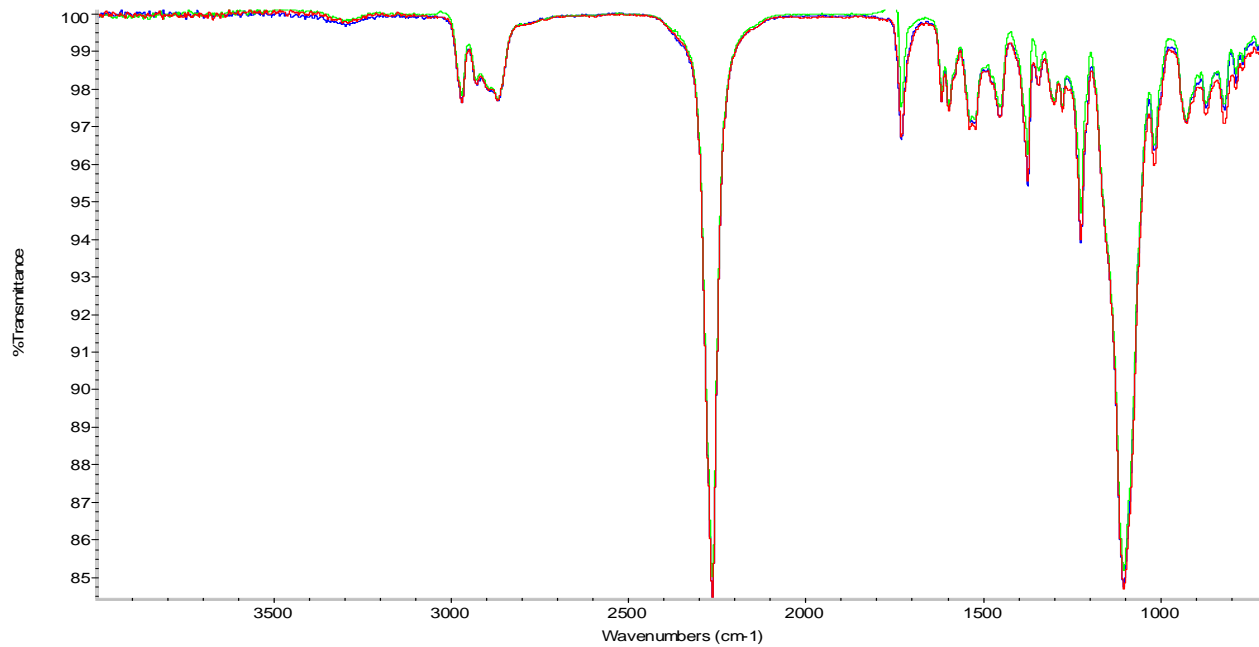
Figure 6.27: CSRP 1 A – Batch 1 Jan 09 (Green), Batch 1 July 09 (Red), Batch 2 July 09 (Blue).
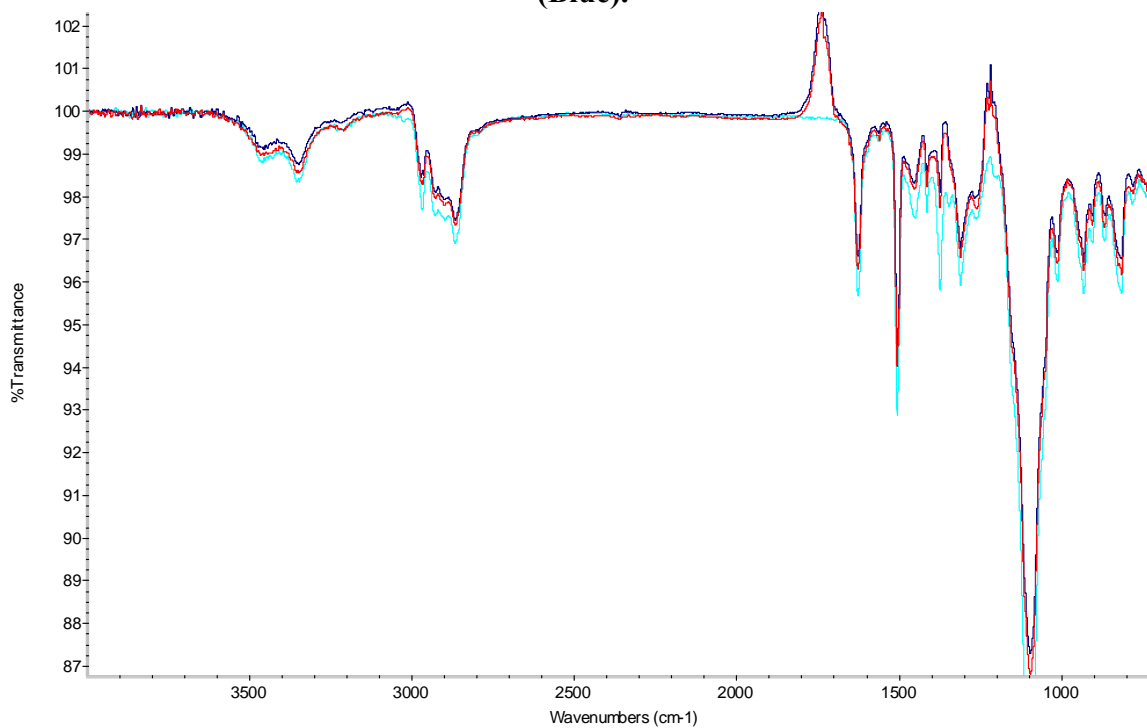
Figure 6.28: CSRP 1 B – Batch 1 Jan 09 (Light Blue), Batch 1 July 09 (Blue), Batch 2 July 09 (Red).
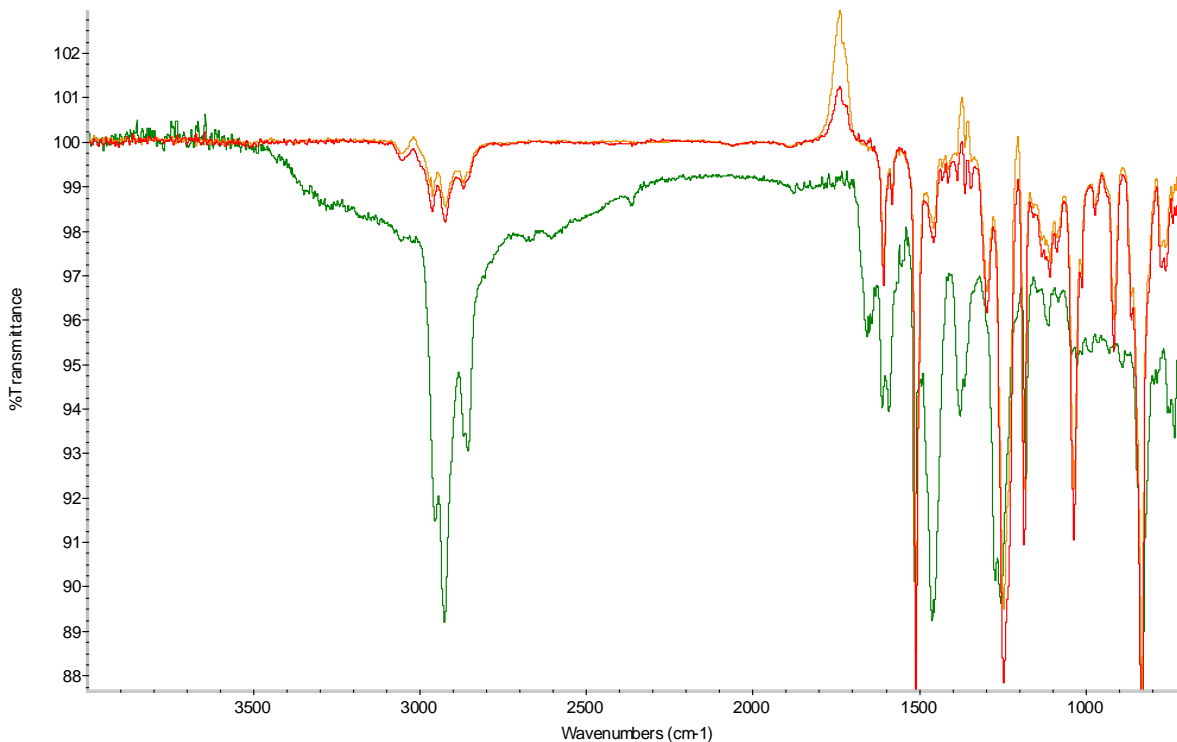
Figure 6.29: CSRP 4 A – Batch 1 Jan 09 (Green), Batch 1 July 09 (Orange), Batch 2 July 09 (Red).
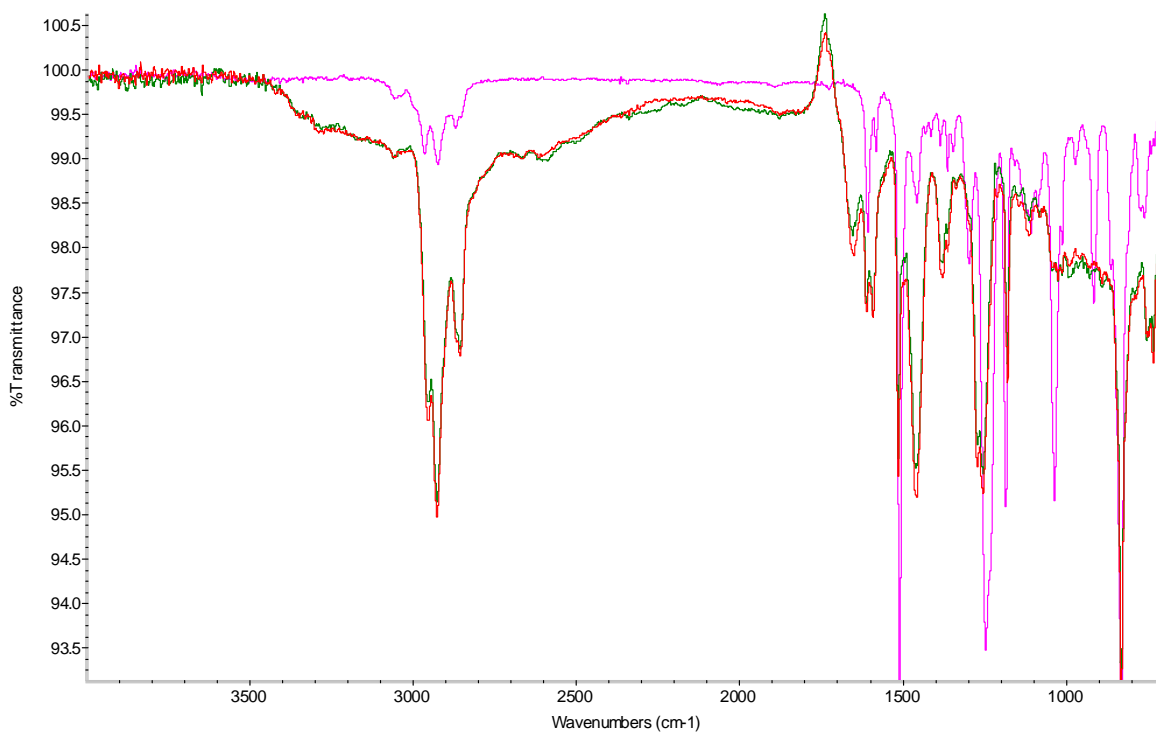
Figure 6.30: CSRP 4 B – Batch 1 Jan 09 (Red), Batch 1 July 09 (Pink), Batch 2 July 09 (Green).
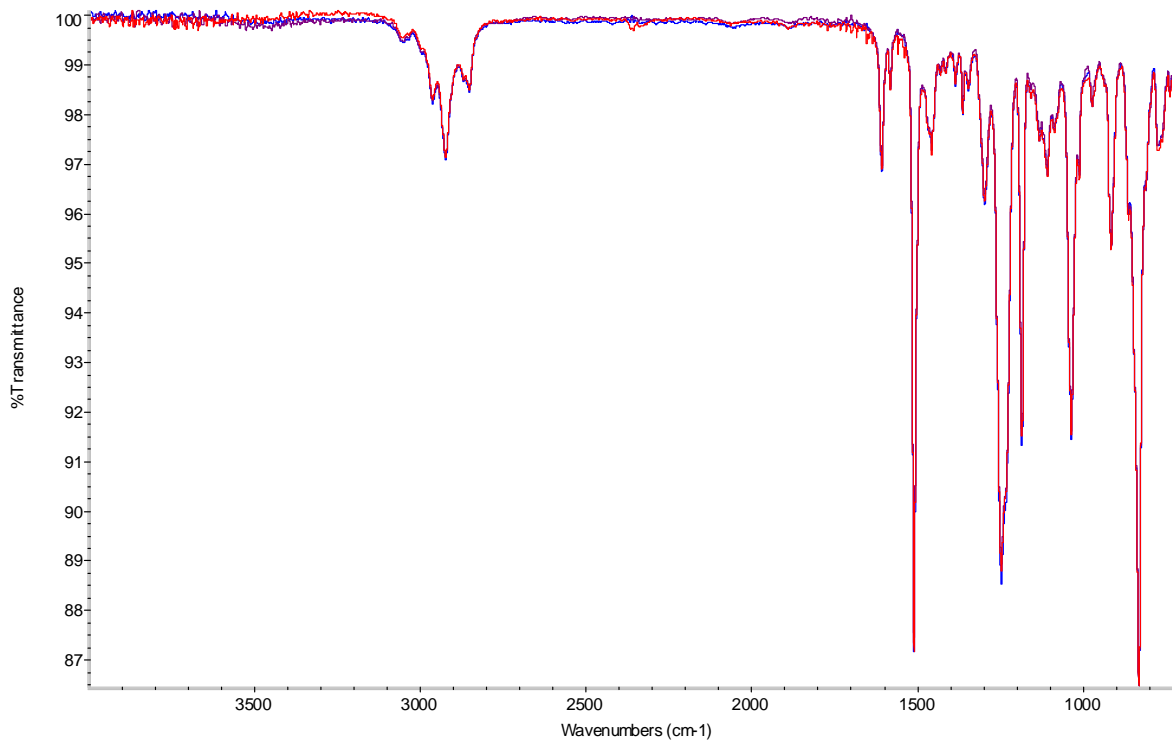
Figure 6.31: CSRP 3 A – Batch 1 Jan 09 (Orange), Batch 1 July 09 (Red), Batch 2 July 09 (Blue).
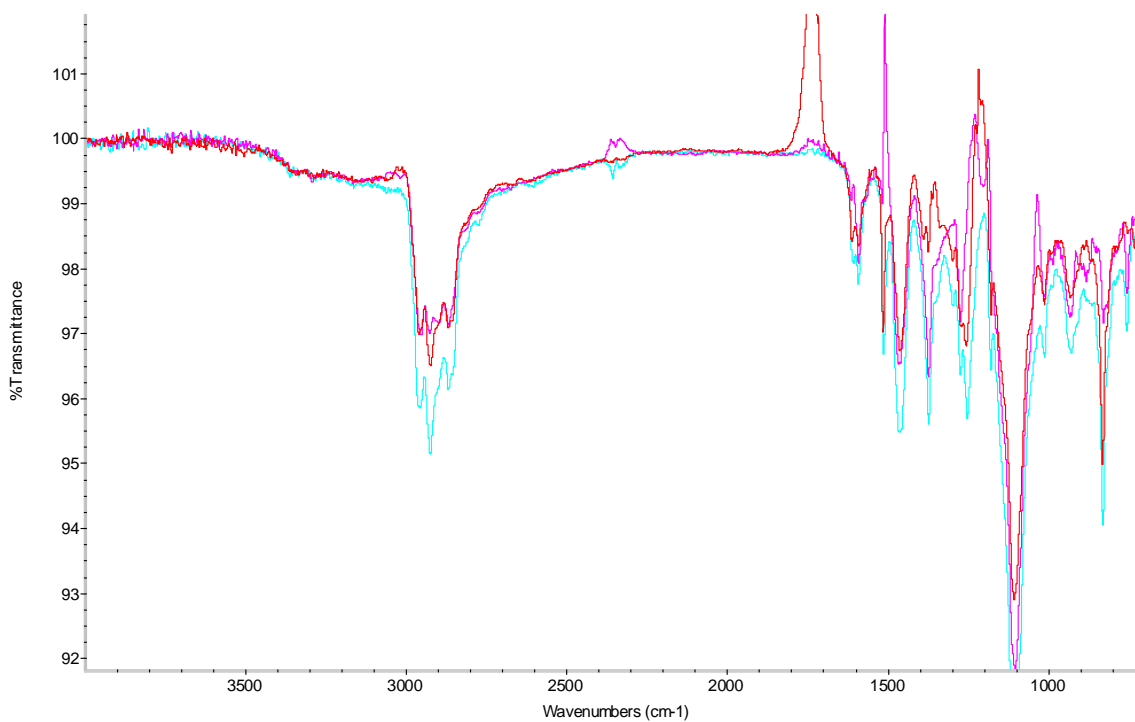
Figure 6.32: CSRP 3 B – Batch 1 Jan 09 (Light Blue), Batch 1 July 09 (Red), Batch 2 July 09 (Pink).

6.8 Summary

Samples of commercial concrete patching materials commonly used by TxDOT in spall repair of concrete pavements (CSRP 1, CSRP 2, CSRP 3, and CSRP 4) were acquired from manufacturers. FTIR fingerprints of all components of the epoxy systems (component A, component B, and a catalyst) were produced and are presented in Figures 6.1-6.26. The two methods of ATR and transmission were employed for this task. A protocol was developed for FTIR spectra acquisition of all types of concrete patching materials for both ATR and transmission methods. The testing protocol for FTIR spectrum collection and analysis is given in section 6.2. Based on collected FTIR spectra for the samples analyzed using spectrometer available at UNT, it was observed that spectra collected using the ATR method were generally noisier than the spectra collected using the transmission method. The level of noise varied from one sample to another and transmission spectra were generally smoother than ATR counterparts. The noise level was not significant and did not interfere with qualitative identification of major components. However, noise associated with a given collected FTIR spectra will impact baseline corrections for quantitative analysis. Identification of functional groups present in each sample was performed using the available library.

Two batches of all four concrete spall repair epoxy materials were obtained and analyzed. Similar spectra for all samples in a given variety were produced, which show uniformity of the products between batches. In addition, keeping epoxy materials at room temperature for six months was shown to not change the chemistry of these materials as evidenced by their respective FTIR spectra.

7. QUALITY AND UNIFORMITY OF CONCRETE CURING MEMBRANES AND EVAPORATION RETARDANTS

Proper hydration of freshly placed concrete pavement depends strongly on preservation of concrete moisture during curing. Availability of moisture during curing of cement determines whether or not required compressive strength and durability is likely to develop. It is widely accepted that the minimum relative humidity needed for proper hydration of Portland concrete cement (PCC) is estimated to be about 80% below which hydration of cement virtually stops, and no further improvement of concrete properties are achieved. In order to prevent moisture evaporation in concrete, a common practice followed by all departments of transportation is to use chemical compounds referred to as "Curing Membranes" and "Evaporation Retardants."

7.1 Classification of Curing Membrane Compounds

ASTM C 309-07 standards classify curing membrane compounds as:
Type I – Clear or translucent without dye
Type I-D Clear or translucent with fugitive dye
Type 2 – White pigmented
The solids dissolved in the vehicle shall be one of the following classes: class A with no restriction, and class B, which must be resin based.

Effectiveness and standard compliance methods for curing compounds do not exist and development of a simple testing technique to assess quality and uniformity of these materials is in great demand. TxDOT requires two applications of curing compounds with a maximum of 180 sf./gal. per each application (TxDOT Project 0-5106). In TxDOT Project 0-5106, four types of curing membranes, namely a solvent-borne resin, a wax emulsion, a solvent-borne acrylic, and an acrylic emulsion, were studied. Researchers of project 0-5106 found that for the moisture loss, the wax emulsion compound performed the best and was almost three times less than that of non-cured concrete. They also concluded that high Volatile Organic Compound (VOC) containing curing compounds show slower moisture loss compared to low VOC compound, but VOC content appeared not to be a good indicator of the curing compound performance. N.M. Whiting et al. (2003) fingerprinted low and high VOC for Minnesota DOT and concluded that neither high VOC nor low VOC curing compounds performed as well as samples cured with water or plastic sheeting.

Two issues in applications of curing membrane are lack of an acceptable compliance testing method for effectiveness of the application of curing membranes and lack of a rapid and reliable evaluation of curing membrane compounds. In this project, emphasis will be on the latter aspect. It is envisioned that FTIR could be a suitable technique to assess quality and uniformity of typical curing membrane compounds.

In this research, two batches of two curing membrane compounds (CMC 1 and CMC 2) and most of the evaporation retardants were investigated. Test Procedure for Cement Moisture Barriers and Evaporation Retardants is presented in Appendix C.

7.2 Results

Figures 7.1-7.4 show FTIR spectra of dried concrete curing membrane compounds and Figures 7.5 through 7.10 present FTIR spectra of a number of evaporation retardants currently being used by TxDOT. Two batches (# 60903, # 90360) of CMC 1 containing white pigment showed similar FTIR fingerprints. Two sets of spectra for each batch were produced to ensure reproducibility of the results (Figures 7.1-7.4). In addition, two batches (#9FG012, #9FG018) of CMC 2 water-based, resin-based concrete curing compound were dried and analyzed. FTIR spectra of these compounds that are distinctly different than the CMC 1 sets are shown in Figures 7.3-7.4. Absorption bands observed in the spectra of CMC 1 samples were matching those of Polyethylene and Kaolinite, as shown in Figure 7.11. Absorption bands in the spectra of CMC 2 curing compound matches with those of Poly(acrylamide) and Ammonium d4deuteroxide as shown in Figure 7.12. Comparing FTIR spectra of curing compounds for both batches, one can see uniformity of these products in different batches. Evaporation retardants products received from different suppliers showed their corresponding FTIR fingerprint spectra, which were different enough to distinguish them from another.
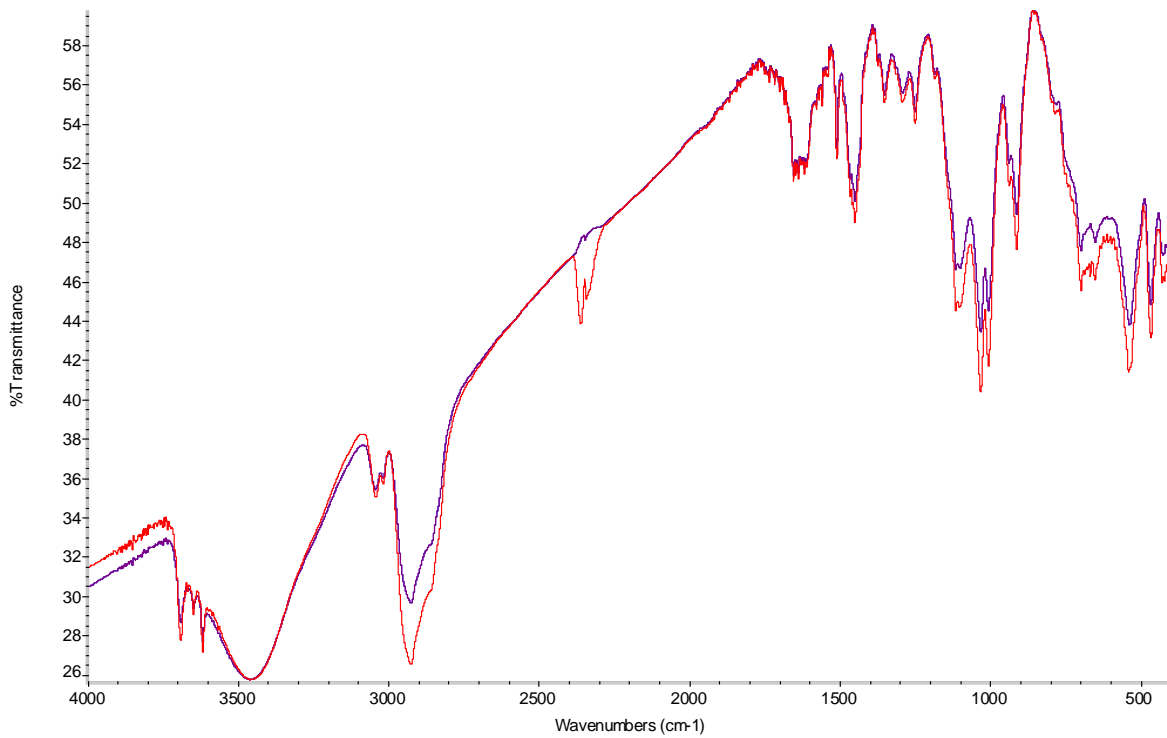
Figure 7.1: FTIR Spectra of Curing Membrane CMC 1 Batch # 60903.
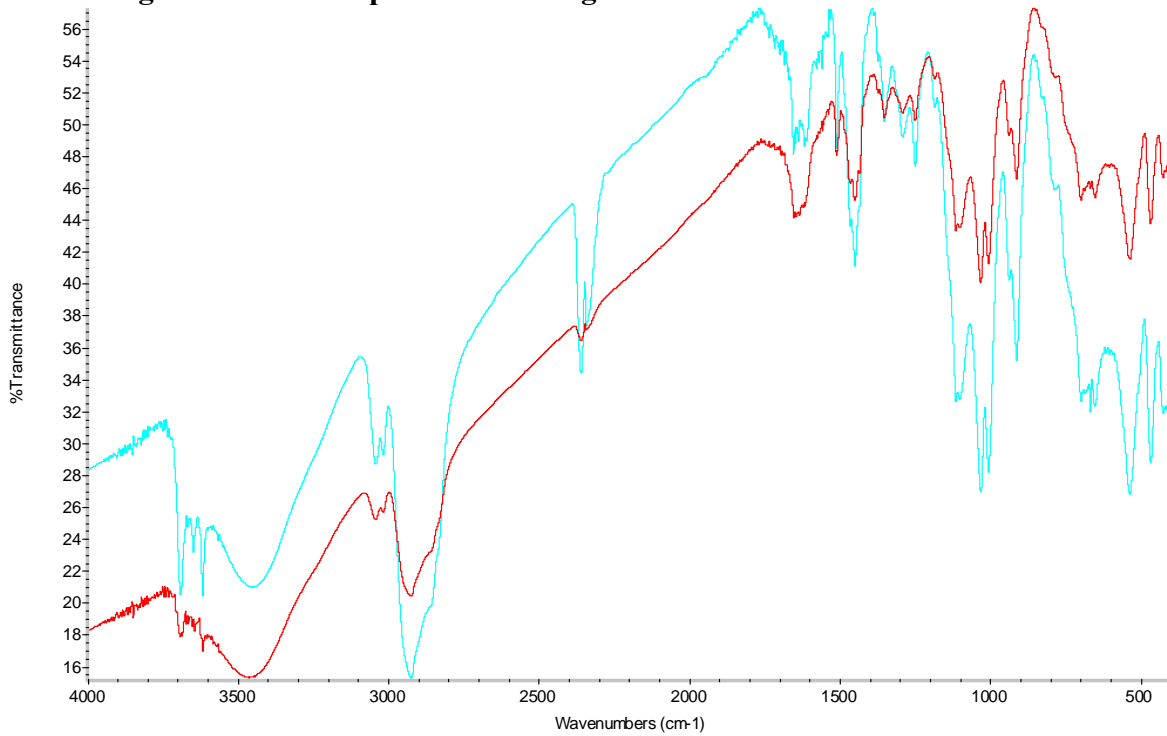
Figure 7.2: FTIR Spectra of Curing Membrane CMC 1 Batch # 90360.
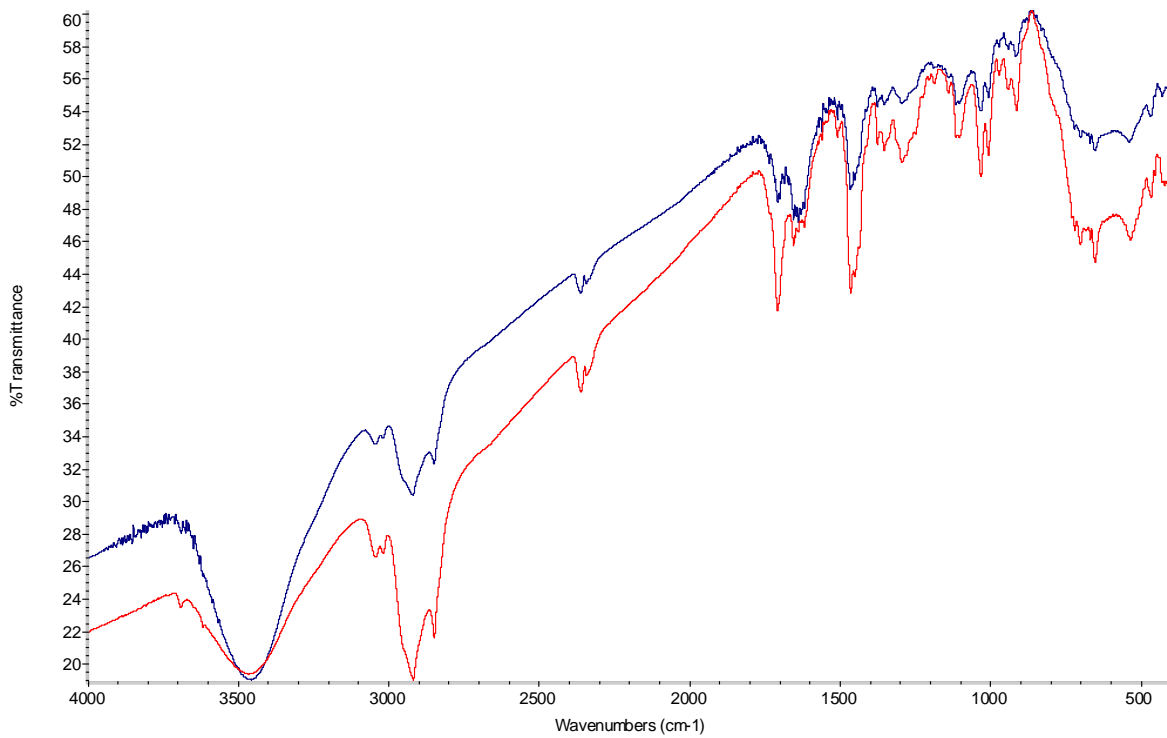
Figure 7.3: FTIR Spectra of Curing Membrane CMC 2 Batch #9FG012.
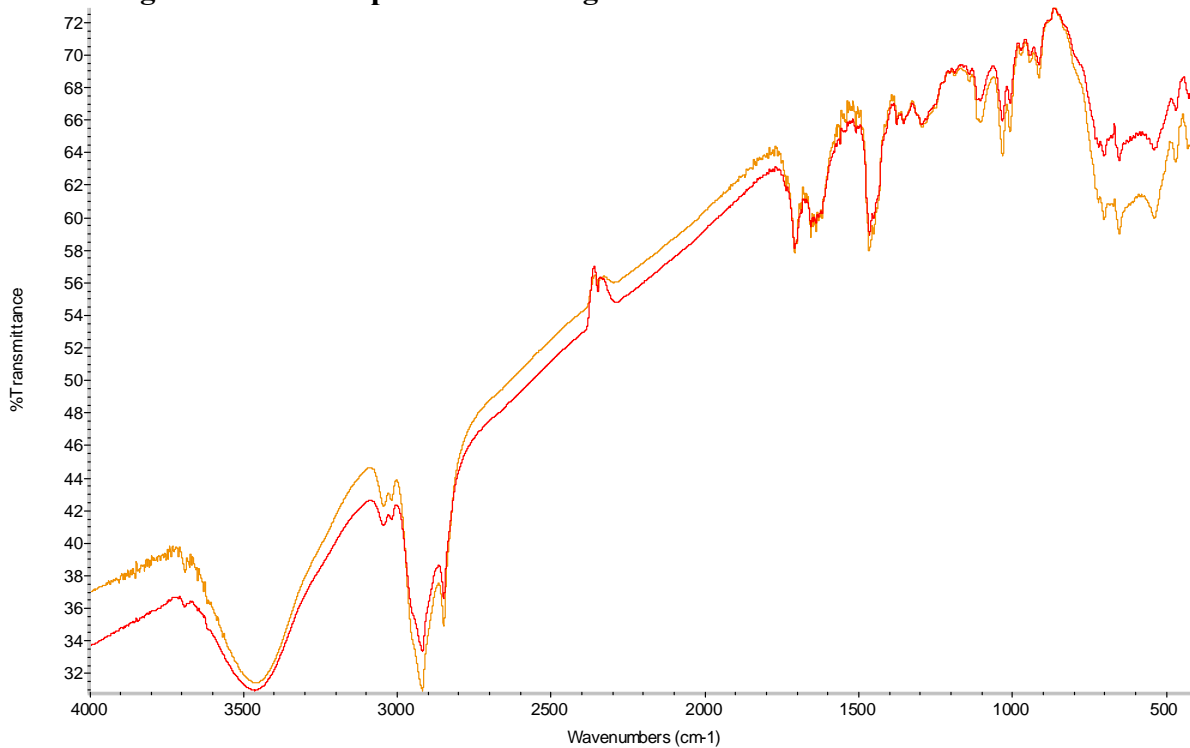
Figure 7.4: FTIR Spectra of Curing Membrane CMC 2 Batch #9FG018.
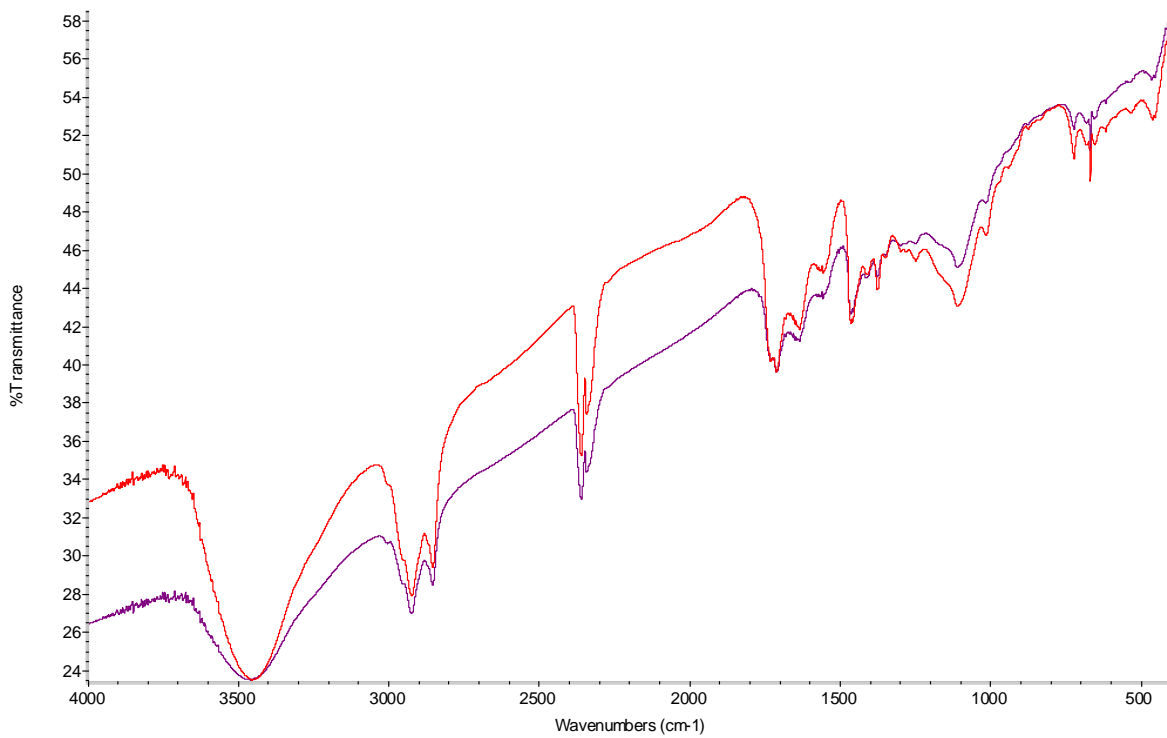
Figure 7.5: FTIR Spectra of Evaporation Retardant Product 1.
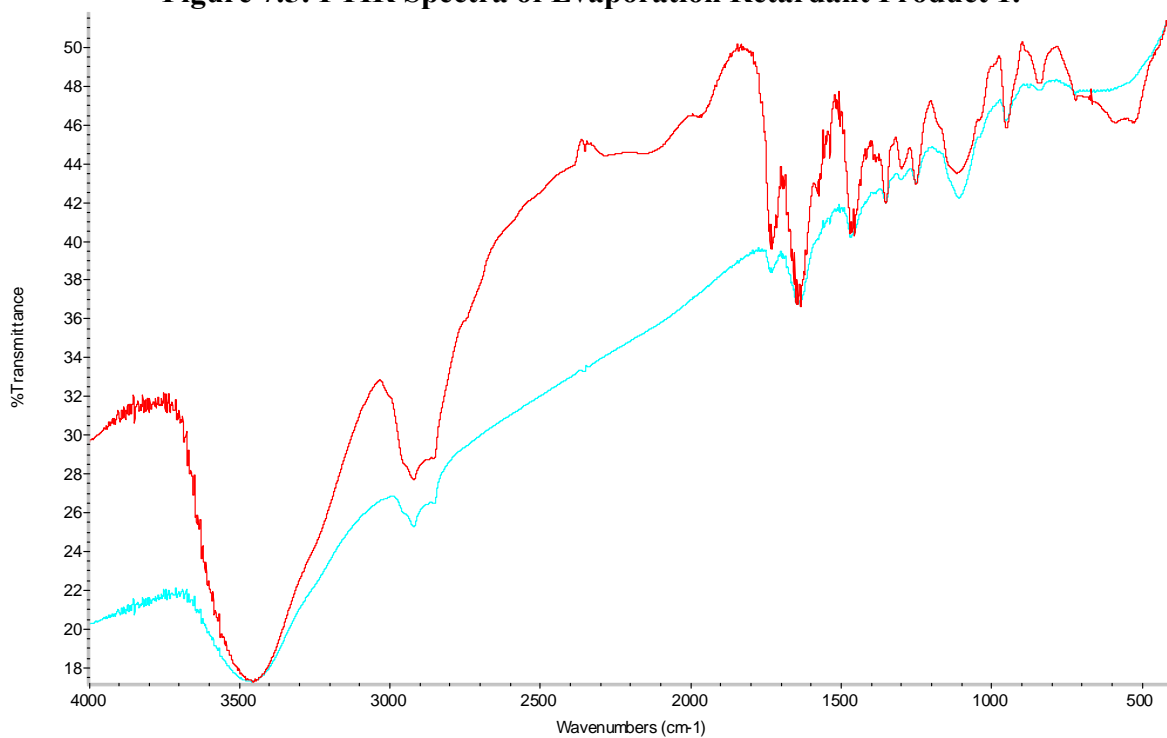
Figure 7.6: FTIR Spectra of Evaporation Retardant Product 2.
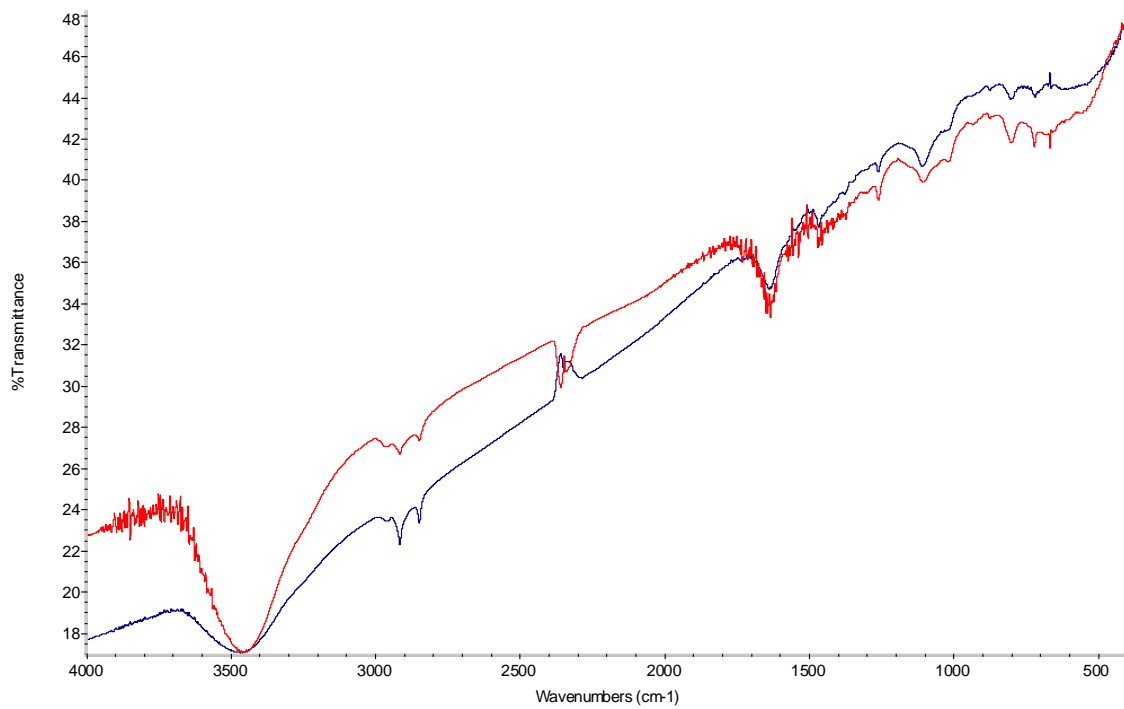
Figure 7.7: FTIR Spectra of Evaporation Retardant Product 3.
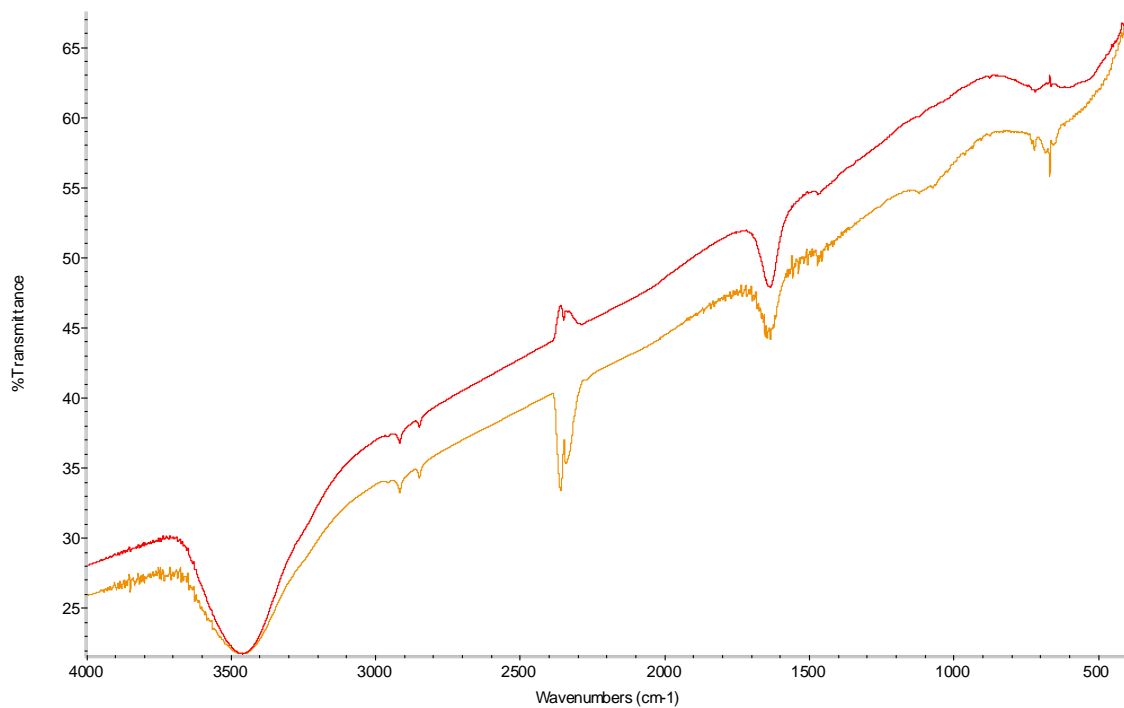
Figure 7.8: FTIR Spectra of Evaporation Retardant Product 4.
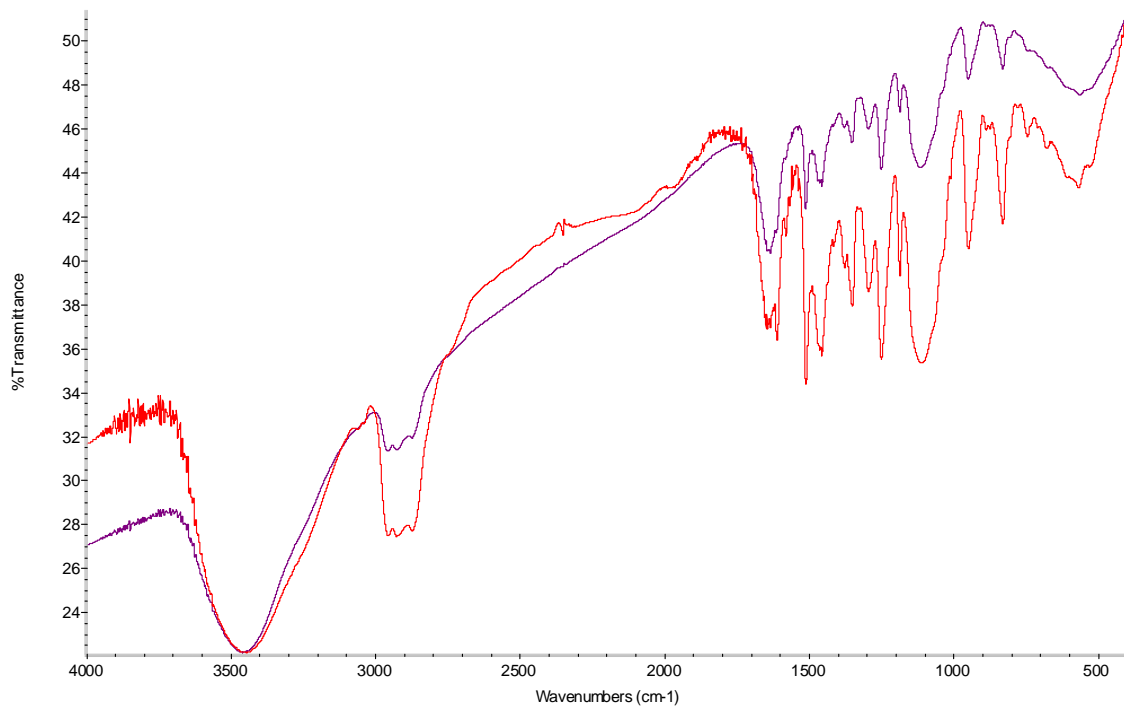
Figure 7.9: FTIR Spectra of Evaporation Retardant Product 5.
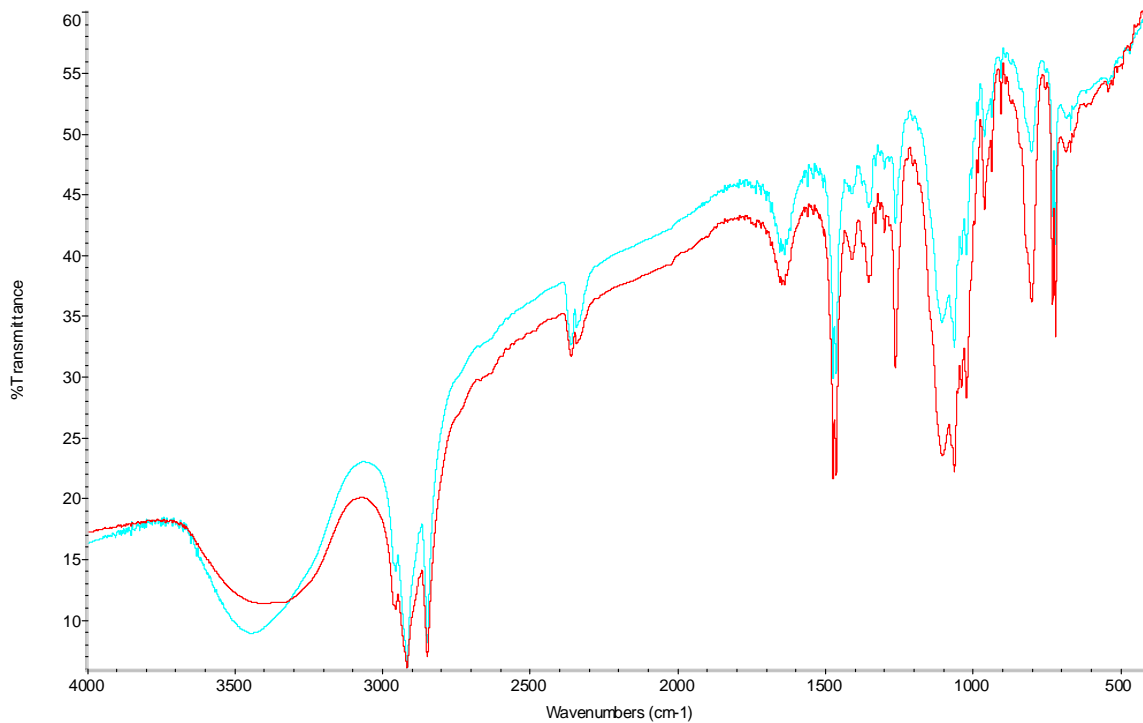
Figure 7.10: FTIR Spectra of Evaporation Retardant Product 6.
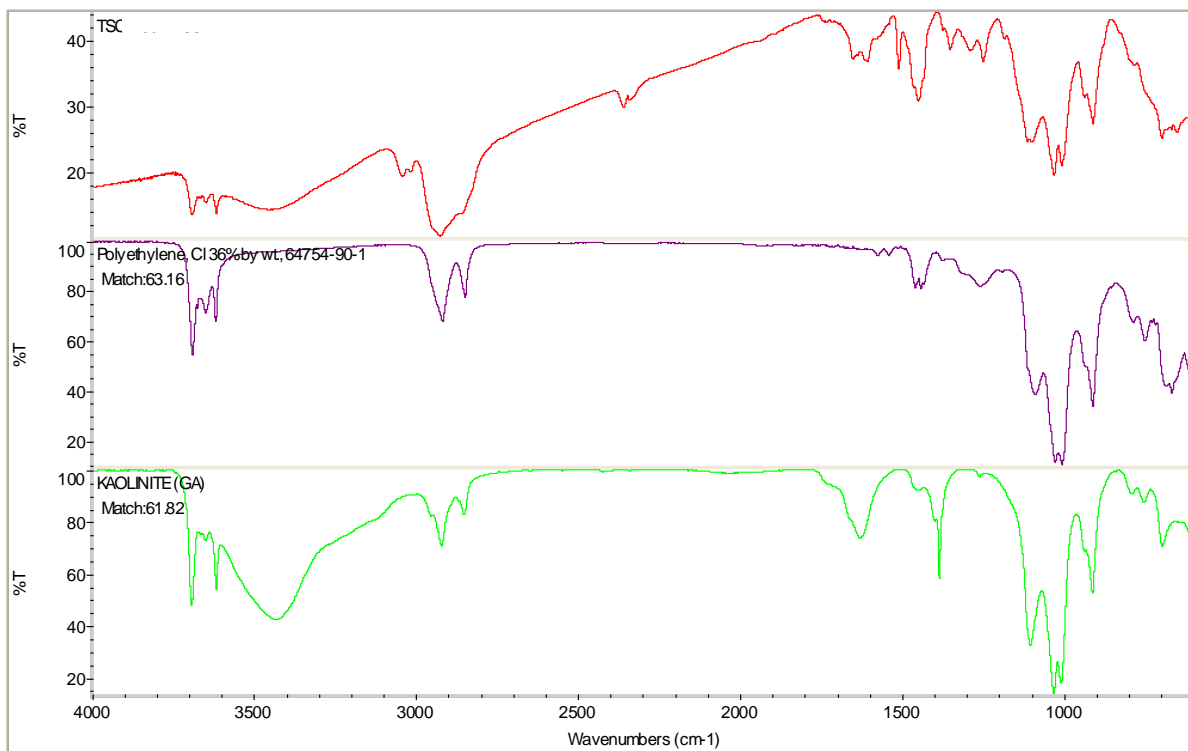
Figure 7.11 Comparison of FTIR Spectra of CMC 1 Curing Compound with Polyethylene and Kaolinite.
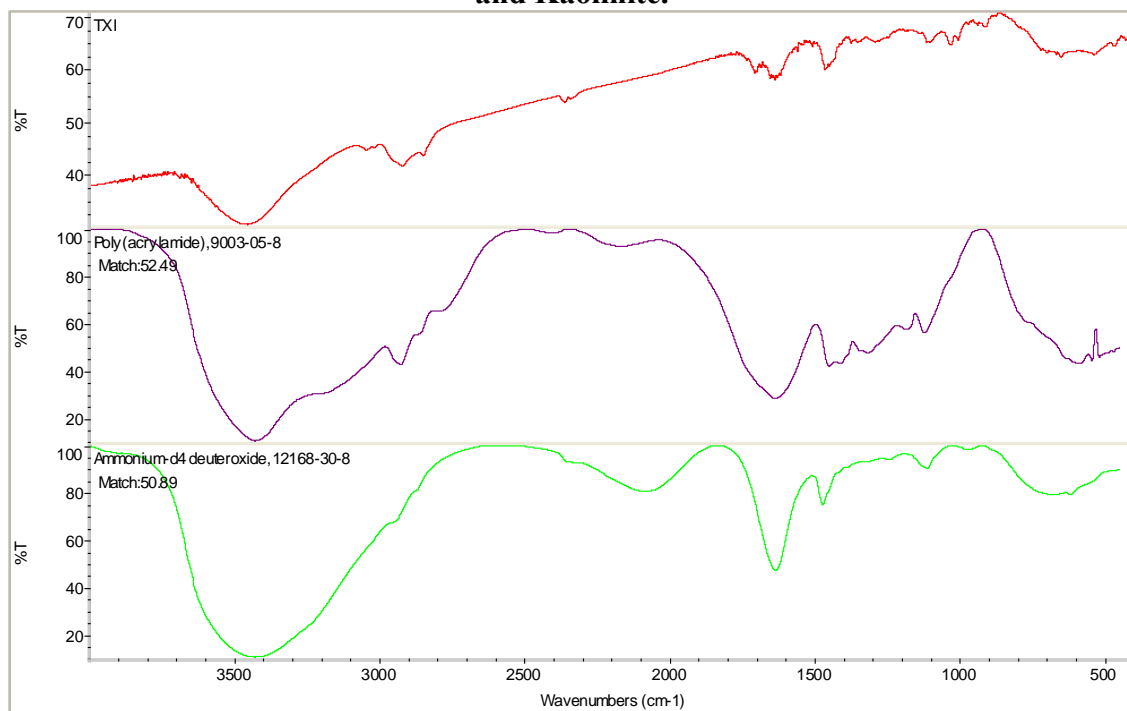
Figure 7.12: Comparison of FTIR Spectra of CMC 2 Curing Compound with Poly(arcylamide) and Ammonium 4d Deutroxide.

8. CEMENT AND FLY ASH QUALITY AND UNIFORMITY

Excessive expansion of concrete due to reaction of alkali in cement and siliceous aggregates in the presence of moisture results in concrete cracking and is termed Alkali Silica Reaction (ASR). TxDOT engineers have experienced this mode of premature concrete degradation and have addressed this issue in Item 421 of "Standard Specifications for Construction and Maintenance of Highways, Streets, and Bridges" adopted by TxDOT on June 1, 2004.

TxDOT has sponsored Project 0-4085 entitled "Preventing Premature Concrete Deterioration due to ASR/DEF in New Concrete," conducted at the University of Texas' Center for Transportation Research. Results of this project confirmed and expanded earlier findings on possible methods to prevent ASR. Limiting the alkali concentration in hydraulic cement to four pounds per cubic yard as calculated by the following equation (mix design option 7 in Item 421) was one of the preventive measures adopted by TxDOT:

lb. alkali per cu. yd. = [(lb cement per cu. Yd.) X (%Na_2O equivalent in cement)] / 100

Considering high volume usage of concrete in the state of Texas (> 60 million cubic yards in 2006), the ability of FTIR to identify and quantify alkali content in given concrete cement will be of great importance. Ease of FTIR testing and interpretation of its spectra along with quantification capability can be an asset in performing quality control at an acceptable cost. This section presents our findings and that of others researchers on applications of FTIR in cement and fly ash analysis.

8.1 FTIR Analysis of Concrete Cement and Fly Ash (C, F)

According to C. Estakhri and D. Saylak (2005), 6.6 million tons of fly ash will be produced annually in Texas from 18 power plants located throughout the state and 40% of it is used in concrete. This group suggested that if 60% of the Portland cement used in Texas concrete production were replaced with fly ash, carbon dioxide emission could potentially be reduced by 6.6 million tons annually by the year 2015. This reduction would have a sizable impact on the environment, as well as potentially reducing costs resulting from environmental issues. It is striking to know that that one ton of carbon dioxide is produced for production of one ton of cement product and therefore, for every ton of FA replacement with Portland cement, one

expects to reduce one ton of carbon dioxide. Samples of concrete cement and fly ash grades C and F listed in Table 8.1 were analyzed and their respective spectra are shown in Figures 8.1-8.5 and Figures 8.11-8.17, respectively. Major FTIR absorption bands for all concrete cements are tabulated in Table 8.2.

Table 8.1: List of Concrete Cement and Fly Ash Samples Analyzed in This Project.

Material	Sources and Types
Concrete Cement	Cement Source 1 I/II
Concrete Cement	Cement Source 2 I
Concrete Cement	Cement Source 3 I/II
Concrete Cement	Cement Source 4 I/II
Concrete Cement	Cement Source 5 I/II
Fly Ash	Fly Ash Source 1 Class C
Fly Ash	Fly Ash Source 2 Class C
Fly Ash	Fly Ash Source 3 Class C
Fly Ash	Fly Ash Source 4 Class F
Fly Ash	Fly ash Source 5 Class F
Fly Ash	Fly Ash Source 6 Class F
Fly Ash	Fly Ash Source 7 Class F
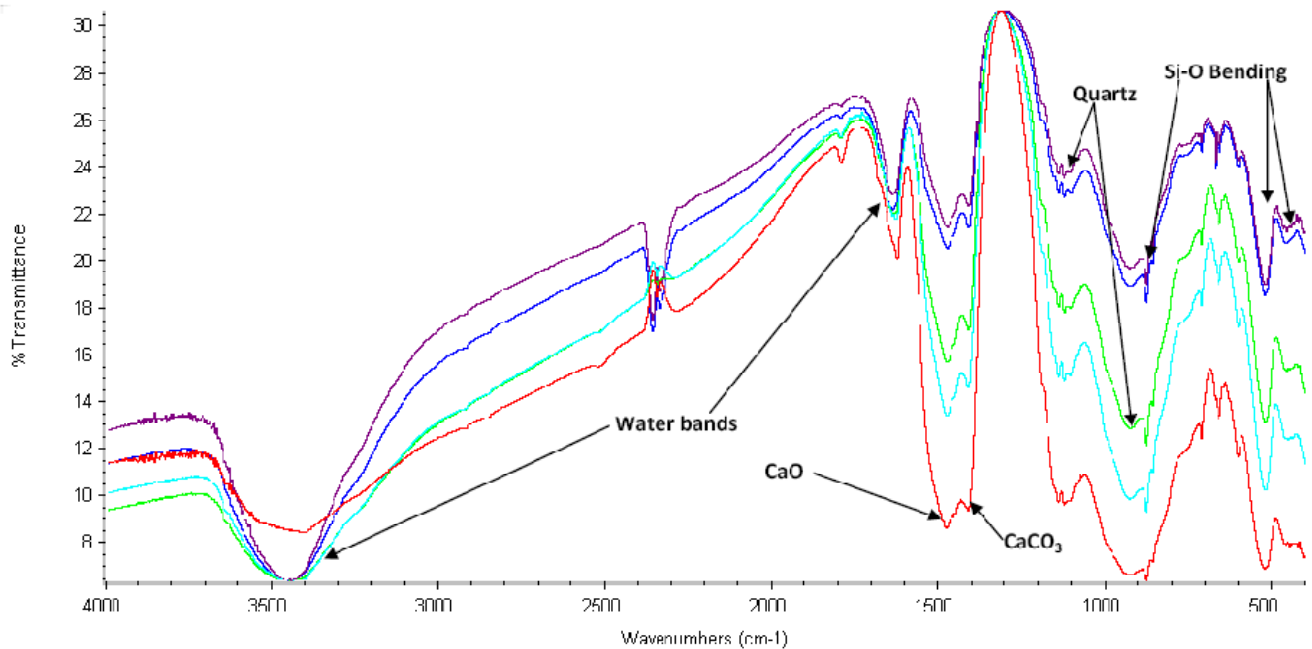
Figure 8.1: FTIR Spectra of Cement Source 1 Type I/II.
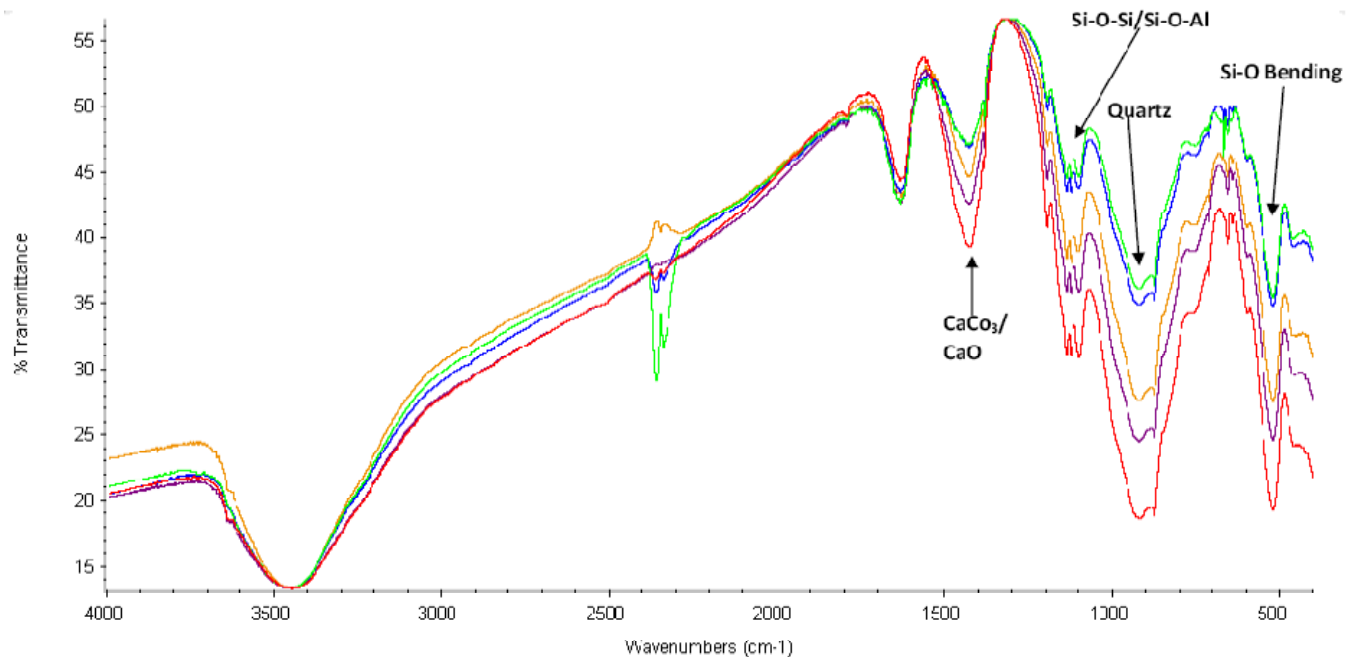
Figure 8.2: FTIR Spectra of Cement Source 2 Type I.
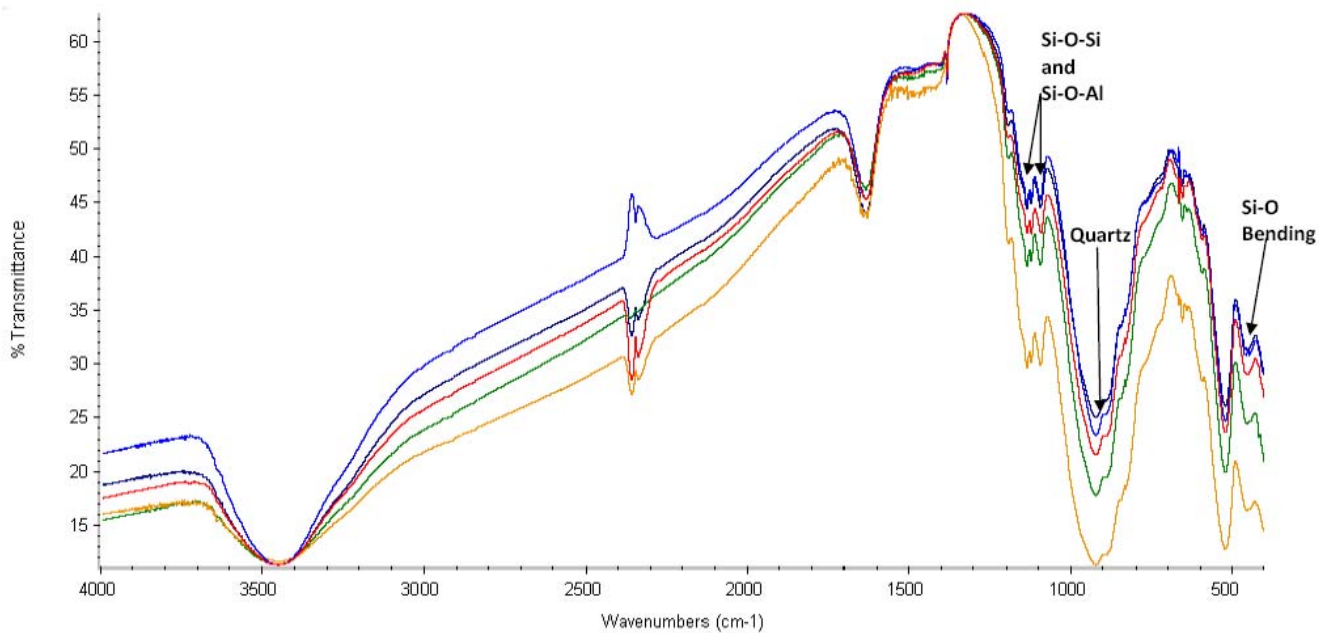
Figure 8.3: FTIR Spectra of Cement Source 3 Type I/II.
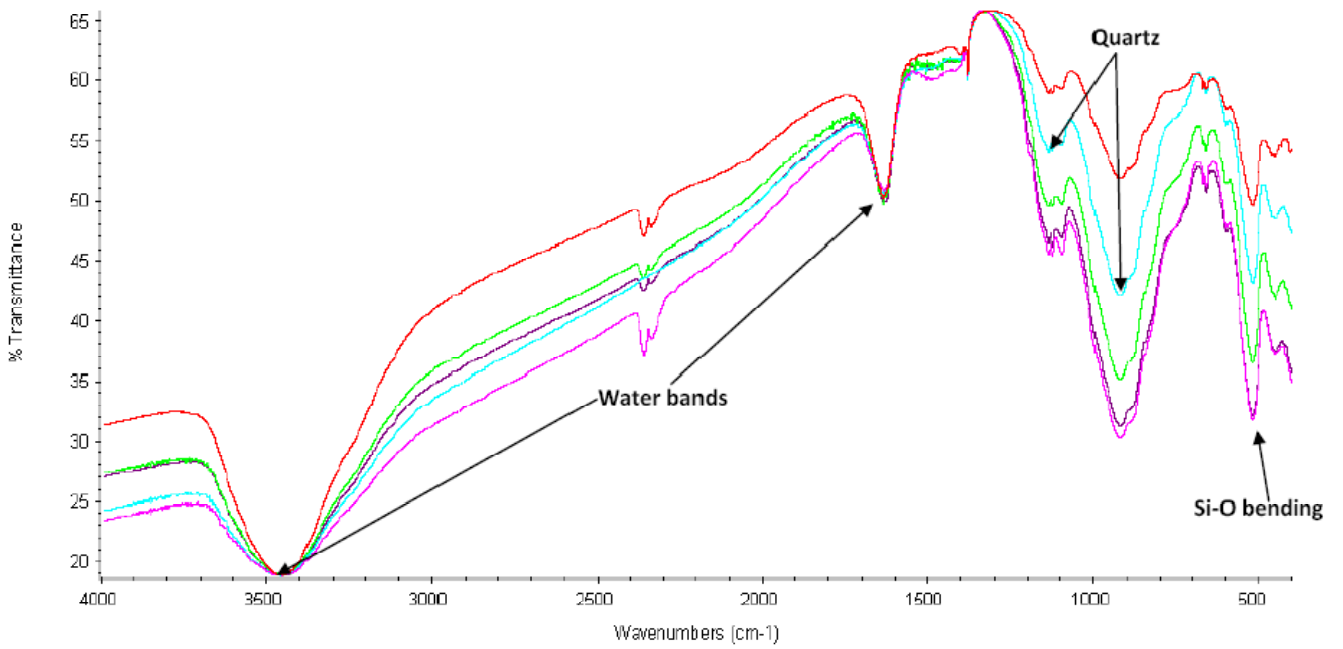
Figure 8.4: FTIR Spectra of Cement Source 4 Type I/II.
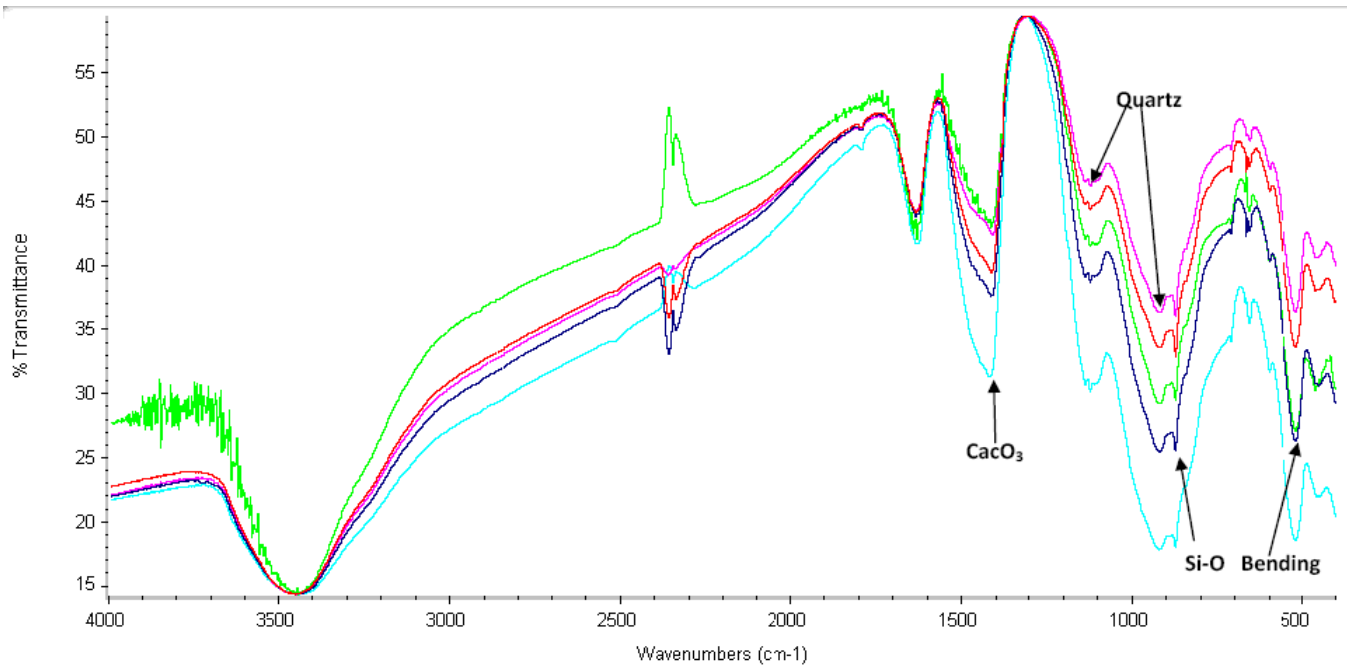
Figure 8.5: FTIR Spectra of Cement Source 5 Type I/II.

Table 8.2: Major FTIR Absorption Bands of Concrete Cement Types I and I/II.

Cement I/II:							
Cement Source 1	3453.95	1636.00	1473.74	1123.94	875.17	668.49	520.10
Cement Source 3	3453.44	1636.03	1384.48	1124.85	923.58	668.62	522.49
Cement Source 4	3459.10	1635.44	1384.53	1124.77	923.20	658.16	521.84
Cement Source 5	3453.71	1636.32	1418.71	1124.36	923.01	668.66	521.26
Cement I:							
Cement Source 2	3448.43	1636.52	1429.26	1124.94	920.31	657.48	521.40

8.2 Analysis of FTIR Spectra of Cement Samples

FTIR spectra of all five varieties of the cement samples are similar. Major absorption bands in all samples include: 3453 cm^{-1} and 1638 cm^{-1} bands assigned to H-O-H stretching and H-O-H bending respectively (generally known as water bands); 1384 cm^{-1} – 1473 cm^{-1} associated with CaO and $CaCO_3$; 1123 cm^{-1} and 923 cm^{-1} bands assigned to Si-O-Si and Si-O-Al bonds, respectively; and 668 cm^{-1} and 521 cm^{-1} assigned to Si-O bending. Assigned bands are based on literature data. Despite a high degree of similarity, there is a unique difference in concrete cement samples containing various amounts of alkali. Specifically, a narrow band centered around 750 cm^{-1} is uniquely present in the spectra of samples with high alkali content. In this research, samples of cement from five different source with types I and I/II were analyzed. Historically, samples from cement samples from sources 1 and 2 have shown high alkali content, cement source 4 samples has shown medium alkali content and cement sources 3 and 5 samples have shown low alkali content. TxDOT records of chemical compositions of all cement samples measured by XRF are presented in Appendix D. The trend from high to low alkali content in cement samples is observed in the FTIR spectra of these concrete cement samples on the band centered around 750 cm^{-1} , as shown in Figures 8.1-8.5. Overlay of FTIR spectra of all five cement samples and an enlarged region of interest is shown in Figures 8.6 and 8.7, respectively.
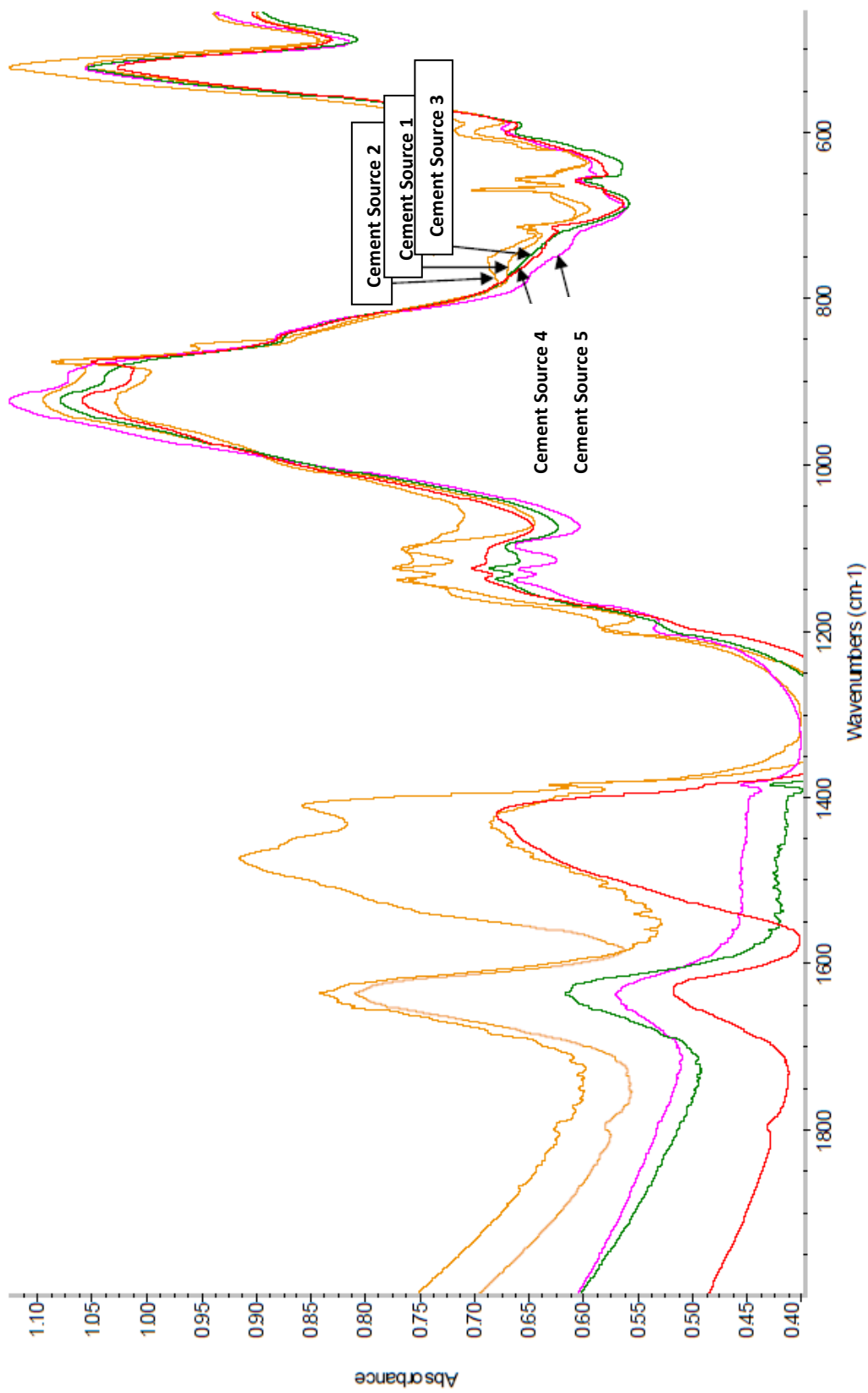
Figure 8.6: Overlay of Cement Samples Showing 750 cm⁻¹ FTIR Absorption Band Intensity Variations in Various Cement Sources
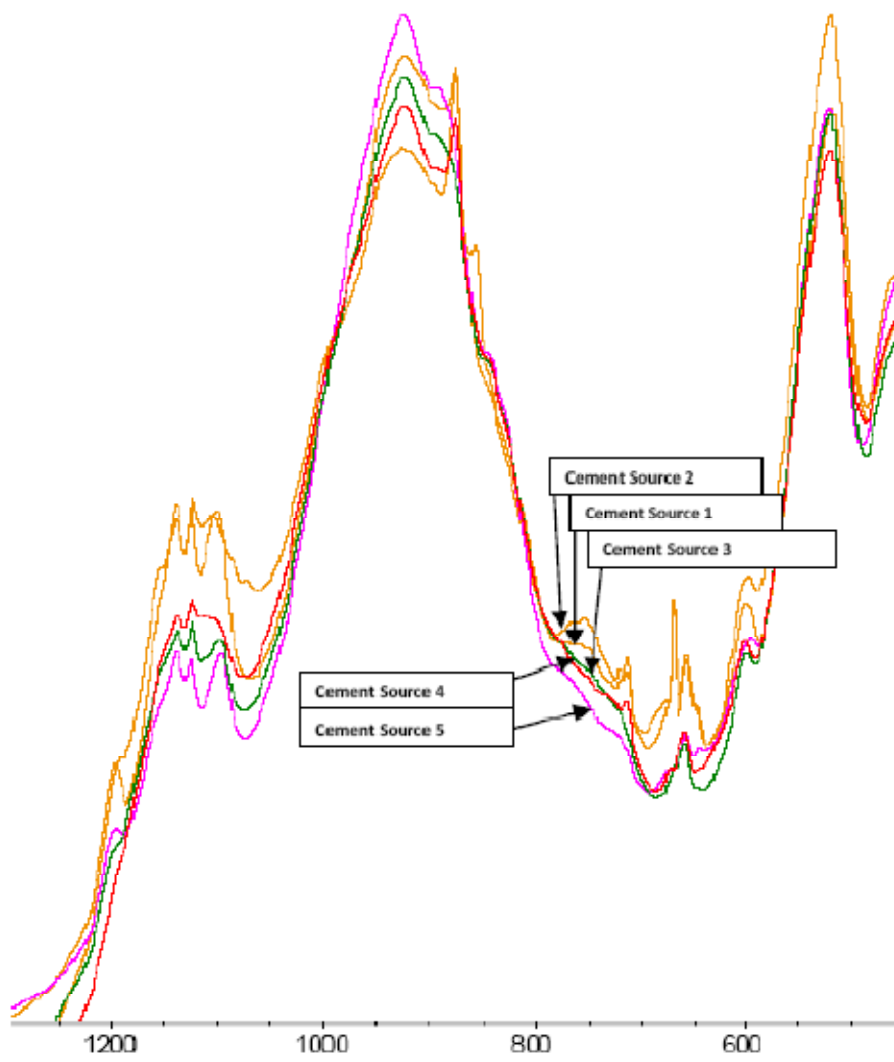
Figure 8.7: Enlarged Overlay of FTIR Spectra for Cement Samples from Various Sources with Emphasis on Region of interest (750 cm^{-1} band.

8.3 Alkali Content Quantification of Concrete Cement Samples

Due to the importance of limiting alkali concentration in concrete for the sake of preventing ASR and Delayed Ettringite Formation (DEF), it was desirable to quantify alkali content in cement using the fast and reliable technique of FTIR. In this research, peak area ratio for areas under the bands at 750 cm^{-1} to 923 cm^{-1} were measured for two sets of samples (sets #1 and #2), and an average of five samples for each data point was calculated. The plot of Peak Area ratio to Na_2O equivalent (Na_2O_e) as measured with XRF is plotted in Figures 8.8 and 8.9. When data from both sets #1 and #2 were averaged, a plot shown in Figure 8.10 was obtained. As can be seen from these plots, a high degree of linearity exists between peak area ratio and Na_2O_e as measured with XRF. R^2 values for data sets #1, #2, and a combined set is shown as 0.978, 0.974, and 0.979, respectively. Presented data in Figures 8.8 through 8.10 suggests that the minimum detectable level for Na_2O_e measurements using FTIR appears to be around 0.42%. Appendix E contains all numerical values of individual measurements along with standard deviations for each of five measurement sets for five cement samples. Procedure to follow for alkali quantification using FTIR is given in Appendix F.
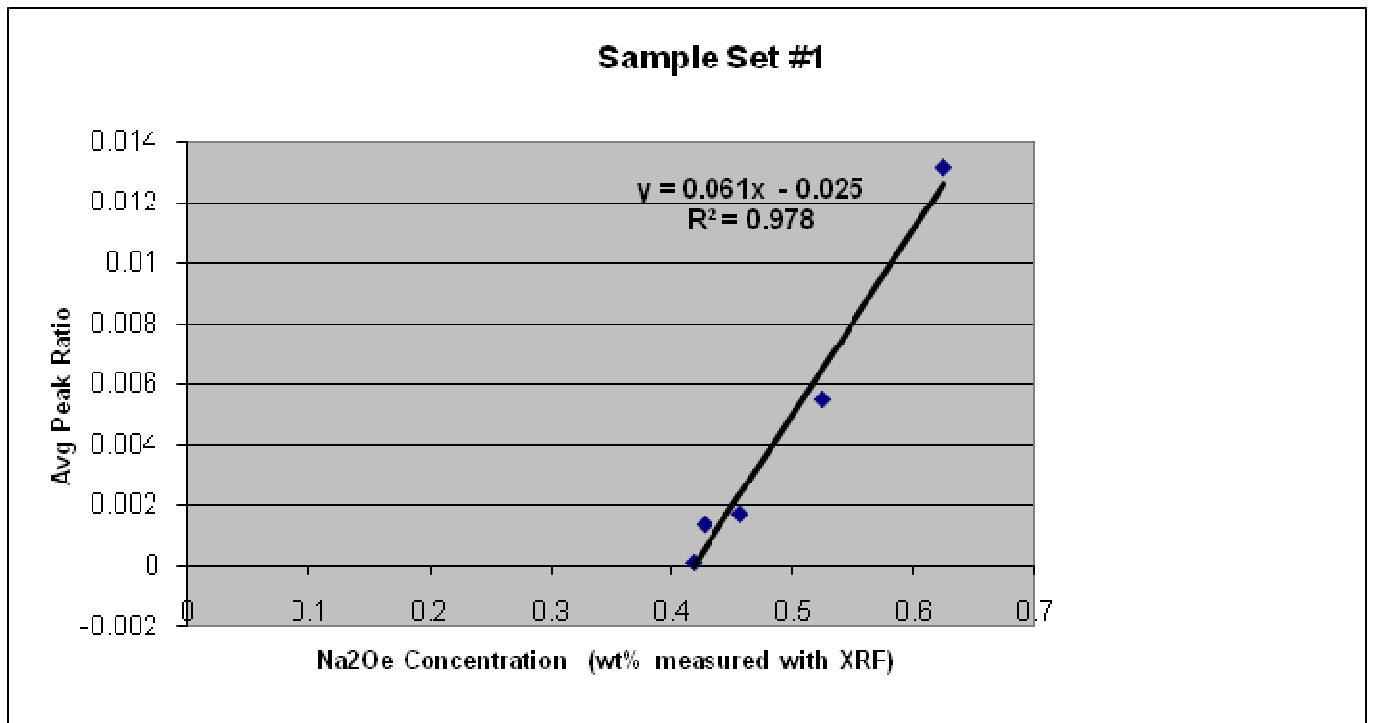
Figure 8.8: Plot of Average 750/923 cm^{-1} Bands Ratio to Na_2O_e (Data Set #1).
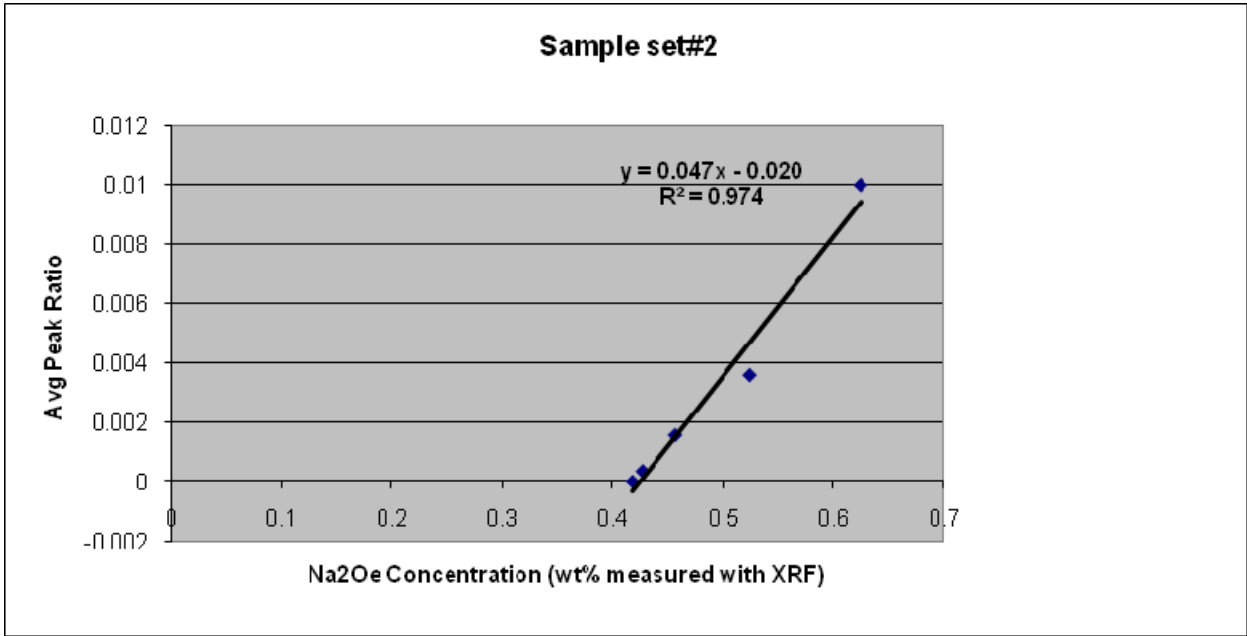
Figure 8.9: Plot of Average 750/923 cm^{-1} Bands Ratio to Na$_2$O$_e$ (Data Set #2).
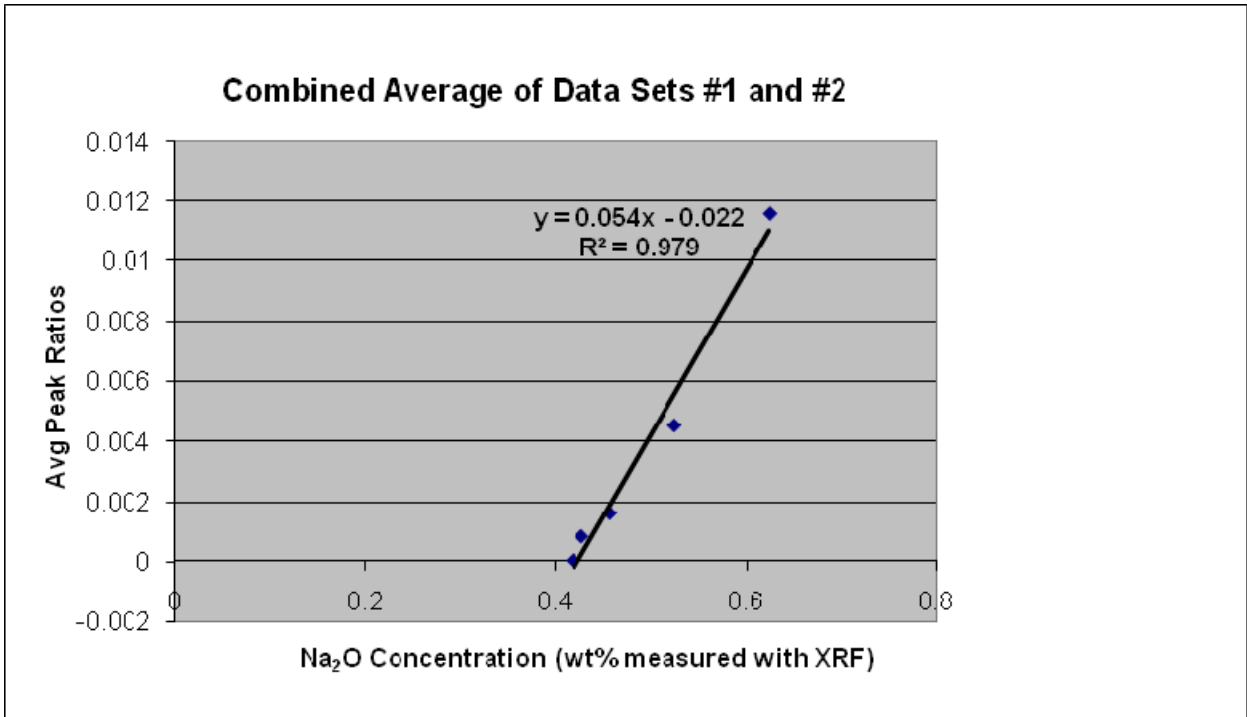
Figure 8.10: Plot of Average 750/923 cm^{-1} Bands Ratio to Na$_2$O$_e$ (Combined Data Sets 1-2).

8.4 Justification for Using Band Ratio for Quantification of Alkali in Cement

L. Stoch and M. Sroda (1999) applied infrared spectroscopy to investigate oxide glasses and indicated that the FTIR absorption band at 750 cm^{-1}belongs to K$_2$O·2SiO$_2$. A. Palomo et al. (2007) studied Opc-fly ash cementitious systems and showed FTIR absorption band of 927 cm^{-1}

belongs to clinker. T. Hughes et al. (1995) used FTIR to determine cement composition and showed a linear relationship between their predicted models (based on FTIR absorption bands) and measured weight percentages of K_2O and Na_2O using Inductively Coupled Plasma. C.E. Tambelli et al. (2006) studied alkali-silica reaction gel by high- resolution Nuclear Magnetic Resonance spectroscopy and pointed to literature data giving a number of FTIR bands associated with: amorphous silica related to asymmetric and symmetric stretching of Si-O (1154 cm^{-1} and 1037 cm^{-1} respectively); stretching of Si-O-X, where X=K or Na (953 cm^{-1}); symmetric stretching of O-Si-O (783 cm^{-1}); and bending of O-Si-O (457-600 cm^{-1}).

8.5 FTIR Analysis of Fly Ash Samples

Several fly ash samples of both F and C grades were fingerprinted and FTIR spectra of all fly ash samples are shown in Figures 8.11-8.17. Major FTIR absorption bands of fly ash (C and F) samples are tabulated in Table 8.3.
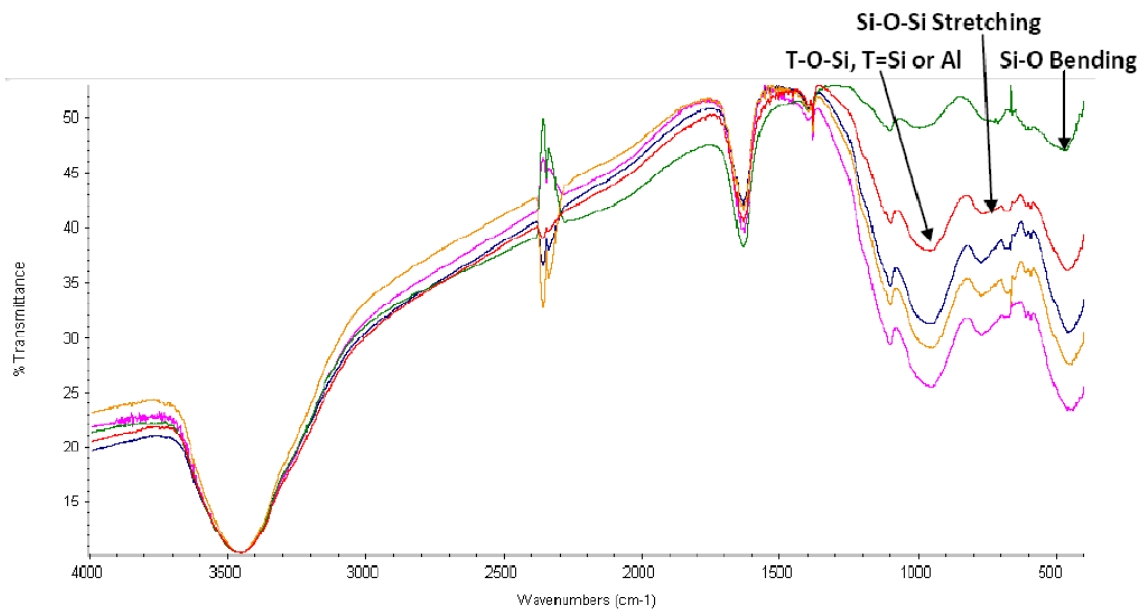
Figure 8.11: FTIR Spectra of a Sample for Fly Ash (C) Source 1.
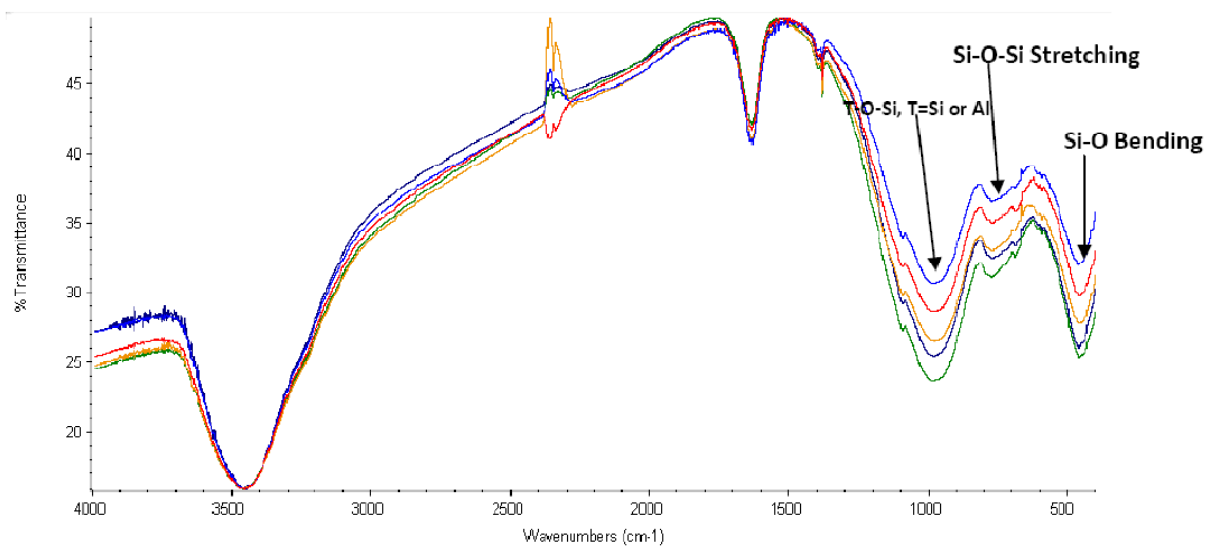
Figure 8.12: FTIR Spectra of a Sample for Fly Ash (C) Source 2.
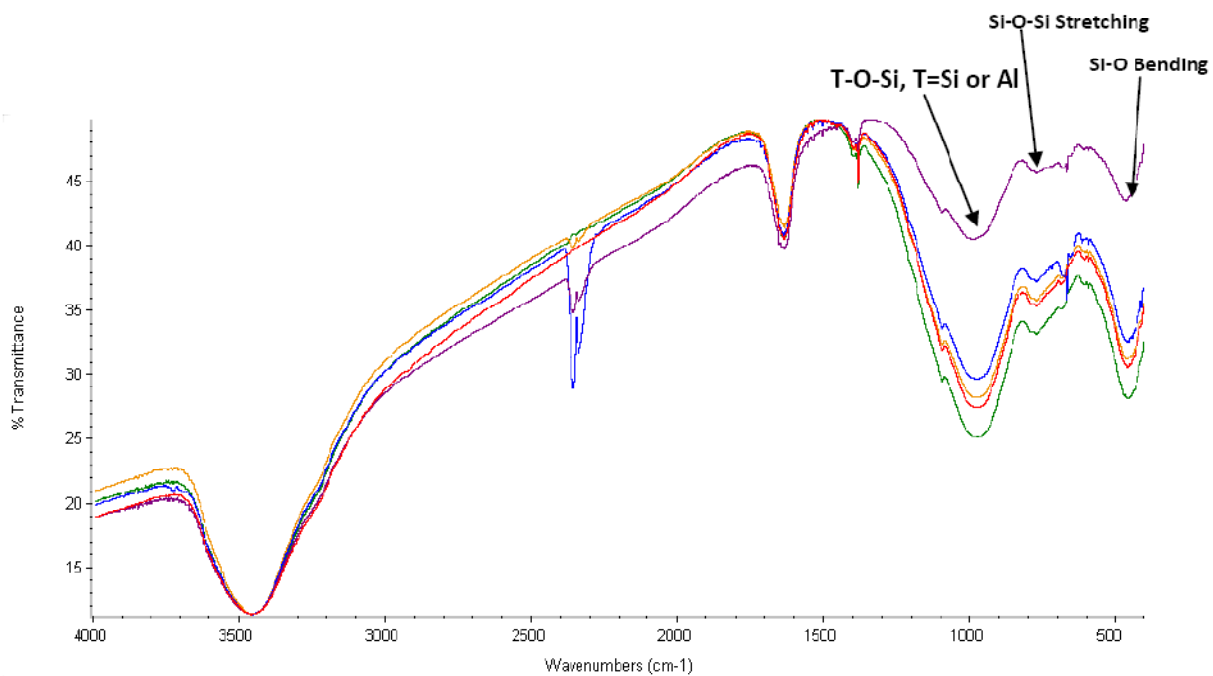
Figure 8.13: FTIR Spectra of a Sample for Fly Ash (C) Source 3.
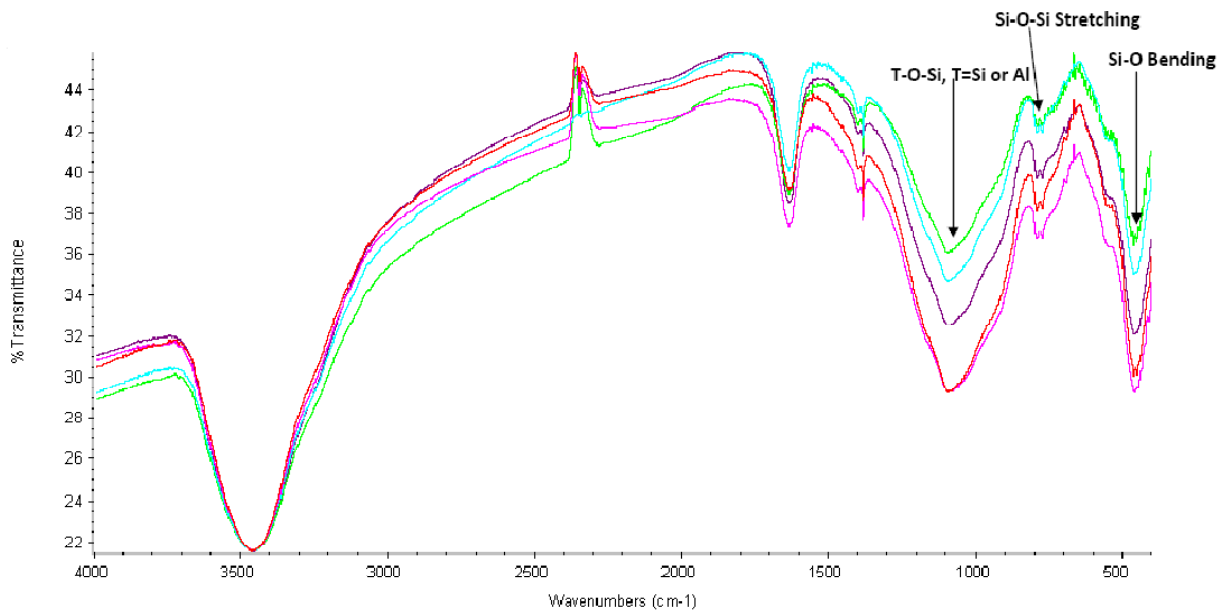
Figure 8.14: FTIR Spectra of a Sample for Fly Ash (F) Source 4.
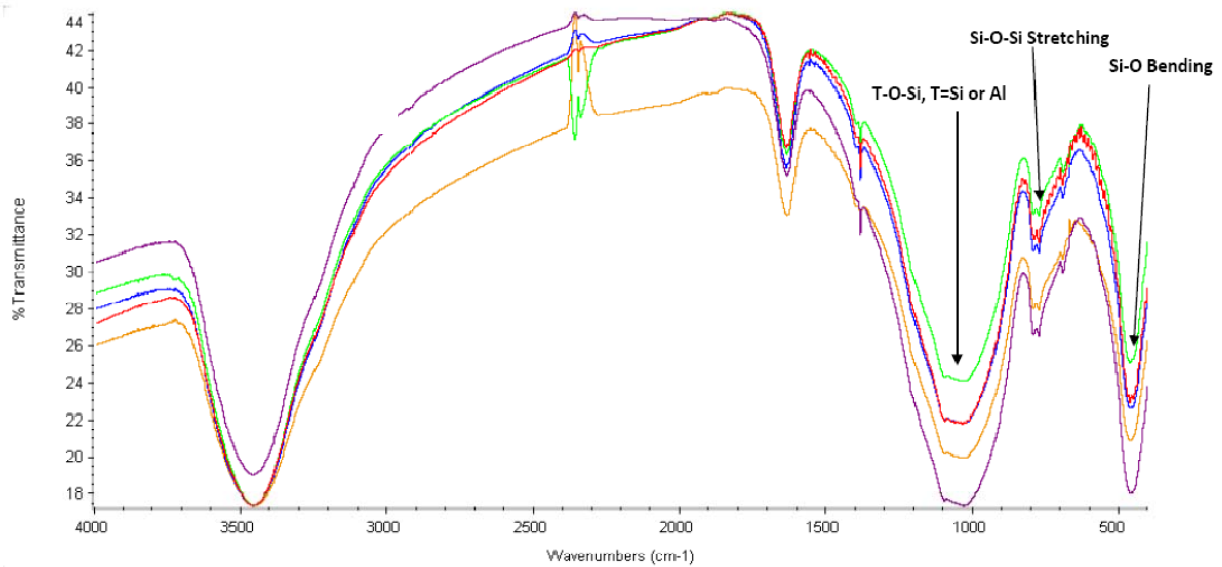
Figure 8.15: FTIR Spectra of a Sample for Fly Ash (F) Source 5.
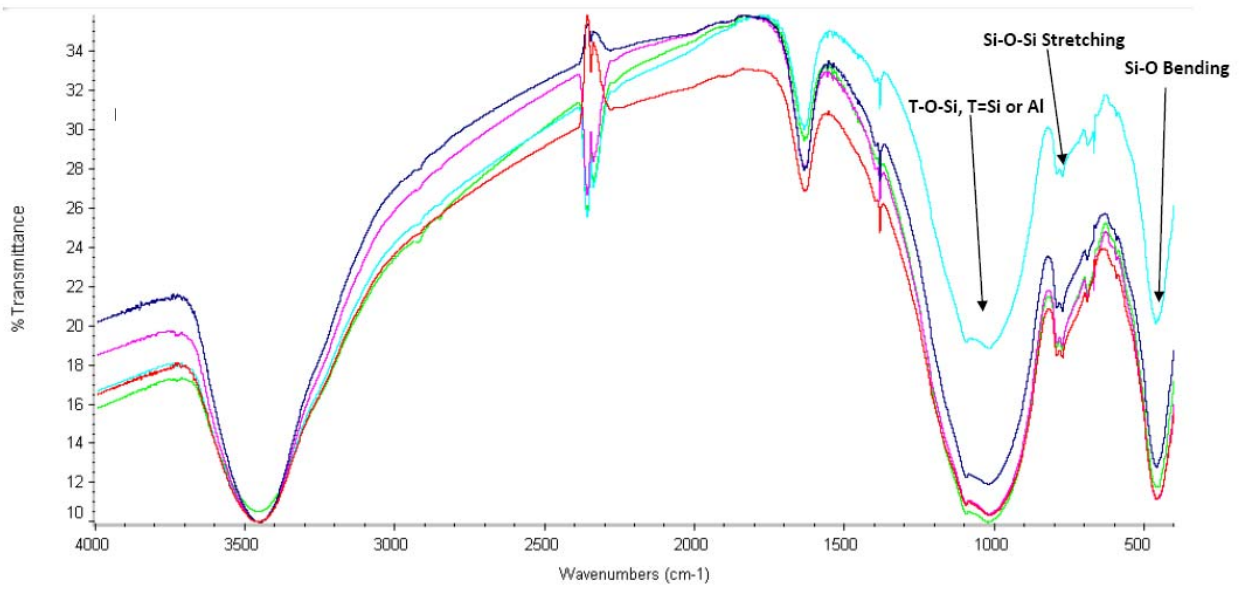
Figure 8.16: FTIR Spectra of a Sample for Fly Ash (F) Source 6.
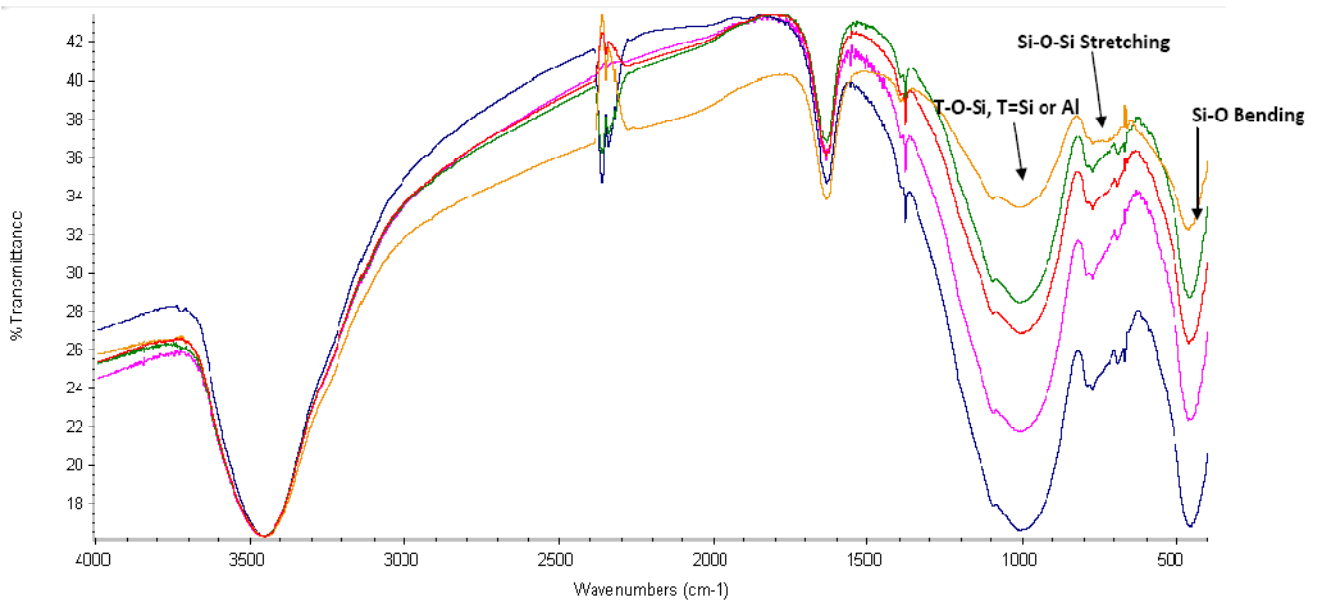
Figure 8.17: FTIR Spectra of a Sample for Fly Ash (F) Source 7.

99

Table 8.3: Major FTIR Absorption Bands of Fly Ash (C and F) Samples Analyzed in this Research.

Absorption Peaks

F-Ash:

Source 6	3462.22	1636.59	1384.13	1023.32	776.22	460.95
Source 5	3457.59	1635.46	1384.19	1031.72	775.73	462.90
Source 7	3462.47	1637.36	1384.14	1015.85	774.17	465.10
Source 4	3458.51	1636.26	1384.27	1095.20	793.71	459.82

C-Ash:

Source 2	3457.74	1635.81	1384.32	985.60	463.42
Source 3	3462.63	1636.65	1384.34	980.97	462.65
Source 1	3463.16	1637.09	1384.34	959.80	456.02

Assigned FTIR absorption bands indicated in Figures 8.11-8.17 are based on documented literature. Table 8.4 lists major bands of fly ash as provided by D. Panias et al. (2007). A. Sarkar et al. (2006) suggested that strong mineral bands observed at wave numbers 1095 cm^{-1}, 1031 cm^{-1} in all fractions of fly ash (magnetic/non-magnetic) belong to Si–O–Si/Si–O stretching those points towards the presence of kaolinite, quartz, and mullite. W.K.W. Lee et al. (2002) assigned bands shown in Table 8.5 based on numerous previous studies.

Table 8.4: Characteristic FTIR Bands of the Used Fly Ash and the Synthesized Geopolymers.

Wave number (cm^{-1})	Assignment
1430 - 1410	Stretching vibration (O-C-O)
1090 - 990	Asymmetric stretching vibration (T-O-Si, T=Si or Al)
882	Si-O stretching, OH bending (Si-OH)
800 - 780	Symmetric stretching vibration (Si-O-Si)
750 - 550	Symmetric stretching vibration (Si-O-Si and Al-O-Si)
470 – 460	Bending vibration (Si-O-Si and O-Si-O)

Table 8.5: Characteristic IR Vibrational Bands of the Gladstone Class F Fly Ash

(W.K.W. Lee et al. (2002)).

Wave numbe (cm^{-1})	Assignment
950 - 1200	Asymmetric stretching (Si-O-Si and Al-O-Si)
1165	Asymmetric stretching (Si-O-Si)
1138	Asymmetric stretching (Si-O-Si and Al-O-Si)
1080	Asymmetric stretching (Si-O-Si and Al-O-Si)
1074	Asymmetric stretching (Si-O-Si and Al-O-Si)
882	Si-O stretching, OH bending (Si-OH)
798	Symmetric stretching (Si-O-Si)
727	Symmetric stretching (Si-O-Si and Al-O-Si)
620	Symmetric stretching (Si-O-Si and Al-O-Si)
561	Symmetric stretching (Ai-O-Si)
466	Bending (Si-O-Si and O-Si-O)

8.6 Summary

Results of alkali quantification in cement samples show that FTIR is capable of quantifying alkali concentrations based on absorption band ratios of 750 cm^{-1} to 923 cm^{-1} bands that belong to alkali and cement clinker, respectively. In addition, FTIR can identify if fly ash is present in a mixture of cement and fly ash by observing absorption band at 460 cm^{-1}. Results of the alkali quantification showed a high degree of linearity between FTIR band ratio and alkali concentration measured using XRF. The minimum detectable level for alkali concentration appears to be approximately 0.42%.

9. CUMULATIVE CONCLUSIONS

Based on the results of this research, the following conclusions can be made:

1. A comprehensive literature review on practical applications of FTIR on characterization of paving materials was performed and a collection of the papers, books, and reports for this purpose is listed in the References section of this report.

2. FTIR is capable of differentiating between polymer and non-polymer-modified binders. Asphalt samples with known SBS content from multiple suppliers were used to generate calibration curves for polymer quantification. Calibration curves showed a linear relationship between band area ratio ($966 \text{ cm}^{-1}/1375 \text{ cm}^{-1}$) and polymer weight percent (as described in AASHTO T 302-05) with R^2 values close to 1.0. Both ATR and transmittance methods of FTIR were shown to be effective in polymer quantifications with transmittance method producing smoother traces, which affects reproducibility of the measurements. The transmittance method is more favorable over ATR due to protection of the ATR crystal (exposure of the ATR crystal to hot asphalt can potentially damage or crack the crystal). In addition, disposing a KBr pellet used in the transmission method is much easier than cleaning solidified asphalt on an ATR crystal.

3. Attempts were made to study antistripping agents in asphalt emulsions of both anionic (SS-1, HFRS-2, and HFRS-2P) and cationic (CHFRS-2, CRS-2, and CRS-2P) forms. Samples of anionic and cationic emulsions were collected from multiple suppliers and analyzed. FTIR spectra of the materials received from different suppliers were very similar in the uniformity of the products, but they did not show discernable absorption bands for antistripping agents present in these samples. Addition of 2% of a known antistripping agent (with known FTIR spectrum) received from TxDOT Cedar Park Laboratory to PG 64-22 asphalt binder did not yield a spectrum exhibiting expected absorption bands. It is possible that volatility of the antistripping agent did not allow mixing with PG 64-22 in the sample preparation stage for FTIR analysis. Bagampadde and Isacsson (2006) indicated "Infrared spectroscopy was found to not be a good tool for measuring amines in the blends, especially at low concentrations." However, FTIR

spectra of cutbacks like MC 30 and RC 250 show absorption bands associated with kerosene that is a constituent of cutbacks.

4. Two batches of all four concrete spall repair epoxy materials were obtained and analyzed. Similar spectra for all samples in a given variety were produced, which show uniformity of the products between batches. In addition, keeping epoxy materials at room temperature for six months was shown to not change the chemistry of these materials as evidenced by their respective FTIR spectra.

5. Two batches of two commercial concrete curing membrane samples were fingerprinted and a protocol was developed for samples preparation for fingerprinting of the curing membranes. In addition, the developed protocol includes samples preparations for a group of evaporation retardants for their fingerprinting.

6. A new method for alkali quantification of concrete cement using FTIR was developed based on the TxDOT XRF data from the past several years. In this research, a correlation model was developed correlating the FTIR band ratio of 750 cm^{-1} / 923 cm^{-1} band versus equivalent alkali (0.658 x %K$_2$O + %Na$_2$O) concentration as calculated based on XRF analysis. R^2 values of two data sets from TxDOT samples were calculated as 0.978 and 0.974. A protocol describing a step-by-step procedure for this method is given in section 8 and Appendix E.

7. Assigned FTIR absorption bands unique to concrete cement were identified based on available literature, and fingerprint spectra obtained will be used for future analysis of variations in concrete cement compositions. Both grades of fly ash (C and F) received from multiple sources were analyzed and as anticipated both types had similar FTIR spectra for both types. Two noticeable distinctive features observed included the presence of an absorption band at wave number 460 cm^{-1} in fly ash samples, while the lowest detected band for concrete cement occurred at wave number 520 cm^{-1}. The other feature observed in the FTIR spectra of fly ash C and F types was the presence of a narrow (in most cases) band in the wave number range of 1384 cm^{-1}-1388 cm^{-1} possibly due to the

presence of $CaCO_3$ or lime in fly ash. Based on ASTM classifications of fly ash, type F should have 10% lime, while type C has up to 20%.

8. Protocols were developed for FTIR analysis of different paving materials including: polymer quantification in asphalt binders (Appendix B), fingerprinting of concrete curing membranes and evaporation retardants (Appendix C), and alkali quantification (Appendix F).

REFERENCES

AEMA, Basic Asphalt Emulsion Manual-section 2 (chemistry), Rev. 1 Mar. 2004, pp. 2-1 through 2-12.

ASTM C 309-07, Standard Specification for Liquid Membrane-Forming Compounds for Curing Concrete, ASTM International, PA USA.

Anderson, G.L. and L.H. Lewandowski (1994) "Additives in Bituminous Materials and Fuel-Resistance Sealers," Report Number DOT/FAA/CT-94/78, DOT/FAA/RD-93/30.

Arnold, M. Rozario-Ranasinghe, and J. Youtcheff, "Determination of lime in hot-mix asphalt," Transportation Research Record 1962 (2006) 113-120.

ASHTOO T-302-05, "Polymer content of polymer-modified emulsion asphalt residue and asphalt binders."

U. Bagampadde and U. Isacsson, "Characterization of chemical reactivity of liquid antistripping additives using potential titration and FTIR spectroscopy," Energy & Fuels, vol. 20, (2006) 2174-2180.

T. Bakharev, "Geopolymeric materials prepared using Class F fly ash and elevated temperature curing," Cement and Concrete Research, vol. 35 (2005) 1224-1232.

W. Britton, "Quantitative analysis of epoxy mixing ratios using partial least-square analysis of FTIR spectra," International Labmate,vol. 16 (1991) 1.

C. R. Brundle, C. A. Evans, S. Wilson, Encyclopedia of Materials Characterization, Butterworth-Heinemann Publishing, USA, 1992.

J. Canavate, X. Colom, P. Pages, and F. Carrasco,"Study of the curing process of an epoxy resin FTIR spectroscopy," Polymer Plastic Technology Engineering, vol. 39 no.5 (2000) 937-943.

L.B. Canto, G.L. Mantovani, E.R. deAzevedo, T.J. Bonagamba, E. Hage and L.A. Pessan, "Molecular Characterization of Styrene-Butadiene-Styrene Block Copolymers (SBS) by GPC, NMR, and FTIR," Polymer Bulletin vol. 57 (2006) 513–524.

John M. Chalomers and Geoffery Dent, Industrial Analysis with Vibrational Spectroscopy, Published by the Royal Society of Chemistry, Thomas Graham House, Science Park, Milton Road, Cambridge CB4 4WF, UK, 1997.

C. Chen, A. Tayebali, and D. R.U. Knappe, "A procedure to quantify antistrip additives in asphalt binders and mixes," Journal of Testing and Evaluation, vol. 34 no. 4 (2006) 269-274.

C.W. Curtis, D. I. Hanson, S. T. Chen, G-J Shieh, and M. Ling "Quantitative determination of polymers in asphalt cements and hot-mix asphalt mixes," Transportation Research Record 1488. Transportation Research Board, Washington, DC, (1995) 52-61.

C. Curtis, "A literature review of liquid antistripping and tests for measuring stripping," Strategic Highway Research Program, SHRP-A/UIR-90-016, Washington DC July 1990.

I. E. dell'Erba, and R.J.J. Williams, "Synthesis of oligomeric silsesquioxanes functionalized with (β-carboxyl) ester groups and their use as modifiers of epoxy networks," European Polymer Journal, vol. 43 (2007) 2759-2767.

S. Diefendefer, "Detection of polymer modifiers in asphalt binder," FHWA/VTRC 06-R18, Virginia Department of Transportation, Richmond Virginia, January 2006.

F. Djouani, C. Connan, M. M. Chehimi, and K. Benzarti," Interfacial chemistry of epoxy adhesives on hydrated cement paste", Surface and interface Analysis, DOI 10.1002/sia.2783 (www.interscience.com).

C. Estakhri and D. Saylak, Reducing Greenhouse Emission in Texas with High Volume Fly Ash Concrete, 84th annual conference of Transportation Research Board, pp. 167-174 (2005).

M. Fernandez-Berridi, Gonzalez, N., Mugica, A., Bernicot, C., Thermochimica Acta 444 (2006) 65-70.

A. Fernandez-Jimenez and F. Puertas, "Effect of activator mix on the hydration and strength behaviour of alkali-activated slag cements," Advances in Ceramic Research vol. 15 no. 3 (2003) 129-136.

P. Fletcher, P.V. Coveney, T.L. Hughes, and C.M. Methven, "Predicting quality and performance of oilfield cements with artificial neural network and FTIR spectroscopy," JPT February 1995 129-130.

S. Garrigues, J.M. Andrade, M. de la Guadia, D. Prada, Analytica Chimica Acta 317 (1995) 95-105.

G.N. Ghebremeskel, S.R. Shield, and A. Synpol, "Characterization of binary/tertiary blends of SBR, NBR and PVC by IR spectroscopy," Rubber World 2003, 26-46.

T. Hughes, C. Methven, T. Jones, S. Pelham, P. Fletcher, and C. Hall, "Determining cement composition by Fourier Transform Infrared Spectroscopy," Advanced Cement Based Materials 2, (1995) 91-104.

A. James, Overview of Asphalt Emulsion, Transportation Research Circular Number E-C102, Asphalt Emulsion Technology, August 2006.

Q.M. Jia, M. Zheng, Y.C. Zhu, J.B. Li, and C.Z. Xu, "Effects of organophilic montmorillonite on hydrogen bonding, free volume and glass transition temperature of epoxy resin/polyurethane interpenetrating polymer networks," European Polymer Journal vol. 43 (2007) 35-42.

G. King, "Additives in Asphalt," J. Assoc. Asphalt Paving Technol A 68 (1999) 32-69.

J. Lamontagne, P. Dumas, V. Mouillet, and J. Kister, "Comparison by Fourier transform infrared (FTIR) spectroscopy of different ageing techniques: application to road bitumens," Fuel 80 (2001) 483- 488.

W.K.W. Lee and J.S.J. van Deventer, "Structural Reorganisation of Class F Fly Ash in Alkaline Silicate Solutions," Colloids and Surfaces A: Physicochem. Eng. Aspects 211 (2002) 49- 66.

F. Lima, and L. Leite, "Determination of asphalt cement properties by Near Infrared Spectroscopy and Chemometrics," Petroleum Science and Technology vol. 22, no. 5 & 6 (2004) 589-600.

Y. Li, J. Cheng, "Quantitative analysis methods of Thiirane/epoxy resin of Bisphenol A," Advanced Materials Research vol. 11-12 (2006) 379-382.

S. Lin, B. Bulkin, E. Pearce, "Epoxy resins III. Applications of Fourier Transform IR to degradation studies of epoxy systems," Journal of Polymer Science vol. 17 (1978) 3121-3148.

A.A.P. Mansur, D.B. Santos, and H.S. Mansur, "A microstructural approach to adherence mechanism of Polyvinylalcohol modified cement systems to ceramic tiles," Cement and Concrete Research vol.37 no. 2 (2007) 270-282.

J-F Masson, L. Pelletier, P. Collins, "Rapid FTIR method for quantification of Styrene-Butadiene type copolymers in bitumen," J. of Applied Polymer Science vol. 79 (2001) 1034-1041.

E.A. Mercado, A.E. Martin, E.S. Park, C. Spiegelman, and C. Glover, "Factors affecting binder properties between production and construction," Journal of Materials in Civil Engineering ASCE/ January/February 2005 89-98.

P. Musto, "Two dimensional FTIR spectroscopy studies on the thermal-oxidative degradation of epoxy and epoxy-Bis(maleimide) network," Macromolecules vol. 36 (2003) 3210-3221.

S. Nasrazadani and H. Namduri, "Study of Phase Transformation in Iron Oxides Using Laser Induced Breakdown Spectroscopy (LIBS)," Spectrochimica Acta, Part B 61 (2006) 565-571.

S. Nasrazadani, "Application of IR Spectroscopy for Study of Phosphoric and Tannic Acids Interactions with Magnetite, Goethite, and Lepidocrocite," Corrosion Science, Vol. 39, No. 10-11(1997) 1845-1859.

S. Nasrazadani and A. Raman, "The Application of Infrared Spectroscopy to the Study of Rust Systems," Corrosion Science, Vol 34, No. 8(1993) 1355-1365.

T. Nguyen, E. Byrd, D. Bentz, and J. Seller, "Development of a method for measuring water-stripping resistance of asphalt/siliceous aggregate mixtures," NISTIR 5865, U.S. Department of Commerce, Gaithersburg MD, July 1996.

C. Ouyang, S. Wang, Yong Zhang, and Yinxi Zhang, "Improving the aging resistance of styrene-butadiene-styrene tri-block copolymer modified asphalt by addition of antioxidants," Polymer Degradation and Stability 91 (2006) 795-804.

C. Ouyang, S. Wang, Yong Zhang, and Yinxi Zhang, "Improving the aging resistance of asphalt by addition of Zinc dialkyldithiophosphate," Fuel 85 (2006) 1060-1066.

A. Palomo, A. Fernandez-Jimenez, G. Kovalchuk, L.M. Ordoňez and M.C. Naranjo, "Opc-fly ash cementitious systems: Study of gel binders produced during alkaline hydration, "Journal of Materials Science 10.1007/s10853-006-0585-7, published online 22 February 2007. (http://www.springerlink.com/content/jq631288076322ng/fulltext.html viewed 8/8/2009)

D. Panias, I. P. Giannopoulou, T. Perraki, "Effect of synthesis parameters on the mechanical properties of fly ash-based geopolymers," Colloids and Surfaces A: Physicochem. Eng. Aspects 301 (2007) 246–254.

J.C. Petersen, H. Plancher, and S. M. Dorrence,"Identification of chemical types in asphalts strongly adsorbed at the asphalt-aggregate interface and their relative displacement by water," Proceedings Association of Asphalt Pavement Technologists, vol. 46, 1977.

J.C. Petersen, "Quantitative functional group analysis of asphalts using Differential Infrared Spectrometry and Selective Chemical Reactions -theory and applications," Transportation Research Record 1096. Transportation Research Board, Washington, DC, (1986).

N. Poisson, G. Lachenal, H. Sautereau, "Near- and mid-Infrared spectroscopy studies of an epoxy reactive system," Vibrational Spectroscopy vol. 12 (1996) 237-247.

F. Puertas, S. Martinez-Ramirez, S. Alonso, and T. Vazquez, "Alkali-activated fly ash/slag cement strength behaviour and hydration products," Cement and Concrete Research, 30 (2000) 1625-1632.

F. Puertas, A. Fernandez-Jimenez, "Mineralogical and microstructural characterization of alkali-activated fly ash/slag pastes," Cement & Concrete Research vol. 25 (2003) 287-292.

F. L. Roberts, P. S. Kandhal, E. R. Brown, D. Lee, and T.W. Kennedy, "Hot Mix Asphalt Materials, Mixtures Design, and Construction," NAPA Research and Education Foundation.

M. A. Rodriguez –Valverde, P. Ramon-torregrosa, A. Paez-Dueňas, M.A. Cabrizo-Vilchez, R. Haidalgo-Alvarez, "Imaging techniques applied to characterize bitumen and bituminous emulsion," Advances in Colloid and Interface Science vol. 136 (2008) 93-108.

N.J. Saikia, P. Sengupta, P.K. Gogoi, and P.C. Borthakur, "Hydration behaviour of lime-co-calcined kaolin-petroleum effluent treatment plant sludge," Cement and Concrete Research vol. 32 (2002) 297-302.

K. Saravanan, S. Sathiyanarayanan, M. Muralidharan, S. Syed Azim, and G. Venkatachari, "Performance evaluation of polyaniline pigmented epoxy coating for corrosion protection of steel in concrete environment," Progress in Organic Coatings vol. 59 (2007) 160-167.

A. Sarkar, Ruma Rano, G. Udaybhanu, A.K. Basu, "A comprehensive characterization of fly ash from a thermal power plant in Eastern India," Fuel Processing Technology 87 (2006) 259 – 277.

M. Sanchez-Soto, P. Pages, T. Lacorte, K. Briceno, F. Carrasco, "Curing FTIR study and mechanical characterization of glass bead filled trifunctional epoxy composites," Composite Science and Technology vol. 67 (2007) 1974-1985.

T. Scherzer, (2003) Journal of Applied Polymer Science vol. 58 no.3 (2003) 501-514.

T. Scherzer, "Rheo-optical FTIR Spectroscopy of Amine Cured Epoxy Resins," Journal of Molecular Structure vol. 348 (1995) 465-468.

M. Siddiqui, "Infrared study of hydrogen bond types in asphaltenes," Petroleum Science and Technology vol. 21, no. 9 & 10 (2003) 1601-1615.

J. Stevens, R. Theimer, S. Nasrazadani, and H. Namduri "Secondary System Oxide and Lead Study at Comanche Peak," Proceeding of International Conference on Water Chemistry of Nuclear Reactor Systems, Jeju Island, South Korea, October 2006.

L. Stoch and M. Sroda, "Infrared Spectroscopy in the Investigation of Oxide Glasses Structure," Journal of Molecular Structure, vol. 511-512 (1999) 77-84.

C.E. Tambelli, J.F. Schneider, N.P. Hasparyk, and P.J.M. Monteiro, "Study of the structure of alkali-silica reaction gel by high-resolution NMR spectroscopy," Journal of Non-Crystalline Solids 352 (2006) 3429-3436.

TEX-533-C, "Determination of polymer additive percentages in polymer modified asphalt cements," Test method TEX-533-C, Materials and Tests Division, Texas State Department of Transportation August 1999.

M.J. Varas, M. Alvarez de Buergo, and R. Fort, "Natural cement as the precursor of Portland cement: Methodology for its identification," Cement and Concrete Research vol. 35 (2005) 2055-2065.

J. Vega-Baudrit, M. Sibaja-Ballestero, P. Vazquez, R. Torregrosa-Macia, J. M. martin-Martinez, "Properties of thermoplastic polyurethane adhesive containing nanosilicas with different specific surface area and silanol content," International Journal of Adhesion & Adhesives, vol. 27 (2007) 469-479.

R.K. Vempati, H.V. Lauer, Jr., "Fractionation and characterization of Texas lignite class "F" fly ash by XRD, TGA, FTIR, and SFM," Cement and Concrete Research vol. 24, no. 6 (1994) 1153-1164.

Y. Yildirim, "Polymer modified asphalt binders," Construction and Building Materials vol. 21 (2007) 66-72.

B.Yilmaz, A. Olgun, "Studies on cement and mortar containing low-calcium fly ash, limestone, and dolomite limestone," Cement and Concrete Composites, vol. 30 (2008) 194-201.

N.M. Whiting, and Snyder M. B., "Effectiveness of Portland Cement Concrete Curing Compound," *Transportation Research Record*, No. 1834(2003) 59–68, 2003.

Y. Zhang, J. Xu, Z. Chen, C. Qin, and Y. Dou, "Vibration spectroscopic investigation of light-induced polymerization process of epoxy resin, polytetrahydrofuran and spirobislactone," Polymer International, vol. 56 (2007) 914-918.

FTIR SPECTRA OF SELECTED POLYMER-MODIFIED ASPHALT SAMPLES

0156
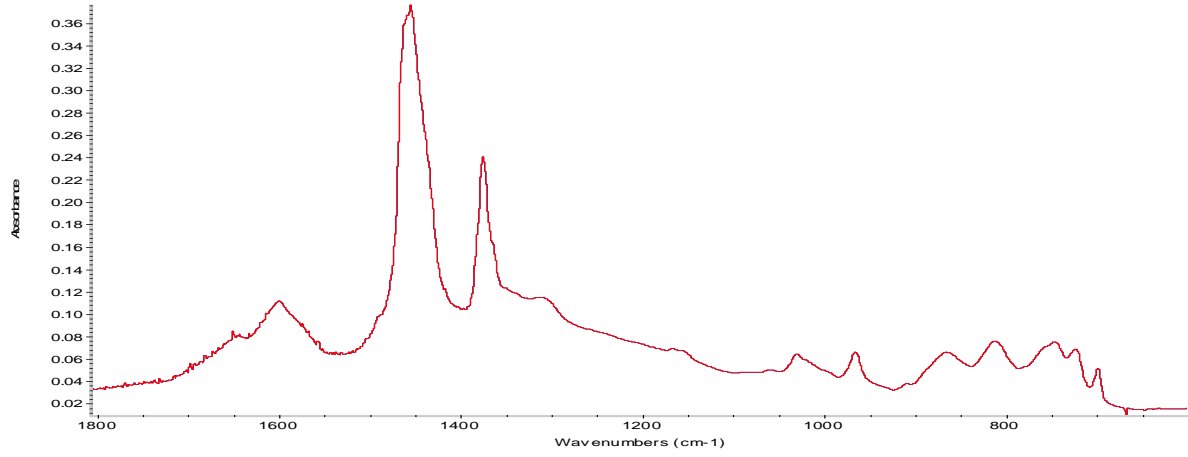
Calibration Curve	Supplier A	Supplier B
% Polymer	3.012522 %	3.213283 %

0157
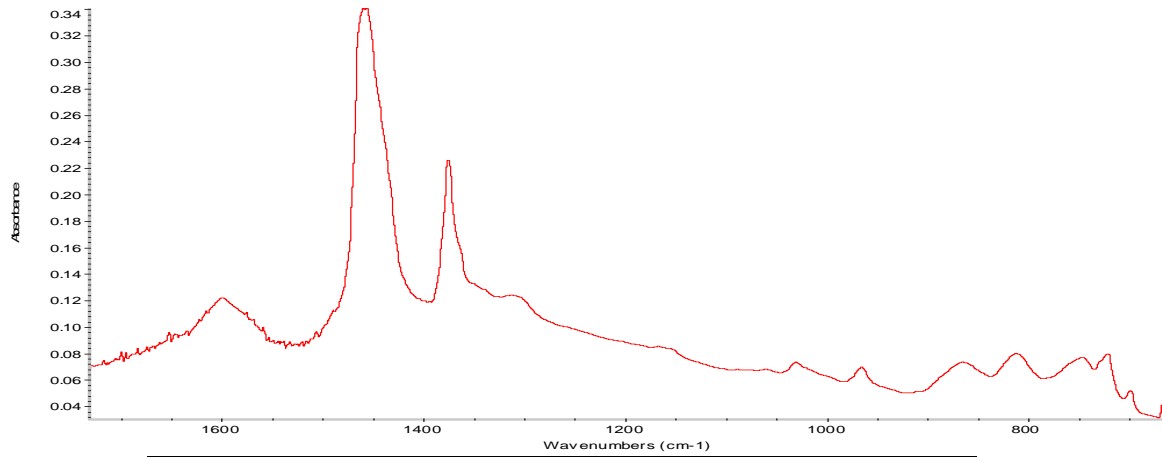
Calibration Curve	Supplier A	Supplier B
% Polymer	1.925708 %	1.560909 %

142
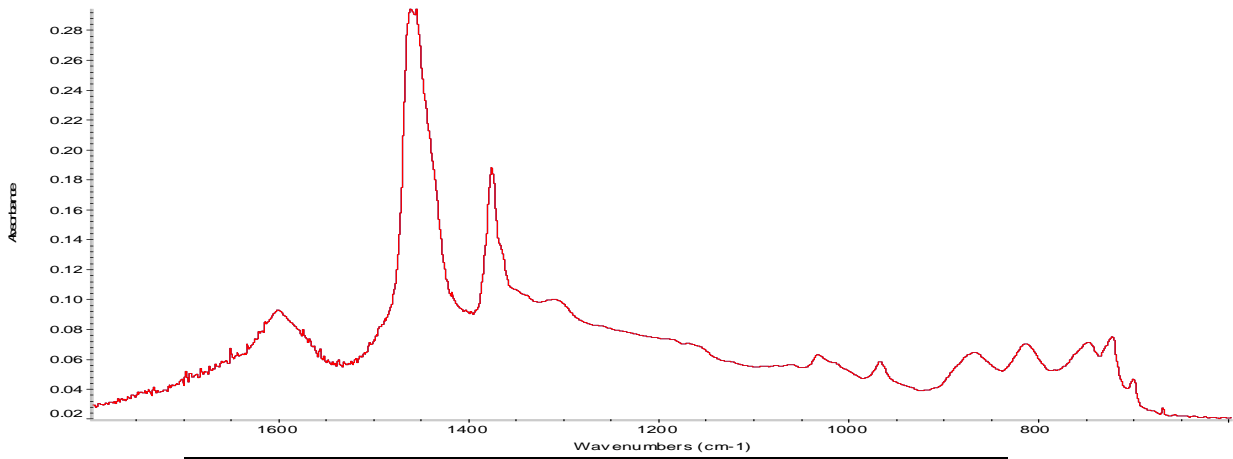
Calibration Curve	Supplier A	Supplier B
% Polymer	1.793887 %	1.360489 %

==

0143

Sat Feb 23 12:52:23 2008 (GMT-06:00)
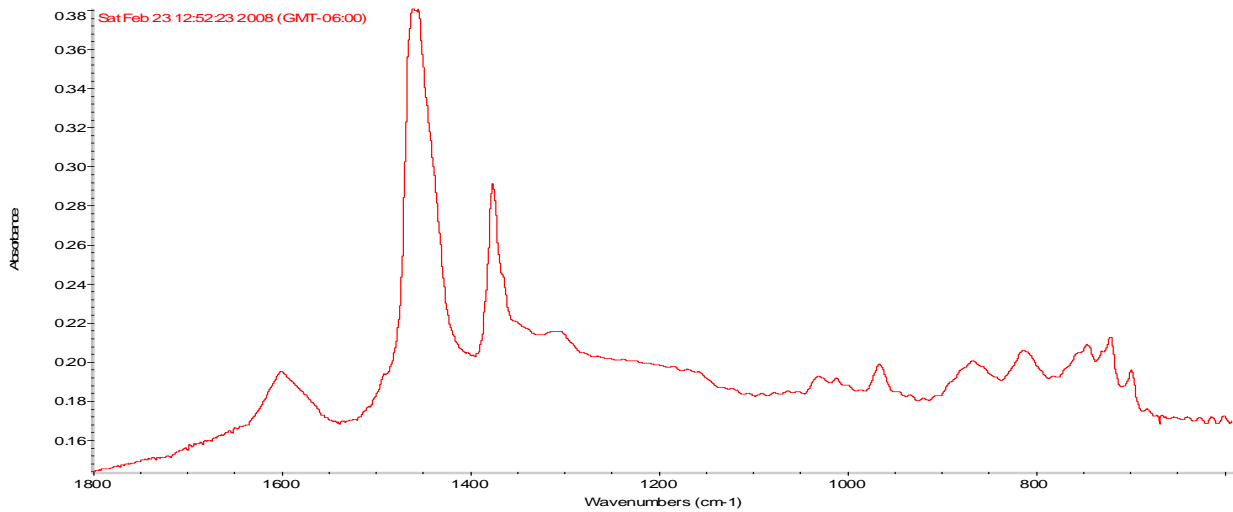
Calibration Curve	Supplier A	Supplier B
% Polymer	2.905299 %	3.050263 %

144

Mon Feb 25 17:45:09 2008 (GMT-06:00)
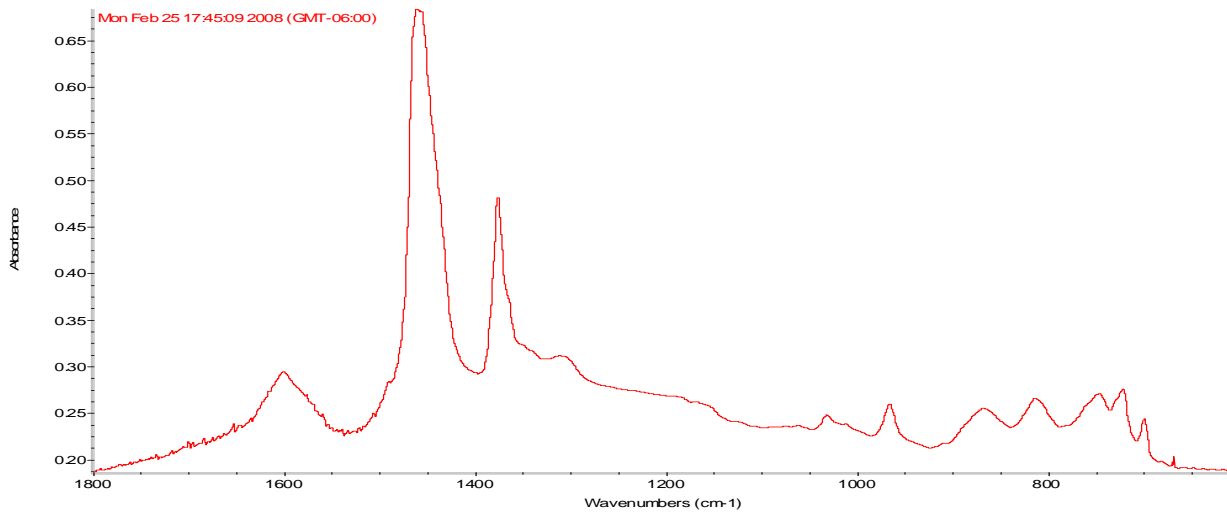
Calibration Curve	Supplier A	Supplier B
% Polymer	3.117443 %	3.372803 %

===

145
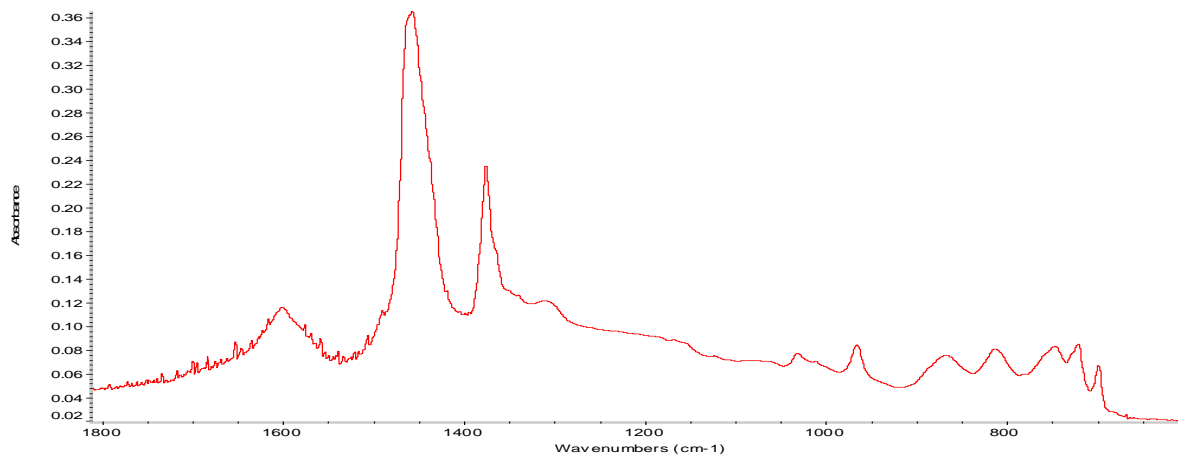
Calibration Curve	Supplier A	Supplier B
% Polymer	3.228446 %	3.54156 %

===

07B

Mon Feb 25 14:02:45 2008 (GMT-06:00)
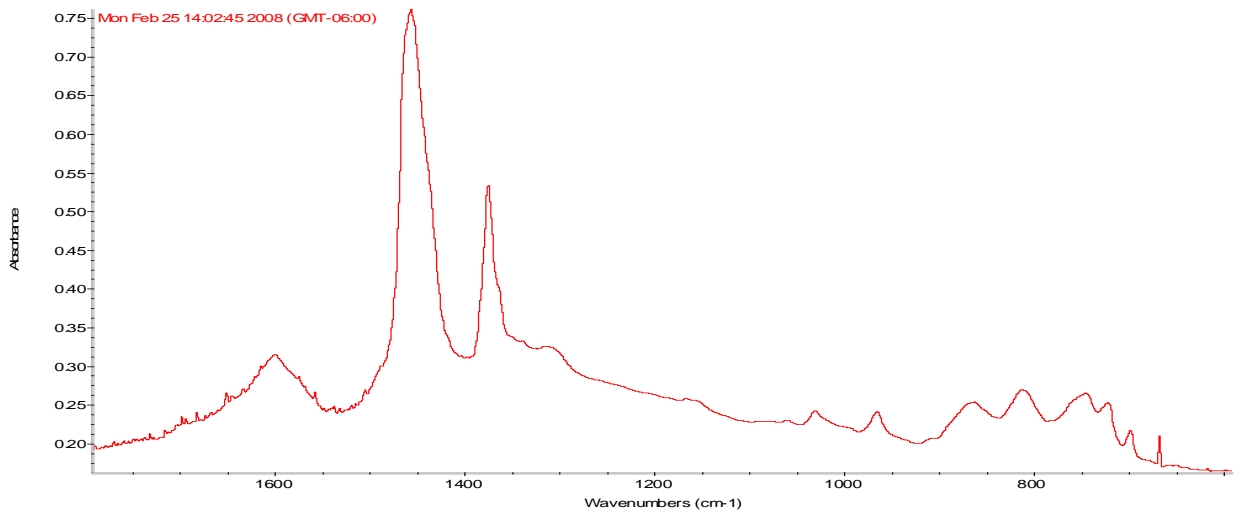
Calibration Curve	Supplier A	Supplier B
% Polymer	1.986765 %	1.653738 %

TEST PROCEDURE FOR POLYMER QUANTIFICATION IN POLYMER MODIFIED ASPHALT

Test Procedure for

QUANTIFICATION OF POLYMER CONTENT OF POLYMER MODIFIED ASPHALT BY FTIR

TxDOT Designation:

Effective Date:

_____

1.SCOPE

1.1   Use this method to determine the concentrations of various polymeric additives in asphalt binder, including the following:
- styrene-butadiene-styrene block copolymer (SBS)

- Styrene-butadiene-rubber random copolymer (SBR)

 1.2   This test procedure contains several parts:
- Part I – Determining polymer content of an unknown sample
- Part II – Generating calibration curves for specific asphalt/additive combination

- Part III – General procedure for collecting sample data by light transmission through a Potassium Bromide (KBr) pellet.
- Part IV- Using ATR method for polymer quantification (This part is an alternative to Part III.)
- Part V- Data Collection and Analysis

_____

PART I – DETERMINING POLYMER CONTENT OF AN UNKNOWN SAMPLE
_____

2.SCOPE

2.1   Use the following procedure to measure the polymer content of an unknown sample of modified asphalt.

_____

3.PROCEDURE

3.2   If one does not exist, generate a calibration curve for the polymer-modified asphalt using the method described in Part II.

3.3   Generate an IR spectrum using the method described in Part III.

3.4   Calculate the peak height ratio for the appropriate polymer type in the unknown.

3.5   Calculate the polymer content from the measured peak height ratio.

___

PART II – GENERATING CALIBRATION CURVES FOR SPECIFIC ASPHALT/ADDITIVE COMBINATION
___

4. SCOPE

4.1   Because the infrared response is different for each asphalt crude source and each polymer brand, generate a calibration curve for each asphalt/polymer combination. The producer of the modified asphalt is required to submit samples of the asphalt and polymer for generation of a calibration curve.

5.   APPARATUS

5.1   Fourier Transform Infrared Spectrometer

5.2   Balance, readable to 0.1g, accurate to 0.5g.

5.3   Hot plate.

5.4   Wax paper.

5.5   Insulating gloves.

5.6   Metallic canisters.

5.7   Mercury thermometer, marked in 5°F (3°C) divisions or less, or digital thermometer, capable of measuring the temperature specified in the test procedure.

___

6.   MATERIALS

6.1   Asphalt cement containing 1-5% (wt%) polymer.

___

7.   DATA COLLECTION AND CURVE GENERATION

7.1   Collect standard blends from asphalt manufacturer.

7.2   Perform IR scans of all standards and of the unmodified asphalt, using the method described in Part III.

7.3   When using the transmission method (Part III), measure the appropriate peak height from a baseline adjustment between 1055 and 920 cm^{-1}. The peak for SB in SBS and SBR is 965 cm^{-1}, (due to butadiene mid-block).

7.4   Plot the peak ratio of the height of the peak 965 cm^{-1} by the height of peak 1375 cm^{-1} versus the polymer concentration, and perform a curve fit by using linear least squares or other convention. (IR software may be equipped to do this.) The resulting equation serves as calibration curve.

___

PART III – GENERAL PROCEDURE FOR COLLECTING DATA BY TRANSMISION THROUGH A KBr PELLET

8. APPARATUS

8.1   Fourier Transform Infrared Spectrometer

8.2   Balance, readable to 0.1g, accurate to 0.5g.

8.3   Hot plate.

8.4   Wax paper.

8.5   Insulating gloves.

8.6   Mercury thermometer, marked in 5°F (3°C) divisions or less, or digital thermometer, capable of measuring the temperature specified in the test procedure.

MATERIALS

8.7   Asphalt cement.

9. PREPARING SAMPLES

9.1   Heat 100g of asphalt sample to no more than 100°C for 20 minutes.

9.2   Apply approximately 1g of liquid asphalt to wax paper using spatula.

9.3   Measure 100 mg of KBr powder.

9.4   Place KBr powder into 13 mm die press for 2 minutes at 10,000 psi.

9.5   Place KBr pellet on top of 1g of asphalt sample and heat to no more than 100°C for 30 seconds.

9.6   Apply another wax paper on top of KBr pellet and gently press until a thin transparent coat of asphalt is applied to KBr pellet.

10. SAMPLE ANALYSIS

10.1   Prepare the sample using the method described in Section 9.

10.2   Place the KBr pellet in the cell holder and position the most uniform region of the pellet in the path of the beam.

10.3   Scan the sample from 4000 to 400 cm^{-1}, and record data.

PART IV – FTIR ATR METHOD

## 11.	SCOPE

11.1	This is the general procedure for collecting IR data by Attenuated Total Reflectance (ATR) Method.

## 12.	APPARATUS

12.1	Fourier Transform Infrared Spectrometer with ATR accessory.

12.2	Balance, readable to 0.1g, accurate to 0.5g.

12.3	Hot plate.

12.4	Insulating gloves.

12.4.1	Mercury thermometer, marked in 5°F (3°C) divisions or less, or digital thermometer capable of measuring the temperature specified in the test procedure.

## 13.	MATERIALS

13.1	Asphalt cement.

## 14.	PREPARING SAMPLES

14.1	Heat asphalt sample to no more than 100°C for 20 minutes and stir it to homogenize.

14.2	Apply a thin film of liquid asphalt over the center of germanium crystal using wax paper. Ensure no bubbles are formed by pressing on the wax paper.

14.3	Prepare an ATR crystal using the manufacturer's guidelines

---

## 15.	SAMPLE ANALYSIS

15.1	Prepare the sample using the method described in Section 14.

15.2	Place germanium crystal into ATR accessory.

15.3	Scan the sample from 4000 to 500 cm^{-1}, and record data.

PART V – DATA COLLECTION AND ANALYSIS

## 16.	DATA ANALYSIS

16.1   Using either transmittance or ATR method, acquire spectra on the prepared KBr or crystal for each sample with known polymer content. Background collection is recommended before a sample analysis.

16.2   Once a FTIR spectrum such as the one shown in Figure 1 is collected, draw a baseline covering both 965 cm^{-1} and 1375 cm^{-1} absorption bands using manufacturer's software.

16.3   Measure absorbance height for bands at 965 cm^{-1} and 1375 cm^{-1}.

16.4   Calculate ratio of band areas ($H_{965 \text{ cm-1}}/H_{1375 \text{ cm-1}}$)

16.5   Repeat steps 16.3 and 16.4 for all samples with known polymer concentration

16.6   Plot ($H_{965 \text{ cm-1}}/H_{1375 \text{ cm-1}}$) versus polymer concentration as shown in Figure 2.

16.7   Perform a regression analysis to obtain a mathematical relationship between area ratios and polymer content.

16.8   Use the obtained mathematical relationship and area ratio measured for an unknown sample to find polymer concentration of in the unknown sample.
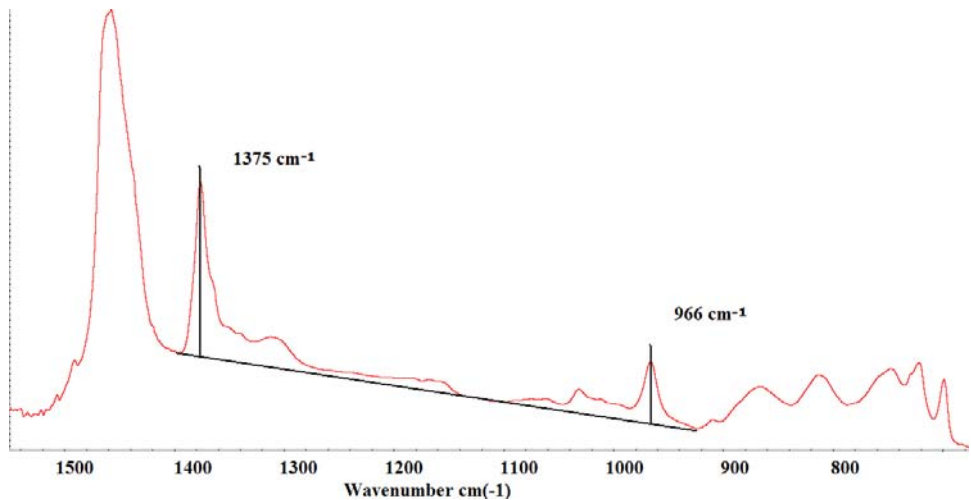
Figure 1: FTIR Spectrum of a Polymer-Modified Asphalt Sample.
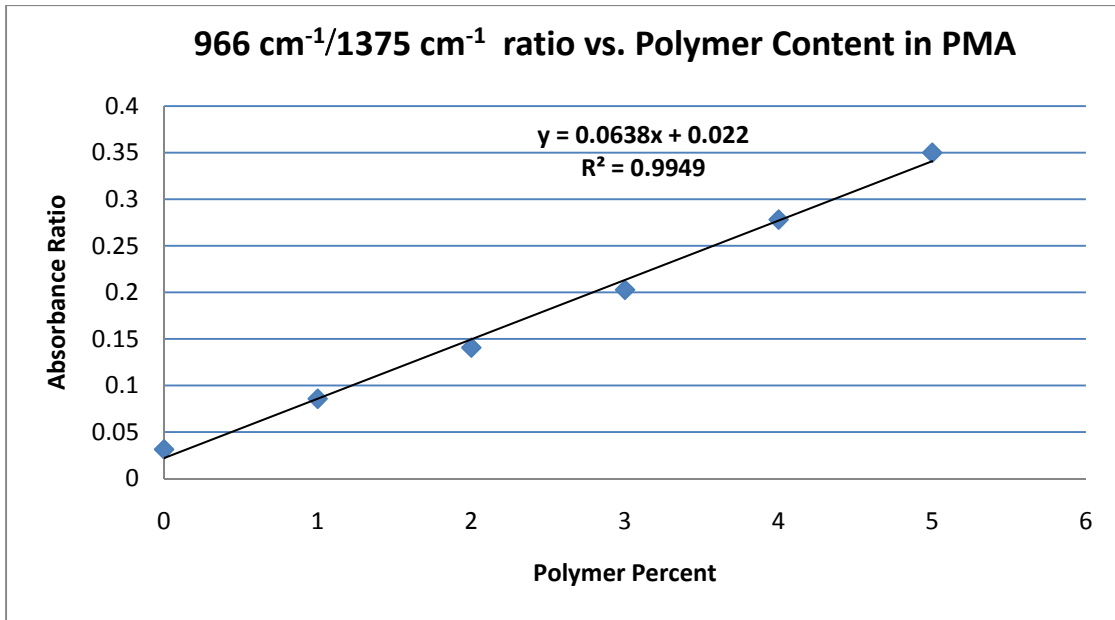
Figure 2: A Calibration Curve for Polymer Quantification of a Polymer-Modified Asphalt Binder.

TEST PROCEDURE FOR UNIFORMITY ANALYSIS OF MOISTURE BARRIERS AND EVAPORATION RETARDANTS

TXDOT DESIGNATION:

Effective Date: August 1999

---

1.   SCOPE

1.1   Use this procedure to determine uniformity of moisture barriers and evaporation retardants.

1.2   This test procedure is in several parts:

- ■   Part I—Drying procedure for moisture barriers and evaporation retardants

- ■   Part II—Sample preparation for moisture barriers

- ■   Part III—Sample preparation for evaporation retardants

- ■   Part IV—Spectra analysis

PART I— DRYING PROCEDURE FOR MOISTURE BARRIER AND EVAPORATION RETARDANTS

2.   SCOPE

2.1   Use the following procedure to dry moisture barriers and evaporation retardants.

---

3.   PROCEDURE

3.1   Prepare a glass slide by labeling it with material information.

3.2   Using a spatula scoop some of the material and place it on the glass slide. Spread the material over the glass slide without touching the film.

3.3   Place the slide in an oven or over a hot plate at 95 °C and heat it for 3 hours. (Some color change in the sample may occur)

3.4   Allow glass slide to cool to room temperature. This may take about one hour.

PART II—SAMPLE PREPARATION FOR MOISTURE BARRIERS

4.   SCOPE

4.1   This procedure prepares a KBr pellet for a moisture barrier sample.

5.   APPARATUS

5.1   *Hydraulic press with 12000 psi capacity*

5.2   *Mortar and pestle set*

5.3   *Hot plate*

5.4   *Oven*

5.5   *KBr powder*

5.6   *Wax paper*

5.7   *Spatulas*

5.8   *Glass slide*

6.   PREPARING KBR PELLET FOR MOISTURE BARRIER SAMPLES

6.1   Weigh approximately 100 mg of KBr powder in a wax paper.

6.2   Weigh approximately 2 mg of dried (dried according to procedure given in part 1) moisture barrier.

6.3   Mix and grind KBr and dried moisture barrier and using mortar and pestle set to obtain a fine powdery mixture.

6.4   Pour the mixture prepared in step 6.3 into a stainless steel die and apply 10,000 psi pressure on the mixture for 3-5 minutes. Use a mechanical pump to remove any moisture and air from pressed mixture during pellet making step.

PART III— SAMPLE PREPARATION FOR EVAPORATION RETARDANTS

7.   PREPARING KBR PELLET FOR EVAPORATION RETARDANT SAMPLES

7.1   Weigh approximately 100 mg of KBr powder in a wax paper.

7.2   Prepare a blank KBr pellet using 100 mg powder.

7.3   Using a spatula, smear paste like evaporation retardant over a glass slide.

7.4	Place the slide containing evaporation retardant over the pre-fabricated KBr pellet.
7.5	Press firmly, move the slide on the pellet in a small circular motion to transfer the material to the face of the pellet.

PART IV— SPECTRA ANALYSIS

8.   DATA COLLECTION

8.1	Transfer either moisture barrier or evaporation retardant pellet to the sample holder of FTIR spectrometer
8.2	Run FTIR analysis in 4000 cm-1 to 400 cm-1.
8.3	Use FTIR software to overlay spectra and compare fingerprints of the sample from different patches to assess uniformity of the same material from different batches.

APPENDIX D:

HISTORICAL DATA OF CEMENT COMPOSITION ANALYZED BY XRF

This historical data is provided here to show that a large number of samples from different cement suppliers have been chemically analyzed using XRF and results of this analysis consistently show different alkali content in these cement samples.

Cement Source 1

SiO_2	Al_2O_3	Fe_2O_3	CaO	MgO	SO_3	Na_2O	K_2O	DATE_RECEIVED
19.52	5.24	2.66	59.17	1.16	2.96	0.17	0.88	1/1/1988 0:00
19.55	5.31	2.83	63.9	1.13	5.05	0.12	0.81	1/1/1988 0:00
19.95	5.57	2.58	63.42	1.22	3.45	0.11	0.68	1/1/1988 0:00
19.73	5.31	2.93	63.33	1.22	3.53	0.11	0.93	2/15/2001 0:00
20.57	5.27	2.49	63.73	1.32	3.39	0.1	0.66	4/19/2001 0:00
13.87	3.68	2.06	52.27	0.79	2.47	0.14	0.85	6/15/2001 0:00
16.08	4.32	2.31	58.52	1.08	3	0.19	0.76	8/14/2001 0:00
20.34	5.14	2.72	63.36	1.21	3.3	0.16	0.99	10/5/2001 0:00
20.83	4.76	4.05	63.22	2.64	1.97	0.19	0.5	10/30/2001 0:00
20.35	5.95	2.74	62.2	1.4	3.17	0.25	0.83	12/2/2001 0:00
19.75	5.68	2.5	63.73	1.22	3.21	0.18	0.89	4/26/2002 0:00
19.89	5.25	2.67	64.04	1.18	3.23	0.19	0.87	7/31/2002 0:00
20.17	5.26	2.48	63.93	1.13	3.21	0.12	0.92	10/15/2002 0:00
19.93	5.46	2.36	64.14	1.14	3.2	0.11	0.91	11/27/2002 0:00
19.69	5.28	2.39	64.21	1.12	3.42	0.11	1.02	12/20/2002 0:00
19.65	5.26	2.67	63.76	1.1	3.51	0.14	1.09	1/31/2003 0:00
19.66	5.16	2.5	64.13	1.16	3.29	0.1	0.94	3/6/2003 0:00
20.13	5.03	3.91	64.5	0.65	3.34	0.07	0.94	3/10/2003 0:00
19.63	5.19	2.51	63.97	1.12	3.31	0.11	0.94	3/27/2003 0:00
18.86	5.04	2.73	63.16	1.11	3.4	0.1	0.97	4/28/2003 0:00
18.78	4.76	2.64	59.89	1.03	2.79	0.08	0.78	5/28/2003 0:00
19.9	5.22	2.64	64.29	1.14	3.29	0.15	0.9	7/31/2003 0:00
19.74	5.1	2.82	63.81	1.16	3.16	0.35	0.88	8/25/2003 0:00
19.21	5.5	2.7	67.87	1.09	3.11	0	1.02	9/25/2003 0:00
19.5	5.63	2.29	64.42	1.25	3.3	0.12	0.89	10/29/2003 0:00
19.38	5.52	2.85	63.75	1.16	3.41	0.19	0.93	11/1/2003 0:00
18.92	4.42	2.34	61.98	1.37	2.75	0.14	0.92	2/17/2004 0:00
20.29	5.31	2.46	64.43	1.14	3.41	0.12	0.91	2/26/2004 0:00
20.95	4.88	2.46	65.18	1.49	2.96	0.14	0.94	3/17/2004 0:00
20.38	5.42	2.37	64.56	1.1	3.32	0.12	0.92	4/22/2004 0:00
20.83	4.61	2.48	65.01	1.49	2.97	0.13	0.94	5/18/2004 0:00
19.75	5.11	2.49	64.07	1.11	3.33	0.09	0.94	6/4/2004 0:00
19.45	5.68	2.59	63.5	1.12	3.19	0.16	0.91	7/15/2004 0:00
20.072	5.003	2.4	63.842	1.119	3.287	0.069	0.908	11/1/2004 0:00
20.372	4.139	3.137	64.139	2.077	2.506	0.181	0.512	12/2/2004 0:00
19.91	5.23	2.65	63.25	1.076	3.33	0.105	0.855	2/18/2005 0:00
19.794	5.512	2.41	63.315	1.084	3.178	0.108	0.983	4/28/2005 0:00
19.542	5.441	2.667	63.166	1.096	3.349	0.087	0.928	5/19/2005 0:00
20.118	5.59	2.299	63.976	1.257	3.073	0.095	0.852	10/31/2005 0:00
19.436	5.581	2.337	63.87	1.17	3.314	0.098	0.895	12/5/2005 0:00

SiO$_2$	Al$_2$O$_3$	Fe$_2$O$_3$	CaO	MgO	SO$_3$	Na$_2$O	K$_2$O	DATE_RECEIVED
20.128	5.234	2.692	63.762	1.261	3.459	0.083	0.689	1/31/2006 0:00
19.48	5.601	2.332	64.315	1.208	3.442	0.117	0.983	3/31/2006 0:00
19.695	5.383	2.629	63.315	1.2	3.245	0.109	0.903	4/28/2006 0:00
20.049	5.788	2.28	63.244	1.4	2.852	0.102	0.926	6/14/2006 0:00
20.523	5.242	3.662	63.104	0.895	2.672	0.085	0.483	7/20/2006 0:00
19.773	5.27	2.343	63.541	1.115	3.14	0.11	0.87	11/17/2006 7:53
20.555	5.265	2.526	64.127	1.179	3.196	0.123	0.892	1/3/2007 16:24
19.004	4.825	2.661	62.444	1.097	2.887	0.083	0.92	2/16/2007 16:14
19.18	5.243	2.261	63.346	1.125	2.753	0.108	0.999	3/28/2007 0:00
18.825	5.081	2.367	61.204	1.021	3.301	0.107	0.921	5/25/2007 0:00
19.229	5.347	2.589	61.914	1.056	3.489	0.118	0.928	7/2/2007 0:00
19.284	5.006	2.815	62.888	1.08	3.305	0.114	0.903	9/30/2007 0:00
18.966	4.541	3.756	63.554	0.986	2.798	0.354	0.329	2/20/2008 8:08
18.752	4.987	2.312	61.436	1.243	3.376	0.148	0.851	2/20/2008 9:07
19.86	5.491	2.327	61.386	1.363	3.357	0.147	0.946	5/7/2008 0:00
18.857	5.314	2.642	59.963	1.396	3.408	0.15	0.906	6/5/2008 16:23
18.676	5.373	2.599	61.588	1.14	3.615	0.128	1.078	8/19/2008 8:09
19.015	5.296	2.739	61.319	1.283	3.385	0.141	0.963	9/3/2008 0:00
18.593	4.475	3.864	61.195	1.072	2.745	0.16	0.562	12/31/2008 9:05
17.576	4.81	2.928	61.086	1.119	3.299	0.137	0.907	2/3/2009 16:44
18.213	5.455	2.65	61.401	1.18	3.555	0.145	1.054	3/5/2009 12:52
17.82	5.061	2.69	62.603	1.148	3.381	0.127	0.966	4/9/2009 8:09
17.963	5.183	2.447	63.502	1.082	3.371	0.12	0.938	5/12/2009 14:24
18.808	5.271	2.613	63.003	1.158	3.383	0.115	0.835	6/10/2009 14:43

Cement Source 4	Type I/II							
SiO$_2$	Al$_2$O$_3$	Fe$_2$O$_3$	CaO	MgO	SO$_3$	Na$_2$O	K$_2$O	DATE_RECEIVED
20.2	4.89	1.9	59.91	1.33	2.91	0.15	0.64	1/1/1988 0:00
20.15	4.99	1.85	64.71	1.32	4.26	0.11	0.6	1/1/1988 0:00
20.58	5.09	1.78	63.95	1.38	3.02	0.09	0.59	2/5/2001 0:00
20.9	4.82	2.26	63.57	1.39	2.94	0.14	0.58	4/6/2001 0:00
21.68	4.8	3.09	66.01	1.3	2.73	0.19	0.52	7/12/2001 0:00
21.61	5.02	1.95	66.17	1.29	3.15	0.12	0.65	10/8/2001 0:00
20.74	5.08	2.14	65.9	1.27	3.23	0.19	0.64	11/19/2001 0:00
21.01	4.97	1.89	65	1.31	3.01	0.18	0.61	1/10/2002 0:00
20.49	4.98	1.93	64.85	1.3	3.18	0.15	0.63	2/11/2002 0:00
19.34	4.71	1.72	61.98	1.26	2.86	0.18	0.63	4/8/2002 0:00
21.3	5.2	1.96	64.93	1.24	2.92	0.6	0.6	5/6/2002 0:00
21.5	5.18	2.17	63.63	1.17	2.98	0.19	0.56	6/7/2002 0:00
20.81	5.03	1.91	65.66	1.16	2.91	0.17	0.57	7/22/2002 0:00
20.41	5.03	2.01	64.68	1.28	3.31	0.21	0.57	8/6/2002 0:00
20.56	5.03	1.98	64.59	1.3	3.23	0.14	0.6	9/6/2002 0:00
20.19	4.96	1.95	64.87	1.26	3.06	0.15	0.62	11/13/2002 0:00
20.83	5.21	1.95	65.35	1.23	3.1	0.12	0.65	12/10/2002 0:00
20.61	5.11	1.83	64.58	1.26	3.12	0.1	0.67	3/18/2003 0:00
20.89	5.29	1.79	64.64	1.43	3.08	0.11	0.64	4/9/2003 0:00
20.82	5.2	1.9	64.65	1.28	3.16	0.13	0.63	2/17/2003 0:00
18.82	4.66	1.88	60.69	1.22	3.09	0.21	0.58	6/2/2003 0:00
20.69	5.12	1.86	64.59	1.3	3.23	0.08	0.58	6/9/2003 0:00

20.4	5.16	1.84	65.46	1.26	3.14	0.12	0.61	7/18/2003 0:00
20.81	5.19	1.88	65.44	1.25	2.94	0.16	0.63	8/15/2003 0:00
20.26	5.14	1.88	64.16	1.15	3.19	0.33	0.68	9/11/2003 0:00
20.49	5.28	1.95	65.11	1.15	3.24	0.14	0.67	10/5/2003 0:00
21.1	5.47	2.1	64.71	1.36	3.24	0.18	0.59	11/1/2003 0:00
20.76	5.12	1.9	64.71	1.05	3.26	0.14	0.75	11/10/2003 0:00
20.7	5.12	2.06	64.37	1.12	3.24	0.14	0.67	12/8/2003 0:00
20.73	5.22	1.92	63.64	1.07	3.38	0.14	0.69	1/12/2004 0:00
21.38	5.36	1.99	64.49	1.07	3.51	0.12	0.74	2/10/2004 0:00
20.08	5.09	1.97	65	1.14	3.31	0.1	0.6	3/8/2004 0:00
20.65	5.16	1.93	63.6	1.14	4.63	0.12	0.65	4/5/2004 0:00
19.87	5.09	1.86	62.39	1.14	3.24	0.11	0.66	4/8/2004 0:00
20.13	4.94	1.92	61.56	1.06	3.44	0.11	0.71	5/7/2004 0:00
20.73	4.96	1.97	64.78	1.1	3.23	0.1	0.63	6/4/2004 0:00
20.63	5.81	2.06	65.72	1.23	3.23	0.16	0.64	7/5/2004 0:00
20.59	5.26	2	64.67	1.18	3.41	0.14	0.69	8/9/2004 0:00
20.8	5.24	2	64.85	1.12	3.36	0	0	9/5/2004 0:00
20.873	4.697	1.719	64.982	1.156	3.403	0.056	0.642	10/26/2004 0:00
20.9	4.795	1.837	64.405	1.189	3.363	0.073	0.663	10/26/2004 0:00
21.312	5.18	1.807	65.972	1.204	3.532	0.112	0.64	11/15/2004 0:00
20.26	4.65	1.899	64.312	1.486	3.551	0.078	0.665	12/7/2004 0:00
20.45	5.38	1.9	64.89	1.267	3.03	0.12	0.635	1/25/2005 0:00
20.55	5.1	1.91	64.37	1.57	3.45	0.106	0.636	2/8/2005 0:00
20.099	5.063	1.407	63.241	1.233	3.573	0.102	0.555	3/7/2005 0:00
20.256	5.155	2.262	64.317	1.303	3.441	0.126	0.639	4/14/2005 0:00
20.291	5.435	2.186	64.63	1.253	3.399	0.089	0.602	5/16/2005 0:00
20.31	5.361	1.941	64.386	1.21	3.399	0.086	0.592	6/6/2005 0:00
19.641	5.152	1.956	64.239	1.137	4.218	0.099	0.591	7/26/2005 0:00
20.456	5.241	2.036	65.372	1.244	3.568	0.119	0.557	8/31/2005 0:00
20.098	5.133	1.938	64.834	1.128	3.308	0.112	0.646	9/8/2005 0:00
20.248	5.151	1.947	64.749	1.275	3.51	0.108	0.684	10/26/2005 0:00
20.229	5.283	1.946	65.125	1.442	3.37	0.105	0.611	11/14/2005 0:00
19.714	5.278	2.014	64.17	1.28	4.385	0.14	0.531	12/12/2005 0:00
20.294	5.101	1.934	64.1	1.237	3.589	0.118	0.487	1/12/2006 0:00
21.339	5.401	1.721	64.191	1.305	2.996	0.309	0.5	2/6/2006 0:00
20.547	5.442	1.912	65.817	1.304	3.37	0.151	0.517	3/8/2006 0:00
20.467	4.949	3.936	62.928	1.03	3.117	0.082	0.806	4/12/2006 0:00
19.394	5.043	3.726	62.546	0.988	2.954	0.06	0.743	5/8/2006 0:00
20.436	5.167	1.928	64.007	1.268	3.284	0.133	0.524	6/5/2006 0:00
19.532	4.99	1.796	63.405	1.332	3.292	0.113	0.561	7/12/2006 0:00
19.93	5.245	1.813	63.43	1.278	3.343	0.105	0.525	8/28/2006 0:00
19.852	5.132	1.839	63.355	1.268	3.224	0.096	0.492	9/26/2006 0:00
18.425	4.878	1.688	58.685	1.212	3.173	0.102	0.508	10/11/2006 0:00
19.787	5.046	1.765	65.116	1.17	3.185	0.099	0.559	11/17/2006 6:41
20.51	5.212	1.702	65.368	1.246	3.335	0.137	0.571	12/21/2006 15:22
19.511	4.984	1.72	63.71	1.196	3.22	0.103	0.51	1/29/2007 14:56
19.877	4.91	1.708	63.856	1.232	2.856	0.109	0.61	2/16/2007 16:00
20.607	5.301	1.686	64.157	1.445	3.115	0.107	0.596	3/5/2007 14:57
20.821	5.56	1.58	62.765	1.57	3.269	0.135	0.512	4/11/2007 0:00
19.747	5.163	1.537	63.279	1.359	2.996	0.128	0.456	5/15/2007 0:00

19.567	4.979	1.548	63.098	1.304	3.962	0.126	0.471	6/13/2007 0:00
19.563	5.238	1.491	63.353	1.35	3.557	0.115	0.468	7/9/2007 0:00
20.142	5.274	1.491	63.065	1.459	3.648	0.118	0.483	8/23/2007 9:01
20.076	5.367	1.507	63.075	1.533	3.468	0.131	0.504	9/30/2007 0:00
19.859	5.354	1.534	63.521	1.479	3.611	0.124	0.465	10/15/2007 0:00
18.665	4.771	1.609	61.067	1.447	3.616	0.154	0.466	12/5/2007 9:47
18.939	4.834	1.686	62.131	1.396	3.721	0.157	0.512	1/22/2008 8:52
18.286	4.616	1.683	62.791	1.205	3.598	0.167	0.555	4/9/2008 11:20
19.576	5.197	1.762	61.859	1.472	3.466	0.132	0.514	6/5/2008 14:27
20.325	5.329	1.682	63.014	1.625	3.694	0.136	0.474	8/19/2008 8:41
18.604	4.926	1.712	59.977	1.288	3.48	0.138	0.49	9/11/2008 8:57
20.423	5.374	1.666	62.714	1.436	3.583	0.139	0.494	10/10/2008 8:35
19.665	5.231	1.611	60.658	1.378	3.215	0.13	0.449	11/12/2008 15:31
18.909	5.062	1.694	61.026	1.389	3.542	0.126	0.465	12/15/2008 12:52
20.8	5.434	1.643	61.032	1.467	3.608	0.166	0.5	1/16/2009 8:59
17.229	4.469	1.532	56.48	1.229	3.284	0.116	0.453	2/10/2009 11:25
19.921	5.282	1.582	61.439	1.489	3.53	0.121	0.477	3/12/2009 9:29
19.133	5.307	1.66	61.681	1.478	3.341	0.122	0.51	4/15/2009 10:48
19.013	5.264	1.708	61.702	1.412	3.439	0.116	0.507	5/7/2009 9:05
19.197	5.205	1.663	61.498	1.367	3.63	0.107	0.509	6/8/2009 9:12

Cement Source 5

SiO$_2$	Al$_2$O$_3$	Fe$_2$O$_3$	CaO	MgO	SO$_3$	Na$_2$O	K$_2$O	DATE RECEIVED
20.37	4.52	3.09	59.67	1.36	2.73	0.14	0.4	1/1/1988 0:00
20.41	4.8	3.3	64.85	1.2	4.27	0.1	0.37	1/1/1988 0:00
20.79	4.78	3.49	63.67	1.43	2.8	0.11	0.31	1/1/1988 0:00
20.68	4.79	3.14	62.77	1.37	2.93	0.16	0.36	2/15/2001 0:00
20.03	4.72	3.37	62.55	1.41	2.91	0.21	0.37	4/19/2001 0:00
20.65	5.05	3.45	64.03	1.43	2.87	0.22	0.41	6/15/2001 0:00
20.24	4.9	3.7	64.06	1.49	2.88	0.24	0.37	4/30/2001 0:00
20.54	5.14	3.5	65.4	1.02	3.78	0.15	0.67	7/26/2001 0:00
20.33	5.06	3.86	63.63	1.68	3.11	0.23	0.38	8/14/2001 0:00
21.86	5.2	3.42	66.61	1.57	3.5	0.15	0.39	10/30/2001 0:00
20.61	5.03	3.69	63.25	1.5	3.18	0.22	0.37	2/28/2002 0:00
19.79	5.25	3.72	63.08	1.64	3.23	0.24	0.43	7/26/2002 0:00
19.67	5.31	3.84	63.42	1.61	3.15	0.16	0.39	8/29/2002 0:00
20.2	5.14	3.56	63	1.71	3.24	0.26	0.41	9/16/2002 0:00
20.68	5.38	2.25	64.42	1.26	3.38	0.14	0.59	10/15/2002 0:00
20.36	4.99	3.5	63.66	1.59	3.04	0.17	0.38	11/26/2002 0:00
20.51	4.95	3.51	63.76	1.64	3.17	0.13	0.4	12/30/2002 0:00
22.23	3.48	4.37	62.77	1.58	3.15	0.13	0.71	1/31/2003 0:00
20.54	5.12	3.62	63.85	1.66	2.75	0.14	0.37	3/6/2003 0:00
20.17	5.3	3.69	63.33	1.66	3.04	0.18	0.42	3/27/2003 0:00
21.03	4.99	3.24	64.34	1.51	2.79	0.14	0.37	4/28/2003 0:00
21.11	5.05	3.53	64.19	1.63	2.46	0.17	0.35	5/28/2003 0:00
20.04	4.8	3.28	61.02	1.44	2.54	0.15	0.32	6/30/2003 0:00
20.3	5.1	3.53	64.18	1.58	2.71	0.21	0.33	7/31/2003 0:00
20.09	4.89	3.43	63.95	1.51	2.64	0.38	0.36	8/25/2003 0:00
20.32	5.04	3.65	61.95	0.84	3.46	0.22	0.23	9/25/2003 0:00

20.08	5	3.51	64.3	1.52	2.61	0.17	0.39	10/29/2003 0:00
20.72	5.23	3.4	64.36	1.62	2.91	0.16	0.39	2/26/2004 0:00
20.7	5.53	3.52	63.9	1.8	2.88	0.15	0.38	3/17/2004 0:00
20.15	5.31	3.27	63.35	1.7	2.75	0.24	0.38	4/20/2004 0:00
20.2	5.25	3.46	63.8	1.64	2.83	0.18	0.36	6/4/2004 0:00
20.1	5.35	3.02	63.5	1.46	2.8	0.21	0.4	7/15/2004 0:00
20.09	4.94	3.23	63.49	1.41	2.58			8/31/2004 0:00
21.88	5.2	3.02	62.52	1.46	2.74			9/16/2004 0:00
20.31	3.85	3.1	64.45	2.16	2.38			9/28/2004 0:00
20.204	4.508	3.025	63.907	1.443	2.852	0.14	0.373	11/1/2004 0:00
20.908	4.13	3.303	64.857	1.475	2.607	0.034	0.476	12/2/2004 0:00
20.33	4.58	2.98	64.19	1.39	2.83	0.14	0.405	1/20/2005 0:00
19.9	5.05	3.073	64.27	1.232	2.83	0.112	0.375	2/18/2005 0:00
20.607	4.726	2.51	62.383	1.474	2.993	0.106	0.556	3/31/2005 0:00
20.164	4.687	3.092	64.202	1.651	2.716	0.232	0.431	4/28/2005 0:00
20.372	4.7	3.319	64.176	1.456	2.804	0.169	0.456	5/19/2005 0:00
20.18	4.803	3.05	63.344	1.469	2.78	0.151	0.425	6/10/2005 0:00
20.856	4.674	2.885	63.145	1.466	2.769	0.169	0.452	7/26/2005 0:00
19.99	4.81	3.119	64.605	1.262	2.795	0.114	0.366	8/31/2005 0:00
20.648	4.94	3.043	62.792	1.486	2.821	0.18	0.582	9/9/2005 0:00
20.701	4.928	3.041	62.739	1.484	2.843	0.183	0.59	9/9/2005 0:00
21.332	4.899	3.125	61.994	2.121	2.604	0.186	0.432	10/25/2005 0:00
19.515	4.319	3.644	62.509	1.516	3.194	0.152	0.624	10/26/2005 0:00
21.19	4.789	3.025	62.122	2.045	2.681	0.173	0.454	10/26/2005 0:00
20.9	4.762	3.01	61.677	2.028	2.935	0.168	0.42	10/31/2005 0:00
20.867	4.869	3.139	61.083	1.947	2.739	0.212	0.438	12/5/2005 0:00
20.87	4.654	2.815	62.274	1.761	2.933	0.193	0.382	1/31/2006 0:00
20.628	4.931	3.144	61.413	2.009	2.957	0.231	0.479	3/31/2006 0:00
15.627	3.618	2.624	54.656	1.494	2.298	0.183	0.371	4/28/2006 0:00
19.539	4.937	3.141	60.448	1.904	2.655	0.2	0.4	6/14/2006 0:00
20.708	5.258	3.361	61.414	2.026	2.766	0.227	0.46	6/30/2006 0:00
19.786	5.043	3.331	64.832	0.924	2.461	0.094	0.47	7/20/2006 0:00
20.235	4.56	2.966	59.656	1.869	2.423	0.208	0.38	9/26/2006 0:00
19.86	4.602	3.63	63.867	1.57	2.49	0.199	0.462	11/17/2006 7:55
20.427	4.695	3.51	65.316	1.148	2.427	0.213	0.559	1/3/2007 16:24
19.744	4.647	3.526	62.806	1.623	2.403	0.153	0.49	1/29/2007 11:10
19.489	4.634	3.283	60.949	1.81	2.506	0.165	0.465	2/16/2007 16:13
19.637	4.649	3.441	62.914	1.704	2.381	0.17	0.468	2/21/2007 0:00
19.195	5.177	2.243	63.456	1.109	2.756	0.091	1.001	3/28/2007 0:00
20.166	4.71	2.913	63.281	1.484	2.792	0.172	0.458	4/25/2007 0:00
20.226	4.743	3.275	62.107	1.584	2.714	0.178	0.435	5/25/2007 0:00
20.091	4.727	3.286	62.266	1.576	2.693	0.175	0.437	5/25/2007 0:00
18.897	4.203	2.958	60.411	1.349	2.586	0.152	0.39	5/25/2007 0:00
20.816	4.032	2.615	61.483	1.394	2.851	0.16	0.376	7/2/2007 0:00
21.021	4.431	2.932	63.438	1.711	2.664	0.169	0.396	8/6/2007 14:17
20.175	4.272	2.895	61.853	1.698	2.617	0.178	0.383	10/31/2000 0:00
20.047	4.428	3.512	61.791	1.836	2.618	0.188	0.408	9/30/2007 0:00
19.135	4.232	3.145	62.295	1.735	2.313	0.172	0.396	2/20/2008 8:16
19.447	4.283	3.113	60.869	1.853	2.391	0.184	0.394	2/20/2008 9:10
19.304	4.187	3.046	61.72	2.009	2.367	0.196	0.411	4/9/2008 11:30

20.977	4.734	2.819	62.502	1.954	2.429	0.181	0.413	6/5/2008 14:12
20.198	4.782	3.295	61.532	1.873	2.51	0.173	0.393	8/19/2008 8:17
20.465	4.841	3.416	61.805	1.76	2.364	0.169	0.402	9/3/2008 0:00
20.284	4.774	3.364	61.061	1.747	2.342	0.161	0.392	10/24/2008 9:57
19.826	4.766	3.184	61.063	1.924	2.304	0.187	0.422	12/31/2008 9:11
20.352	4.848	3.244	61.217	1.893	2.538	0.189	0.44	7/15/2008 7:02
18.682	4.768	3.414	59.768	1.234	2.084	0.146	0.444	1/16/2009 9:01
19.88	4.332	3.373	63.73	1.217	2.35	0.143	0.456	2/3/2009 16:47
18.013	4.168	3.235	60.978	1.282	2.282	0.15	0.415	3/5/2009 12:51
18.958	4.329	3.018	63.727	1.689	2.507	0.159	0.424	5/18/2009 9:03
20.349	4.528	3.124	63.472	1.276	2.302	0.153	0.41	6/10/2009 14:48

Cement Source 2

SiO_2	Al_2O_3	Fe_2O_3	CaO	MgO	SO_3	Na_2O	K_2O	DATE RECEIVED
19.52	5.24	2.66	59.17	1.16	2.96	0.17	0.88	1/1/1988 0:00
19.55	5.31	2.83	63.9	1.13	5.05	0.12	0.81	1/1/1988 0:00
19.95	5.57	2.58	63.42	1.22	3.45	0.11	0.68	1/1/1988 0:00
19.73	5.31	2.93	63.33	1.22	3.53	0.11	0.93	2/15/2001 0:00
20.57	5.27	2.49	63.73	1.32	3.39	0.1	0.66	4/19/2001 0:00
13.87	3.68	2.06	52.27	0.79	2.47	0.14	0.85	6/15/2001 0:00
16.08	4.32	2.31	58.52	1.08	3	0.19	0.76	8/14/2001 0:00
20.34	5.14	2.72	63.36	1.21	3.3	0.16	0.99	10/5/2001 0:00
20.83	4.76	4.05	63.22	2.64	1.97	0.19	0.5	10/30/2001 0:00
20.35	5.95	2.74	62.2	1.4	3.17	0.25	0.83	12/2/2001 0:00
19.75	5.68	2.5	63.73	1.22	3.21	0.18	0.89	4/26/2002 0:00
19.89	5.25	2.67	64.04	1.18	3.23	0.19	0.87	7/31/2002 0:00
20.17	5.26	2.48	63.93	1.13	3.21	0.12	0.92	10/15/2002 0:00
19.93	5.46	2.36	64.14	1.14	3.2	0.11	0.91	11/27/2002 0:00
19.69	5.28	2.39	64.21	1.12	3.42	0.11	1.02	12/20/2002 0:00
19.65	5.26	2.67	63.76	1.1	3.51	0.14	1.09	1/31/2003 0:00
19.66	5.16	2.5	64.13	1.16	3.29	0.1	0.94	3/6/2003 0:00
20.13	5.03	3.91	64.5	0.65	3.34	0.07	0.94	3/10/2003 0:00
19.63	5.19	2.51	63.97	1.12	3.31	0.11	0.94	3/27/2003 0:00
18.86	5.04	2.73	63.16	1.11	3.4	0.1	0.97	4/28/2003 0:00
18.78	4.76	2.64	59.89	1.03	2.79	0.08	0.78	5/28/2003 0:00
19.9	5.22	2.64	64.29	1.14	3.29	0.15	0.9	7/31/2003 0:00
19.74	5.1	2.82	63.81	1.16	3.16	0.35	0.88	8/25/2003 0:00
19.21	5.5	2.7	67.87	1.09	3.11	0	1.02	9/25/2003 0:00
19.5	5.63	2.29	64.42	1.25	3.3	0.12	0.89	10/29/2003 0:00
19.38	5.52	2.85	63.75	1.16	3.41	0.19	0.93	11/1/2003 0:00
18.92	4.42	2.34	61.98	1.37	2.75	0.14	0.92	2/17/2004 0:00
20.29	5.31	2.46	64.43	1.14	3.41	0.12	0.91	2/26/2004 0:00
20.95	4.88	2.46	65.18	1.49	2.96	0.14	0.94	3/17/2004 0:00
20.38	5.42	2.37	64.56	1.1	3.32	0.12	0.92	4/22/2004 0:00
20.83	4.61	2.48	65.01	1.49	2.97	0.13	0.94	5/18/2004 0:00
19.75	5.11	2.49	64.07	1.11	3.33	0.09	0.94	6/4/2004 0:00
19.45	5.68	2.59	63.5	1.12	3.19	0.16	0.91	7/15/2004 0:00
20.072	5.003	2.4	63.842	1.119	3.287	0.069	0.908	11/1/2004 0:00
20.372	4.139	3.137	64.139	2.077	2.506	0.181	0.512	12/2/2004 0:00
19.91	5.23	2.65	63.25	1.076	3.33	0.105	0.855	2/18/2005 0:00

SiO₂	Al₂O₃	Fe₂O₃	CaO	MgO	SO₃	Na₂O	K₂O	DATE RECEIVED
19.794	5.512	2.41	63.315	1.084	3.178	0.108	0.983	4/28/2005 0:00
19.542	5.441	2.667	63.166	1.096	3.349	0.087	0.928	5/19/2005 0:00
20.118	5.59	2.299	63.976	1.257	3.073	0.095	0.852	10/31/2005 0:00
19.436	5.581	2.337	63.87	1.17	3.314	0.098	0.895	12/5/2005 0:00
20.128	5.234	2.692	63.762	1.261	3.459	0.083	0.689	1/31/2006 0:00
19.48	5.601	2.332	64.315	1.208	3.442	0.117	0.983	3/31/2006 0:00
19.695	5.383	2.629	63.315	1.2	3.245	0.109	0.903	4/28/2006 0:00
20.049	5.788	2.28	63.244	1.4	2.852	0.102	0.926	6/14/2006 0:00
20.523	5.242	3.662	63.104	0.895	2.672	0.085	0.483	7/20/2006 0:00
19.773	5.27	2.343	63.541	1.115	3.14	0.11	0.87	11/17/2006 7:53
20.555	5.265	2.526	64.127	1.179	3.196	0.123	0.892	1/3/2007 16:24
19.004	4.825	2.661	62.444	1.097	2.887	0.083	0.92	2/16/2007 16:14
19.18	5.243	2.261	63.346	1.125	2.753	0.108	0.999	3/28/2007 0:00
18.825	5.081	2.367	61.204	1.021	3.301	0.107	0.921	5/25/2007 0:00
19.229	5.347	2.589	61.914	1.056	3.489	0.118	0.928	7/2/2007 0:00
19.284	5.006	2.815	62.888	1.08	3.305	0.114	0.903	9/30/2007 0:00
18.966	4.541	3.756	63.554	0.986	2.798	0.354	0.329	2/20/2008 8:08
18.752	4.987	2.312	61.436	1.243	3.376	0.148	0.851	2/20/2008 9:07
19.86	5.491	2.327	61.386	1.363	3.357	0.147	0.946	5/7/2008 0:00
18.857	5.314	2.642	59.963	1.396	3.408	0.15	0.906	6/5/2008 16:23
18.676	5.373	2.599	61.588	1.14	3.615	0.128	1.078	8/19/2008 8:09
19.015	5.296	2.739	61.319	1.283	3.385	0.141	0.963	9/3/2008 0:00
18.593	4.475	3.864	61.195	1.072	2.745	0.16	0.562	12/31/2008 9:05
17.576	4.81	2.928	61.086	1.119	3.299	0.137	0.907	2/3/2009 16:44
18.213	5.455	2.65	61.401	1.18	3.555	0.145	1.054	3/5/2009 12:52
17.82	5.061	2.69	62.603	1.148	3.381	0.127	0.966	4/9/2009 8:09
17.963	5.183	2.447	63.502	1.082	3.371	0.12	0.938	5/12/2009 14:24
18.808	5.271	2.613	63.003	1.158	3.383	0.115	0.835	6/10/2009 14:43

Cement Source 3

SiO₂	Al₂O₃	Fe₂O₃	CaO	MgO	SO₃	Na₂O	K₂O	DATE RECEIVED
21.38	3.89	3.71	65.76	2.55	2.91	0.07	0.58	1/1/1988 0:00
21.48	3.7	3.41	64.68	2.44	3.56	0.05	0.62	1/1/1988 0:00
22.6	3.42	3.42	64.8	2.58	2.5	0.11	0.76	1/1/1988 0:00
21.27	3.49	3.33	63.15	2.38	2.66	0.08	0.66	2/20/2001 0:00
22.43	3.64	3.29	63.24	2.32	2.65	0.07	0.68	4/24/2001 0:00
22.24	3.7	3.28	64.22	2.23	2.66	0.17	0.64	6/26/2001 0:00
21.6	3.61	3.2	65.58	2.5	2.69	0.2	0.64	10/22/2001 0:00
21.11	3.39	3.32	63.42	1.89	2.68	0.18	0.62	3/8/2002 0:00
21.15	3.6	3.67	64.93	2.12	2.77	0.18	0.67	7/22/2002 0:00
21.38	3.41	3.6	64.47	2.32	2.52	0.11	0.55	9/30/2002 0:00
21.33	3.61	3.67	64.01	2.27	2.63	0.12	0.61	10/20/2002 0:00
21.63	3.67	3.65	64.33	2.49	2.48	0.13	0.69	12/2/2002 0:00
21.98	3.65	3.73	63.95	2.04	2.62	0.08	0.78	12/30/2002 0:00
23.06	3.68	3.6	62.54	1.9	2.9	0.22	0.76	1/24/2003 0:00
20.77	3.31	3.57	64.14	2.38	2.84	0.08	0.68	2/28/2003 0:00
20.85	3.18	3.77	64.37	2.17	2.98	0.15	0.62	3/24/2003 0:00
21.25	3.42	3.64	64.72	1.81	2.94	0.19	0.67	4/22/2003 0:00
21.4	3.3	3.75	64.48	1.99	2.72	0.14	0.57	6/9/2003 0:00

19.45	2.96	3.33	59.85	2.27	2.52	0.17	0.41	6/27/2003 0:00
21.76	3.42	3.8	63.64	2.79	2.49	0.2	0.53	7/18/2003 0:00
21.4	4.05	4.13	68.7	2.43	2.9	0	0.64	9/25/2003 0:00
21.23	3.42	3.57	65.66	2.91	2.04	0.23	0.44	10/25/2003 0:00
21.69	3.7	3.29	63.81	2.83	2.4	0.23	0.4	11/25/2003 0:00
21	3.94	3.24	62.35	3.37	2.59	0.26	0.45	12/18/2003 0:00
21.31	4.48	2.9	63.72	2.26	2.61	0.28	0.41	1/24/2004 0:00
20.94	3.75	3.86	62.04	2.77	2.82	0.25	0.5	2/25/2004 0:00
20.96	3.91	3.27	62.51	3.29	2.56	0.27	0.47	3/22/2004 0:00
21.83	3.83	3.54	61.39	3.03	2.79	0.28	0.59	4/22/2004 0:00
20.04	4.86	3.14	62.51	3.95	2.72	0.21	0.53	5/3/2004 0:00
21.89	4.03	3.35	61.26	2.55	2.7	0.25	0.82	5/27/2004 0:00
22.03	3.9	3.91	62.72	1.95	2.65	0.17	0.59	6/28/2004 0:00
21.62	4.09	3.33	61.99	2.21	2.82	0.2	0.79	7/23/2004 0:00
20.78	4.19	3.29	61.34	2.5	2.76	0	0	8/30/2004 0:00
20.75	3.7	3.17	61.6	2.41	2.83			9/27/2004 0:00
21.741	3.386	3.553	62.265	2.561	2.992	0.128	0.676	10/26/2004 0:00
21.572	3.283	3.915	63.015	2.206	2.654	0.11	0.578	12/2/2004 0:00
21.16	3.279	3.783	62.293	2.192	2.834	0.122	0.626	12/27/2004 0:00
20.66	4.3	3.3	61.48	2.61	3.04	0.157	0.647	2/23/2005 0:00
21.05	3.988	2.629	61.121	2.305	2.865	0.155	0.574	3/31/2005 0:00
20.991	4.113	3.567	62.416	2.318	2.845	0.19	0.733	4/28/2005 0:00
20.649	3.654	4.335	61.145	2.403	2.698	0.133	0.574	6/22/2005 0:00
20.507	3.682	4.312	61.338	2.937	2.645	0.122	0.653	8/31/2005 0:00
20.445	3.62	3.93	63.368	2.855	2.506	0.099	0.635	8/31/2005 0:00
21.451	3.611	3.364	64.345	2.637	2.684	0.036	0.703	9/29/2005 0:00
22.459	3.64	3.361	63.2	3.566	2.214	0.069	0.59	10/26/2005 0:00
21.467	3.704	3.127	61.992	2.994	2.786	0.091	0.726	11/28/2005 0:00
21.306	3.621	3.859	63.028	2.516	3.099	0.086	0.714	12/19/2005 0:00
20.636	3.437	3.855	62.282	3.108	2.99	0.108	0.676	1/24/2006 0:00
21.646	3.693	3.892	63.253	3.475	3.013	0.11	0.788	2/27/2006 0:00
21.008	3.429	3.831	63.329	3.764	2.928	0.111	0.769	3/23/2006 0:00
20.148	3.551	3.972	61.229	3.674	2.715	0.082	0.658	5/24/2006 0:00
20.818	3.556	3.76	63.19	3.37	2.556	0.08	0.711	5/24/2006 0:00
20.471	3.437	4.088	62.609	3.362	2.598	0.065	0.662	6/26/2006 0:00
20.405	3.48	3.953	62.651	2.639	2.572	0.072	0.697	7/26/2006 0:00
20.826	3.402	4.364	61.109	2.933	2.748	0.057	0.601	8/28/2006 0:00
21.454	3.336	3.209	61.079	2.793	2.363	0.078	0.64	9/26/2006 0:00
19.691	4.505	3.538	63.546	1.103	2.729	0.2	0.553	11/17/2006 6:43
21.12	3.974	3.543	63.605	2.743	2.637	0.145	0.846	12/12/2006 9:13
19.336	3.617	3.425	59.645	2.5	2.927	0.09	0.753	1/3/2007 16:26
20.414	3.905	3.622	61.716	2.778	2.913	0.115	0.873	1/29/2007 11:17
19.914	3.997	3.603	62.605	2.913	1.692	0.123	0.72	2/20/2007 0:00
20.192	3.93	3.533	63.003	3.141	2.353	0.113	0.851	3/15/2007 0:00
20.417	3.465	3.861	61.961	2.877	2.444	0.111	0.666	4/25/2007 0:00
19.933	3.376	3.939	60.331	2.756	2.527	0.101	0.627	5/25/2007 0:00
21.297	3.829	3.851	61.116	2.789	2.691	0.109	0.668	6/13/2007 0:00
20.55	3.746	3.685	60.525	2.188	2.643	0.114	0.687	6/21/2007 0:00
20.386	3.974	3.859	63.293	2.189	2.474	0.094	0.719	7/23/2007 11:18
20.907	3.59	4.137	62.193	2.172	2.493	0.104	0.658	9/30/2007 0:00

19.155	3.291	4.086	63.394	2.013	2.423	0.082	0.605	9/30/2007 0:00
19.436	3.854	3.583	61.366	3.334	2.515	0.083	0.687	12/4/2007 15:43
19.792	3.7	3.842	63.822	2.227	2.513	0.089	0.761	12/19/2007 11:18
19.826	3.197	4.309	62.979	2.108	2.684	0.102	0.66	2/20/2008 8:04
19.17	3.586	3.937	61.925	2.46	2.459	0.105	0.743	4/9/2008 10:45
20.785	3.399	4.195	62.299	2.975	2.454	0.093	0.616	6/5/2008 14:33
20.42	3.843	4.129	62.522	2.731	2.413	0.094	0.714	8/26/2008 13:27
18.123	4.162	3.787	61.83	1.347	2.644	0.126	0.605	9/26/2008 0:00
20.345	3.883	4.36	63.512	1.996	2.711	0.077	0.746	10/17/2008 0:00
20.116	3.643	3.609	62.064	2.532	2.624	0.118	0.662	12/4/2008 10:18
20.393	3.927	4.012	61.184	2.436	2.846	0.085	0.788	12/31/2008 8:36
20.013	3.655	3.741	61.93	2.689	2.85	0.082	0.702	2/3/2009 16:42
18.416	3.247	3.897	60.76	2.124	2.66	0.098	0.626	3/26/2009 11:04
19.584	3.541	4.142	63.079	1.988	2.702	0.082	0.6	4/15/2009 11:19
16.734	3.389	3.665	59.82	1.999	2.138	0.136	0.658	5/12/2009 15:03
21.343	3.72	3.777	63.96	2.588	2.42	0.074	0.623	6/10/2009 12:15

APPENDIX E:

ABSORPTION BAND RATIO (750 CM^{-1}/960 CM^{-1}) FOR ALKALI QUANTIFICATION

	Set 1				Set 2			
	960 cm-1	750 cm-1	Ratio	Avg	960 cm-1	750 cm-1	Ratio	Avg
Cement Source 2	27.342	0.381	0.0139		22.381	0.212	0.0095	
	19.926	0.265	0.0133		29.465	0.259	0.0088	
	35.873	0.478	0.0133		33.875	0.375	0.0111	
	18.594	0.243	0.0131		70.877	0.774	0.0109	
	45.572	0.518	0.0114	0.012999	65.567	0.644	0.0098	0.010015
Cement Source 1	16.789	0.09	0.00536		59.225	0.173	0.0029	
	11.6412	0.0881	0.00757		17.035	0.082	0.0048	
	33.803	0.156	0.00461		50.165	0.162	0.0032	
	44.424	0.188	0.00423		50.137	0.156	0.0031	
	41.139	0.234	0.00569	0.005492	44.029	0.173	0.0039	0.003601
Cement Source 5	62.533	0.003	0.000048		50.909	-0.22	-0.0043	
	19.652	0.003	0.0001527		52.068	-0.315	-0.0060	
	35.552	0.003	0.0000844		47.739	-0.237	-0.0050	
	22.004	0.003	0.0001363		40.096	-0.179	-0.0045	
	10.5476	0.0013	0.0001233	0.000109	31.693	-0.208	-0.0066	-0.00527
Cement Source 3	47.37	0.061	0.001288		71.561	0.108	0.0015	
	30.798	0.056	0.001818		59.757	0.08	0.0013	
	92.346	0.171	0.001852		74.289	0.096	0.0013	
	59.043	0.101	0.001711		77.746	0.091	0.0012	
	41.091	0.073	0.001777	0.001689	38.108	0.097	0.0025	0.001571
Cement Source 4	34.384	0.041	0.001192		66.937	-0.002	0.0000	
	26.89	0.047	0.001748		71.645	0.11	0.0015	
	20.971	0.021	0.001001		54.265	-0.026	0.0005	
	36.72	0.026	0.000708		20.393	0.02	0.0010	
	8.9095	0.018	0.002020	0.001334	46.289	0.016	0.0003	0.000471

Note: Negative values represent area below baseline and it should be treated as zero.

Set 1					
Cement Source 2	Cement Source 1	Cement Source 5	Cement Source 3	Cement Source 4	
0.0139	0.00536	0.000048	0.006988	0.001192	
0.0133	0.00757	0.0001527	0.001818	0.001748	
0.0133	0.00461	0.0000844	0.001852	0.001001	
0.0131	0.00423	0.0001363	0.001711	0.000708	
0.0114	0.00569	0.0001233	0.001777	0.00202	
0.000943	0.001299	4.2384E -05	0.002326	0.00054	**SDEV**
Set 2					
Cement Source 2	Cement Source 1	Cement Source 5	Cement Source 3	Cement Source 4	
0.0095	0.0029	0	0.0015	0	
0.0088	0.0048	0	0.0013	0.0015	
0.0111	0.0032	0	0.0013	0	
0.0109	0.0031	0	0.0012	0.001	
0.0098	0.0039	0	0.0025	0.0003	
0.000968	0.000779	0	0.000537	0.000666	**SDEV**

Test Procedure for Quantification of alkali content in cement
TxDOT Designation:

Effective Date:

1.   SCOPE

1.1   Use this procedure to determine the concentrations of Na_2O_e content in cement

1.2   This test procedure is in several parts:

- ■   Part I—Sample preparation for determining alkali content of an unknown sample
- ■   Part II— General Procedure for collecting sample data by light transmission through a KBr pellet
- ■   Part III— Sample Analysis

PART I— SAMPLE PREPARATION FOR DETERMINING ALKALI CONTENT OF AN UNKNOWN SAMPLE

2.   SCOPE

2.1   Use the following procedure to measure the Alkali content of an unknown cement sample.

3.   PROCEDURE

3.1   Use the existing calibration curve for the quantification of alkali content in cement. (The background collection method used by the IR may account for variations in the prisms or KBr pellet. If so, calibration curves need generation only periodically. Refer to the instrument manufacturer's recommendations to determine the necessary frequency of calibrations.)

3.2   Generate a FTIR spectrum using KBr pellet and light transmission method described below.

3.3   Integrate the appropriate peak, or calculate the peak ratio for the alkali content in the unknown cement sample.

3.4   Calculate the alkali content from the measured peak area ratio the previously generated calibration curve.

PART II— GENERAL PROCEDURE FOR COLLECTING SAMPLE DATA BY LIGHT TRANSMISSION THROUGH A KBR PELLET

4.   SCOPE

4.1   Procedure for producing a KBr pellet and collection transmission data

5.   APPARATUS

5.1   Fourier Transform Infrared Spectrometer

5.2   Balance, readable to 0.1g, accurate to 0.5g

5.3   Hydrallic press with 12000 psi capacity

5.4   A set of mortar and pestle

5.5   Wax paper

6.   PREPARING STANDARD

6.1   Using wax paper, measure 100 mg of KBr powder (it is highly recommended to keep KBr in an oven at ~ 60 °C to prevent moisture absorption)

6.2   Add 2 mg of cement to the 100 mg of KBr powder prepared in step 6.1

6.3   Grind the mixture prepared in part 6.2 and place it into 13 mm die press for 3 minutes at 10,000 psi. Use a mechanical pump to remove air and moisture from the die while powder is being pressed.

6.4   Remove the pellet from the die.

6.5   Run a background spectrum (4000 cm^{-1} to 400 cm^{-1}) without any sample placed in the path of IR light using FTIR manufacturer recommended procedure

6.6   Place the pellet prepared in steps 6.1 through 6.4 and collect spectrum of the sample for 4000 cm^{-1} to 400 cm^{-1}.

PART III— SAMPLE ANALYSIS

ALKALI QUANTIFICATION

7.   CALCULATIONS

7.1   Use peak area measurement for absorption band around 750 cm^{-1} (this band belongs to alkali constituent) using integral area calculation feature of the FTIR manufacturer software and assign its value to $A_{750 \, cm-1}$

7.2   Use peak area measurement for absorption band around 960 cm^{-1} (this band belongs to cement) using integral area calculation feature of the FTIR manufacturer software and assign it to $A_{960\ cm-1}$

7.3   Calculate area ratio ($A_{750\ cm-1}/A_{960\ cm-1}$)

7.4   Use calibration curve generated previously (shown below) and calculate alkali content of the sample.

7.5   Locate measured area ratio on the "Avg Peak Ratio" axis and intersect calibration curve.

Combined Average of Data Sets #1 and #2

$$y = 0.054x - 0.022$$
$$R^2 = 0.979$$

Avg Peak Ratios vs. Na$_2$O Concentration (wt% measured with XRF)
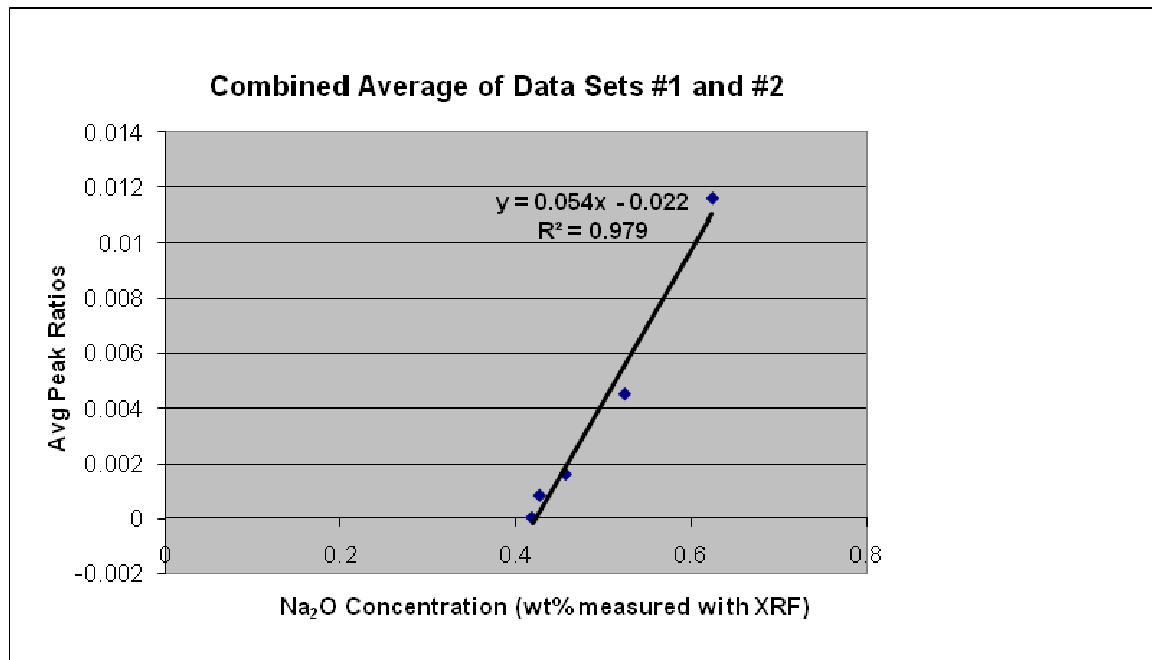
7.6   Calculate for alkali in cement using equation y = 0.054 x -0.22. In this equation x represent Na$_2$Oe present in the sample under analysis.

7.7   Total equivalent alkali content can be calculated from

lb. alkali per cu. yd. = [(lb cement per cu. Yd.) X (%Na$_2$O equivalent in cement)] / 100

FTIR SPECTRA OF EMULSION ASPHALT BINDERS
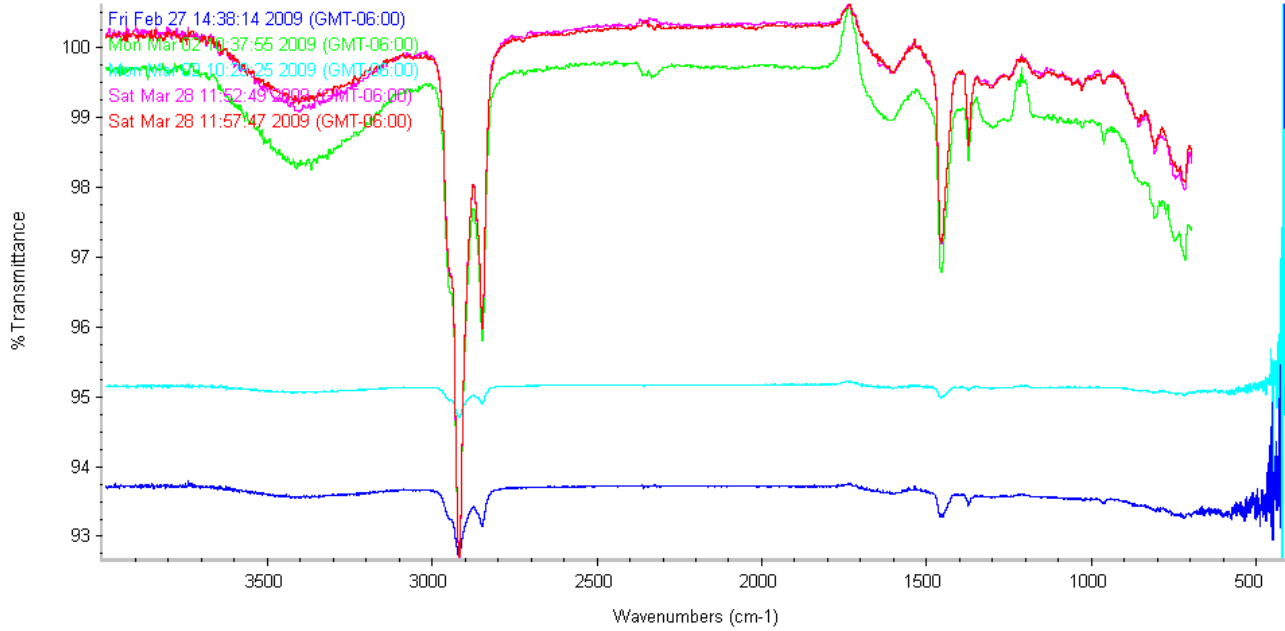
Figure 5.21: FTIR Spectra of CRS-2 Samples Received from Supplier B (batch 1).
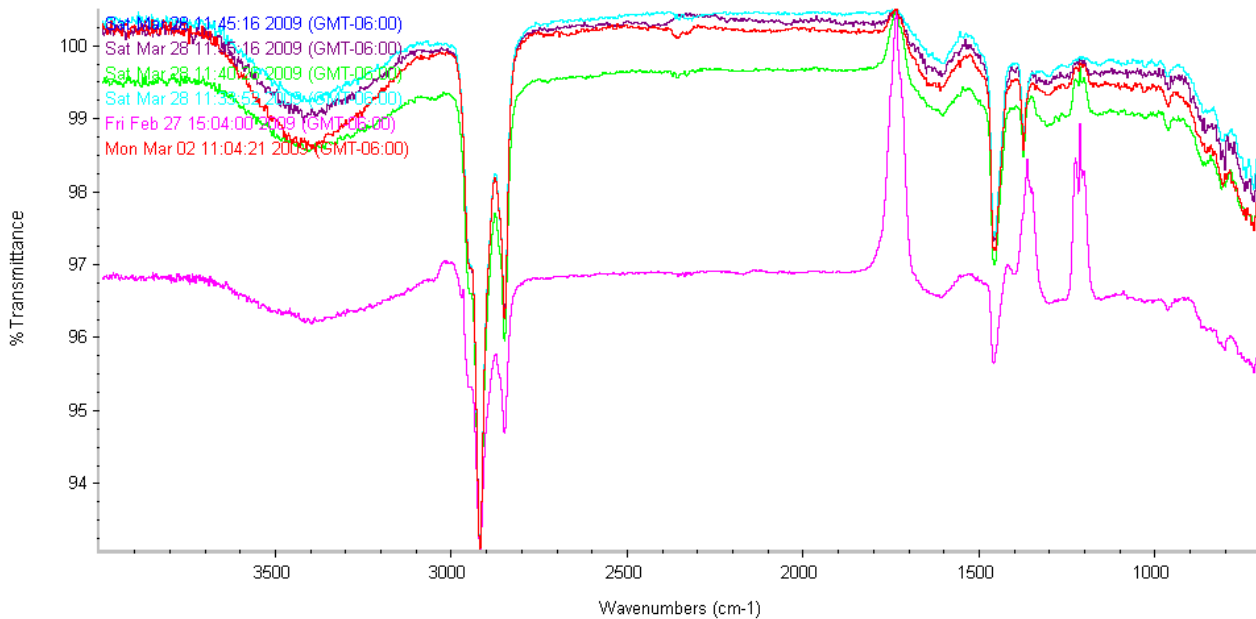
Figure 5.22: FTIR Spectra of CRS-2P Samples Received from Supplier B (batch 1).
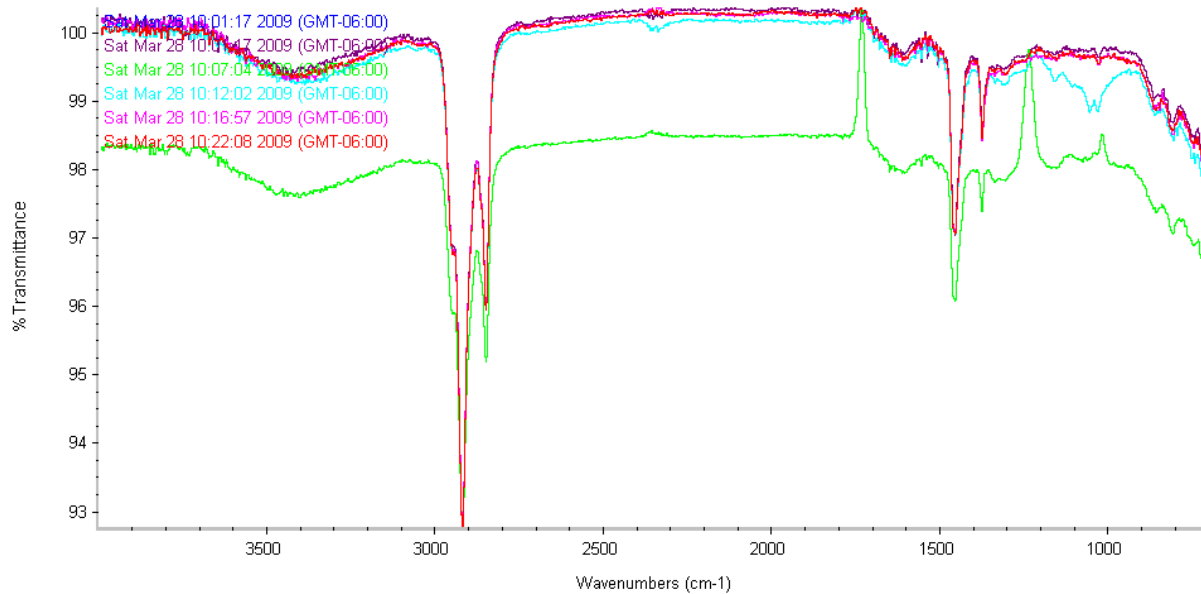
Figure 5.23: FTIR Spectra of CRS-2 Samples Received from Supplier B (batch 2).
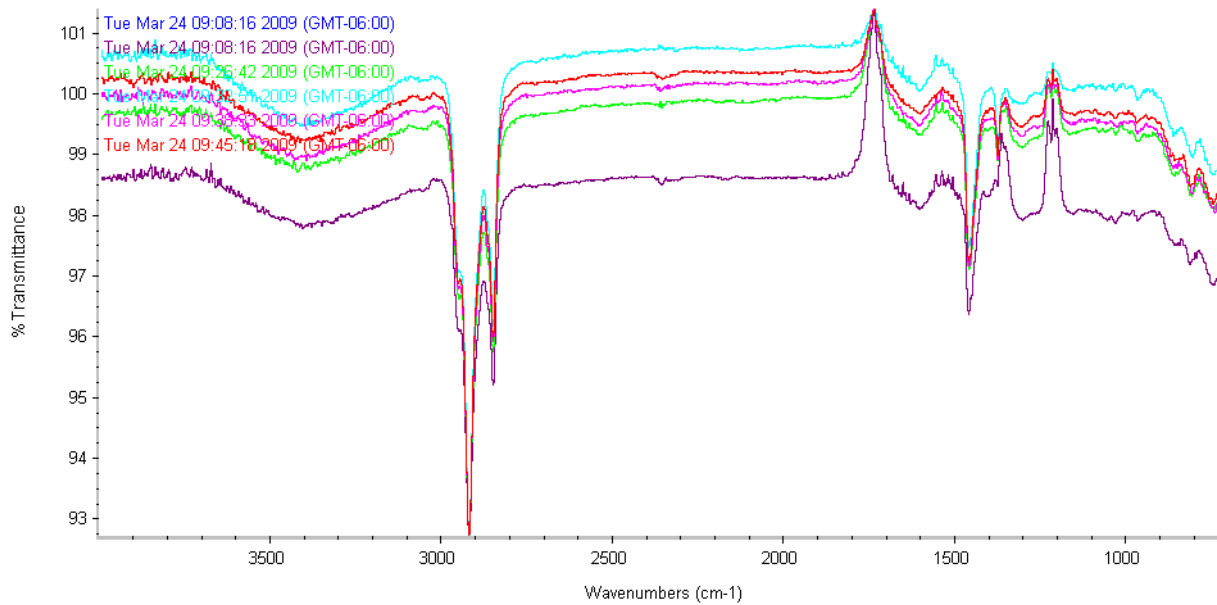
Figure 5.24: FTIR Spectra of CRS-2P Samples Received from Supplier B (batch 2).
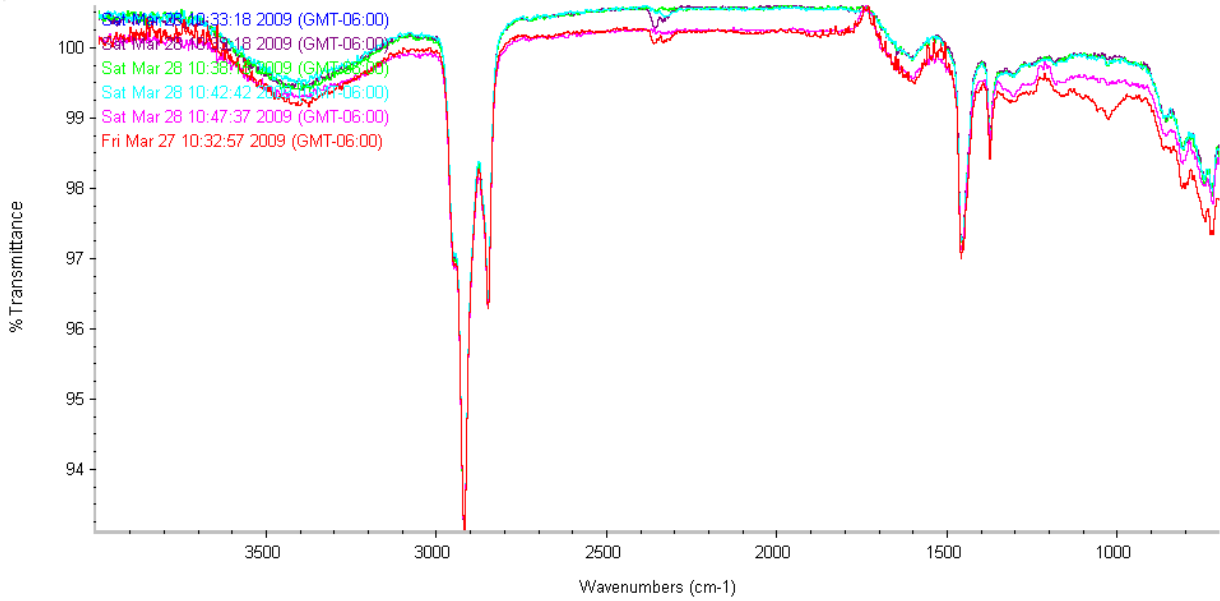
Figure 5.25: FTIR spectra of HFRS-2 Samples Received from Supplier A.
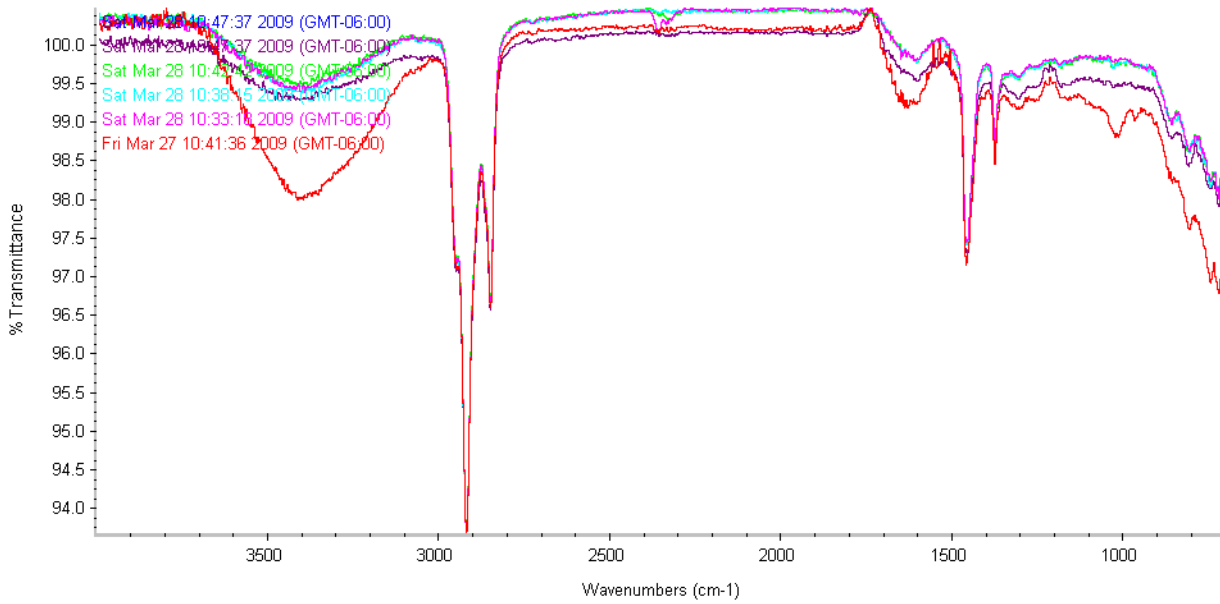
Figure 5.26: FTIR spectra of HFRS-2P Samples Received from Supplier A.
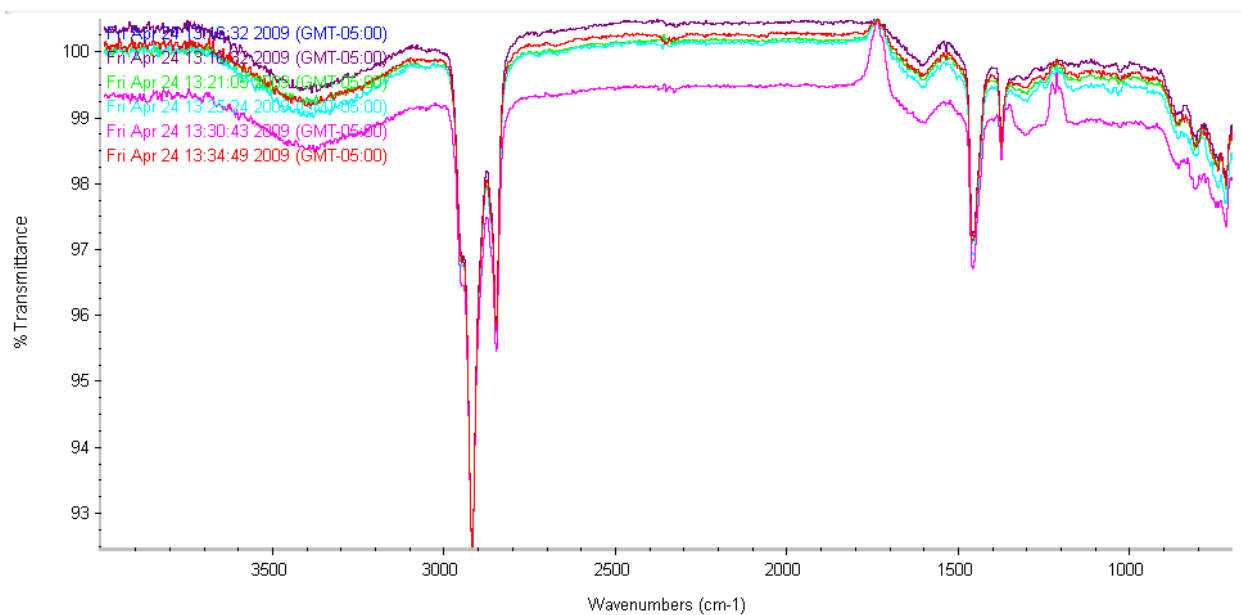
Figure 5.27: FTIR Spectra of CRS-2 Samples Received from Supplier D.
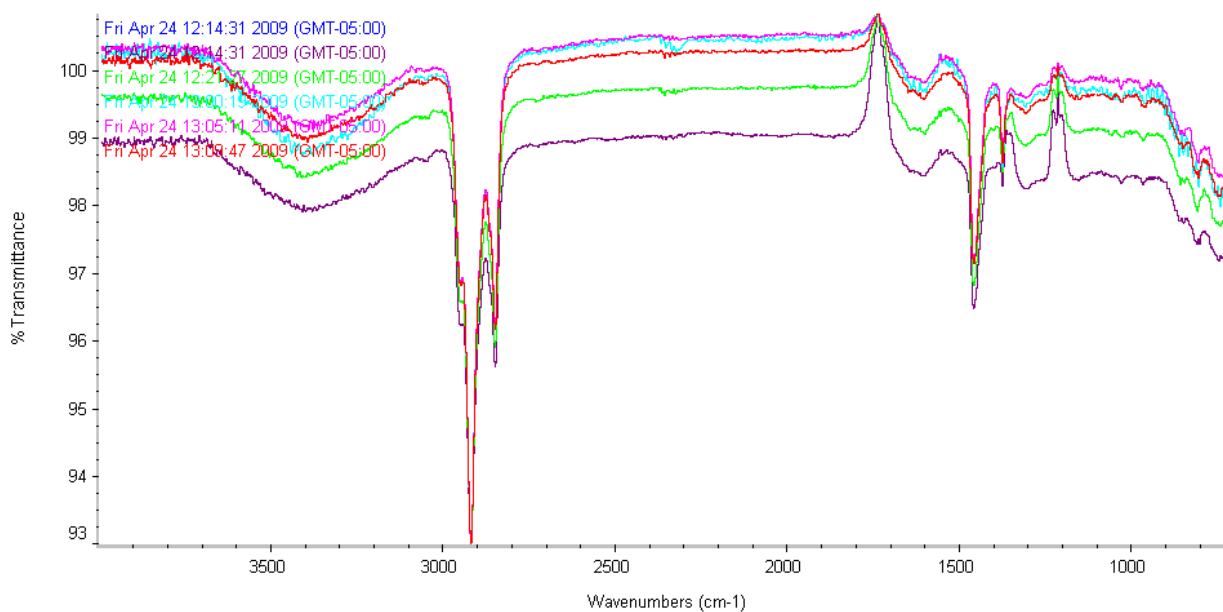
Figure 5.28: FTIR Spectra of CRS-2P Samples Received from Supplier D.
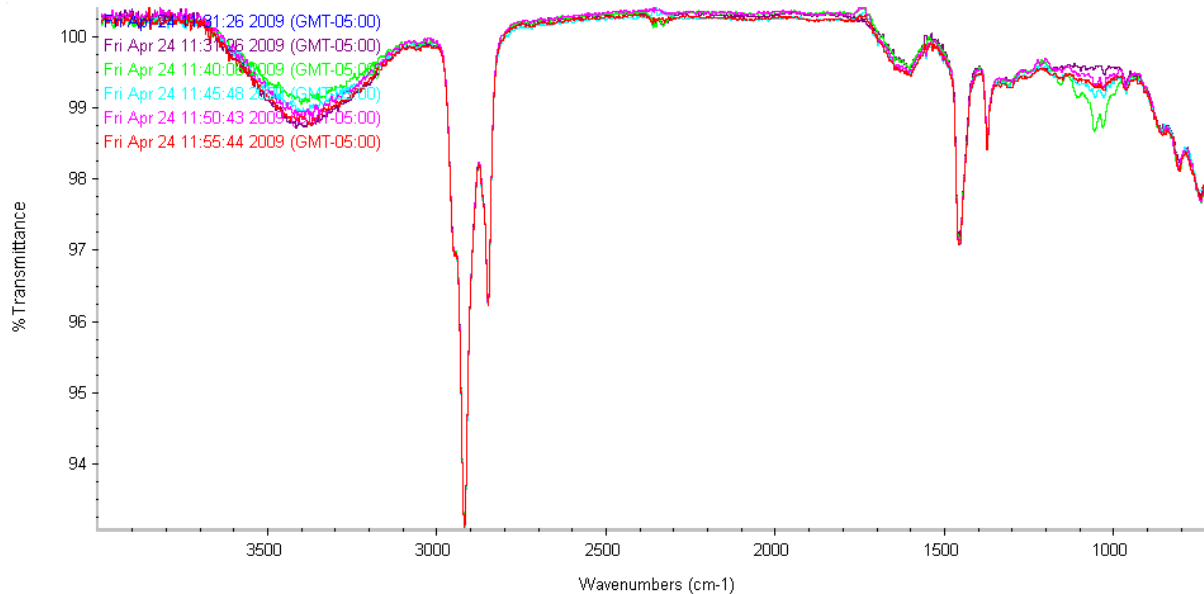
Figure 5.29: FTIR Spectra of CHFRS-2P Samples Received from Supplier D.
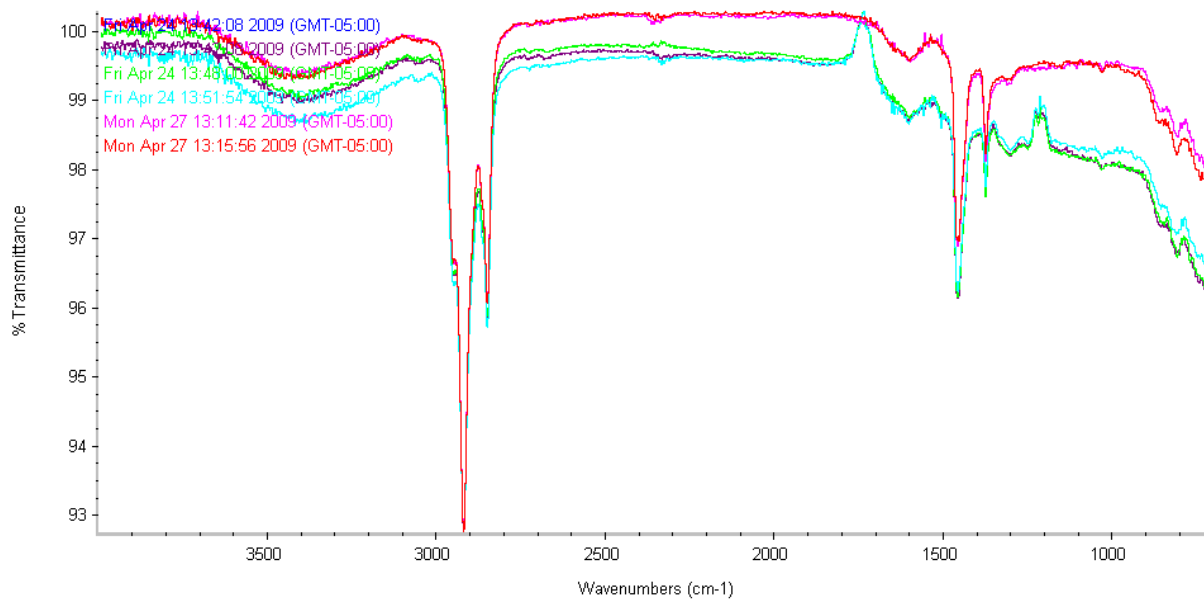
Figure 5.30: FTIR Spectra of HFRS-2 Samples Received from Supplier D.
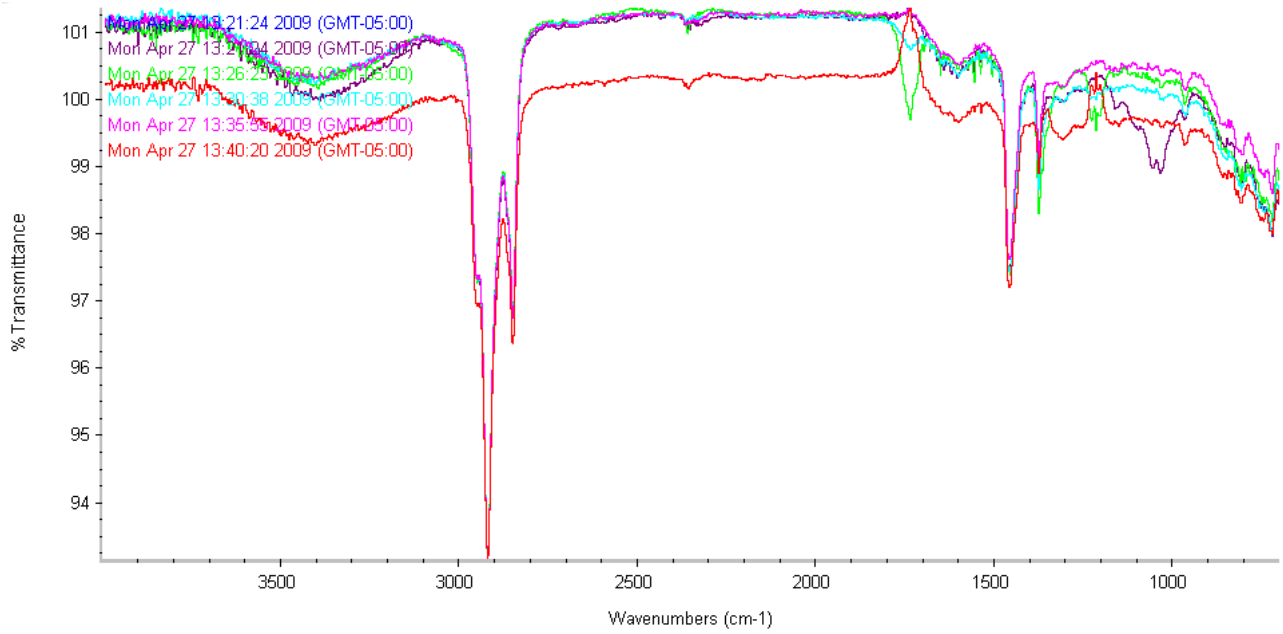
Figure 5.31: FTIR Spectra of HFRS-2P Samples Received from Supplier D.

University of North Texas
Denton, Texas